Vascular smooth muscle cell heterogeneity and plasticity in models of cardiovascular disease

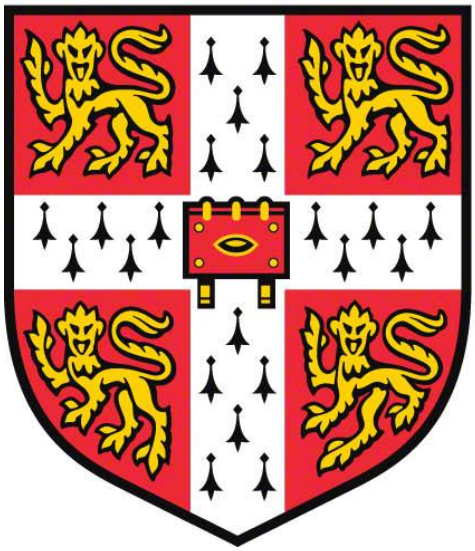

Joel Stephen Chappell

Darwin College

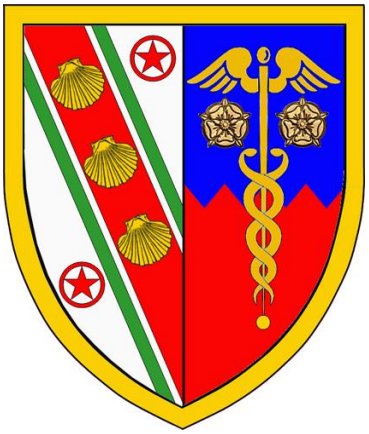

This dissertation is submitted for the degree of Doctor of Philosophy

University of Cambridge

16/10/2017

Preface

Declaration

This dissertation is the result of my own work and includes nothing which is the outcome of work done in collaboration except as declared in the Preface and specified in the text.

It is not substantially the same as any that I have submitted, or, is being concurrently submitted for a degree or diploma or other qualification at the University of Cambridge or any other University or similar institution except as declared in the Preface and specified in the text. I further state that no substantial part of my dissertation has already been submitted, or, is being concurrently submitted for any such degree, diploma or other qualification at the University of Cambridge or any other University or similar institution except as declared in the Preface and specified in the text.

It does not exceed the prescribed word limit for the relevant Degree Committee.

The studies which form the basis of Chapters 4-6 were published in Chappell et al., 2016. Figures taken from this published work are referenced within the Figure legends.

- Jennifer L. Harman, aided in the immuno-staining of cryo-sections
- Vagheesh M. Narasimhan, aided in statistical analysis of data
- Haixiang Yu and Kirsty Foote, aided in performing and teaching the carotid ligation technique
- Benjamin D. Simons, aided in statistical analysis and discussion concerning the experimental design/results
- Martin R. Bennett, was involved in discussions concerning the experimental design/results
- Helle F. Jorgensen, supervised this work and was involved in the experimental design and mouse breeding

The work within Chapter 7 is based on a collaboration between the groups of Dr. Helle Jorgensen and Prof. Ziad Mallet

- Mini-pump surgery, tissue removal and tissue fixation was performed by Dr. Marc Clement

The work within Chapter 8 is based on a collaboration between the groups of Dr. Helle Jorgensen and Dr. Mikhail Spivakov.

- Lina Dobnikar aided in the analysis of sequencing data

Acknowledgments

I would like to thank and acknowledge all those who have contributed to this project:

To Helle, I feel incredibly lucky to have had you as my PhD supervisor. You have been a fantastic mentor these past three years, and have pushed me to work hard and develop skills necessary to be a better scientist. Thank you for investing time in me, for putting up with my doodling throughout our meetings and for your kindness. Most of all, thank you for trusting me to carry out this project in my own way, even after months of me spending almost no time in our lab (particularly in the mornings). I hope, being your first PhD student, you have also learnt something from this experience and will continue to be such a brilliant supervisor to all future students.

To The Jorgensen Group, thank you for being such an engaging group who always have time to discuss life and work, and generally whatever topic I felt necessary to go on about, it has been a pleasure working with you all. In particular, I would like to thank: Jenny, for being there from the start, showing me where to find things in the lab (which I still seem to need help with), and always helping me out in any way you could; and Lina, for guiding me through this new world of single cells and help while writing this thesis.

To everyone within the Division of Cardiovascular Medicine, I should probably start this by saying thank you for the patience you have all shown me during the last three years, for the good times, the lunch breaks, the lessons and the numerous trips to the all you can eat restaurants which has made my time in this lab so enjoyable. Particular thanks to Nikki, Allie, Suzy and Katja, for everything you do which I am clueless of, allowing me to focus on this project.

To my Parents, somehow I made it to Cambridge to do a PhD, and it is because of you both that I did. Thank you for the continual love and support you give me, and for always letting me choose what I wanted to do in life, even if I didn't call home as often as I should.

To Will, Cristina, Anjali and Raya, thank you for help with proof reading this thesis and for being some of the best friends I could ask for.

To the badminton guys, for all the matches and whisky, keep smashing it.

To The GalapaGoGos/Darwin College Band, the best memories I will take away from Cambridge will mainly consist of my time playing music and spending time with you all. Without a doubt you have been my escape from the hard things and the long days.

To Snarky Puppy, out of all the music I have listened to during my PhD, yours has undeniably been the soundtrack to it. Thank for all the countless nights I spent just listening.

To the mice, it was always the hardest part, but without each of you, none of this was possible.

Abstract

Vascular smooth muscle cell (VSMC) accumulation is a hallmark of atherosclerosis and vascular injury. However, fundamental aspects of proliferation and the phenotypic changes within individual VSMCs, which underlie vascular disease remain unresolved. In particular, it is not known if all VSMCs proliferate and display plasticity, or whether individual cells can switch to multiple phenotypes. To assess whether proliferation and plasticity in disease is a general characteristic of VSMCs or a feature of a subset of cells, multi-colour lineage labelling is used to demonstrate that VSMCs in injury-induced neointimal lesions and in atherosclerotic plaques are oligo-clonal, derived from few expanding cells, within mice. Lineage tracing also revealed that the progeny of individual VSMCs contribute to both alpha Smooth muscle actin (aSma)-positive fibrous cap and Mac-3-expressing macrophage-like plaque core cells. Co-staining for phenotypic markers further identified a double-positive aSma+ Mac3+ cell population, which is specific to VSMC-derived plaque cells. In contrast, VSMC-derived cells generating the neointima after vascular injury generally retained expression of VSMC markers and upregulation of Mac3 was less pronounced. Monochromatic regions in atherosclerotic plaques and injury-induced neointima did not contain VSMC-derived cells expressing a different fluorescent reporter protein, suggesting that proliferation-independent VSMC migration does not make a major contribution to VSMC accumulation in vascular disease. Similarly, VSMC proliferation was examined in an Angiotensin II perfusion model of aortic aneurysm in mice, oligo-clonal proliferation was observed in remodelling regions of the vasculature, however phenotypic changes were observed in a large proportion of VSMCs, suggesting that the majority of VSMCs have some potential to modulate their phenotype. To understand the mechanisms behind the inherent VSMC heterogeneity and observed functionality, the single cell transcriptomic techniques Smart-seq2 and the Chromium 10X system were optimized for use on VSMCs. The work within this thesis suggests that extensive proliferation of a low proportion of highly plastic VSMCs results in the observed VSMC accumulation after injury, and the atherosclerotic and aortic aneurysm models of cardiovascular disease.

Contents

List of figures

List of tables

Abbreviations

Abbreviation	Extension
AAA	Abdominal aortic aneurysm
Ang II	Angiotensin II
ApoE	Apolipoprotein E
$ApoE^{-/-}$	$ApoE^{tm1Unc}$
aSMA	α-Smooth Muscle Actin
BAC	Bacterial artificial chromosome
bHLH	Basic helix-loop-helix
BM-MSC	Bone marrow mesenchymal stem cell
BrdU	5-Bromo-2´-Deoxyuridine
BSA	Bovine serum albumin
C+S+	Confetti+ Sca1+
C+S-	Confetti+ Sca1-
C-S+	Confetti- Sca1+
CA	Carotid arteries
CArG	$CC(AT)_6GG$
ChIP	Chromatin immunoprecipitation
CRBP-1	Cellular retinol binding protein 1
CVD	Cardiovascular disease
CFP	Cyan fluorescent protein
DA	Descending aorta
DAPI	4',6-diamidino-2-phenylindole
DMEM	Dulbecco's Modified Eagles Medium
ECs	Endothelial cells
ECM	Extracellular matrix
EdU	5-Ethynyl-2'-deoxyuridine
EMT	Epithelial to mesenchymal transition
EtOH	Ethanol
FACS	Fluorescence-activated cell sorting
FoxO4	Forkhead Box O4
FU	Fluorescent Units
GFP	Green fluorescent protein
H3ac	Histone H3 acetylation
H3K4me2	Histone H3 lysine 4 dimethylation
H3K79me2	Histone H3 lysine 79 dimethylation
H4ac	Histone H4 acetylation
HDAC4	Histone deacetylase 4
Herp2	HES-related repressor protein
HFD	High fat diet
Hox	Homeobox
IEL	Inner elastic lamina
IMH	Intramural haematoma
ISPCR	Universal primers
KLF2	Kruppel-like factor 2
KLF4	Kruppel-like factor 4
LCA	Left Carotid Artery
Ldlr	low density lipoprotein receptor

miRNAs	MicroRNAs
MMPs	Matrix metalloproteinases
MSC	Mesenchymal stem cell
MVSMC	Multipotent Vascular Smooth Muscle Cell
MYH11/ SM-MHC	Smooth muscle-myosin heavy chain 11
NF-κB	Nuclear factor kappa-light-chain-enhancer of activated B cells
NO	Nitric oxide
PBS	Phosphate Buffered Saline
PDGF	Platelet-derived growth factor
PIAS1	Protein inhibitor of activated stat 1
Pol II	RNA polymerase II
Prx1	Paired-related homeobox gene 1
RCA	Right Carotid Artery
RFP	Red fluorescent protein
RRI	Recombinant ribonuclease inhibitor
RT	Room temperature
RT PCR	Reverse transcription PCR
scRNA-seq	Single cell RNA sequencing
Sm22α	Transgelin
SM-MHC	Smooth Muscle-Myosin Heavy Chain
SMC	Smooth muscle cell
SMemb	Smooth muscle myosin heavy chain
SRF	Serum response factor
Stat6	Signal transducers and activators of transcription 6
Tcf21	Transcription Factor 21
TGF-β	Transforming growth factor-β
TIMPs	tissue inhibitors of MMPs
TSO	Template switching oligo
UMI	Unique molecular identifier
VSMC	Vascular smooth muscle cell
WHO	World Health Organisation
YFP	Yellow fluorescent protein

CHAPTER 1: Introduction

In 2015, cardiovascular disease (CVD), was the primary global cause of non-communicable disease death (17.9 million, 95% UI) and morbidity. This figure has risen 12.5% from 2005, however when standardised for age, deaths from CVD fell 15.6%, primarily from the decrease in deaths due to cerebrovascular diseases, such as stroke (Wang et al. 2016). While CVD has, in the past, been a 'Western' problem, this is no longer the case. The number of deaths CVD is responsible for per year is predicted to rise in the next few decades (23.6 million by 2030), with developing countries expecting the largest increase (Mathers and Loncar 2005). Many of the molecular mechanisms underlying CVD are yet to be discovered. The experiments within this thesis attempt to elucidate certain molecular events which take place in the progression of CVD, and improve our understanding of the disease which currently carries a lifetime risk of 60% (Mozaffarian et al. 2015).

1.1 The Cardiovascular system

The cardiovascular system comprises the heart, blood and blood vessels, and permits the delivery of nutrients and oxygen to cells whilst removing CO_2 and other waste products. The arterial component of the cardiovascular system carries blood away from the heart, oxygenated regarding the systemic circulation and deoxygenated regarding the pulmonary circulation. Based on the position in the arterial tree, arteries can be classified as either conducting, conduit or resistance arteries, each characterised by a slightly different compositional structure. Conducting arteries, are the largest within the body and are highly elastic, relative to other arteries, allowing them to deal with highly oscillating blood pressures. The aorta, carotid arteries and pulmonary arteries are examples of conducting arteries (McEniery, Wilkinson, and Avolio 2007). These larger arteries branch into conduit arteries, which function primarily to direct blood flow to different regions of the body, and include the femoral and brachial arteries (Pugsley and Tabrizchi 2000). Conduit arteries branch out to resistance arteries. Highly innervated by sympathetic nerves, resistance arteries form part of the microvasculature which allow arterioles to regulate blood flow by vaso-dilation/constriction (Rhodin 1980).

Arteries typically have thick walls, necessary for coping with high blood pressure, composed of three distinct cellular layers; the adventitia, the media and the intima (**Figure 1**). Each layer is dissimilar in its cellular composition, histology and functionality, and contributes to vascular homeostasis and response to injury in different ways (Stenmark et al. 2013).

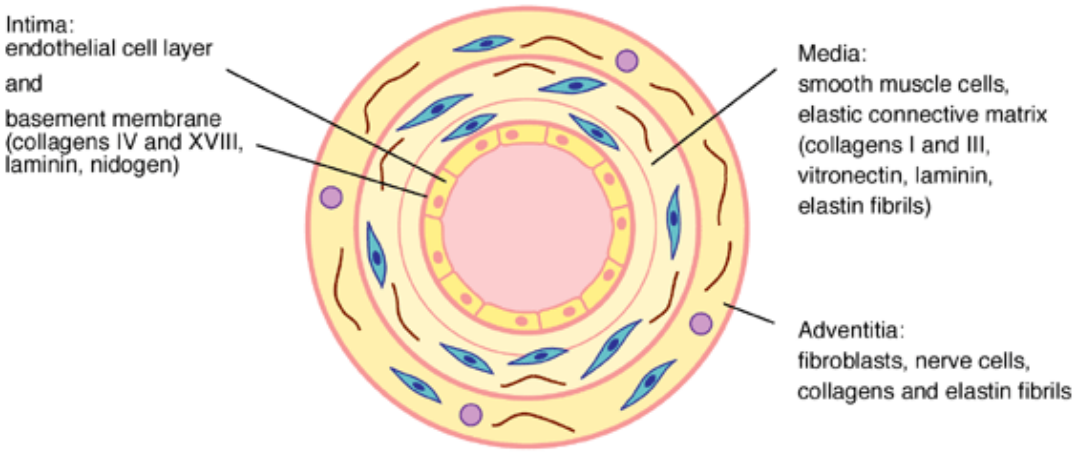

Figure 1: Schematic view of an arterial cross section
The arterial wall has three recognisable layers; the intima, media and adventitia. Each layer has a unique cellular and matrix composition. The intima contains endothelial cells and a basement membrane, this layer acts as the interface between the blood and subsequent layers. The media contains vascular smooth muscle cells (VSMCs), responsible for vascular tone, and extracellular matrix. The adventitia is home to numerous cell types including fibroblast, stem and immune-cells and has roles in trafficking immune cells and signalling molecules across all layers. From: Cambridge Clinical School. Clinical and Biomedical Computing Unit., 1997.

The adventitia is the outer most layer of an artery. Composed of multiple cell types, lymphatic vessels and autonomic nerves, this layer is the most diverse of the three arterial layers. Adventitial fibroblasts and extracellular matrix (ECM) act to protect and anchor blood vessels in place while resident macrophage, T, B, mast and dendritic cells are involved in immune response (Galkina et al. 2006; Tieu et al. 2009; Swedenborg, Mayranpaa, and Kovanen 2011). Recently, the adventitia has been recognised as a stem/progenitor cell compartment, containing cells positive for Sca1+, c-kit, CD34 and Flk1, which has been proposed to maintain the intimal and medial cellular compartments, possibly in response to arterial injury (Zengin et al. 2006; Hu et al. 2004; Majesky et al. 2011). Furthermore, as the adventitia is the site where micro-vessels (e.g. vasa vasorum in the aorta) penetrate it has an important role in supplying nutrients to subsequent layers, trafficking immune/inflammatory cells and mediating communication between the three layers (Gutterman, 1999; Haurani et al., 2007). There is evidence that the adventitia activates early in CVDs, such as atherosclerosis, with the proliferation of fibroblast cells, increased NADPH oxidase production of superoxide and expansion of the vasa vasorum, driving the delivery of inflammatory signals/ immune cells to subsequent layers (Stenmark et al. 2013; Dourron et al. 2004; Ogeng'o et al. 2014). Further, confirmed and theorised, roles of the adventitia in CVD will be discussed in **section 1.5**.

The intima is the innermost layer of the vessel wall. In mice the intima is composed of a single cell thick layer of endothelial cells (ECs) on top of a basal and elastic lamina, within humans the intima also contains vascular smooth muscle cells (VSMCs). Acting as the interface and barrier between the blood

and the vessel wall, these cells play a critical role in responding to environmental stimuli and maintaining tissue homeostasis. ECs can metabolise and synthesise a range of molecules responsible for auto and paracrine effects on the surrounding tissue (Cines et al. 1998), and serves as a semi-permeable barrier to regulate the transfer of small and large molecules (Galley and Webster 2004). Importantly the endothelium maintains a protective, non-thrombogenic interface between tissue and blood, regulating platelet adherence, thrombosis, blood flow and vascular tone. Endothelial dysfunction, often characterised by a reduced production of bio-available nitric oxide (NO), is regarded as a key early step in the progression of many diseases, including atherosclerosis, and pulmonary and systemic hypertension (Kinlay and Ganz 1997; Galley and Webster 2004).

The media, or middle layer of an artery, is the thickest of the three arterial layers and is characterised by the presence of concentric layers of VSMCs and the ECM components: elastin, collagen type I and III and proteoglycans. VSMCs are arranged circumferentially around the media separated by elastic fibres, this highly ordered matrix provides structural integrity to the vasculature and enables VSMCs to carry out their primary function of contraction. The number of concentric layers is variable throughout the vasculature, and while the mechanisms determining number of VSMC layers is still unknown, luminal diameter is a primary determining factor (Wolinsky and Glagov 1967; Pfaltzgraff and Bader 2015). Manipulating animal size or matrix composition does not change the number of layers in a region (Dilley and Schwartz 1989), with studies suggesting that other compensatory mechanisms can cope with the increases in vascular demand (Dilley and Schwartz 1989; Faury et al. 2003). Medial thickening is, instead, regarded as a characteristic of CVD (Grobbee and Bots 1994). The medial layer's involvement, and in particular, VSMC involvement in CVD will be a focus of this thesis.

1.2 Vascular development and VSMC origins

De novo vascular networks are laid down via the process of vasculogenesis, first occurring within the yolk sac of mammalian embryos and later within the actual embryo. This process is driven, firstly, by the recruitment of epiblast cells through the primitive streak, where they undergo epithelial to mesenchymal transition (EMT), and subsequently form mesoderm (Tam and Behringer 1997). Endothelial precursors, derived, mainly, from the splanchnic mesoderm, accumulate in networks which will define the earliest vasculature (Bellairs and Osmond 2009). These early endothelial tracks are then refined via angiogenesis/vascular remodelling and subsequent recruitment of VSMC pre-cursor cells (Yao et al. 2014).

Both platelet-derived growth factor (PDGF)-B and transforming growth factor-β (TGF-β), are important chemoattractants responsible for recruiting and differentiating VSMC pre-cursor cells (Yao et al 2014). Other signalling pathways responsible for recruiting VSMC progenitor cells can differ throughout the vasculature, as does the origin of these cells. **Figure 2** shows which embryonic cell population VSMCs are derived from and their position within the vasculature (Wang et al. 2015).

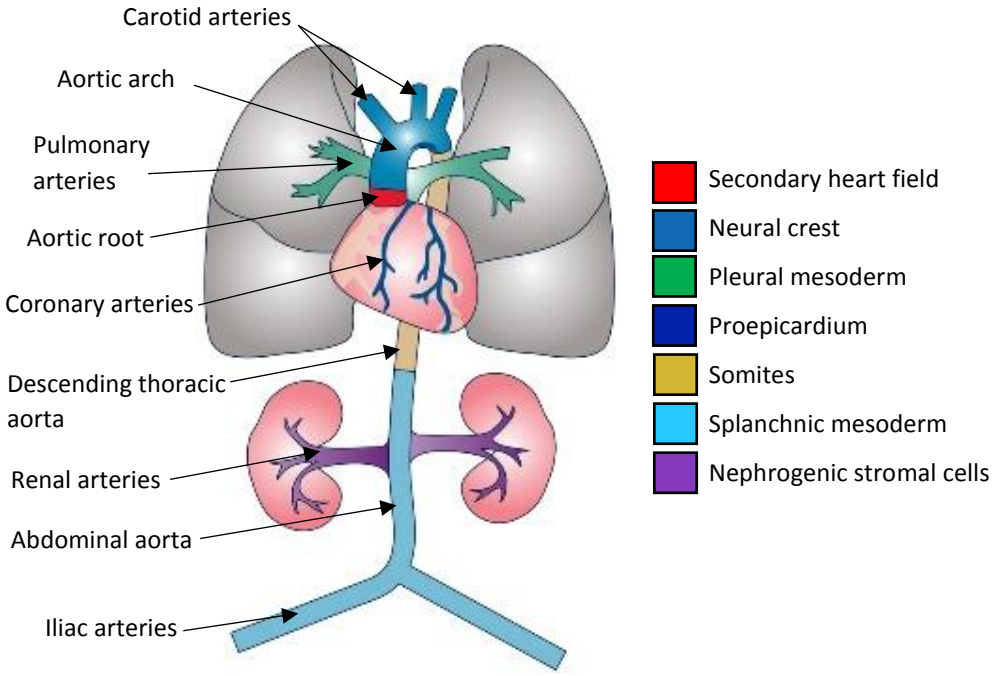

Figure 2: Developmental fate map for VSMCs
VSMC are derived from various embryological origins, the coloured vasculature relates to the origin depicted in the key. Adapted from Wang et al., 2015.

Using a Wnt1-Cre driven recombination of the LacZ reporter system in mice, Jiang et al. (2000) were able to show that the carotid arteries and aortic arch VSMCs are derived from the neural crest, a structure present in early embryo as a strip of cells between the neural and non-neural ectoderm (Jiang et al. 2000; Mayor and Theveneau 2013). As embryogenesis proceeds neural crest cells contribute to various mesenchymal structures, including craniofacial bone/cartilage, VSMCs and melanocytes, however the mechanisms underlying the contribution of neural crest-derived VSMCs to the aortic arch and carotid arteries is not fully understood (Wang et al. 2015). VSMCs in the descending thoracic aorta are derived from the somites, itself derived from the paraxial mesoderm, these structures are transient and contribute to the development of organs and tissues including the vertebrae, ribs and back muscles (Sato 2013). Based on Quail-chick chimera analysis, the sclerotome, part of the somite responsible for giving rise to bone/skeletal tissue, has been shown to be the exact cellular location which contributes the majority of VMCS to the descending thoracic aorta (Pouget, Pottin, and Jaffredo 2008). Interestingly each somite seems to contribute to descending aortic VSMCs

in a segmented way so that VSMC progenitors from each somite are restricted to specific local domains (Majesky 2007).

Several studies suggest that the embryonic origin of VSMCs affects their underlying biology, regarding gene expression (Zhang et al. 2012) and predisposition to disease (Haimovici and Maier 1971). Diseases such as atherosclerosis and aortic aneurysm typically locate to specific locations in the vasculature (discussed in **sections 1.4 and 1.9**, respectively), which could potentially be, in part, due to the embryonic origins of the VSMCS within these regions (Ruddy et al. 2008; DeBakey, Lawrie, and Glaeser 1985; Sinha, Iyer, and Granata 2014). For example, the normally atherosclerotic resistant thoracic aorta in a mouse model of atherosclerosis has a higher expression of Homeobox (Hox) genes compared to the atherosclerotic-prone aortic arch. The inverse relationship between Hox9a and nuclear factor kappa-light-chain-enhancer of activated B cells (NF-κB) expression (Trigueros-Motos et al. 2013) provides a possible disease regulatory processes founded in embryological origin (Bennett, Sinha, and Owens 2016). Congenital defects also occur at the boundaries where VSMCs from different embryonic origins meet, for example, coarctation and interruption of the aortic arch (Jacobs et al. 1995; Tanous, Benson, and Horlick 2009). However, the extent to how VSMCs in different vascular beds differ, the underlying mechanisms for these differences and the consequences of these differences are still not fully understood, requiring further inquiry (Pfaltzgraff and Bader 2015).

Differentiating, embryonic VSMCs are highly proliferative and migratory and secrete a large amount of ECM proteins vital for angiogenesis (Shang et al. 2008). Following the recruitment of VSMC pre-cursor cells to the developing vasculature they encircle the vessel and differentiate into mature VSMCs, this initial patterning occurs rapidly and is later remodelled through angiogenesis once the heart begins to beat and perfuse the vessels with blood (Blatnik, Schmid-Schönbein, and Sung 2005; Chen and Tzima 2009). Indeed, as will be discussed (**sections 1.4 and 1.5**), hemodynamic forces serve as a potent force in remodelling the vasculature.

1.3 VSMC function and heterogeneity

The primary purpose of mature, differentiated, VSMCs is to maintain tone of blood vessels and regulate blood flow through vaso-constriction/dilation of resistance arterioles, thus ensuring intravascular pressure and tissue perfusion is maintained (Stegemann, Hong, and Nerem 2005). VSMCs, therefore have characteristics which make them suitable for this role. Morphologically, they are elongated in shape, aligned in an organised structure with surrounding VSMCs. Biochemically, they

can be characterised by their expression of particular calcium handling proteins, ion channels, cell surface receptors and contractile proteins, most notably: α-smooth muscle actin (aSMA), smooth muscle-myosin heavy chain 11 (MYH11/SM-MHC), Transgelin (SM22α) and Smoothelin (Rensen, Doevendans, and van Eys 2007). Healthy, mature VSMCs are quiescent and divide with a half-life ranging from 270 – 400 days (Neese et al. 2002).

However, this description is an over simplification of the mature VSMC phenotype, in reality this is one phenotype at the extreme end of a spectrum. As discussed above, during vasculogenesis, a VSMCs primary act is that of proliferation and ECM synthesis, required to build the vascular wall. This phenotype can here be considered the other end of the spectrum on which VSMCs lie (Pfaltzgraff and Bader 2015). The VSMC spectrum ranges from the 'contractile' phenotype to the 'synthetic' phenotype. Synthetic VSMCs are epithelioid or rhomboid in shape and contain a higher number of organelles, necessary for protein synthesis, replacing the contractile filaments found in contractile VSMCs. Furthermore, synthetic VSMCs are more proliferative and migratory than their contractile counter parts (Hao, Gabbiani, and Bochaton-Piallat 2003). Gene expression also differs along the spectrum, with synthetic VSMCs expressing higher levels of certain matrix metalloproteinases (MMPs) and collagens, the embryonic smooth muscle myosin heavy chain (SMemb) protein and cellular retinol binding protein 1 (CRBP-1). Lower levels of contractile markers such as Myh11 and Smoothelin also typically accompany this phenotype (Rensen, Doevendans, and van Eys 2007).

What is remarkable about VSMCs, and unique when compared to cardiac and skeletal muscle, is that they are not terminally differentiated and retain a large degree of plasticity, able to move along the spectrum of phenotypes and, as will be discussed later, even trans-differentiate into other cells types (**section 1.5**). The process by which VSMCs can change their phenotype is known as phenotypic modulation/switching, and can be induced by a variety of environmental stimuli. Typically, this process is studied in the direction of contractile to synthetic, and is vital in allowing a rapid response to vascular injury and fluctuating environments, permitting remodelling and re-vascularisation (Alexander and Owens 2012).

Morphological differences between synthetic and contractile VSMCs were first recognised when cultured and in vivo VSMCs were compared (**Figure 3A**). Initially, studies examined visceral smooth muscle cells (SMCs), which when cultured lose myofilaments and gain organelles, including golgi apparatus, rough endoplasmic reticulum and mitochondria (Campbell et al. 1971; Rensen, Doevendans, and van Eys 2007). Moreover, when primary SMCs are seeded at a high density and via

proliferation become confluent they begin to form an organised structure/pattern initially described as “hills and valleys”. After an additional few days of culture, these SMCs return to their original spindle shape, regain their myofilaments and begin to contract. This work concludes that SMCs not only have the potential to phenotypically switch, but that this ‘switch’ is reversible. Interestingly, if the cultured primary SMCs are seeded sparsely, by the time they reach confluency they seem unable to revert to their original phenotype (Campbell et al. 1971). Further work confirmed that the ability to reverse to a contractile state is dependent on the number of cell doubling events (<5 doublings/cells = reversible, >9 doublings/cells = irreversible (Chamley-Campbell and Campbell 1981)).

Phenotypic heterogeneity of VSMCs is also observed in vivo in healthy tissue, immunohistochemistry has shown differential expression of VSMC contractile markers, as well as adhesion molecules and gap junctional proteins, between adjacent VSMCs (Christen et al. 2001; Frid, Moiseeva, and Stenmark 1994; Moiseeva 2001). Distinct VSMC populations, within the same artery, have been seen in rats (Bochaton-Piallat et al. 1996), pigs (Christen et al. 2001; Hao et al. 2002) and in humans (Li et al. 2001), phenotypes of which remain distinctive in vitro. Furthermore, these VSMC populations react differently to similar culture conditions, and can be differentially coaxed to adopt a synthetic or contractile state by varying the culture conditions (Li et al. 1999; Hao et al. 2002). Based on these studies, Rensen et al. (2007) propose a hypothetical phenotypic spectrum occupied by multiple VSMCs populations, each with distinct characteristics and phenotypic switching potential (**Figure 3B**). Furthermore, Rensen et al. (2007) suggest, that there is likely an epigenetic foundation for the observed VSMC heterogeneity, through which the environment can act on to regulate phenotypic switching.

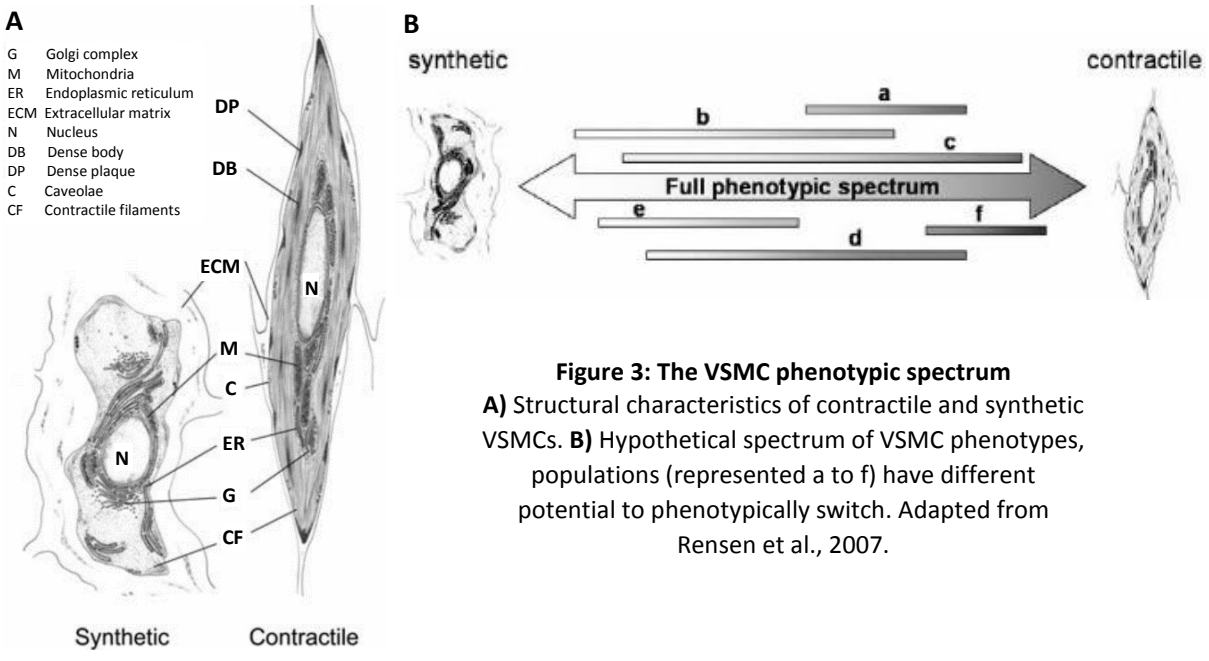

Figure 3: The VSMC phenotypic spectrum
A) Structural characteristics of contractile and synthetic VSMCs. **B)** Hypothetical spectrum of VSMC phenotypes, populations (represented a to f) have different potential to phenotypically switch. Adapted from Rensen et al., 2007.

The plasticity of VSMCs has likely evolved, as the ability for VSMCs to phenotypically switch to a synthetic phenotype and participate in vascular repair has conferred a survival advantage. However, a consequence of this plasticity is that VSMCs can be exposed to environmental stimuli which contribute to adverse/dysregulated phenotypic switching, which, in turn, contributes to the progression/development of vascular disease (Owens, Kumar, and Wamhoff 2004). Indeed, hyper-proliferation of VSMCs is integral in the formation of atherosclerotic plaques (Sherif and Zahradka 2010).

1.4 Cardiovascular disease: Atherosclerosis

CVD encompasses an array of diseases affecting the heart and/or blood vessels, including, among others; ischaemic heart disease, stroke, cardiomyopathy and aortic aneurysm. Of the 15.6 million deaths relating to CVD in 2015, 85.1% were attributable to ischaemia and stroke. These diseases are the clinical manifestation of atherosclerosis, a chronic inflammatory condition, which locates to the arterial wall. Atherosclerosis is typically characterised by the accumulation of lipids, inflammatory molecules, immune cells and VSMCs, resulting in the formation of an atherosclerotic plaque. Plaque rupture, and subsequent flow limiting stenosis, results in the aforementioned diseases. (Newman et al., 1986; Virmani et al., 1987; PDAY research Group, 1990).

Atherosclerosis often begins early in life and remains asymptomatic for several decades. The initiating factor for atherogenesis is typically vascular injury or dysfunction of ECs. Proposed causes are oscillating shear forces (from blood flow) caused by hypertension, increased low-density and decreased high density plasma lipoproteins, increased toxin levels in the blood (e.g. from smoking) and diabetes (Fuster 1994; Ross 1999; Zaman et al. 2000). The development and progression of atherosclerotic plaques (**Figure 4**) has been proposed to occur in five main steps: 1) Endothelial dysfunction and sub-endothelial accumulation of low-density lipoproteins. 2) Infiltration of leukocytes and subsequent formation of foam cells. 3) VSMC proliferation and trans-differentiation. 4) Production of connective tissue. 5) Plaque stabilisation or erosion/rupture leading to symptomatic complications (Tedgui and Mallat, 2006). However, plaque development is not necessarily orderly, neither does it always follow the linear classification system of plaques (type I to VI) defined by The American Heart Association Committee (Stary et al., 1995).

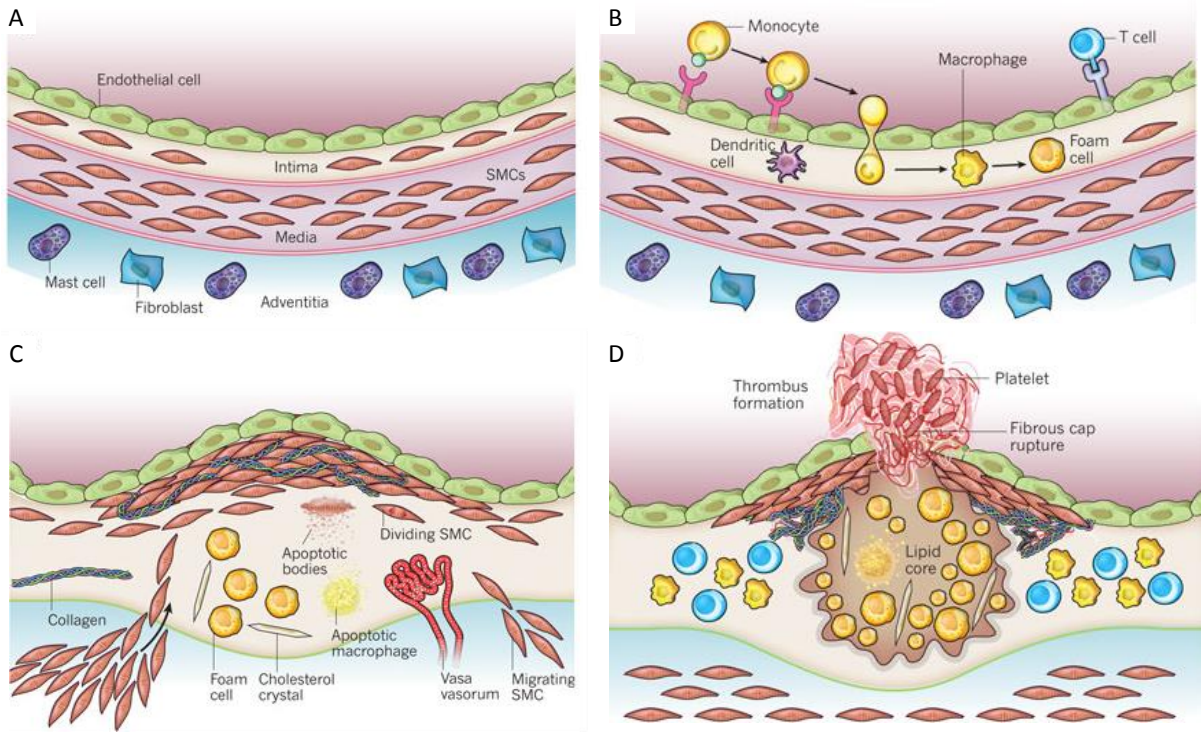

Figure 4: A schematic view of atherosclerotic plaque development

A) Cross section of the wall of healthy vasculature. **B)** The initial steps of atherosclerosis. Blood circulating immune cells bind ECs, leukocytes infiltrate the sub-endothelial space and monocytes mature to macrophages and uptake lipids to form foam cells. **C)** VSMCs infiltrate the intima, a proportion of these cells become foam cells within the core of the plaque, and those which locate to the cap produce collagen and elastin, forming a mature plaque. **D)** Rupture of the atherosclerotic plaque and subsequent thrombus formation due to the coagulation of blood components. The resulting thrombus can occlude an artery, limiting blood flow. From Libby et al., 2011.

Atherosclerotic plaques develop in a spatially non-random and temporally non-linear process, and typically affects athero-prone regions of the vasculature (Tabas et al., 2015). Lesion prone areas are often found where the vasculature experiences oscillatory shear blood flow compared to the relatively uniform high-pressure flow experienced within 'athero-protected' regions (Chiu and Chien, 2011). **Figure 5A** shows that it is typically bifurcating and bending regions of the vasculature which develop atherosclerosis. Within athero-protective regions, ECs (as described in **section 1.1**) are exposed to steady laminar flow which activates signal transduction promoting EC production of NO, Kruppel-Like Factor 2 (KLF2) and superoxide dismutase, which actively prevents atherogenesis (Cai and Harrison, 2000; De Caterina et al., 1995; Dekker et al., 2005; Dimmeler et al., 1999). Within athero-prone regions, ECs display characteristics typical of a dysfunctional, pro-inflammatory and pro-thrombotic phenotype. Athero-prone ECs prime the NF-kB signalling pathway which is further amplified by accumulating lipoproteins, causing the influx of monocytes into the neo-intima and subsequent activation of VSMC phenotypic switching (**Figure 5B**, Chiu and Chien, 2011). This activation of VSMCs

(**Figure 4C**) is perhaps the most interesting aspect in the progression of this disease, particularly in the context of this thesis. Concerning the migration, proliferation, trans-differentiation and synthetic capacity of VSMCs in atherosclerotic plaques, this stage (**Figure 4 C**) is often regarded as the transitional point whereby what was once just a site of accumulating macrophage derived foam cells becomes a fibrous lesion containing a lipid core, with future symptomatic prospects (Kolodgie et al., 2007).

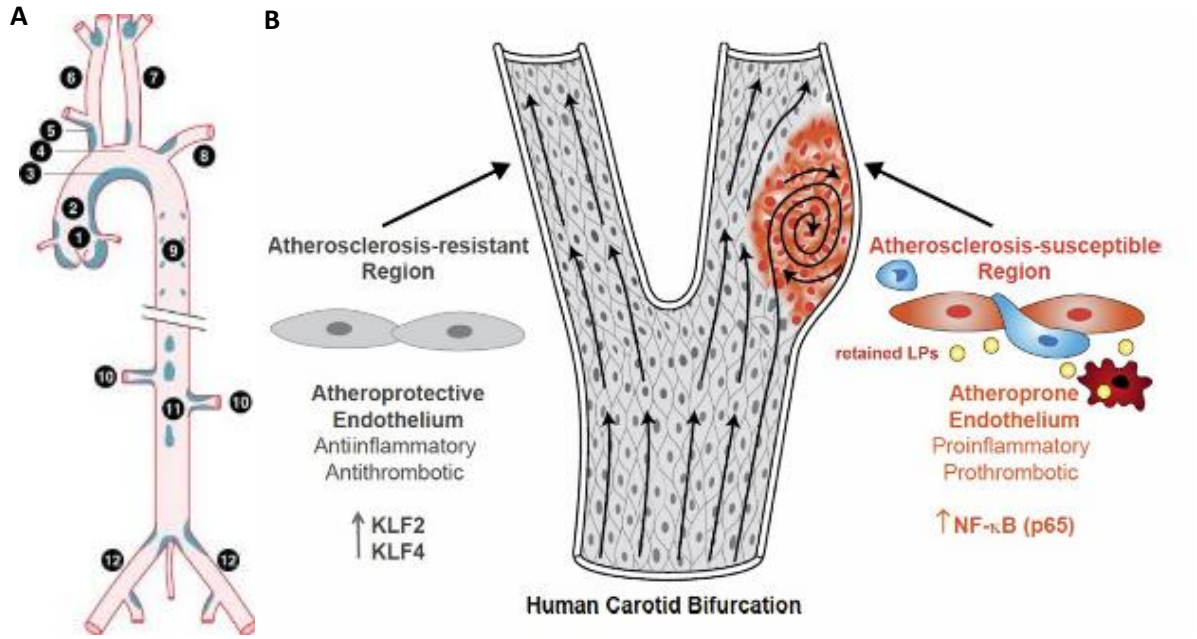

Figure 5: Atherosclerotic plaques preferentially develop at sites of arterial branching and curvature
A) Schematic of the major arterial vasculature illustrating the observed distribution of atherosclerotic plaques. 1, Aortic sinus; 2, ascending aorta; 3, inner (lesser) curvature of aortic arch; 4, outer (greater) curvature of aortic arch; 5, innominate artery; 6, right carotid artery; 7, left carotid artery; 8, left subclavian artery; 9, thoracic aorta; 10, renal arteries; 11, abdominal aorta; 12, iliac artery (adapted by Chiu and Chien, 2011; originally VanderLaan et al., 2004). **B**) Oscillatory sheer stress and pressure gradients promote EC dysfunction, NF-κB signalling and inflammation. Adapted from Tabas et al., 2015.

1.5 VSMCs in atherosclerosis - Origin and plasticity

VSMC contribution to atherosclerosis has been studied in a variety of disease models in rats and mice (several of which will be discussed in detail in **sections 2.2 and 2.3**) as well as in samples from humans. The models mentioned in this section fall into two categories, (1) injury-induced models of neo-intimal growth, in which animals undergo surgery (wire-injury, balloon-injury, carotid ligation) to cause a growth in the number of cells within the intima (neo-intima); and (2) diet-induced models of atherosclerosis, which involve feeding a high fat diet (HFD) to mice on either a low density lipoprotein

receptor (Ldlr) or Apolipoprotein E (ApoE) knockout background, resulting in atherosclerotic plaque development.

The extent to which phenotypic modulation of fully differentiated VSMCs contribute to the development and overall proportion of an atherosclerotic plaque and the extent to which they can trans-differentiate, contributing to other cell types, has been hotly debated in recent years. Initially this debate was confounded by the fact that downregulation and non-specificity of VSMC contractile markers made it difficult to definitively identify VSMC-derived cells after phenotypic switching (Gomez and Owens, 2012). Several papers claimed that the majority of cells forming the plaque/neointima, which were positive for several VSMC markers, may be of adventitial (Hu et al., 2004) or myeloid origin (Sata et al., 2002). However, these claims were later refuted, Iwata et al. (2010) and Benzton et al. (2007) showed that while bone marrow-derived cells contribute to vascular inflammation they do not differentiate into VSMC lineages in models of injury induced neo-intima growth or atherosclerosis. Nemenoff et al. (2011) were the first to use a specific marker of VSMCs for lineage tracing purposes following vascular injury. Utilising mice harbouring the Myh11-CreER(T2) transgene and Rosa26-floxStop/βGal reporter they tracked VSMCs following femoral artery wire-injury in mice. The Myh11-CreER(T2) transgene here recombines the Rosa-26floxStop/βGal allele following tamoxifen administration allowing specific labelling of VSMCs. This study identified that VSMC-derived cells accumulate in the neo-intima, furthermore no bone marrow-derived VSMCs were detected.

Contrastingly, in 2012, Tang et al. claimed that mature VSMCs were not capable of phenotypically switching and do not contribute to the development of neointima/atherosclerotic plaques (i.e. they are terminally differentiated). They suggested an alternative, a pre-cursor/stem cell population of multipotent VSMCs (MVSMCs) which exist in the media and are responsible for VSMC-like cells seen in disease/injured tissue. To substantiate this claim, Tang et al. (2012) first show that these MVSMCs exists within the media in rats, are negative for Sm-mhc (Myh11) and express the stem cell markers Sox17, Sox10 and S100β when cultured. They further suggest that neointimal VSMCs following a wire-injury model are derived from these MVSMCs, instead of mature, Myh11 expressing, VSMCs. This statement, however, is not definitively backed by experimental evidence, but is based on the following observations: (1) no injury-induced, neointimal cells were GFP+ following lineage tracing using the Myh11-Cre; Rosa26-loxP-GFP mouse suggesting that Myh11-expressing cells do not contribute. And (2), most cells within the neointima and surrounding media express S100β, which MVSMCs also express. However, neither of these results definitively lineage trace MVSMCs and therefore cannot determine their involvement. Furthermore, the methods utilised by Tang et al., (2012) were highly criticised in a paper co-authored by many experts within the field (Nguyen et al., 2013), in particular

their use of a non-conditional lineage tracing system, and therefore the inability to rigorously label mature VSMCs at a given time point. It was also suggested that their model of injury was so severe that it killed all GFP+ VSMCs within the media. This work lead to definitive experiments to answer questions regarding VSMC involvement and trans-differentiation in atherosclerosis.

Gomez et al. (2013) were the first to use the inducible Myh11-CreER(T2); Rosa26-STOP-floxedYFP; ApoE$^{-/-}$ mice to show that in a model of atherosclerosis, induced by HFD, that VSMC-derived cells contributed to large regions of an atherosclerotic plaque. Furthermore, they show that >95% of these cells are unidentifiable as VSMCs using conventional immuno-staining for VSMCs (aSma and Myh11), suggesting they have phenotypically modulated. Herring et al. (2014) confirmed the study of Nemenoff et al. (2011), using Myh11-CreER(T2)/R26R-mTmG mice, in the carotid ligation injury model as opposed to the femoral wire injury model. The mTmG reporter gene marks all cells with mTomato prior to tamoxifen administration and specifically marks Myh11-expressing cells irreversibly with mEGFP post tamoxifen-induced Cre-mediated recombination. Tamoxifen injected mice then underwent carotid ligation surgery. Most cells (79 ± 17%) within the neo-intima were mEGFP positive, and were therefore the progeny of Myh11-expressing, differentiated VSMCs prior to injury. Inter-mouse variability in the proportion of VSMC derived neo-intimal cells in the carotid ligation (5-70%) and femoral injury wire injury (0-85%) models has since been reported (Yang et al., 2015).

To investigate the extent to which VSMCs phenotypically switch/trans-differentiate, Shankman et al. (2015) also utilised the Myh11-CreER(T2); Rosa26-STOP-floxedYFP; ApoE$^{-/-}$ mice on HFD to lineage trace VSMCs in a model of atherosclerosis. And combined with immunohistochemistry showed that a large proportion of cells and cell types within mature atherosclerotic lesions were VSMC derived. Shankman et al. (2015) quantify that 30% of VSMC-derived cells had trans-differentiated into macrophage-like (express LGALS3), 12% into myofibroblast-like (express aSMA and PDGF-B), 7% into mesenchymal stem cell (MSC)-like (express SCA1) and 32-51% into an indeterminate like – cell type. Furthermore, 36% of the total macrophage marker LGALS3^{+} cells within the lesion were of VSMC origin, a proportion of which were lipid laden, suggesting that VSMC-derived macrophage-like cells do indeed take on some phagocytic properties. However, in vitro experiments showed that VSMC-derived MSC-like cells could not differentiate into osteoblasts and adipocytes and therefore do not take on the multipotent properties of true MSCs. VSMCs that locate to the outer most region or cap of the plaque express contractile markers (aSMA), resembling a typical VSMC seen in healthy vasculature (Shankman et al., 2015).

The studies discussed here clearly demonstrate that a large proportion of an atherosclerotic plaque is VSMC-derived and that VSMCs can trans-differentiate into multiple like-cell types. A major limitation of these lineage tracing systems is that they require the use of genetically modified organisms and cannot be performed in the same way in humans. To address this, Shankman et al. (2015) used an in situ hybridization proximity ligation assay (developed by Gomez et al., 2013), to trace cells positive for Histone H3 lysine 4 dimethylation (H3K4me2) within the *MYH11* locus. Only VSMCs express this epigenetic mark at this locus, and it is retained in trans-differentiated VSMCs. This work showed that VSMCs can transition to macrophage-like cells within lesions from human samples. Combined these works shows that VSMCs can trans-differentiate into multiple cell types, some of which preferentially locate to distinct regions of an atherosclerotic plaque (**Figure 6**). What in unknown, however, is whether individual VSMCs can generate phenotypically distinct VSMC-derived cells (i.e. multipotent) or if these cells originate from different unipotent VSMCs[1].

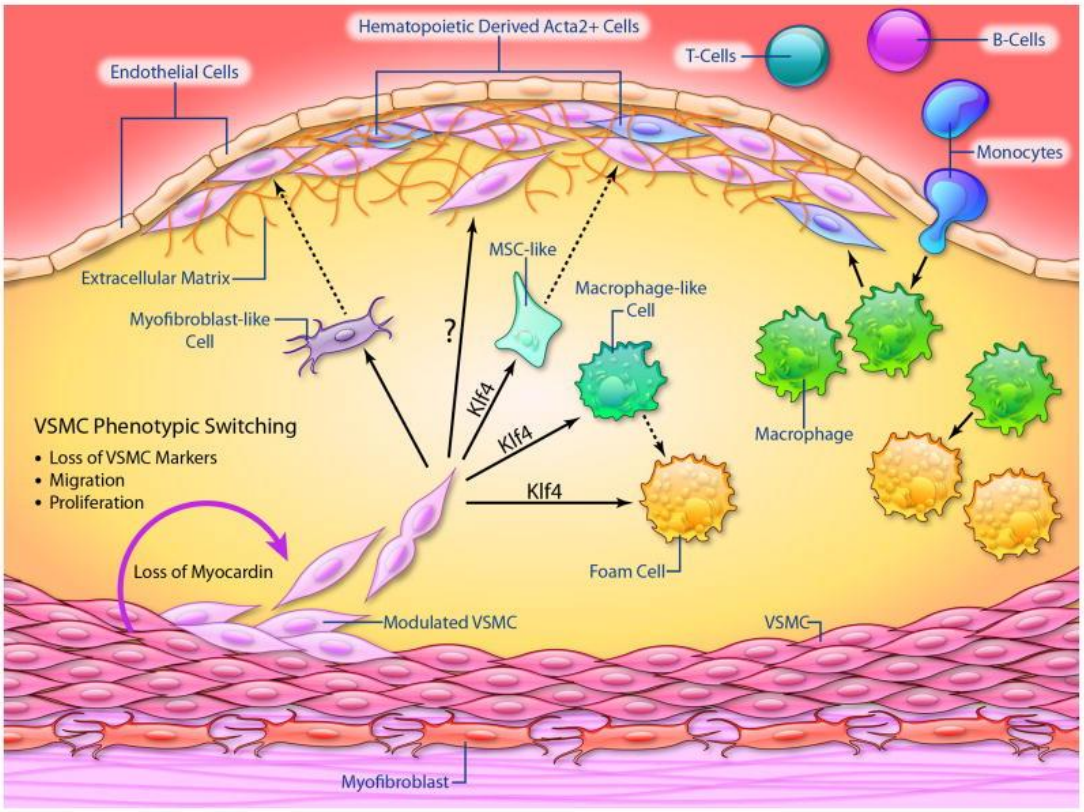

Figure 6: Schematic of an atherosclerotic plaque and origin of plaque cells
VSMCs retain a large degree of plasticity and undergo phenotypic switching to multiple distinct phenotypes within atherosclerotic lesions. VSMCs within the core of the plaque take on properties of macrophage and stem cells while those which locate to the cap resemble a contractile VSMC. From Bennett, Sinha, and Owens, 2016.

[1] Thesis aim 1: Determine if phenotypically distinct VSMC-derived plaque cells are generated from single (multi-potent) VSMCs or if distinct VSMCs produce a single or subset of these (uni/oligo-potent)

However, the origin of all cells (positive or negative for VSMC markers) within a plaque/arterial disease is still currently under intense investigation. Kramann et al. (2016), show that in a wire-injury model of the femoral artery, that a large proportion of aSma+ cells within the neo-intima are derived from Gli1+ MSC-like adventitial cells. Furthermore, they show that Gli1+ adventitial cells can migrate into an atherosclerotic plaque, within the kidney vasculature of animals with chronic kidney disease, and contribute to osteoblast-like cells which in-turn contribute to vascular/plaque calcification (Kramann et al. 2015). They further suggest, but do not definitively show that these cells go through an intermediate VSMC stage before trans-differentiation into the osteoblast-like cells. Nurnberg et al., (2015) identified that medial and adventitial cells expressing Transcription factor 21 (Tcf21) prior to injury, migrate and give rise to VSMC marker-positive cells within the cap and subcapsular regions of late stage plaques. Typically, few cells within the media express Tcf21 and there is minimal overlap with VSMC markers (aSma). Other studies have re-visited the idea of myeloid derived-VSMCs, using a LysM-Cre, Albarrán-Juárez et al. (2016) suggests that up to 30% of all aSma+ cells within atherosclerotic plaque have a myeloid origin. This Cre is however constitutively active, therefore VSMC-derived cells which induce LysM expression will be labelled in this model. The same study, using the Myh11-CreER(T2) transgene did indeed find that a large proportion of plaque cells are VSMC derived, including 16% of CD68+ cells (Albarrán-Juárez et al. 2016).

Other groups have focused on Sca1+ adventitial cells, showing that they are capable of dedifferentiating into VSMCs in response to PDGF-B in vitro (Hu et al. 2004). Furthermore, when adventitial Sca1+ cells are transferred to the adventitial side of a vein graft they can be lineage traced to the neointima of an atherosclerotic plaque in $ApoE^{-/-}$ mice (Hu et al. 2004) and neointima of wire-injured mice arteries (Yu et al. 2016). Yu et al. (2016) further suggest that it is the release of chemokines CCL2 and CXCL1 from pre-existing VSMCs which drives this migration of Sca1 adventitial cells, where they then dedifferentiate into VSMCs. Others have even suggested that there exists a VSMCs progenitor population of Sca1+ cells within the media (based on flow cytometry analysis), which can differentiate into VSMCs in vitro (Sainz et al., 2006).

Finally, the Song group, that previously identified Sox10+ MVSMCS as VSMC progenitors (Tang et al., 2012) performed experiments which suggests the existence of two types of neointima following carotid ligation or wire-injury methods (Yuan et al., 2017). Type I is VSMC-derived, based on lineage tracing using a Myh11-Cre; Rosa-loxP-RFP mouse. Type II is not VSMC-derived and is possibly derived from $Sox10^{+}$ vascular stem cells. However, this is not definitively shown as specific lineage tracing is not used. Indeed, much of the work investigating potential progenitor cells rely on immuno-

staining/use markers which do no clearly define the origins of the cell type nor exclude VSMCs as a pre-cursor. Unfortunately, many of the proposed adventitial stem cell-precursor-cells lack cell specific markers to use for lineage tracing (Bennett, Sinha, and Owens 2016).

Considering the work discussed here it seems there is still a degree of debate surrounding the origin of VSMC-like cells within the plaque. While mature VSMCs seem capable of trans-differentiation and migration in to neointima/atherosclerotic plaques in some studies, they may not be the only source from which plaque VSMC-like cells are derived. Furthermore, given the known heterogeneity of VSMCs (**section 1.3**) it is not known whether all VSMCs have the potential to contribute to plaque growth or if only a proportion of VSMCs are capable[2].

1.6 VSMCs in atherosclerosis - The clonality hypothesis

In 1973, Benditt and Benditt proposed that VSMCs within atherosclerotic plaques may be mono-clonally derived, this was based on a study of X-inactivation patterns of the X-linked glucose-6-phosphate dehydrogenase protein in female humans (Benditt and Benditt, 1973). Their study revealed that the majority of atherosclerotic plaques, including plaques exceeding a diameter of >0.5 cm, predominately contained one of the protein isotypes, while relatively small patches of healthy media (<0.1 mm^3) contained both isotypes (Benditt and Benditt, 1973). However, this notion came under scrutiny when more sensitive methods to measure X-inactivated genes found large medial patches expressing the same X-inactivation pattern (Schwartz and Murry, 1998), suggesting that plaques would, inevitably, have the same inactivated X-chromosome. Furthermore, as has been discussed (**section 1.2**) VSMCs within distinct regions of the vasculature have different embryological origins, the ascending aorta, arch and carotid arteries derive from the neural crest, the descending aorta from the somites, the aortic root from the lateral plate mesoderm and the coronary arteries from the proepicardium (Majesky, 2007; Wasteson et al., 2008; Jiang et al., 2000). As X-inactivation occurs prior to gastrulation (Rastan, 1982) all cells within each region would therefore be expected to share the same inactivated X-chromosome (i.e. local proliferation of VSMC progenitors sharing the same inactivation pattern build the vessel wall), which also explains why this would be the case for a plaque.

Feil et al. (2014), have more recently, suggested that VSMC-derived macrophages and indeed the entire plaque is clonally derived. The mice in this study contained the multi-colour R26R-Confetti

[2] Thesis aim 2: Determine the proportion of VSMCs which respond in vascular disease/ injury

reporter (discussed in **section 2.1**) and the inducible Sm22α Cre recombinase. While this study does not definitively confirm clonality, due to various limitation discussed later (**section 5.2**), if shown to be true would imply that a single VSMC can differentiate into multiple distinct cell types known to occupy the plaque[3]. It would also raise questions concerning the proliferative potential of all VSMCs and whether the underlying heterogeneity of this population has functional consequences.

1.7 VSMCs in atherosclerosis - Proliferation and migration

The ability of VSMCs to cross the elastic lamina and enter the intima and contribute to plaque development relies on the upregulation of ECM degrading MMPs released by multiple cell types including VSMCs (Newby, 2006). It is not fully understood whether phenotypically switched cells preferentially activate proliferative or migratory responses in turn or simultaneously (Sherif and Zahradka, 2010). Zahradka et al. (2004) suggest that migration of VSMCs into the neo-intima can take place independently of VSMC proliferation, as inhibiting DNA synthesis did not inhibit migration in cell culture or neointimal formation in a porcine organ culture system. However, blocking migration, through inhibition of MMPs, did inhibit neo-intimal formation in this system. De Donatis et al. (2008), identified a PDGF gradient-dependant, differential response, in fibroblast cells, with low PDGF concentration activating migration and high PDGF concentrations activating proliferation without migration. Although this has not yet been confirmed within VSMCs, PDGF is key in inducing both proliferation and migration in VSMCs (De Donatis et al., 2008). Sherif and Zahradka (2010) suggest that the known release of cyclin-dependant kinase inhibitors post vascular injury which prevents G_1/S transition may initially cause a preferentially state of migration. Several studies have attempted to label all proliferating cells following vascular injury models using either ^{3}H-thymidine loaded mini-pumps (inserted into rats, Clowes and Schwartz 1985)) or 5-bromo-2'-deoxyuridine (BrdU) loaded drinking water (given to mice, Yu et al. 2011)). Results from these studies indicate that a large proportion (>40%) of neointimal cells have migrated independent of proliferation, as they have not incorporated either molecule, both studies claim this specifically refers to VSMCs, although neither use definitive lineage tracing strategies to confirm this (Clowes and Schwartz 1985; Yu et al. 2011). Furthermore, these strategies for labelling proliferating cells may not be 100% efficient. The notion that migration may occur prior to or independent from proliferation is, perhaps, not expected if plaques are mono-clonal.

[3] Thesis aim 3: Determine if VSMC remodelling occurs by the clonal expansion of single VSMCs or proliferation of numerous VSMCs

1.8 VSMCs in atherosclerosis - Function and consequences

The contribution of VSMCs to the development of an atherosclerotic plaque is without doubt, at least when considering certain research, however the implications are still questioned. Typically, the accumulation of lipids within the sub-endothelial space precedes the development of advanced atherosclerotic plaques, however this early phenotype does not always proceed on to the advanced stage. Accumulation of fibrous tissues in the cap region, the bulk of which is synthesised by VSMCs, in plaques is the hallmark of an advanced stage (Libby., 2005). It is unclear whether the overall contribution of VSMCs to plaque development is beneficial or detrimental in the progression of atherosclerosis.

Trans-differentiation of VSMCs into macrophage like-cells and their subsequent formation of foam cells increases the lipid content of the plaque core (Shankman et al. 2015). Foam cell necrosis as well as VSMC-mediated cytokine release have both been shown to induce a negative, inflammatory, plaque phenotype (Jaulmes et al., 2006; Hofnagel et al., 2004; Okura et al., 2000). Furthermore, VSMCs which become senescent within atherosclerotic plaques actively contribute to the chronic inflammatory plaque phenotype through the release of interleukin-1α which primes adjacent cells to a pro-atherosclerotic state (Gardner et al. 2015). However, EMC-producing VSMCs which locate to the cap of the plaque, encapsulating the necrotic core, stabilise the plaque and protect against rupture and thrombosis (Schwartz, Virmani and Rosenfeld 2000). The normal adult artery has very low rates of proliferation and apoptosis, however within the plaque, multiple factors including inflammatory cytokines, inflammatory cells and oxidised lipoproteins alter the balance between proliferation and apoptosis (Bennett, 2002). Furthermore, VSMCs are intrinsically more sensitive to apoptosis within a plaque than healthy tissue (Bennett et al., 1995), expressing death receptors (e.g. interleukin-1 converting enzyme, Geng and Libby, 1995). Loss of plaque VSMCs often, therefore, occurs by apoptosis (**Figure 7**, Bennet, 1999) and subsequent thinning of the VSMC containing fibrous cap is associated with rupture (Newby et al., 1999). Indeed, plaques which rupture and directly lead to heart attack show a scarcity of cap VSMCs compared to stable lesions (Davies et al., 1993). Replicative senescence is also thought to contribute to VSMCs inability to replace apoptosed cells in late stage plaques due to observed shortened telomeres (Matthews et al., 2006).

It therefore appears VSMCs have both a positive and negative impact on atherosclerotic plaque progression, their involvement is thought necessary for plaque growth and the development of the necrotic core (Shankman et al. 2015). However, while their contribution is vital for stabilising a plaque

their subsequent apoptosis/senescence results in plaque rupture (**Figure 7,** Bennett, Sinha, and Owens, 2016; Schwartz, Virmani and Rosenfeld, 2000). VSMC accumulation is also known to contribute to in-stent restenosis (Marx, Totary-Jain, and Marks, 2011), but the role of VSMCs in other CVDs has not been as intensively studied.

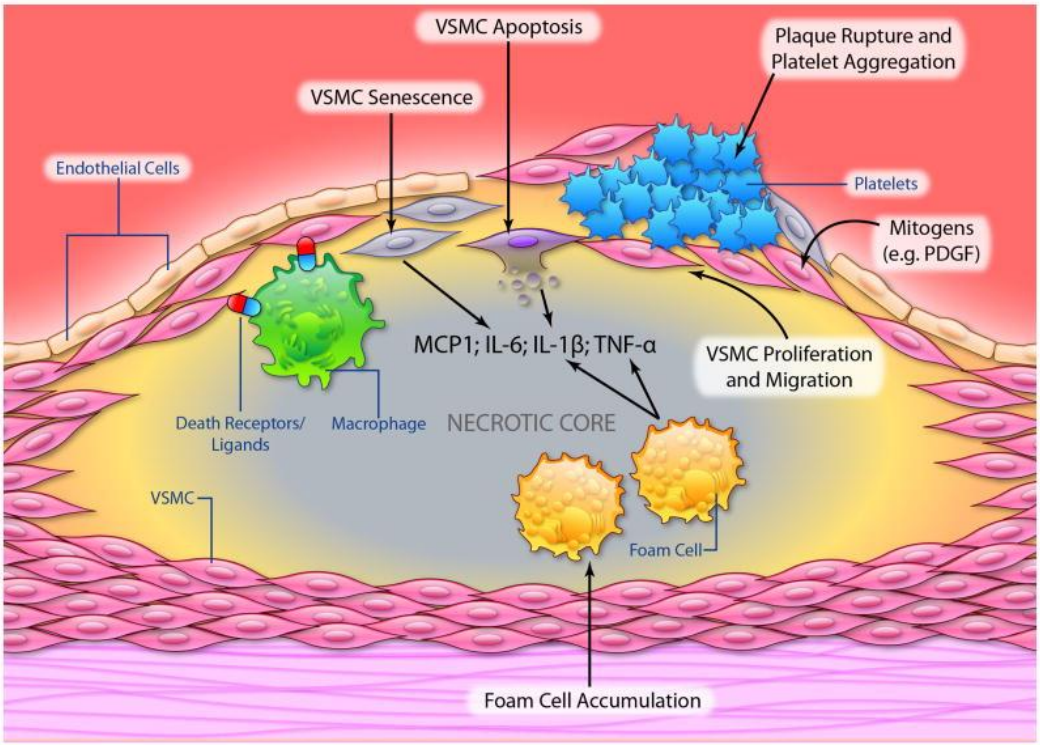

Figure 7: Schematic of an advance atherosclerotic plaque and a number of processes VSMCs undergo Within a late stage plaque, the balance between VSMC proliferation and apoptosis/senescence begins to change leading to a thinning of the fibrous cap. Additionally, senescent and apoptosed VSMCs release molecules which contribute to the development of the necrotic core, subsequently leading to plaque rupture. From Bennett, Sinha, and Owens, 2016.

1.9 Cardiovascular disease: Aortic aneurysm

Abdominal aortic aneurysm (AAA) is defined as the permanent dilatation of the abdominal aorta (the region extending from the diaphragm to the bifurcating iliac arteries, **Figure 8**) of >30 mm or >50% the size of normal diameter (Johnston et al. 1991). AAA is prevalent in 8.2% of men and 1.7% of women, however, this prevalence is not uniformly distributed across all age ranges and dramatically increases with age (Singh et al. 2001). Inflammatory biomarkers are present systemically in patients with AAA (Tambyraja et al. 2007), however, local irregular aortic enlargement is the primary identifier (Singh et al. 2001). As vessel diameter increases, so does the risk of AAA rupture (Filardo et al. 2012), which carries with it a high risk of mortality (60-80% which reduces to 30-65% if reaching a hospital alive) (Basnyat et al. 1999; Samy, Whyte, and Macbain 1994) accounting for 1% of deaths in the Western

world (Collin et al. 1988). Treatment of AAA relies on pre-rupture diagnosis followed by elective surgery to repair the aneurysm. This is however problematic as the majority of AAA remain asymptomatic prior to rupture (Scott et al. 1995).

AAA and atherosclerosis share many risk factors (age, smoking, hypercholesterolemia, and hypertension) and features such as inflammation. Historically, they were thought to be causally related, with AAA the result of atherosclerotic degeneration of the vascular wall. However current research suggests that while there is a significant correlation between the occurrence of both diseases within an individual, these diseases are distinct entities (Johnsen et al. 2010; Tromp et al. 2010).

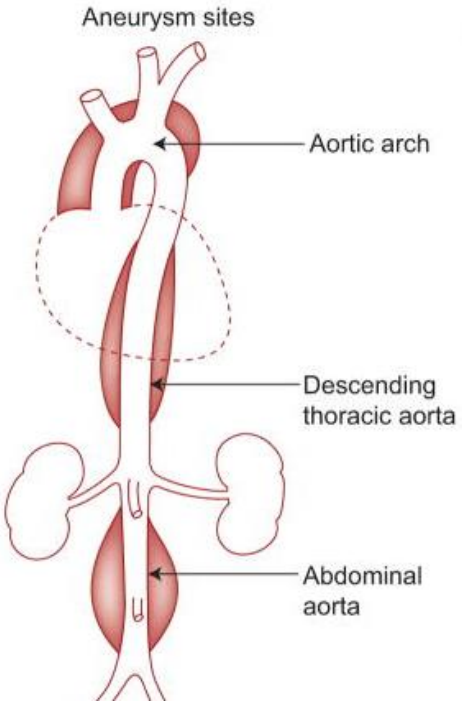

Figure 8: Aneurysm susceptible sites across the aorta
Aneurysms typically locate to the abdominal and descending thoracic aorta, and the aortic arch. Adapted from Tromp et al., 2010.

AAA pathogenesis is a complex process involving the destructive remodelling of the affected vasculature, the main stages are typically characterised by: (1) chronic inflammation, pro-inflammatory cytokine release and neo-vascularisation within the outer wall of the aorta; (2) dysregulated production of MMPs; (3) degradation of the structural matrix proteins collagen and elastin, resulting in arterial weakening and dilatation, and; (4) VSMC death and impaired replacement of connective tissue (Thompson, 1996). The risk of rupture relies on several variables, including the biochemical, hemodynamic and proteolytic conditions of individual regions of the diseased vasculature (Choke et al., 2005). Traditionally biomechanical factors were thought to be the best predictor for aneurysm rupture, with areas of the diseased tissue under the highest tensile strength thought to be the most at risk (Stringfellow et al., 1987). However, factors relating to enzyme activity are now thought to contribute substantially, for example, Vallabhaneni et al. (2004), identified local

'hot spots' of MMP hyperactivity, which could lead to weakening, and hence rupture, of the aortic wall in areas under relatively low intraluminal pressure. MMP activity fluctuates during normal remodelling of the aortic wall, however during AAA the activated MMPs aggressively degrade collagen and elastin. Annabi et al. (2002), for example, show that MMP-1, MMP-9 and MMP-12 are all upregulated in AAA tissue compared to healthy tissue. Furthermore, the balance between MMPs and proteins which regulate MMPs, tissue inhibitors of MMPs (TIMPs), favours the degradation of elastin and collagen (Elmore et al., 1998). TIMP-1 and TIMP-2, lack upregulation in AAA contributing to an imbalanced proteolytic state (Howard et al., 1991; Tamarina et al., 1997).

1.10 VSMCs in abdominal aortic aneurysm

As described above (**sections 1.1 and 1.3**) VSMCs are important structural components of the vascular wall, as such their role in aortic aneurysm where degeneration of the vascular wall is observed, is likely important. Rowe et al. (2000), confirming the results of Lopez-Candales et al. (1997), found that VSMC apoptosis was increased in AAA samples from humans, in conjunction with a decrease in VSMC density when compared with healthy aortas and aortas with aortoiliac occlusive disease. Furthermore, Parastatidis et al. (2013) showed that by specifically augmenting expression of catalase, a H_2O_2 scavenging enzyme, in VSMCs within a model of AAA they could reduce apoptotic cell death and protect from AAA. Liao et al. (2000) further suggest that replicative senescence of VSMCs within AAA contribute to an exhaustive repair potential of these cells, which could in turn be the reason large AAA had a reduced capacity for connective tissue repair (Thompson, 2002; Choke et al., 2005).

While it is known that VSMC loss relates to the reduction of the vascular wall's synthetic capacity and structural weakening (Airhart et al., 2015), there is also growing evidence that dysregulated VSMCs contribute directly to the degeneration of the vascular wall. Multiple studies have shown that MMPs released directly from VSMCs into the ECM are involved in AAA formation (Ailawadi, Eliason, and Upchurch 2003; Airhart et al. 2014). VSMCs cultured from AAA and healthy vasculature exhibit differential gene expression, further still they differ from those extracted from atherosclerotic plaques, supporting the notion that these two diseases are distinct and the AAA phenotype unique (Airhart et al., 2014). Compared to healthy tissue, AAA VSMCs upregulate expression of MMP-2 and MMP-9 and cysteine proteases with properties ideal for elastolysis. Mutations within VSMC genes have also been shown to contribute to aneurysm, mutations in aSMA and MYH11 result in abnormal VSMC contraction and aortic aneurysms (Guo et al., 2007; Pannu et al., 2007). Ailawadi et al. (2009), suggest that VSMCs undergo phenotypic switching early on in AAA. Using an elastase-perfusion model

for AAA within mice they show that by day 7 post-surgery VSMC marker genes (aSma and Sm22a) were downregulated, consistent with VSMC phenotypic modulation, prior to aneurysm formation. Furthermore, human aortic aneurysms extracted at time of resection had significantly less aSMA compared to aortic tissue extracted during coronary artery bypass grafting, and significantly higher MMP-2 and apoptosis marker Caspase-3 expression. While this study implies that VSMCs are changing in AAA, the extent of these phenotypic changes and associated VSMC proliferation cannot be definitively determined.

VSMCs within AAA clearly have an important role, the extent of which remains unknown, similar to the early atherosclerosis experiments describe above (**section 1.5**), phenotypic switching makes these cells difficult to track without using mice carrying the Myh11-Cre transgene, which has yet to be performed in AAA.

1.11 Molecular mechanisms of VSMC phenotypic switching

The stimuli inducing VSMC phenotypic switching are numerous and wide ranging, factors such as vascular injury, mechanical force, growth factors/inhibitors, inflammatory/oxidative stress and cell – cell/matrix interactions are all known to induce such an event (Owens 1995).

The VSMC cytoskeleton and surrounding medial ECM play a key role in phenotypic modulation and migration/proliferation of VSMCs. For example, type I collagen present in the ECM, induces VSMC production of cyclin-dependant kinase 2 inhibitors, preventing VSMC proliferation (Koyama et al. 1996). The cytoskeleton of VSMCs, a 3D structure composed of protein microfilament/tubules, remains intact in contractile VSMCs. However, actin cytoskeletal degradation, induced by loss of tensile stress in an organ culture system, inhibits VSMC marker gene expression (e.g. Myocardin) thereby enhancing phenotypic switching (Zheng et al. 2010).

A significant step forward in understanding the regulatory processes behind phenotypic switching was the identification of promoter/enhancer regions within a selection of VSMC marker genes, conferring specific expression in VSMCs in mice (Mericskay et al., 2000; Li et al., 1996; Mack and Owens, 1999; Kim et al., 1997; Masen et al., 1998). The transcriptional regulation of these regions within VSMC marker genes rely on a multitude of factors which are expressed ubiquitously or selectively by VSMCs (**Figure 9**). The best characterised model of transcriptional regulation is the 'CArG-SRF dependant regulation model'. Studies have identified that expression of many VSMC specific/marker genes rely

on CArG elements ($CC(AT)_6GG$) within enhancer/promotor sites. These elements bind serum response factor (SRF, a MADS-box transcription factor) which coordinate gene expression. Myocardin, a potent SRF activator which is exclusively expressed within SMCs and cardiomyocytes, plays an important role in promoting interactions between CArG boxes and SRF, and subsequent recruitment of RNA polymerase II (Pol II) specifically within VSMCs (McDonald et al., 2006; Yoshida et al., 2003). In fact, within the majority of CArG-dependant VSMC marker genes tested, including aSMA, MYH11, SM22α and Calponin, Myocardin induces selective expression (Du et al., 2003; Yoshida et al., 2003; Alexander and Owens, 2011). Disruption of Myocardin-induced SRF-CArG binding is thought to play a role in phenotypic switching, Wang et al., (2004) showed that PDGF-BB – induced decreases in VSMC marker genes was, in part, due to phosphorylation of Elk-1, which subsequently competed with Myocardin for CArG-SRF binding. Tang et al. (2008) further showed that NFκB also binds Myocardin to reduce its interaction with SRF and CArG. Conversely Angiotensin II (Ang II) increases the expression of VSMC marker genes, mediated through the upregulation of paired-related homeobox gene 1 (Prx1) which promotes CArG-SRF-Myocardin interactions (**Figure 9**, Yoshida, Hoofnagle, and Owens 2004).

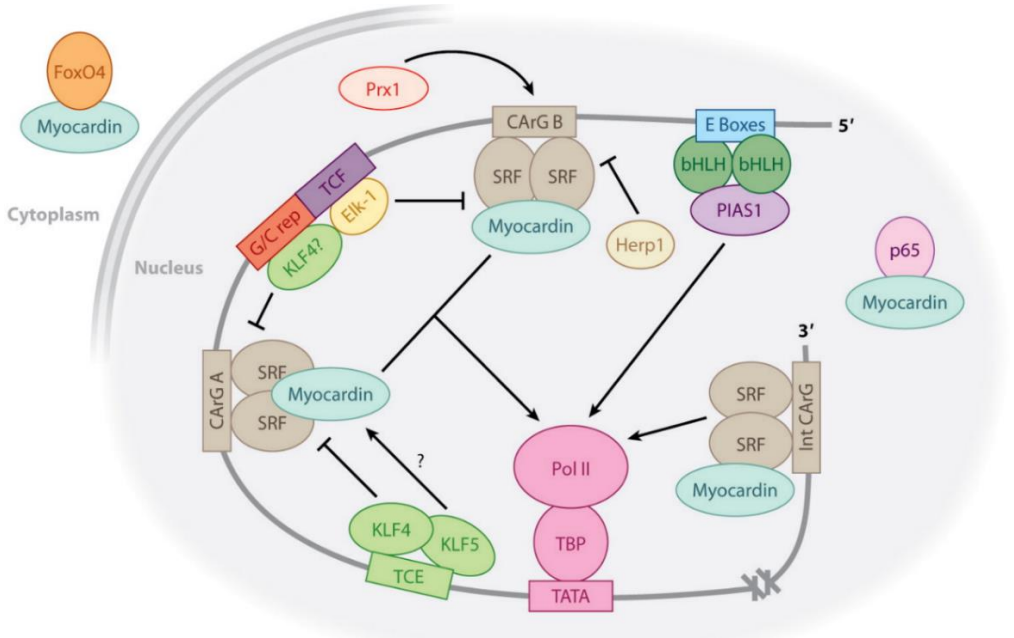

Figure 9: Transcriptional regulation of VSMC marker genes

VSMC-selective gene expression is mediated through a complex process of combinatory cis-regulatory elements and transcription factors. Myocardin acts as a potent co-activator of SRF binding to CArG elements within promoters of VSMC marker genes, which promotes the recruitment of Pol II to initiate transcription. Other factors such as paired-related homeobox gene 1 (Prx1) and protein inhibitor of activated stat 1 (PIAS1) complexed with basic helix-loop-helix (bHLH) factors at E-box cis regulatory elements promote Myocardin-SRF-CArG interactions. Transcription factors KLF4, Elk-1 and HES-related repressor protein (Herp2) act to repress VSMC marker gene expression, at least in part by inhibiting Myocardin-SRF-CArG interactions. Transcription factor Forkhead Box O4 (FoxO4) and the p65 subunit of NFκB compete with SRF to bind Myocardin, inhibiting VSMC marker gene expression. From Alexander and Owens, 2011.

Epigenetic factors also play a crucial role in the ability of SFR to bind CArG containing regions of VSMC genes (**Figure 10**). Studies have identified that the histone modifications Histone H4 acetylation (H4ac), H3K4me2, Histone H3 acetylation (H3ac) and Histone H3 lysine 79 dimethylation (H3K79me2) are involved in the ability of Myocardin-SRF to bind to CArG sites, activating VSMC gene expression programmes and the differentiation of VSMC precursor-cells (Qui and Li, 2002; Cao et al., 2005; Manabe and Owens, 2001; Macdonald et al., 2006). Furthermore, PDGF-B treatment of cultured VSMCs and an in vivo balloon-injury model induced VSMC phenotypic switching in conjunction with a reduction in histone H4 acetylation at CArG elements and SRF binding (McDonald et al., 2006).

McDonald et al. (2006) further suggest that H4 deacetylation is due to the recruitment of histone deacetylase 4 (HDAC4) by KLF4. Indeed, KLF4 had previously been shown to be a potent repressor of VSMC marker genes, both by down regulating Myocardin expression and inhibiting Myocardin-SRF binding to CArG elements (**Figure 9**, Liu et al., 2005). H3K4me2, however, was unaffected in phenotypically switched VSMCs induced by either PDGF-B or the balloon injury models. Thought to represent a lineage memory mark, H3K4me2 may allow VSMCs to reverse the process of phenotypic switching and, as discussed previously (**section 1.5**), acts as a useful marker to examine phenotypically switched VSMCs in humans (McDonald et al. 2006; Gomez et al. 2013). Furthermore, global DNA hypomethylation and expression of DNA methyltransferases are increased in VSMCs within atherosclerotic plaques compared to those in healthy media (Hiltunen et al., 2002).

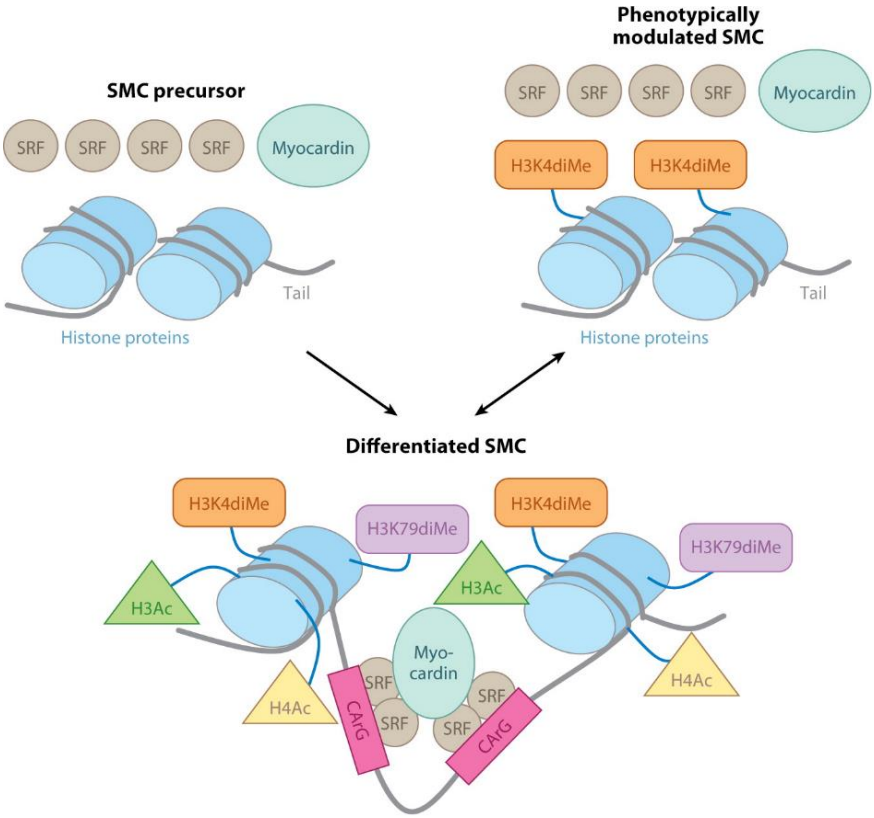

Figure 10: Epigenetic regulation of VSMC phenotype
During VSMC differentiation histone proteins within promotors of VSMC marker genes (e.g. aSMA and MYH11) are modified. Acetylation of H3 and H4 and dimethylation of lysine's 4 and 79 on H3 open allow binding of SRF-Myocardin to CArG elements. VSMCs induced to phenotypically switch/modulate undergo loss of histone modifications H3/H4 acetylation and H3K79 dimethylation, inhibiting CArG accessibility.
From Alexander and Owens,
2011.

MicroRNAs (miRNAs), a group of single stranded 20-25 nucleotide, non-coding RNAs active in many post-transcriptional regulatory processes within a cell act to indirectly regulate transcription and within VSMCs. Several studies have now implicated miR-145 and miR-143 in regulation VSMC phenotype, in part by degrading KLF4 (a zinc finger transcription factor) transcripts, promoting the contractile phenotype. Furthermore, miR-145 and miR-143 are both downregulated in injured and atherosclerotic vasculature (Cordes et al., 2009; Xin et al., 2009; Cheng et al., 2009). Multiple other miRNAs are involved in maintaining the contractile phenotype/causing the switch to a synthetic phenotype (reviewed in Zhang et al., 2016).

Studies on the epigenetic and molecular regulation of VSMC differentiation and phenotypic modulation are plagued by the use of cells from culture systems which do not faithfully recapitulate the in vivo environment. Furthermore, ex vivo bulk tissue processing, necessary for techniques such

as chromatin immunoprecipitation (ChIP)/ChIP-seq, are inevitably contaminated by other cells types (Gomez, Swiatlowska, and Owens 2015). To further understand the mechanistic processes underlying VSMC behaviour it is becoming increasingly necessary to employ new techniques capable of performing analyses at the single cell level either in vivo or on tissue taken directly from living animals. Techniques available include those capable of single-cell epigenetic analysis (Bheda and Schneider, 2014), single cell RNA sequencing[4] (scRNA-seq, Tang et al., 2009) and single cell genome wide DNA methylation analysis (Smallwood et al., 2014).

[4] Thesis aim 4: Optimise scRNA-seq methods for VSMCs

1.12 Aims and hypothesis

VSMCs, which are typically contractile and quiescent, have remarkable plasticity, able to phenotypically switch and trans-differentiate in response to multiple environmental stimuli and vascular diseases. The non-random positional occurrence of atherosclerotic lesions and aortic aneurysms within the vasculature suggests that very particular environmental stimuli are required to activate the dysregulated response of VSMCs in either disease. Furthermore, as mentioned above there is a large degree of heterogeneity in the VSMC population. This raises the question of the relative contribution of cell intrinsic and external factors, in particular, whether all VSMCs have the same potential to phenotypically switch. For example, cells which proliferate in response to injury/disease could belong to specific sub-population of VSMCs or all VSMCs may be equipotent, capable of activating in response to disease. The experiments conducted within this thesis attempt to understand these questions, first by assessing clonal VSMC proliferation within multiple disease models and secondly by understanding heterogeneity at the level of the single cell.

Hypothesis: The reported heterogeneity within the VSMC population results in differences in VSMC functionality in models of CVD

Aims:

1. Determine if phenotypically distinct VSMC-derived plaque cells are generated from single (multi-potent) VSMCs or if distinct VSMCs produce a single or subset of these (uni/oligo-potent)
2. Determine the proportion of VSMCs which respond in vascular disease/ injury
3. Determine if VSMC remodelling occurs by the clonal expansion of single VSMCs or the proliferation of numerous VSMCs
4. Optimise scRNA-seq methods for analysis of VSMCs heterogeneity

CHAPTER 2: Methodology

To investigate the described aims, a system of methods will be employed, the principles of several of these methods are described here for later reference and to aid the understanding of the results.

2.1 VSMC specific, multi-colour lineage tracing – the Confetti system

Lineage tracing within this study utilises an inducible Cre-lox system to drive the stochastic recombination of the multi-colour confetti reporter, specifically within VSMCs (**Figure 11**). This multi-colour labelling is advantages over single or dual colour systems as clonal proliferation can be detected while using a much higher labelling frequency, due to the unlikely event that only cells of the same colour proliferate by chance.

The Cre recombinase used here is fused to a triple mutant form of the human oestrogen receptor, which binds the synthetic oestrogen 4-hydroxytamoxifen (and not its natural ligand, 17β-estradiol). Confined to the cytoplasm of a cell, CreER(T2) can only access the nucleus following tamoxifen administration. Thus, allowing recombination to be induced when desired. To ensure that CreER(T2) activity was specific to VSMCs upon tamoxifen administration the CreER(T2) sequence was inserted into the ATG site of a bacterial artificial chromosome (BAC) carrying the Myh11 gene, the most specific marker of VSMCs (Nguyen et al., 2013). The 180 kb BAC was then injected into the pro-nuclei of mice oocytes. Myh11-CreER(T2) transgenic mice where the transgene had integrated into the Y chromosome were chosen for breeding on to the C57BL/6 background (Wirth et al., 2008). This Cre is therefore only present in male animals, hence the reason only male animals are used in these studies. It should be noted that sex bias in biomedical research, i.e. the neglect of females, is common place. This, however, should be avoided where possible and should have been considered by those who performed the mouse transgenics, as tangible differences can often be seen between sexes (Beery and Zucker 2011). While the activation of this transgene seems to faithfully recapitulate endogenous expression of the true Myh11 gene (Wirth et al. 2008; Nemenoff et al. 2011), it should always be considered that differences in chromosome location/local genomic environment, may affect a transgene's promotor activity relative to the endogenous protein's promotor (Liu 2013).

The confetti reporter (**Figure 11**), located in the Roas26 locus, contains (1) a CAG promoter, which permits high levels of gene expression, (2) a loxP flanked stop cassette, such that protein translation in this system is Cre-recombinase dependant and (3) the Brainbow 2.1 sequence, containing the floxed

cDNA for red (RFP), yellow (YFP), cyan (CFP) and green (GFP) fluorescent proteins. Cre driven recombination of this construct causes the stochastic expression of one of the four fluorescent proteins. RFP and YFP localise to the cytoplasm, whereas tagging results in recruitment of CFP to the membrane and GFP to the nucleus (Snippert et al., 2010; Livet et al., 2007). Without further Cre activity, the progeny of a labelled cell express the same fluorescent protein at equal intensity to the pre-cursor cell.

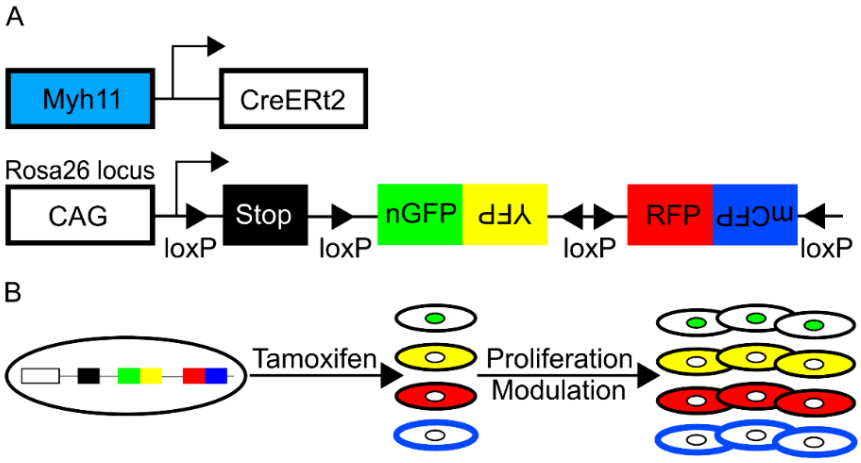

Figure 11: Schematic of the 'Confetti' multi-colour lineage tracing system
A, Schematic of the Myh11-CreERt2 transgene (top) and the Rosa26-Confetti reporter allele (below). **B,** Schematic illustrating tamoxifen-induced recombination at the Rosa26-Confetti locus resulting in expression of one of four fluorescent proteins, which are stably propagated independent of Myh11 expression within progeny. From Chappell et al. (2016)

2.2 The ApoE$^{-/-}$, high fat diet model of atherosclerosis

The C57BL/6 mice strain was found to be one of the most susceptible inbred strains to atherosclerosis, primarily when subjected to HFD, and has since been commonly used as a diet induced atherosclerosis model (Paigen et al., 1987; Nakashima et al., 1994). However, the lesions which develop in these mice when given HFD typically resemble large fatty streaks with little involvement from VSMCs (Paigen et al., 1987). To develop more efficient models of atherosclerosis, mice have been genetically modified to disrupt gene products involved in cholesterol metabolism. Homozygous mice for the ApoE^{tm1Unc} (ApoE$^{-/-}$) mutation have increased total plasma cholesterol due to their inability to properly catabolise triglyceride-rich lipoproteins (Nakashima et al., 1994). Following six weeks of HFD, in ApoE$^{-/-}$ animals, there is evidence of cell adhesion to the endothelium and foam cell formation within the sub-endothelial space, after ten weeks mice develop 'intermediate lesions' consisting of multiple cell types including VSMCs and foam cells and by fifteen weeks large fibrous plaques have formed in the branching regions of the aorta and major vessels. The plaques within ApoE$^{-/-}$ mice follow similar

developmental steps seen within humans (Nakashima et al., 1994). The major difference between the ApoE$^{-/-}$ mouse model and humans is that plaques within these mice typically do not rupture and therefore fail to show the final and deadliest stage of atherosclerosis. Additionally, an important distinction between mice and humans is that within human vasculature, VSMCs exist within the intima at certain positions of the vascular tree, primarily at branch sites, prior to disease (Doran et al., 2008). However, despite differences in cardiovascular physiology, lipid profile and cholesterol metabolism, and the differences noted in plaque pathology, this system remains one of the most useful tools in studying atherosclerosis (Meir and Leitersdorf, 2004).

2.3 The carotid ligation injury model of vascular remodelling

Vascular remodelling within carotid arteries, characterised by medial and intimal thickening, is regarded as a phenotypic predictor for CVD in humans, and is seen in the early stages of atherosclerosis (Davis et al., 2001). This can be modelled by performing carotid ligation surgery within mice (**Figure 12**), where blood flow through the vessel is reduced/abolished (Korshunov and Berk, 2003). As mentioned previously (**section 1.4**), haemodynamic forces experienced by a vessel are important in the maintenance and susceptibility of athero-protective and athero-prone phenotypes, respectively. Flow disruption within this model therefore leads to rapid endothelial dysfunction and an acute proliferative response from VSMCs (Nam et al., 2009). Four weeks post ligation, lumen area is reduced by approximately 80%, primarily due to VSMC-rich neointima formation. Typically, monocytes and macrophages are not detectible, however some leukocytes (CD45 positive cells) infiltrate the media and neointima (Kumar and Lindner, 1997). This model, therefore, allows the study of vascular remodeling at the molecular level by causing an acute proliferative VSMC response, which is typically more reproducible and quicker than HFD protocols which generate plaques.

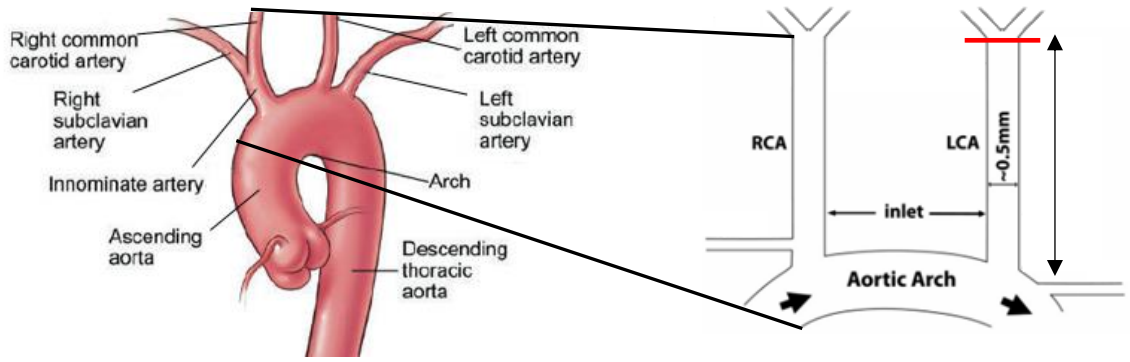

Figure 12: Illustration of carotid ligation surgery of the left carotid artery
Illustration of the aortic arch and protruding vessels and the site of carotid ligation. Within the carotid ligation model of CVD, the left carotid artery is ligated directly below the bifurcation indicated by red line. Adapted from Nam et al., 2009.

2.4 The Angiotensin II perfusion model of aortic aneurysm

There are multiple methods to induce AAA within mice, however, the Ang II perfusion model is the most widely used technique as, it is believed, to faithfully recapitulate AAA and the surgery required is relatively non-invasive compared to other methods (Cao et al., 2010). To perform this method, Ang II containing osmotic mini-pumps are inserted subcutaneously into mice, on one side of the posterior flanks (Daugherty and Cassis, 1999). Typically, $ApoE^{-/-}$ or $Ldlr^{-/-}$ mice fed either normal chow or HFD are used in these studies (Daugherty and Cassis, 1999; Daugherty et al., 2000; Manning et al., 2002). Ang II perfusion will lead to AAA in normocholesterolemic mice (i.e. wild type for ApoE), but at a lower incidence rate (3-4 fold) compared to hyperlipidaemic mice (Deng et al., 2003; King et al., 2006). The mechanisms by which Ang II induces aneurysm are not fully understood, although it has been demonstrated that AAA develops in this model independently of Ang II induced hypertension, but may result from mechanisms related to inflammation (Cassis et al., 2009). Features of the Ang II model include: (1) an early accumulation of macrophages to the adventitia and media of the suprarenal aortic region; (2) medial dissection and an increase in lumen diameter, along with the appearance of thrombi located to the media, contained by the adventitia; (3) abnormal matrix deposition and thrombus resolution 28 days post mini-pump insertion, which continue to remodel and have features associated with immune response and neovascularisation (Saraff et al., 2003; Barisione et al., 2006; Rateri et al., 2011). Wang et al. (2010) combined Ang II perfusion with injections of anti-TGF-β to study the role of TGF-β in the Ang II model of AAA. Results demonstrated that TGF-β neutralisation increased the AAA in the normally resistant, normocholesterolemic, ApoE wild type mice on the C57BL/6 background. However, anti- TGF-β administration in $ApoE^{-/-}$ mice show no difference compared to $ApoE^{-/-}$ receiving Ang II alone (King et al., 2009). Wang et al. (2010) further show that TGF-β is important in controlling excessive monocyte/macrophage activation, thus protecting from AAA. The Ang II + anti-TGF-β model has the advantage that it is not confounded by hypercholesterolemia from the $ApoE^{-/-}$ mice, and is also more reproducible (Wang et al., 2010).

It is difficult to evaluate exactly how similar Ang II induced models of AAA are to human AAA as human samples are typically only collected at the end stage of the disease (Daugherty and Cassis., 2004). However, two main differences/problems noted are: 1) within Ang II perfused mice aneurysms typically locate to the suprarenal, compared to the infrarenal aorta in humans (Saraff et al., 2003); and 2) a large degree of heterogeneity between mice under the same protocol exists, which has led to the development of a classification system from Grade I – IV (Daugherty at al., 2001). The reasons for the difference in position of AAA are considered to be due to potential haemodynamic/mechanical

differences, and/or differences in elastin/collagen matrix composition, between mice and human arteries (Halloran et al., 1995; Saraff et al., 2003). However, no definitive mechanisms responsible for preferential location were known (Daugherty et al., 2011).

These ideas, however, have recently been challenged, and indeed the Ang II model itself as a method of recapitulating AAA. Trachet et al. (2017), published recent work investigating the variability in the shape of the 'dissecting aneurysms' observed in the AAA method, using in vivo ultrasound and ex vivo phase-contrast X-ray tomography microscopy. Trachet et al. (2017) suggest a temporal sequence of events leading to the observed phenotypes in the AAA model. The steps include: 1) micro ruptures around the celiac and mesenteric arteries propagate to a medial tear; 2) the medial tear causes the adventitia to dissect; 3) intramural blood makes small side branches rupture; 4) the dissection is stopped by large side branches; and 5) an intramural haematoma forms with or without a false channel (a second, false, lumen supporting blood flow parallel to the lumen proper). Trachet et al. (2017), first point out that it is the location of the micro tears at the ostium of the celiac and mesenteric arteries within the Ang II model which is the reason why aneurysms locate to the suprarenal region of the aorta. Secondly, they suggest that the variability in the Ang II model can be explained by presence or absence of: 1) medial tears; 2) intramural haematoma (IMH); and 3) a false channel. Trachet et al., (2017) note significant differences between the Ang II model and human AAA, namely, that within the Ang II model, focal tears within the media at specific branch regions initiate aneurysm compared to circumferential medial degradation in human; IMH is caused by adventitial dissection rather than an intraluminal thrombus; and that there is a false channel increase in size in a subset of animals rather than gradual luminal dilatation in all. Based on this information, Trachet et al., (2017) suggest that Ang II infusion in mice is better suited to studying aortic dissection and does not recapitulate human AAA accurately.

Whether the Ang II model will be reclassified regarding the disease it models will be subject to some debate and further work. This does however raise one important conclusion, that all animal models regardless of how well they seem to recapitulate a disease within humans, will differ in many ways and should only be used with this in mind.

2.5 Single cell transcriptomics

In the last decade technologies have been developed/adapted to perform RNA-sequencing on single cells, enabling intra-population heterogeneity and cell-cell transition states to be examined at the

transcript level. Thus, revealing cell subtypes and dynamics in cellular transcription/gene expression, which can be masked by bulk population sequencing (Wills et al., 2013; Trapnell et al., 2014; Liu and Trapnell, 2016). Two methods to perform scRNA-seq are used within this study, the first is Smart-seq2 (Picelli et al., 2013), this method relies on isolating single cells, which can be performed by fluorescence-activated cell sorting (FACS) or laser dissection microscopy (Nichterwitz et al., 2016). Once isolated, cells undergo a protocol in which the RNA from single cells are reversed transcribed to generate full-length cDNA, which are then indexed and pooled to create a sequencing library (**Figure 13**). This method uses 'off the shelf' reagents, a step by step protocol is outlined in **section 3.18**.

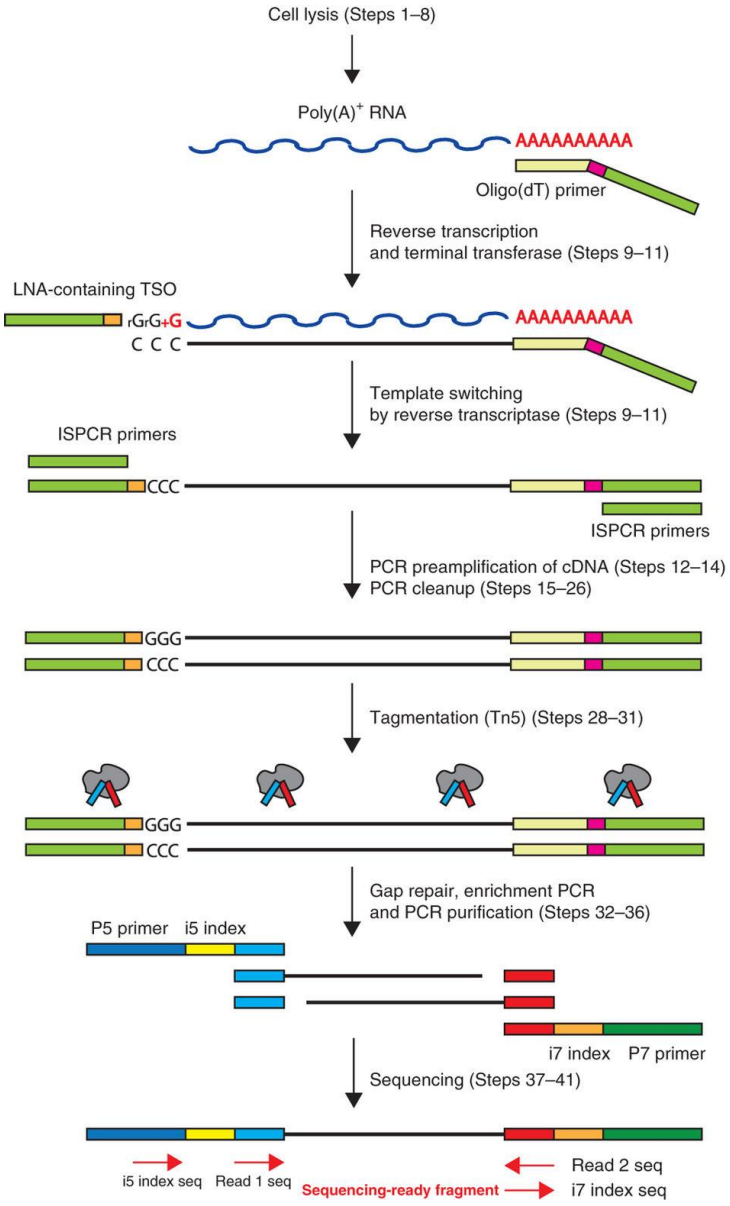

Figure 13: Flow chart for Smart-seq2 protocol
To preform Smart-seq2, single cells are first isolated. Oligo(dT) primer then binds the Poly(A)+ tail of RNA transcripts and reverse transcription is performed. Upon reaching the 5' end of the RNA template the polymerase adds several additional nucleotides (mostly deoxycytidine) to the 3' end of the synthesised cDNA. These bases act as a site for the template switching oligo (TSO) to bind, at which point the polymerase switches templates and continues replication to the end of the 5' end of the TSO. Universal primers (ISPCR) are then added and cDNA amplification performed. To prepare sequencing libraries, a hyperactive derivative of the Tn5 transposon is used to fragment and incorporate predetermined oligonucleotides into the cDNA, which are then PCR enriched. To allow pooling of up to 96 samples, a duel indexing system (index 1 (i7) and index 2 (i5)) is used. Following sequencing, data from individual cells can be extracted based on the unique cell index. From Picelli et al., 2014.

Smart-seq2 is typically performed in 96 well plates (i.e. 96 single cells at a time), and is labour intensive compared to most other methods of scRNA-seq, however it is recognised as one of the most sensitive methods to use when performing scRNA-seq on relatively few cells (Ziegenhain et al., 2017). Compared to scRNA-seq techniques such as MATQ-seq (Sheng et al. 2017), smart-seq2 only captures polyadenylated RNA as it uses oligo(dT) to isolate and purify mRNA, furthermore strand specificity is lost in this method (Picelli et al., 2013).

The second method of scRNA-seq used here utilises the 10X Genomics, Chromium system. This system is a droplet based system in which dissociated cells are loaded into a Chromium machine and are then processed so that individual droplets contain a single cell and a bead, containing the necessary reagents to perform reverse transcription (referred to as single cell gel beads in emulsion, GEMS, Zheng et al. 2017). Reverse transcription then takes place within each GEM, importantly, during first strand cDNA synthesis each transcript is tagged with a cell barcode and a unique molecular identifier (UMI). Following cDNA amplification and library preparation the cDNA is then sequenced. The cell barcode can then be used to aggregate sequencing reads for individual cells similar to the indexing method used in Smart-seq2. One significant advantage of this method compared to methods such as Smart-seq2 is that the UMIs can be used to assign sequencing reads to individual transcript molecules, this helps to remove biases and amplification noise generated from scRNA-seq, furthermore it allows the determination of the relative abundance of different transcripts (Kivioja et al. 2011; Zheng et al. 2017).

Relative to Smartseq-2, the 10x system for scRNA-seq is extremely high throughput, allowing up to 10,000 cells to be captured and processed in one experiment, this is partly due to the early attachment of cell barcodes, during first stand synthesis of cDNA, which allows for multiplexing of the cDNA during amplification (Hashimshony et al. 2012; Jaitin et al. 2014). Furthermore, all steps following tissue dissociation to single cells are automated, meaning the labour costs are low. One disadvantage of this method compared to Smart-seq2 is that only the 3’ ends of each transcript is read during sequencing, this is necessary due to the use of UMIs which only attach to one end of the transcript and must be read. Smart-seq2 however, captures full length transcript data, which increases its sensitivity as lowly expressed transcripts are preferentially detected using full-length transcript methods, this is thought to be due to particular 3’-proximal sequences which are difficult to align to the genome (Ziegenhain et al. 2017).

CHAPTER 3: Methods

This study was conducted within the Cardiovascular Medicine Division, Department of Medicine, University of Cambridge. All animal experiments have been approved by the UK Home Office (PPL70/7565), were performed according to Home Office guidelines and were approved by the local ethics committee.

3.1 Animal experiments

The 'Confetti mice' used here were made by crossing two different genetically modified lines: The Gt(ROSA)26Sortm1(CAG-Brainbow2.1)Cle/J, (R26R-Confetti) mice (Snippert et al., 2010) from The Jackson Laboratory were crossed with the B6.FVB-Tg(Myh11-cre/ERT2)1Soff/J, (Myh11-CreER(T2)) mice (Wirth et al., 2008), also from The Jackson Laboratory. The Myh11-CreER(T2) mice were on an inbred C57Bl/6 background (for at least 10 generations), whereas the R26R-Confetti allele was on a mixed C57Bl/6 / BALB/c background prior to cross breeding.

The $ApoE^{-/-}$ Confetti mice were made by crossing a third genetically modified line, the B6.129P2-$Apoe^{tm1Unc}$/J (Piedrahita *et al.*, 1992) purchased from Charles River Laboratories, to the Confetti mice. The $Apoe^{-/-}$ were on an inbred C57Bl/6 background (for at least 10 generations) prior to cross breeding.

The Myh11-CreER(T2) transgene is Y-linked, therefore all experimental animals in this study are males. Experimental animals used were backcrossed to the C57Bl/6 for 1-6 generations (**Appendix A and C**), no difference in described phenotype between mice from different generations was observed.

3.2 Tamoxifen administration and dose optimisation

Tamoxifen (Sigma-Aldrich) solution was made in batches of 9 ml of 10 mg/ml in corn oil (Sigma-Aldrich). To make, tamoxifen is diluted in pre-warmed (55 ^{o}C) ethanol (EtOH, 200 proof) to a concentration of 10 mg/0.1 ml, and shaken to dissolve. This solution was then diluted into sterile filtered (0.22 µm filter) corn oil warmed to 55 ^{o}C to a concentration of 10 mg tamoxifen/ml, vortexed and aliquoted into 1.5 ml Eppendorf tubes. Three rounds of sonication (Sonics Vibra.Cell), 20 seconds on 60% output, with cooling on ice in-between ensured tamoxifen was fully dissolved. Tamoxifen aliquots were then stored in the dark at -20^{o}C.

When necessary, tamoxifen was further diluted in corn oil to desired concentrations, 100 µl of the tamoxifen solution was injected intraperitoneally into each mouse per injection. Dose optimisation

was completed by injecting various concentrations of tamoxifen (displayed in results) and analysed via confocal microscopy of tissue and flow cytometry of dissociated cells, described below.

3.3 Tissue removal and fixation

Mice were culled via CO_2 asphyxiation prior to perfusion with 10 ml cold phosphate buffered saline (PBS). The left (LCA) and right (RCA) carotid arteries and aorta were removed and cleaned of fat by microdissection under a light microscope. Fixing was performed in fresh 4% paraformaldehyde (Sigma-Aldrich) for 20 mins at room temperature (RT).

3.4 Medial dissociation to single VSMCs

To isolate VSMCs to a single cell suspension, microdissection was used to remove the external fat and to open the aorta into a sheet. The ECs were lightly scraped off the inside of the sheet. A partial digestion step in a mixture of 1 mg/ml Collagenase type IV (Gibco) and 1 U/ml Elastase (Worthington Biochemical) dissolved in Dulbecco's Modified Eagles Medium (DMEM, Sigma-Aldrich) for 8 mins at 37 ^{o}C allowed the separation of the adventitia from the media using forceps. A final digestion in fresh enzyme mixture (1 ml for 1 aorta) at 37 ^{o}C with frequent pipetting using a P1000 was used until a single cell suspension has been achieved, typically 2 hours. Isolated cells were centrifuged at 1000 rpm for 3 mins and re-suspended in 3% bovine serum albumin (BSA) in PBS (this process was repeated 3x) and filtered through a 70 µm cell strainer.

3.5 Flow cytometry

A BD LSR Fortessa was used for flow cytometry. A 405 nm violet laser, 488 nm blue laser and a 561 nm yellow laser combined with 450/50, 530/30 and 610/30 BP filters, detects CFP, GFP/YFP and RFP, respectively. Where possible 10,000 cells were analysed as a minimum. Flowing software (Terho, version 2.5.1) was used to analyse the raw data to determine proportions of labelled cells.

3.6 Blood plasma and bone marrow isolation

Blood was removed from CO_2 asphyxiated mice via cardiac puncture with a 27G needle and collected into heparinized tubes (Microvette® 55LH, SARSTEDT). Red blood cells were lysed by incubation in lysis buffer, composed of 55mM NH4Cl, 10mM KHCO3 and 0.1mM EDTA (pH 7.3) for 10 minutes. White blood cells were pelleted via centrifugation at 300 x g for 5 mins and the supernatant discarded.

Isolated cells were centrifuged at 1000 rpm for 3 mins and re-suspended in 3% bovine serum albumin (BSA) in PBS (this process was repeated 3x) and filtered through a 70 µm cell strainer.

For bone marrow, femurs were removed from mice, the ends of the bone were cut off and the bone marrow flushed out with PBS using a 27G needle. The bone marrow cells were passed through a cell strainer (70 µm) prior to flow cytometry.

3.7 Vibratome sectioning

Following the tissue removal/fixing steps in **section 3.3** the tissue was submerged in liquid 4% low melt agarose (Thermo Scientific) and left at RT until solidified. Sections, 50-100 µm thick, were then cut on a vibratome (LEICA • VT 1200S), on to polysine slides (Thermo Scientific). Sections were then mounted in RapiClear 1.52 (Sunjin lab) with a coverslip.

3.8 Cryo-sectioning

Following the tissue removal/fixing steps in **section 3.3** the tissue was submerged in a 30% sucrose (Sigma Aldrich) solution in PBS overnight at 4^{o}C. Tissue was then transferred to a 50:50 solution of 30% sucrose solution:OCT compound (VWR) for 1 hour at RT before a final incubation of 1 hour in 100% OCT at RT. Samples were then placed into OCT within plastic moulds and snap frozen using dry ice prior to storage at -80 ^{o}C. A cryostat was used to cut 20, 14 or 12 µm thick sections on to Superfrost™ Ultra Plus Adhesion Slides (Thermo scientific), slides were stored at -80 ^{o}C.

3.9 Immuno-staining

All immunostaining was performed on cryo-sections. Sections were briefly rinsed in PBS, permeabilised in 0.5% TritonX-100 in PBS (20 min at RT) and incubated for 1 hour at RT in blocking buffer (1% BSA, 10% normal goat serum (Dako) in PBS). Staining with the following primary or isotype control antibodies diluted in blocking buffer was done overnight at 4˚C: aSMA - biotin, (Abcam, 2.5 µg/ml, ab125057); aSMA-Alexa Fluor 488, (Abcam, 2.5 µg/ml, ab184675); Mac3-Alexa Fluor 647, (Biolegend, 2.5 µg/ml, 08511); Myh11, (Abcam, 2.5 µg/ml, ab53219); Mouse IgG2a, k-biotin, (Biolegend, 2.5 µg/ml, 400203); Rat IgG1, k-Alexa Fluor 647, (Biolegend, 2.5 µg/ml, 400418); Rat IgG2a, k-Alexa Fluor 647, (Biolegend, 2.5 µg/ml, 400526); Rabbit IgG, (Abcam, 2.5 µg/ml, ab27478); Cd41 (eBioscience, 2.5 ug/ml, 14-0411-82). Sections were then washed 3x 5 mins in PBS and incubated with a secondary antibody diluted in blocking buffer where necessary; Streptavidin-Alexa Fluor 647, (Biolegend, 0.5 µg/ml, 405237); Goat Anti-Rabbit IgG-Alexa Fluor 647, (0.5 µg/ml, ab150079). Sections

were then washed 3 times: first in PBS for 5 mins, secondly in in DAPI, (1 µg/ml in PBS, 10 min at RT) and finally in PBS again for 5 mins. Sections were then mounted in RapiClear 1.52 with a coverslip.

3.10 5-ethynyl-2'-deoxyuridine administration and detection

5-ethynyl-2'-deoxyuridine (EdU) is a thymidine analogue able to incorporate into the DNA of proliferating cells. 300 µl EdU diluted in PBS (5 mg/ml) was injected intraperitoneally into mice post carotid ligation surgery (**section 3.11**) or during the high fat diet (**section 3.12**) and AAA (**section 3.13**) protocols at various time points (indicated in figure legends). At the point of choosing, carotid arteries and the aorta were removed and fixed as disused previously (**section 3.3**) and sectioned in the case of the atherosclerosis and AAA studies. The Click-iT® Plus EdU Alexa Fluor® 647 Imaging Kit (Life Tech, C10640) was then used to fluorescently label the incorporated thymidine analogue with the Alexa Fluor 647 dye. The protocol provided with the kit was followed closely for cryo-sections with a few adaptions listed below for the whole mount samples obtained from the ligation experiments. Permeabilisation time was increased from 30 mins to 1 hour in 0.5% Triton X-100 in PBS and incubation time within the Click-iT® Plus reaction mix was increased from 20 mins to 1 hour.

3.11 Carotid ligation protocol

Myh11-CreER(T2); R26R-Confetti mice of at least six weeks old were injected with either 1x 0.1mg, 1x 1 mg or 10x 1 mg of tamoxifen (over 2 weeks) to induce the desired level of recombination of the confetti allele (**Figure 11**). Animals were then rested for at least one week to allow tamoxifen depletion in order to avoid further recombination events.

To perform the ligation surgery, animals were anaesthetised (by inhalation) using a mixture of oxygen (1.5 L/min) with 2.5-3% isoflurane and given a pre-operative analgesic (~0.1 mg/kg body weight, Buprenorphine, Temgesic®) subcutaneously. The neck was shaved and cleaned with antiseptic soap prior to making a 1.5 cm long incision slightly to the left of the midline of the neck. Blunt forceps and retractors were then used to move the salivary gland and muscle out of the way to expose the LCA. Angled forceps were then used to separate the LCA from the surrounding vessels and vagus nerve. A piece of 0.7 braided suture (LOOK™) was then passed under the LCA and tied with two single throws to tighten just below the bifurcation. Several interrupted sutures, 0.7 polyglactin 910 absorbable suture (VICRYL™), were then used to close the incision prior to the mouse being placed in an incubator at 30 ^{o}C to recover. A proportion of mice were injected with EdU every week day following ligation up until and just prior (2 hours) before mice were culled (**section 3.10**). Mice were culled between 1-28 days post ligation surgery, tissue was processed as described (**section 3.3**). Post fixing, nuclei were

stained with 4', 6-diamidino-2-phenylindole (DAPI, 1ug/ml in PBS) for 1 hour at RT. Rapiclear 1.52 was used to clear (approx. 300 µl per aorta) and mount tissues between two coverslips containing a 0.5 mm iSpacer (Sunjin Lab) and imaged via confocal microscopy (**section 3.14**).

3.12 Atherosclerosis, high fat diet protocol

Myh11-CreER(t2); R26R-Confetti; ApoE$^{-/-}$ mice of at least six weeks old were injected with either 1x 0.1 mg, 1x 1 mg or 10x 1 mg of tamoxifen (over 2 weeks) to induce the desired level of recombination of the confetti allele (**Figure 11**). Animals were then rested for at least one week to allow tamoxifen depletion in order to avoid further recombination events.

Mice were then switched from chow to a HFD (Western Rd (p) Product code:829100 SDS, containing 21% fat and 0.2% cholesterol). EdU was injected for 7 days (including 2 hours) prior to culling between 16-19 weeks post switch to HFD (except where animals had to be culled prematurely, see **Appendix A**), tissue was then removed and fixed as described above (**section 3.3**). Samples were either embedded for cryo or vibratome-sectioning (**sections 3.7 and 3.8**), stained for Mac-3, aSma or Edu (**section 3.9 and 3.10**) and imaged by confocal microscopy (**section 3.14**).

3.13 Abdominal aortic aneurysm (AAA) protocol

All surgery, injections and live mouse work in this section was performed by Dr. Marc Clement, everything else was performed by Joel Chappell.

Myh11-CreER(T2); R26R-Confetti mice either on the ApoE$^{-/-}$ or wild type background and at least six weeks old were injected with 10x 1 mg of tamoxifen (over 2 weeks) to induce the desired level of recombination of the confetti allele (**Figure 11**). Animals were then rested for at least one week to allow tamoxifen depletion in order to avoid further recombination events.

Ang II (10 mg/ml in PBS, Sigma, A9525) was loaded in to Azlet model 2004 osmotic mini-pumps (Durect Corporation, Cupertino, CA) following the manufactures protocol, which will release Ang II at an approximate rate of 1000 ng/kg/min (as described in Daugherty and Cassis, 1999). For mini pump surgery, mice were anaesthetised by inhalation, using a mixture of oxygen (1.5 L/min) with 2.5-3% isoflurane and given a pre-operative analgesic (Temgesic, Buprenorphine) subcutaneously. A 1 cm cut was made across the back of the neck, blunt scissors were then inserted into the opening and used to separate the subcutaneous tissue by opening and closing the scissors to create a pocket. The mini-pump was then inserted into the pocket with the delivery portal going in first. The incision point was then closed and glued to seal.

Mice belonging to the Ang II-aTGFb protocol were injected with 250 µg mouse anti-human/mouse TGFb (Bioxcell, clone 1D11, BE0057) 3x per week intraperitoneally for four weeks if they were on a wildtype background and for only the second two weeks if they were on the $ApoE^{-/-}$ background, of the Ang II protocol. EdU was injected in all mice on days 15-21 before being culled day 28 post mini-pump surgery. Tissue was then processed as described (**section 3.3**) and cryo-sectioned in serial, prior to staining.

3.14 Confocal microscopy and image processing

Imaging was performed using confocal laser scanning microscopy (Leica SP5 or SP8), sequential scans with laser lines and detectors set for maximal sensitivity without spectral overlap, typically; DAPI (405 laser, 417-508 nm), CFP (458 laser, 454-502 nm), GFP (488 laser, 498-506 nm), YFP (514 laser, 525-560 nm), RFP (561 laser, 565-650 nm) and Alexa Fluor 647 (633 laser, 650-700 nm). A 20x oil objective (Plan Apochromat, numerical aperture 0.75, Multi-Immersion Correction Collar) was used to scan whole mount aortas, tile scans of Z-stacks totalling ~400 µm (~6-8 µm between each Z-section) were acquired, Z-compensation (laser power and gain) was used to allow for differences in fluorescent protein excitation/detection throughout the tissue. Vibratome sections were imaged using a 20x oil objective with a Z-stack typically totalling 100 µm (~5 µm between each Z-section). Cryo-sections were imaged using a 40x oil objective (Plan Apochromat, numerical aperture 1.30, Oil Immersion) with a Z-stack typically totalling 14 µm (~3 µm between each Z-section). Data was acquired at an optical section resolution of 1024 x 1024 and tiles were stitched using LAS software (Leica).

Imaris 8 software was used for image processing and analysis of whole-mount, vibratome and cryo-section samples. Processing includes brightness and contrast adjustments, generation of maximal projections, virtual cross sectioning and surface rendering. For calculation of patch size within whole-mount samples, surface modelling of individual patches using the surface rendering function within Imaris was used. A ‘patch’ was defined as a large contiguous mass of cells which share the same colour and occupy both neointimal and medial compartments of the vessel. To estimate cell number per patch, the surface volume was divided by the volume of an average of 8 individual VSMCs of the same colour.

Images shown in the results sections are maximal Z-projections (generated in Imaris) where indicated in figure legends or individual scans from a confocal Z-stack generated in FIJI (Schindelin et al., 2012).

3.15 Plaque and neointima scoring

Plaques were analysed from three regions within the vasculature; the carotid arteries (CA) comprising the region from where the right and left CA bifurcate to where they meet the aorta; the aortic arch (Arch) comprising the ascending aorta proximal to the aortic root and the arch region; and the descending aorta (DA) comprising the region distal to the Arch region to the diaphragm. For quantification of imaged cryo-sections, plaques were separated into three distinct regions; the cap region, which was defined as the organized layer of elongated cells on the inner most surface of the plaque adjacent to the lumen; the core region, which was defined as a disorganized mass of cells towards the centre of a plaque; and the shoulder region, which was defined as the mass of cells within the plaque which are immediately adjacent to the arterial wall on either side of the plaque. The neointima, within carotid ligation samples, was defined as the area between the inner elastic lamina (IEL) of the artery wall and the lumen. The few plaque samples observed which did not contain Confetti+ cells were not image and therefore not included in any analysis.

Quantification of labelled (Confetti+) and marker positive (Stain+) cells was performed on immuno-stained cryo-sections (20 µm for plaque and 14 µm for ligated arteries). Cells within an area of 1 mm^2 were counted for each plaque region and neointima. For almost all plaque regions/neointima (>60%, except where they were too small) two areas were scored for each and the average frequency used. Cell scoring was performed on confocal Z-stacks in Imaris in 3D to evaluate staining within Z-sections below and above the cell of interest. This ensures that counts are made on a cell by cell basis in the high-resolution Z-stacks. t-test and two-way ANOVA tests were performed within R (R Core Team, 2016) on selected variables to determine significant differences ($p<0.05$) as indicated in figures.

3.16 Calculating theoretical distribution of plaque colours

To compare the observed distribution of colours per plaque to what would be expected if plaques were generated from proliferation of 1, 2, 3 or 4 cells, a theoretical distribution was calculated as follows. All possible combinations of coloured cells were considered (e.g. if 3 cells proliferate there are 64 possible combinations: red-red-red, red-red-green, red-green-red, red-yellow-blue…). To calculate the probability of each colour combination, the known recombination frequency of each colour was applied (for example: red-red-red = 0.34 x 0.34 x 0.34, red-red-green = 0.34 x 0.34 x 0.07, red-green-red = 0.34 x 0.07 x 0.34, red-yellow-blue = 0.34 x 0.25x 0.33…). The frequencies for colour combinations of 1, 2, 3 and 4 colours were summed; for example, out of the 64 possible combinations of 3 cells there are 4 yielding one colour (red-red-red etc.) with a summed frequency of 0.063, 36x two colour combination (summed frequency=0.563), 24x three colour combinations (summed

frequency=0.375) and 0 x four colour combinations. The expected distribution is shown in **Figure 23 C** for comparison to the observed distribution shown in **Figure 23 B**.

3.17 Statistical analysis of bipotency

A Chi^2 test was used to assess whether monochromatic regions occupying both cap and core were observed more frequently than what would be expected by chance. This analysis was performed by Prof. Ben Simons (from Chappell et al., 2016).

To address the question of bipotency for each Confetti colour the observed data was compared against the null hypothesis that "the VSMC cap and core progenitors are unipotent". The fact that some plaques were observed with lineage labelled cells in either the cap or the core but not both suggests that, following activation, at least some of the cells are unipotent. To assess whether this could be the case, first it is assumed that contiguously labelled patches in the cap or the core region derive from clonal events. Then, according to the null hypothesis, the probability that a patch in the core will be labelled in colour c is given by

$$P_{\mathrm{core},c} = f q_c$$

where f denotes the fraction of fluorescently labelled cells, estimated at around 0.8 in the densely labelled sample, and q denotes the relative labelling efficiency of colour c. Similarly, the probability that a patch in the cap is labelled in colour c is given by $P_{\mathrm{cap},c} = P_{\mathrm{core},c}$. Then the chance that a clone of colour c in the core but not the cap is given by

$$P_{\mathrm{core},c}(1 - P_{\mathrm{cap},c})$$

(similarly cap but no core), while the probability that both core and cap acquire colour c is given by

$$P_{\mathrm{core},c} P_{\mathrm{cap},c}$$

If focus is shifted on to the ensemble of clones that contain colour c in the cap, the core or both, the relative probabilities must be normalized by the factor

$$P = P_{\mathrm{core},c}\left(1 - P_{\mathrm{cap},c}\right) + P_{\mathrm{cap},c}\left(1 - P_{\mathrm{core},c}\right) + P_{\mathrm{core},c} P_{\mathrm{cap},c}$$

So that the relative chance of finding a plaque with core labelling of colour c

$$r_{\mathrm{core},c} = \frac{P_{\mathrm{core},c}(1 - P_{\mathrm{cap},c})}{P}$$

Which is equal to $r_{\mathrm{cap},c}$, while the relative chance of finding both labelled in colour c is given by

$$r_{\mathrm{both},c} = P_{\mathrm{core},c} P_{\mathrm{cap},c} / P$$

Finally, for an ensemble of clonal events, it is expected that the statistical error on the measured fractions should become defined by the standard error of the mean, given by

$$r_{\mathrm{core},c}(1 - r_{\mathrm{core},c})/N)^{1/2}$$

where N denotes the total number of plaques sampled that contain colour c.

Thus, the observed Cap+Core frequencies are significantly higher for all four Confetti colours:

RFP	Cap	Core	Cap+Core	N
Observed	6	9	48	63
Calculated (r*N)	26	26	11	
error (SEM)	1.6	1.6	0.5	

YFP	Cap	Core	Cap+Core	N
Observed	3	4	20	27
Calculated (r*N)	12	12	3	
error (SEM)	1.1	1.1	0.2	

nGFP	Cap	Core	Cap+Core	N
Observed	1	1	8	10
Calculated (r*N)	5	5	0.4	
error (SEM)	0.8	0.8	0.02	

mCFP	Cap	Core	Cap+Core	N
Observed	4	3	20	27
Calculated (r*N)	12	12	4	
error (SEM)	1.1	1.1	0.2	

“Observed” is the measured number of cap only, core only and cap+core clones, “Calculated” is the expected number against the null hypothesis, and “Error” denotes the expected error (SEM) given the total number of clones that are measured (N).

3.18 Smart-seq2 protocol

The protocol used for Smart-seq2 is adapted from Picelli et al., 2014. Steps and reagents which encountered cells post FACS but prior to cDNA amplification were performed/prepared in a designated (pre-PCR, scRNA-seq) isolation hood. Where possible, all steps, unless otherwise stipulated, were performed on ice, cold block or at 4°C.

Sample preparation and **FACS/index sorting**

Aortas and carotid arteries were dissected and dissociated to single cells as described above (**sections 3.3 and 3.4**). The single cells suspension was initially washed in PBS and pelleted (1000 rpm for 5 mins) and re-suspended in a solution consisting of Zombie near infrared viability dye (Zombie NIR, Biolegend, 423105) diluted 1:100 in PBS (total volume ~150 µl), for 20 mins at RT. Cells were then washed in 0.5% BSA in PBS, to block non-specific binding of immunoglobulin to the Fc receptors, cells were then re-suspended in TruStain fcX (BioLegend, 101320, diluted 1:100 in 0.5% BSA in PBS) for 10 mins at 4°C. To this solution Anti-Sca1-APC (Miltenyi Biotec, 130-102-343) or Rat-IgG2a-APC (Miltenyi Biotec, 130-102-655) was added so to be diluted 1:10 and incubated for 15 mins at 4°C. Cells were then washed in 0.5% BSA in PBS twice before being re-suspended in a final volume of 300 µl 0.5% BSA in PBS and filtered through a 70 µm cell strainer.

Single Confetti+, Zombie NIR-negative VSMCs were isolated/sorted by FACS, into individual wells of a 96 well plate (Thermo Scientific) containing 2.3 µl recombinant ribonuclease inhibitor (RRI, 40 U/µl, Clontech) diluted to 1:20 in 0.2% TritonX (in RNase-free dH_2O, Sigma-Aldrich), per well. Following FACS sorting the plate was sealed (Microseal 'B', BIO-RAD), spun down (1 min at 1000 rpm, 4°C) and placed in a -80°C freezer for ~30 mins.

Reverse transcription PCR (RTPCR)

After allowing the cells to thaw, 2 µl of annealing mixture, containing: 0.1 µl ERCC (stock product was previously diluted 1:400,000 in dH_2O, Invitrogen, 4456740), 0.1 µl Oligo-dT (100 µM, Biomers.net, 5'–AAGCAGTGGTATCAACGCAGAGTAC(T30)VN-3'), 1 µl dNTP (10 mM, Life Technologies, R0192) and 0.8 µl dH_2O was pipetted into each well of the 96 well plate. The plate was spun down (1 min at 1000 rpm, 4 °C) and incubated at 72°C for 3 mins before being immediately placed on ice. 5.7 µl of reverse transcription mixture, containing 0.5 µl PrimeScript Reverse Transcriptase (200 U/µl, Clontech), 0.125 µl RRI, 2 µl 5X PrimeScript Buffer (Clontech), 0.5 µl 1,4-Dithiothreitol (DTT, 100 µM, Sigma), 2 µl Betaine (5 M, Sigma, B0300), 0.06 µl $MgCl_2$ (1 M, Invitrogen), 0.1 µl Template switching oligo (TSO, 100 µM, Exiqon, 5'–AAGCAGTGGTATCAACGCAGAGTACATrGrG+G-3') and 0.415 µl dH_2O was then pipetted

into each well of the plate. The plate was spun down and placed in a SimpliAmp Thermal Cycler (Life Technologies) with the following conditions:

Cycle no.	Temperature (°C)	Time
1	42	90 mins
10	50	2 mins
	42	2 mins
1	70	15 mins
-	4	hold

cDNA amplification

Following RTPCR, 15 µl of PCR mixture, containing: 12.5 µl KAPA HiFi Hotstart (Kapa Biosystems), 0.25 µl ISPCR oligo (10 µM, Biomers.net, 5'-AAGCAGTGGTATCAACGCAGAGT-3') and 2.25 µl dH_2O, was added to each well. The plate was then spun down and placed in a thermal cycler under the following conditions:

Cycles no.	Temperature (°C)	Time
1	98	3 min
24	98	20 secs
	67	15 secs
	72	6 mins
1	72	5 mins
-	4	hold

PCR clean up

A bead clean-up method was then used to clean the sample of left over reagents/unwanted material, Ampure XP beads (Agencourt) were equilibrated at RT for 15 mins and vortexed. 25 µl of beads were then added to each well and mixed (by slow vortexing) and incubated at RT for 8 mins. The plate was placed on a magnetic stand (Thermo Fisher) for 5 mins to collect the beads to one edge of each well. The supernatant was then discarded and each well washed twice with 200 µl 80% EtOH (vol/vol) for 30 secs while the plate remains on the magnet. The plate was then spun and any remaining EtOH removed before being left to air dry for 5 mins. 20 µl elution buffer (Qiagen) was then added to each well and mixed (very slowly by vortexing). Finally, the plate is placed on the magnet for a further 2 mins and the cDNA containing supernatant transferred to a new plate.

Quality control

Following bead clean up samples went through a quality control step. In total, 9 samples across the plate were run on an Agilent Bioanalyzer using the Agilent High Sensitivity DNA Chips (Agilent Technologies), to the manufacturers protocol. If samples contain uncontaminated cDNA (i.e. only cDNA is detected within the sample, as in **Figure 49**) the whole plate passes this quality control step.

cDNA from all samples was then quantified using the Quant-iT™ PicoGreen™ assay kit (Thermo Fisher), following the manufacturers protocol. In short each well in a U-bottom plate (PerkinElmer) is filled with 49 µl 1x TE buffer, 50 µl pico-green (diluted 1:200 in TE) and 1 µl of sample (control wells, necessary for calculating standard curve, received 1 µl of Lambda DNA, so that 25 ng, 10 ng, 2 ng, 0.4 ng, 0.08 ng and 0.016 ng samples were represented). The plate was then left to incubate for 5 mins in the dark and read on a plate reader (BioTek, Synergy HT). Finally, samples were diluted so they are roughly the same concentration (typically to ~5 ng/µl).

Library preparation

cDNA library preparation was performed using the Nextera XT kit, the manufacturers protocol followed. In brief, the NT and tagmentation buffers were brought to RT and gently vortexed to mix. Tagmentation DNA buffer and the amplicon tagment mix were mixed to a ratio of 2:1, and 3.75 µl of this mix was added to each well of a new plate. Also added to each well is 1.25 µl of sample cDNA (~6.25 ng). The plate is then sealed and spun at 2000 rpm for 1 min before being placed in a thermal cycler at 55 ^{o}C for 10 mins. Following this incubation, to each well the following was added: 1.25 µl of NT buffer, 3.75 µl Nextera PCR mix, 1.25 µl of index primer 1 and 1.25 µl of index primer 2. Every single well contained a different combination of the index primer 1 and 2 which allows cell identification following sequencing. The plate was then sealed, spun down at 2000 rpm for 1 min and placed on a thermal cycler, under the following conditions:

Cycles no.	Temperature (^{o}C)	Time
1	72	30 secs
12	95	10 secs
	55	30 secs
	72	30 secs
1	72	5 mins
-	10	hold

Library pooling/clean up

Ampure XP beads were again used for post PCR clean-up purposes. Beads were equilibrated at RT for 15 mins and vortexed, 1 µl of cDNA from each well was pooled together and mixed with 87 µl of beads. The pooled sample was mixed by pipetting and incubated at RT for 5 min before being placed on a magnet for 2 mins. Supernatant was then discarded and the beads were washed twice with 180 µl 70% EtOH (vol/vol). The sample was then spun down and any remaining EtOH removed before being left to airdry for 5 mins. 43 µl of elution buffer was then added and the sample vortexed and left to incubate at RT for 2 mins. The sample was then placed on the magnet for a further 2 mins and the supernatant collected into a new tube.

Quality control and library quantification

The pooled sample was checked for quality and contamination on an Agilient Bioanalyzer (described above) and quantified using the KAPA Library Quantification kit (Kapa Biosystems) following the manufacturers protocol.

Sequencing

For sequencing the NextSeq 500 Mid Output 75 bp Paried End system was used in the Babraham Institute's sequencing facility, Cambridge.

3.19 Chromium 10x protocol

To perform scRNA-seq using the 10x Chromium system (10x Genomics), the carotid arteries and aorta were dissected from Confetti mice (**section 3.3**), digested to a single cell suspension (**section 3.4**) and stained with Zombie NIR (**section 3.18**). Single cells were sorted on an Aria-Fusion FACS machine in 0.1% BSA in PBS, using a strict gating strategy in order to collect cells positive for only one of each fluorescent proteins. Following FACS, the cells were spun down at 3000 rpm for 3 mins at 4^{O}C and the supernatant discarded. The collected cells were then re-suspended to a concentration of 6000 cells/33.8 µl in 0.1% BSA in PBS. Cells, on ice, were then delivered to the Genomics core facility in Cancer Research UK, Cambridge Institute and loaded in to the Chromium machine (10x Genomics) where automated RTPCR, cell barcoding and cDNA amplification took place. NextSeq 500 Mid Output 75 bp Paried End sequencing was then performed in the Babraham Institute's sequencing facility, Cambridge.

Chapter 4: Characterisation and specificity of the Confetti reporter

The Confetti reporter (**Figure 11, section 2.1**) is a valuable tool for multi-colour lineage tracing and can, if used correctly, determine clonality. To use the Confetti system effectively and ensure it is functioning as required for subsequent experiments (**Chapters 5-8**) it was important to test its tissue specificity when recombined by the Myh11-CreER(T2), and determine its labelling efficiency given different amounts of tamoxifen. To achieve this, whole-mount imaging and flow cytometry of tissue/cells from tamoxifen injected Myh11-CreER(T2); Rosa26-Confetti mice was analysed.

Aims:

1. Determine optimal tamoxifen dose/concentration for low density (clonal) and high density (mosaic) labelling of VSMCs
2. Determine specificity of the Myh11-CreER(T2) transgene when recombining the Rosa26-Confetti construct
3. Determine the relative activation of each fluorescent protein within the Confetti construct

4.1 Tamoxifen dose and recombination of the confetti reporter

To determine the relationship between tamoxifen dose and recombination frequency of the Confetti allele, different concentrations of tamoxifen were injected intraperitoneally into Myh11-CreER(T2); Rosa26-Confetti mice. Knowing the frequency at which the confetti construct is recombined given an amount of tamoxifen allows the construction of experiments tailored to answering different questions, for example, whether proliferative events can be considered mono or poly-clonal or determining the proportion of cells which proliferate post injury. Low doses of tamoxifen (0.2-0.08 mg) were injected to obtain the optimal dose for 'clonal labelling' of VSMCs. Meaning a recombination frequency sufficiently low that a single labelled cell will be substantially separated from the nearest labelled cell of the same colour. To achieve a high or 'mosaic' labelling frequency, 10 mg of tamoxifen was administered over 2 weeks, this was based on previous studies using the same Cre-transgene, to achieved >95% recombination frequency of a Rosa26-STOP-floxedYFP allele in mice (Gomez et al., 2013).

Initially, whole-mount imaging (**Figure 14**) was used to test the tamoxifen dose-recombination relationship. Despite some variability between mice injected with the same dose of tamoxifen, 0.12

and 0.08 mg doses (**Figure 14, D/G/H**) appeared suitable for the clonal analysis planned for later experiments. Dense, mosaic, labelling was achieved by injecting 10 mg of tamoxifen (**Figure 14, A**) as expected based on a previous study using the same Myh11-CreER(T2) transgene (Gomez et al., 2013).

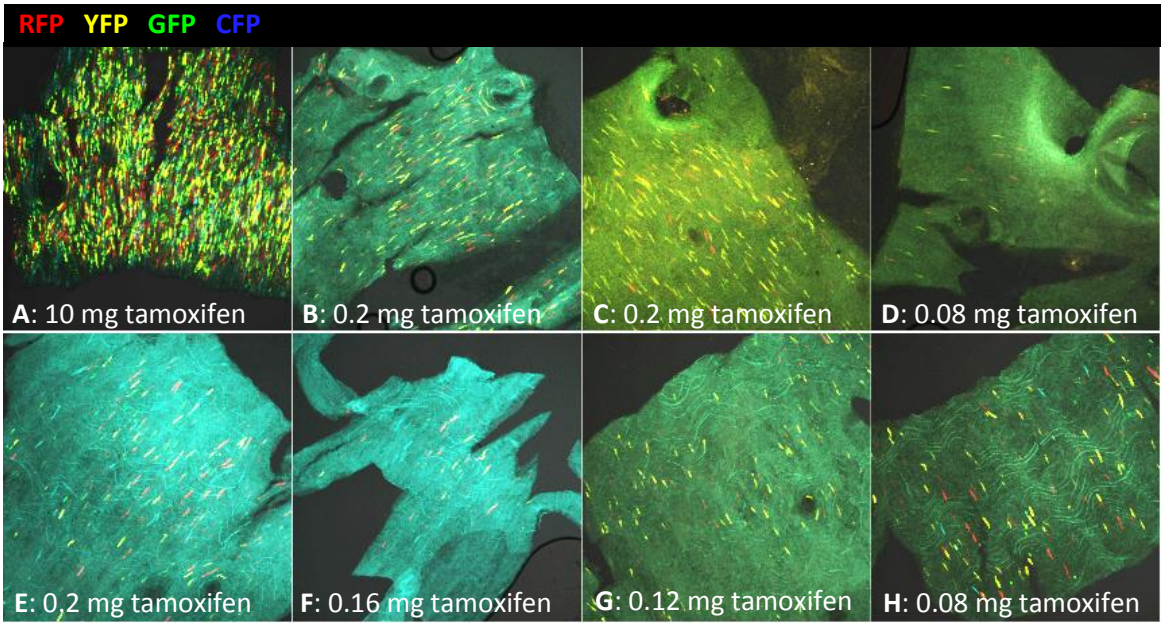

Figure 14: Clonal and mosaic labelling of VSMCs is achievable by varying tamoxifen concentration in Myh11-CreER(T2); R26R-Confetti mice

Images are max projection confocal images of flattened sheets of aortic tissue from Myh11-CreER(T2); R26R-Confetti mice injected with different concentrations of tamoxifen 1 week prior to death. Tamoxifen dose is displayed on each panel.

To quantify the level of recombination at each tamoxifen dose, flow cytometry was used to analyse dissociated cells from the aorta of Myh11-CreER(T2); R26R-Confetti mice injected with different concentrations of tamoxifen. This analysis (**Table 1**), identified that 10 mg of tamoxifen administered over a two-week period resulted in labelling up to 93% of VSMCs, however there was a great deal of variability at this dose (79% ±14%). The doses 0.12 and 0.08 mg, identified by microscopy as a good dose for 'clonal' labelling, labelled approximately 1% of VSMCs.

Cell type, Genotype, Tamoxifen dose (n no.)	Fluorescently labelled (%)			Non-labelled (%)		
	Average	Max	Min	Average	Max	Min
VSMCs wild type, 10 mg (n=1)	0	N/A	N/A	100	N/A	N/A
VSMCs confetti$^+$, 0 mg (n=2)	0.4	0.4	0.3	99.7	99.7	99.6
VSMCs confetti$^+$, 10 mg (n=6)	78.5	92.9	69.6	21.5	30.4	7.1
VSMCs confetti$^+$, 0.2 mg (n=2)	2.9	3.7	2.2	97.1	97.8	96.3
VSMCs confetti$^+$, 0.16 mg (n = 1)	1.7	N/A	N/A	98.3	N/A	N/A
VSMCs confetti$^+$, 0.12 mg (n = 1)	1	N/A	N/A	99	N/A	N/A
VSMCs confetti$^+$, 0.1 mg (n=3)	0.8	1	0.5	99.2	99.5	99
VSMCs confetti$^+$, 0.08 mg (n=2)	0.6	0.7	0.5	99.4	99.5	99.3
VSMCs confetti$^+$, 0.004 mg (n=1)	0.1	N/A	N/A	99.9	N/A	N/A

*NA: Not applicable

Table 1: The tamoxifen dose-recombination relationship within Myh11-CreER(T2); R26R-Confetti mice

Flow cytometry data for isolated VSMCs from Myh11-CreER(T2); R26R-Confetti mice and wild type mice given different doses of tamoxifen. Adapted from Chappell et al., 2016.

When flow cytometry and whole-mount data were considered together, 0.1 mg of tamoxifen was chosen to induce a labelling frequency appropriate for delineating clonal expansion in later experiments. For mosaic labelling of up to 90% of cells, 10 mg was selected, higher doses of tamoxifen were not considered desirable to inject mice with.

It should be noted that there were some issues in optimising flow cytometry analysis of Confetti samples, this was due to the significant number of cells which were detected positive for two fluorescent markers, particularly between the violet and yellow lasers, detecting CFP and RFP, respectively. Confetti+ embryonic stem cells cloned from cells containing each individual fluorescent protein did not give double positive cells (data not shown). It is possible that the VSMC isolation protocol (**section 3.4**) results in the fragmentation of some cells and that these fragments stick to other single cells, this may be particularly prevalent with membrane bound CFP. However, regardless of the reason for the double positive VSMCs this demonstrates the need for strict gating strategies to ensure that single cells can be identified and isolated in future experiments, as will be discussed in **Chapter 8**.

To confirm labelling frequencies and calculate the proportion of cells expressing each colour, aortas/carotid arteries from tamoxifen injected mice were cryo-sectioned and stained with DAPI prior to confocal microscopy. **Figure 15** shows examples of sections from densely (**A**) and clonally (**B**) labelled animals, it is clear from these data that the majority of DAPI positive cells within the media of the high labelled tissue are confetti positive with the reverse true for the clonally labelled tissue. True

for both is that DAPI positive cells within the adventitia and intima are always confetti negative (as indicated by the arrow heads in **A, ii**).

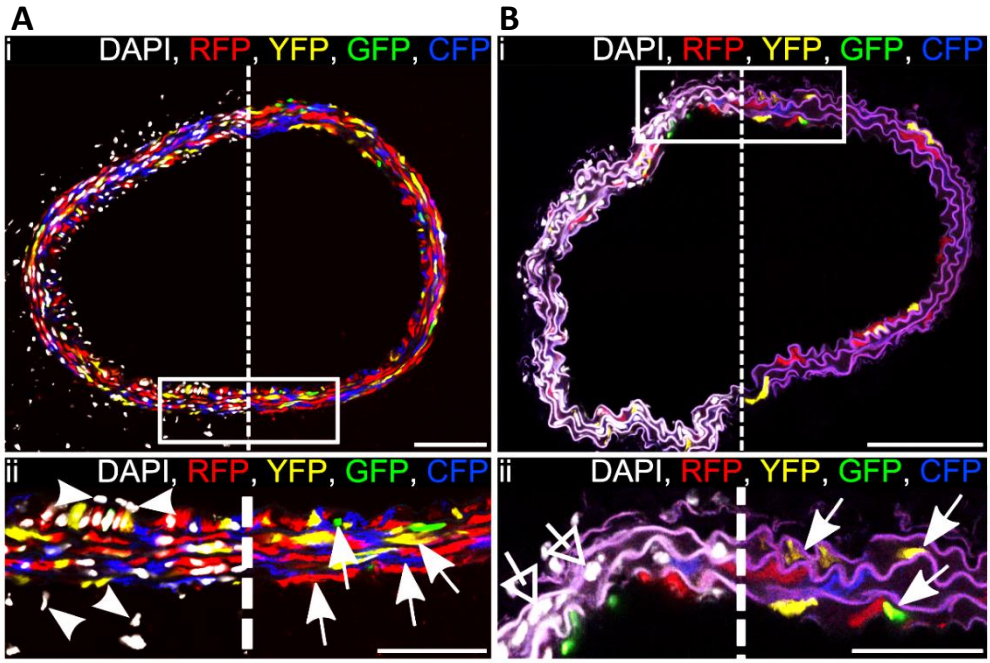

Figure 15: Clonal and dense labelling of VSMCs within arteries from Myh11-CreER(T2); R26R-Confetti mice

Carotid artery cross sections from high density-labelled (**A,** 10x 1 mg tamoxifen) or low density-labelled (**B,** 1x 0.1 mg tamoxifen) animals, region outlined in (**i**) is magnified in (**ii**). Signals for fluorescent proteins are shown with (left) and without (right) nuclear DAPI staining (white). VSMCs, indicated by arrows in (**A and B ii**), are labelled with RFP (red), YFP (yellow), nuclear (n)GFP (green) or membrane associated (m)CFP (blue), whereas cells within the adventitia and endothelium, indicated by arrow heads, are unlabelled. In (**B ii**) arrows point to the few labelled VSMCs, open arrows point to unlabelled VSMCs within the media. Scale bars are 100 µm in (**i**) and 50 µm in (**ii**). Adapted from Chappell et al., 2016.

Quantifying the proportion of cells expressing each colour (**Table 2**) shows that the Confetti construct, following recombination by the Myh11-CreER(T2) transgene, results in a bias against the expression of nuclear GFP relative to the other three proteins, this phenomenon has also been observed in others work under the control of different Cre transgenes (Snippert et al., 2010). The reason for this is not entirely clear, however, one reason could be that GFP may be more toxic compared to the other fluorescent proteins. Resulting in the death of GFP+ cells. A second reason, suggested by Snippert et al., (2010) and The Jackson Laboratory (2015), is that low Cre activity favours the inversion of the loxP-STOP-loxP-GFP-PFY-Pxol sequence (Neo-GFP-YFP region, **Figure 11**) over the excision of the loxP-STOP-loxP sequence, leading to fewer GFP expressing cells.

	Mosaic/dense labelling	Clonal labelling
Fluorescent protein	**Percent of medial cells labelled**	
CFP	31	1
RFP	32	2
GFP	7	0
YFP	23	1
No colour	7	96

Table 2: Proportion of cells within the medial layer of the aorta and carotid arteries which express each of the four fluorescent colours within Myh11-CreERt2; R26R-Confetti mice. Adapted from Chappell et al., 2016.

As the proportion of colours are not equal it is important to factor this knowledge into any statistical calculations that may be used in future experiments which assume that clonality can be determined based on how often groups of cells expressing the same colour are seen. Later sections will explain how this is done in order to identify clonality.

4.2 The tamoxifen activated Myh11-CreER(T2) transgene specifically recombines the R26R-Confetti reporter in VSMCs

As the Myh11-CreER(T2); R26R-Confetti mice will be used to analyse VSMC proliferation within multiple models of CVD, it is vital that the Confetti reporter is specifically expressed in VSMCs. Particularly as the origin of cells within the neointima of injured vessels has been disputed in the past, with evidence supporting that these cells are derived from bone marrow, adventitial and medial stem cells (Albarrán-Juárez et al., 2016; Kramann et al., 2015; Tang et al., 2012, **section 1.5**). Other groups have observed selective expression of other reporter constructs when recombined by the Myh11-CreER(T2) transgene (Gomez et al., 2013; Nemenoff et al., 2011), indicating that the Confetti reporter should also be selectively expressed. Indeed, longitudinal cross sections of the arterial wall (**Figure 16**) identify that only medial cells express the Confetti construct, within the vascular wall following the administration of tamoxifen (10x 1 mg), and that no adventitial or endothelial cells express any of the fluorescent proteins.

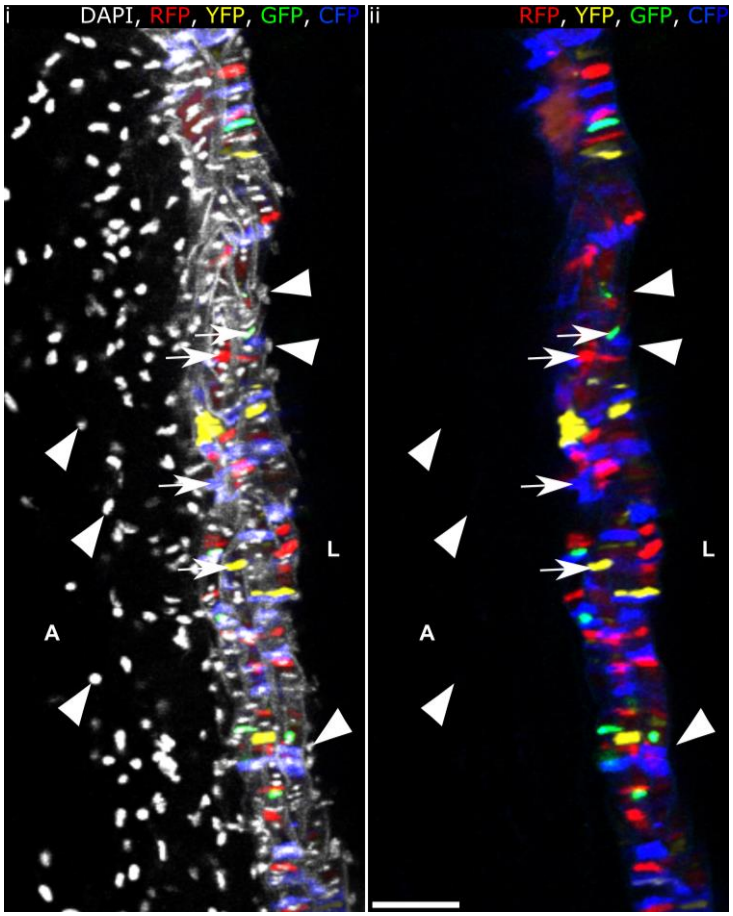

Figure 16: Confetti+ cells are localised to the media of the arterial wall in Myh11-CreER(T2): R26R-Confetti mice
Longitudinal cross section of a whole-mount carotid artery from a Confetti animal labelled at high density (10x 1 mg tamoxifen). Signals for fluorescent proteins are shown with (**i**) and without (**ii**) nuclear DAPI (white). Arrows point to labelled VSMCs within the medial layer, arrow heads point to unlabelled cells within the endothelium and adventitia. The luminal side is denoted as "L" and the adventitial side marked "A". Scale bar is 50 µm. Adapted from Chappell et al., 2016.

To assess the tissue specificity of recombination in other (non-vascular) tissues, fluorescence was analysed from a number of other cell types and tissues. As bone marrow and circulating blood born cells have been implicated in vascular disease, these cells were extracted from mice and analysed via flow cytometry alongside cells dissociated form the aorta of Myh11-CreER(T2); R26R-Confetti mice which had received tamoxifen to induce dense labelling. Out of the three Confetti+ mice analysed (**Table 3**) there were very few events in either the peripheral blood or bone marrow, the few positive events detected occurred at a comparable rate to that seen in Wild type animals, so is therefore likely the result of auto-fluorescence or contamination (e.g. red blood cells or dead cells).

Mouse no.	ID	Sample	Proportion of positive events	Number of singlet events
1	Wild type	Peripheral blood	0.0006	>25000
2	Wild type		0.0003	>65000
3	Wild type		0.00007	>65000
4	Confetti+		0.0001	>65000
5	Confetti+		0.00009	>65000
6	Confetti+		0.0001	>65000
1	Wild type	Bone marrow	0.00002	>400000
2	Wild type		0.00001	>400000
3	Wild type		0.00007	>200000
4	Confetti+		0.00001	>400000
5	Confetti+		0	>400000
6	Confetti+		0.00002	>400000
1	Wild type	Aorta	0.0002	>9000
2	Wild type		0.0001	>30000
3	Wild type		0.0005	>30000
4	Confetti+		0.62	>30000
5	Confetti+		0.63	>30000
6	Confetti+		0.67	>30000

Table 3: Specific labelling of VSMCs in Myh11-CreER(T2); Rosa26-Confetti mice

Flow cytometry analysis demonstrating background levels of fluorescence in bone marrow and peripheral blood from non-tamoxifen treated wild type animals and experimental Myh11-CreER(T2); Rosa26-Confetti animals labelled at high density (10x 1mg tamoxifen). Samples were gated for live cells (FSC-A, SSC-A) and singlets (FSC-A, FSC-H). Positive cells were identified based on gates set on VSMCs from Wild type and Confetti+ animals. Adapted from Chappell et al., 2016

To assess specificity in solid tissues, vibratome sections of liver, skeletal muscle and lung from Myh11-CreER(T2); Rosa26-Confetti mice, injected with 10 mg tamoxifen, were analysed by confocal microscopy. The only detectable florescence from these sections were within the vasculature within each tissue (**Figure 17**) confirming recombination is specific to VSMCs in all tissues/cell types analysed.

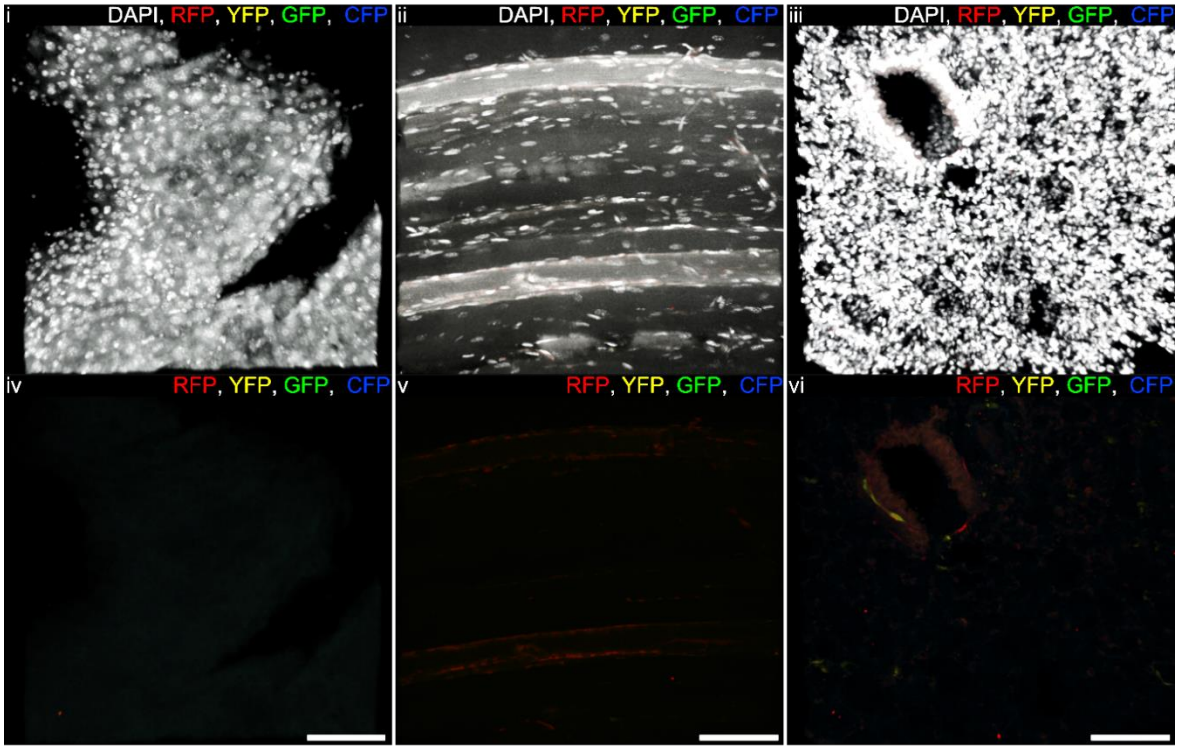

Figure 17: Specific labelling of VSMCs in Myh11-CreER(T2); Rosa26-Confetti mice
Confocal microscopy images showing absence of recombination in liver (**i, iv**), skeletal muscle (**ii, v**) and lung (**iii, vi**) in Confetti animals after tamoxifen treatment (10x 1 mg). Note that labelled cells in (**vi**) correspond to VSMCs lining a blood vessel. Signals for fluorescent proteins are shown with (**i, ii, iii**) and without (white, **iv, v, vi**) nuclear DAPI staining. Scale bars are 100 µm.

4.3 Conclusion from the Confetti characterisation and specificity experiments

Results within this chapter show that the Myh11-CreER(T2) transgene specifically recombines the Confetti construct within VSMCs and that there is a relationship between the quantity of tamoxifen injected and the proportion of cells labelled. Dosing strategies were established for high density (10x 1mg tamoxifen) and low density (1 x 0.1 mg tamoxifen) labelling of VSMCs, which will be used in subsequent experiments (**Chapters 5-8**). It was also noted that there is a slight bias against the expression of nuclear GFP, in favour of the other three fluorescent proteins which are expressed at near equal levels.

Chapter 5: VSMC proliferation and plasticity in a model of atherosclerosis

As discussed in (**sections 1.5 and 1.6**) there has been, in recent years and indeed as far back as the 1970's, some discussion concerning the origins of atherosclerotic plaque cells, for example; VSMC-derived, bone marrow-derived or adventitial-derived, and if they are indeed VSMC-derived whether this is a clonal process arising from the proliferation of few cells (Gomez et al., 2013; Albarrán-Juárez et al. 2016; Kramann et al. 2015; Benditt and Benditt, 1973; Feil et al., 2014). Furthermore, it is known that VSMCs have the potential to trans-differentiate into multiple cell types within a plaque, including: macrophage-like, MSC-like and myofibroblast-like cells (Shankman et al., 2015). It is not, however, clear whether single VSMCs are multi-potent, capable of trans-differentiating into all observed VSMC-derived cell phenotypes or if distinct VSMCs are, for example, uni-potent and produce a single subset of these cells.

If plaques are monoclonal and derived from the proliferation of a single VSMC, then this would suggest that a single VSMC has the potential to trans-differentiate into all known VSMC-derived plaque cells. Furthermore, it would suggest that individual VSMCs which respond to disease may be inherently different to medial VSMCs which do not respond to disease. Plaque mono-clonality was originally hypothesised by Benditt and Benditt (1973), based on their study investigating X-inactivation patterns of the X-linked glucose-6-phosphate dehydrogenase protein. Their work demonstrated that plaques would typically contain only one of the protein isotypes, whereas the media would contain both (Benditt and Benditt 1973). This hypothesis was, however, challenged when more sensitive methods using PCR amplification of an X-inactivated gene showed that large portions of the non-atherosclerotic media also contained only one protein isotype (Schwartz and Murry, 1998). More recently, Feil et al., (2014) used the confetti system (described in **section 2.1 and Chapter 4**) to lineage trace VSMCs in a mouse model of atherosclerosis. Based on this study Feil et al., (2014) suggest that plaques are mono-clonally derived as they appeared to be single coloured, their work was however limited in several ways: (1) plaques were imaged in whole mount, which does not allow investigation of cells within the plaque as the lipid content prevents light penetration; (2) a labelling frequency of 11% was used, meaning there is significant potential for unlabelled VSMCs to contribute to plaques; and (3) the Sm22α-CreER(T2) transgene was used, while Sm22α is a classical marker used to define VSMCs it is not exclusively expressed in VSMCs. Indeed Cre expression in mice containing the Sm22α-Cre has previously been detected in myeloid and lymphoid cells, with the authors suggesting that caution should be taken when analysing data using the Sm22α-Cre given known contributions of myeloid cells to vascular development and CVD (Shen et al. 2012). Espagnolle et al. (2014), have since shown an association between CD146 expression and bone marrow mesenchymal stem cell (BM-MSC)

commitment to a VSMC lineage, with CD146(High) BM-MSCs expressing detectable levels of Sm22α. Others have also detected Sm22α-Cre expression in epithelium (Proweller et al. 2006) and cardiomyocytes (Zhang et al. 2006). Based on these limitations, the experiments by Feil et al. (2014) cannot definitively show that plaques are mono-clonally derived.

To answer the questions regarding plaque clonality and the ability of single VSMCs to trans-differentiate into multiple VSMC-derived cell types, the Myh11-CreER(T2) is used to recombine the Confetti reporter (described in **section 2.1**) in ApoE$^{-/-}$ mice fed a HFD for 16-19 weeks. The ApoE$^{-/-}$ background in combination with HFD is used here as it recapitulates a chronic inflammatory model of atherosclerosis, resulting in the formation of large atherosclerotic plaques by week 16 of HFD feeding (described in **section 2.2**). To investigate clonality, thick vibratome-sections and thin cryo-sections are analysed to visualise every cell within a plaque. Furthermore, cryo-sections are stained for aSma (contractile maker) and Mac3 (macrophage marker) to identify if a single VSMC can give rise to different VSMC-derived cell types. Finally, VSMC contribution to/between: (1) plaques in different regions of the vasculature (aortic arch, descending aorta (DA) and carotid arteries (CA), **Figure 18A**); (2) different regions of a plaque (cap, core and shoulder, **Figure 18 B**); and (3) plaques in individual mice, are investigated.

Aims:

1. Assess the extent of clonal proliferation of VSMCs within atherosclerosis
2. Assess relative contribution of VSMC migration as opposed to proliferation within atherosclerotic plaques
3. Determine if the progeny of a single VSMC can trans-differentiate into multiple cell types

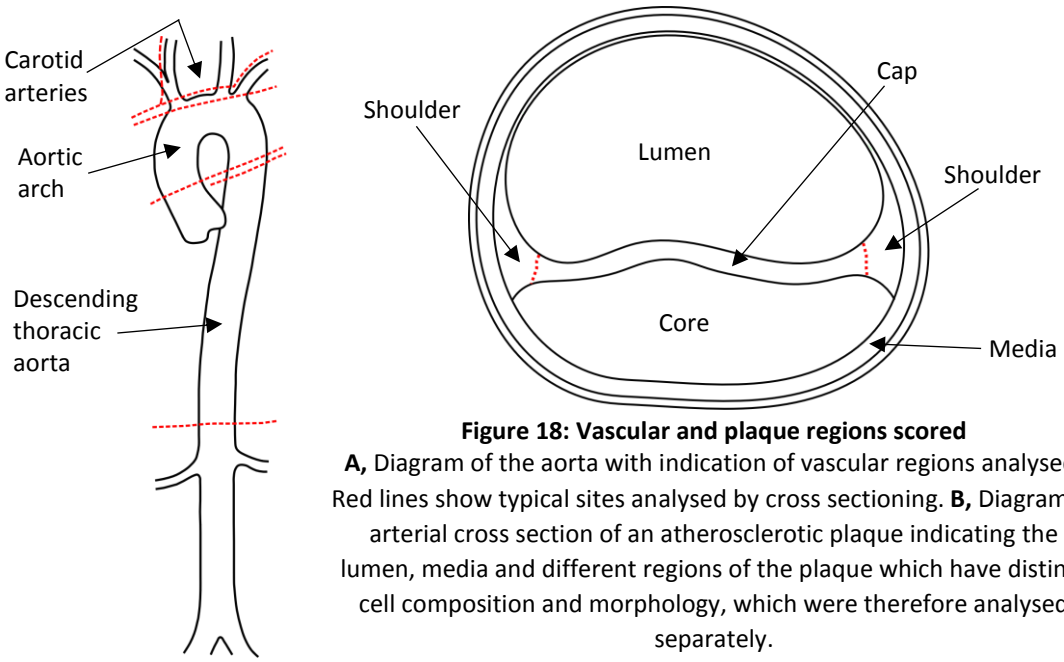

Figure 18: Vascular and plaque regions scored
A, Diagram of the aorta with indication of vascular regions analysed. Red lines show typical sites analysed by cross sectioning. **B,** Diagram of arterial cross section of an atherosclerotic plaque indicating the lumen, media and different regions of the plaque which have distinct cell composition and morphology, which were therefore analysed separately.

5.1 The Confetti reporter is selectively expressed in VSMCs in Myh11-CreER(T2); R26R-Confetti; ApoE$^{-/-}$ mice in the HFD model of atherosclerosis

To test that the ApoE$^{-/-}$ background and/or the 16-week HFD protocol does not cause non-tamoxifen induced recombination of the Confetti reporter or that tamoxifen administration alone does not cause plaque growth, vibratome sections from control animals on HFD were analysed (**Figure 19**). Results demonstrate that: (1) no fluorescence is detectable in Wild type; ApoE$^{-/-}$ mice which received tamoxifen and HFD (**Figure 19, A/B**), (2) tamoxifen and HFD does not cause atherosclerosis in Myh11-CreER(T2); R26R-Confetti; ApoE$^{+/-}$ mice (**Figure 19, C/D**) and (3) HFD does not induce recombination of the confetti allele in Myh11-CreER(T2); R26R-Confetti; ApoE$^{-/-}$ mice (**Figure 19, E/F**). These controls confirm that the Confetti mice are suitable for future studies and that there are no off target effects of either tamoxifen or the Confetti reporter in combination with HFD/the ApoE$^{-/-}$ background.

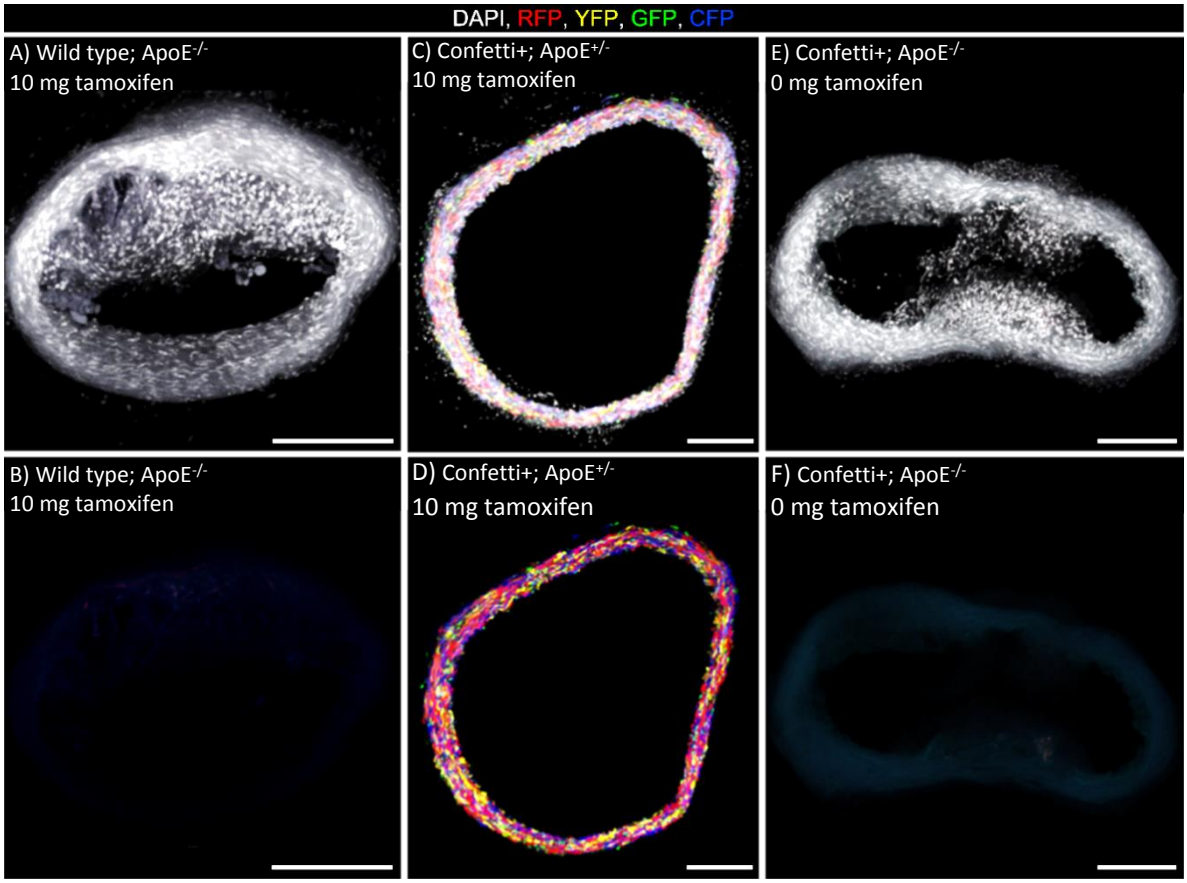

Figure 19: Specificity control data in the HFD model of atherosclerosis
Max projection of confocal scans of 100 µm thick vibratome sections from mouse aortas and carotid arteries of experimental/control animals after 16-weeks of HFD, showing signals from fluorescent proteins with (**A**, **C**, **E**) or without (**B**, **D**, **F**) DAPI. ApoE and Confetti genotype and dose of tamoxifen is displayed on each image. Sections containing plaque are visible in (**A**) and (**E**). Scale bars are 200 µm.

5.2 VSMCs clonally expand to contribute to plaque development

To definitively determine whether VSMC-derived cells within atherosclerotic plaques are clonally derived, 6-8-week-old Myh11-CreER(T2); Rosa26-Confetti; ApoE$^{-/-}$ mice were injected with 10 mg of tamoxifen to induce dense labelling of VSMCs. Mice were then rested for 1 week to allow tamoxifen depletion and avoid further recombination events prior to feeding them an atherosclerosis-inducing HFD for 16-19 weeks (**Figure 20 A**, **Appendix A**).

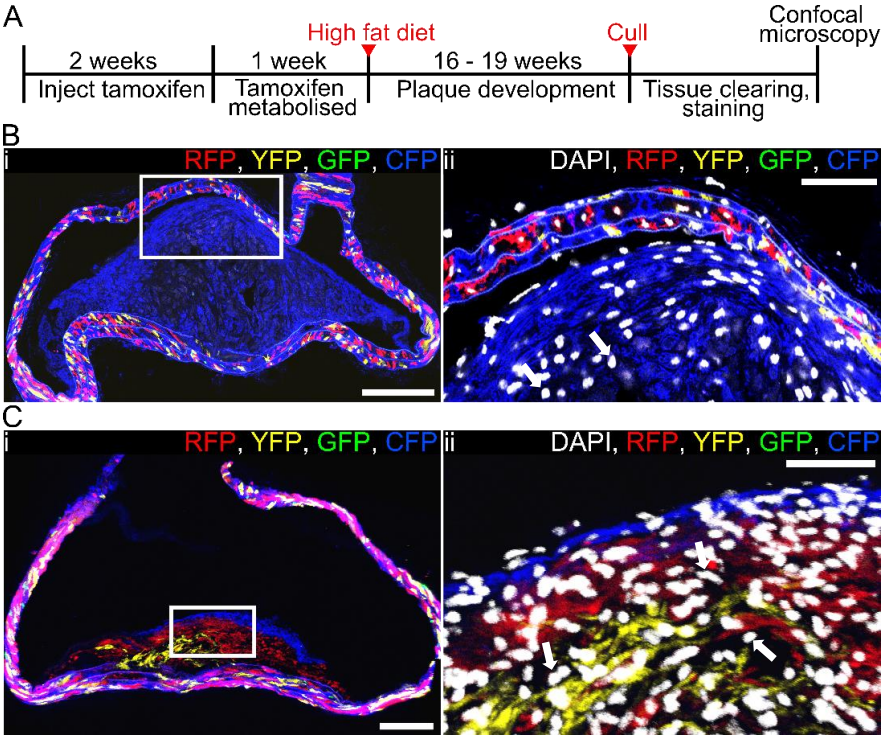

Figure 20: VSMC-derived cells generate oligo-clonal atherosclerotic plaques

A, Experimental protocol for the atherosclerosis studies. **B, C,** Arterial cryo-sections from high density-labelled animals (10x 1 mg tamoxifen) presenting plaques containing VSMC-derived cells of a single colour (CFP/blue, **B**) and more than one colour (RFP/red, mCFP/blue, YFP/yellow. **C**). The region outlined in (**i**) is magnified in (**ii**). Scale bars are 150 µm (**i**) and 50 µm (**ii**). Signals for fluorescent proteins and nuclear DAPI in (**ii**, white) are shown. Arrows in (**ii**) point to non-labelled cells interspersed throughout the plaque. Adapted from Chappell et al., 2016.

Accumulation of VSMC-derived cells was assessed by confocal microscopy of arterial cross sections. Cells expressing the Confetti reporter (Confetti+), and therefore derived from mature Myh11-expressing VSMCs, were observed within atherosclerotic plaques and constituted a significant proportion of the total plaque cell number (**Figure 20 B, C**). In order to assess and compare VSMC contribution to plaques within different regions of the vasculature (Arch, DA and CA) and within different regions of the plaque (cap, core and shoulder) these regions were quantified separately (**Figure 18**). It is important to consider these different vascular and plaque regions as: (1) VSMCs within

different vascular regions are derived from different pre-cursor populations (i.e. Arch and CA from the neural crest and the DA from the somites, Wang et al. 2015, **section 1.2, Figure 2**) which may change the characteristics of these cell types (Bennett, Sinha, and Owens 2016); and (2) different plaque regions contain vastly different environments, with a necrotic, lipid dense core and a fibrous cap (Libby et al., 2011), which may affect the ability of VSMC-derived cells to survive and contribute to these different compartments. On average 65.5% of cells within plaques containing at least one Confetti+ cell, were Confetti+ (**Figure 21**). The proportion of VSMC-derived cells ranged from 41-94% between plaques, this variation however was not explained by plaque region, as a similar VSMC cell contribution to the cap, shoulder and core regions was observed (**Figure 21 A**). Further stratification also showed there was no significant difference between plaques taken from different vascular regions or animals (**Figure 21 B, C**), suggesting inter-plaque variation is not linked to differences between animals, differences in regional hemodynamics and/or VSMC developmental origin which are different across vascular regions (Wang et al., 2015). The proportion of VSMC-derived plaque cells observed here (65.5%) is higher compared to Shankman et al. (2015) who detected 37.6%, using the Myh11-CreER(T2); R26R-floxed-STOP-eYFP mouse. This may be due to differences in the strain of mice used (they do not list their strain) or differences in the way plaques cells were counted.

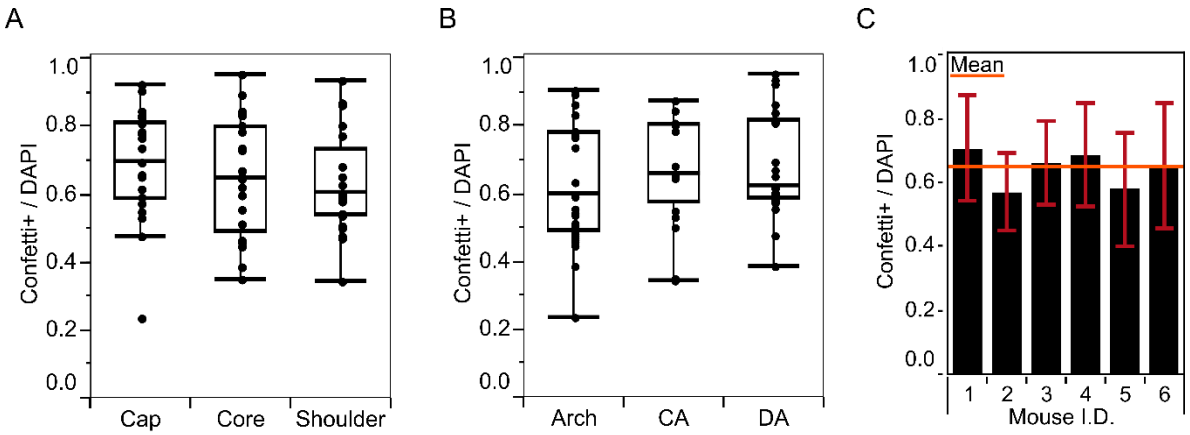

Figure 21: Proportion of atherosclerotic plaque cells derived from VSMCs
A) Box plot showing the proportion of the total number of cells (DAPI) which express the Confetti reporter (Confetti+) within each plaque region (in 23 plaques from 6 animals). **B)** Box plot quantifying the proportion of all cells (DAPI) within plaques from each of the indicated regions of the vasculature (Arch, carotid arteries (CA) and descending aorta (DA)) which express the Confetti reporter (Confetti+), each point represents a plaque region not a whole plaque. **C)** Bar chart showing the proportion of the total number of cells (DAPI), which express the Confetti reporter (Confetti+) within 23 plaques (plaque regions combined) from 6 individual animals. Mean across all animals is indicated by the orange bar (0.65 ±0.16). Adapted from Chappell et al., 2016.

In contrast to the mosaic, stochastic labelling observed in the vascular wall, VSMC-derived cells within plaques were found in large monochromatic regions with little intermixing between colours as shown in 20 µm cryo-sections (**Figure 20 B, C**) and 50-100 µm vibratome sections (**Figure 22**). Where plaques

contained more than a single colour they typically (>90%) localised to very defined regions. For example, in **Figure 20 C** three colours are observed within the plaque, however, these different coloured regions overlap and only mix at their borders. Very few plaques (<10%) showed intermingling of colours (for example GFP+ and YFP+ cells in **Figure 22 B**), and this is likely the result of two proximate cells of different colours expanding at the same time. Monochromatic VSMC-derived patches did contain some interspersed non-labelled cells (arrows in **Figure 20 B ii and C ii**), consistent with known infiltration of monocytes that contribute to lesion development (Tacke et al., 2007). Because VSMC labelling was not 100% (**Table 1 and 2**), it cannot be ruled out that these are unlabelled VSMCs. However, this is unlikely, as no plaques were observed which contained singlet VSMC-derived cells expressing another confetti colour within a monochromatic region. The coloured patterns observed in **Figure 20 and 22** are highly indicative of clonal expansion of VSMCs in atherosclerotic plaques as it is unlikely that such large regions would be observed if multiple VSMCs were to proliferate. To demonstrate this result statistically, the likelihood that the observed result could have occurred by the chance expansion of multiple VSMCs of the same colour can be assessed.

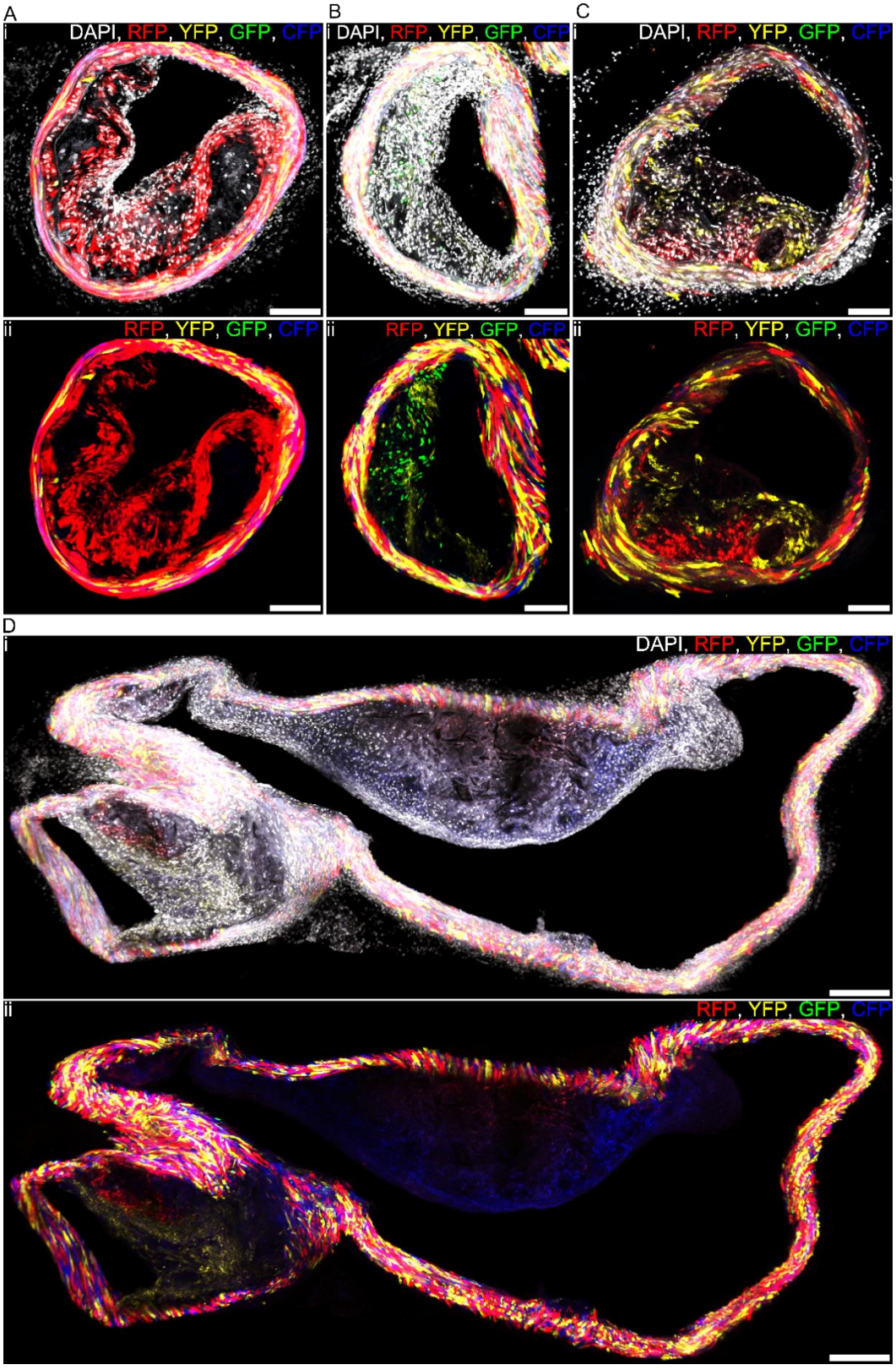

Figure 22: Clonal VSMC expansion in atherosclerotic plaques

Examples of monochromatic plaques (**A**) and plaques containing VSMC-derived cells in more than one colour (**B-D**). **B,** example of a plaque containing two intermingled clones (YFP/yellow and GFP/green). The section shown in panel (**D**) is cut through the top of the aortic arch and includes a portion of the right carotid artery. Signals from fluorescent proteins in 50- 100 µm vibratome sections are shown with (**i**) and without nuclear DAPI staining (white, **ii**). All plaques are from animals labelled at high density (10x 1 mg tamoxifen). Scale bars are 100 µm (**A-C**) and 200 µm (**D**). From Chappell et al., 2016.

Plaques showed substantial variation in colour pattern (**Figure 22**), but the frequency of individual colours was not significantly different compared to the initial labelling frequency, demonstrating that there was no bias towards expansion of VSMC-derived cells expressing a particular fluorescent protein (**Figure 23 A**). Quantification of coloured regions revealed that most plaques contained one (52%) or two (40%) colours, with a small proportion containing three (6%) or four (2%) colours (**Figure 23 B**). To compare the observed distribution of colours per plaque with the expected distribution if plaques were not clonally derived, the number of colours expected per plaque if 1, 2, 3 or 4 coloured cells proliferated can be calculated (**Figure 23 C**) based on the observed recombination frequency in healthy tissue (**Figure 23 A**). The difference between the observed and expected results suggests that very few Myh11-expressing VSMCs undergo massive expansion to contribute to plaque formation. If, for example, more than two cells frequently proliferated, the number of single coloured plaques would be close to zero (**Figure 23 C**). This data, however, also indicates that plaques are not exclusively mono-clonal (48% without taking into account single coloured plaques derived from more than one cell of the same colour, **Figure 23 B**) suggesting that a large proportion of plaques are oligo-clonal, derived from a few proliferating VSMC-derived cells.

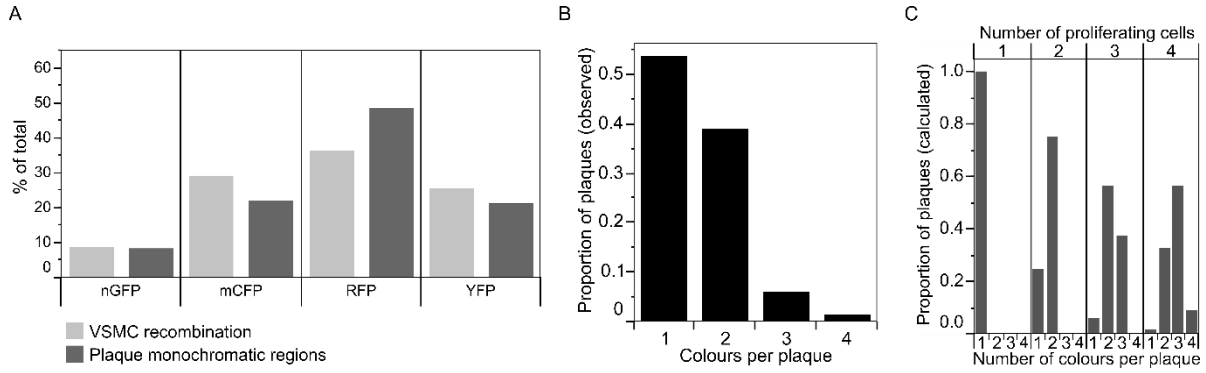

Figure 23: Colour distribution and number of observed and expected colours per plaque
A) Bar chart showing the proportions of each of the Confetti colours in VSMCs directly after recombination (light grey) and in monochromatic regions within atherosclerotic plaques (dark grey). **B)** Bar chart showing the number of colours observed per plaque (82 plaques from 16 animals). **C)** Bar chart showing the theoretical, number of colours per plaque resulting from proliferation of 1, 2, 3 or 4 VSMCs labelled at the recombination frequency observed in high density-labelled animals. All data is from animals labelled at high density (10x 1 mg tamoxifen). Adapted from Chappell et al., 2016.

When stratified into vascular region the proportion of colours per region remained similar throughout (**Figure 24**). The biggest difference was in the number of colours detected per plaque between the aortic arch and the descending aorta (**Figure 24 B and D**). This may result from the fact that the lumen of the aortic arch is large and the plaques observed here were typically larger than the descending aorta. Stratification by plaque region (**Figure 24**) suggests that the number of VSMCs contributing to

each region is consistent and there is no preference for more cells to contribute to the cap or core of a plaque.

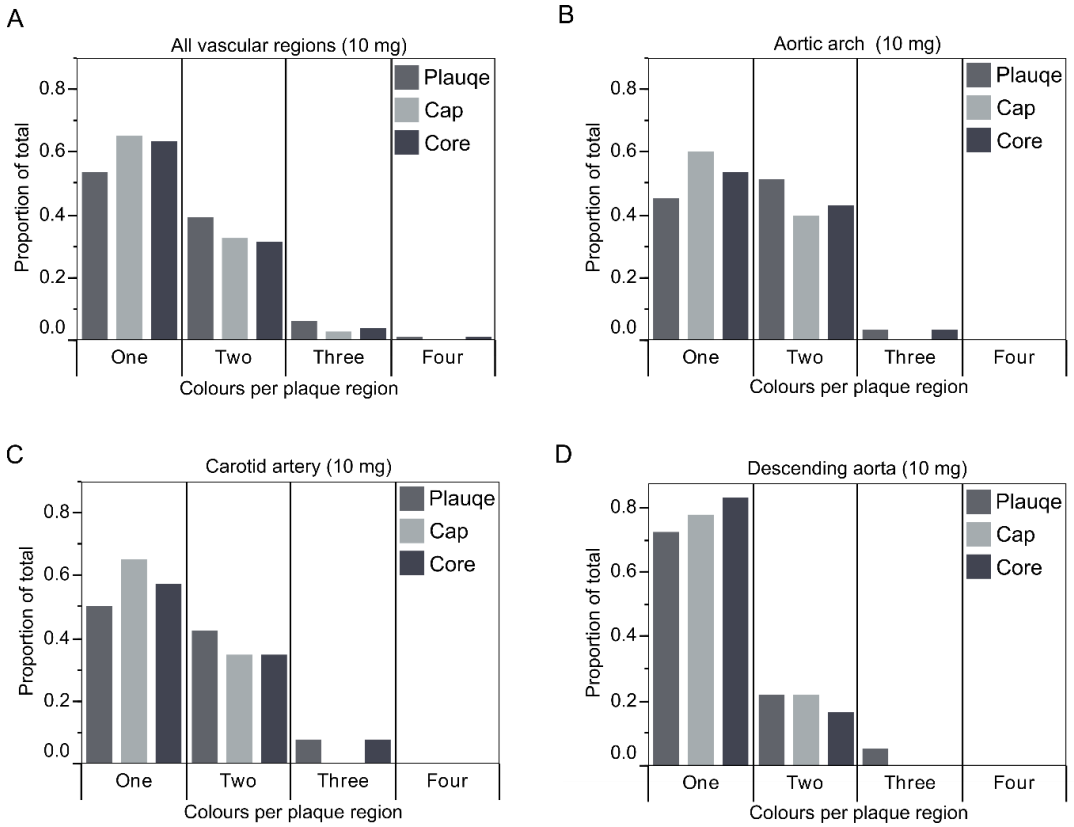

Figure 24: Number and distribution of Confetti colours within atherosclerotic plaques
A-D, Bar charts showing the proportion of plaques in high density (10x 1 mg tamoxifen) labelled animals with one, two, three or four colours. Bars represent the entire plaque (grey, also shown in **Figure 23 B**), the cap (light grey) or the core of the plaque (dark grey). **A**, Data is shown for all plaques (82 plaques from 16 animals). **B**, **C**, **D**, Data is shown for plaques in different vascular regions (**B**, Aortic Arch; **C**, Carotid artery; **D**, Descending aorta;). Arch: aortic arch, DA: descending aorta, CA: carotid artery. Adapted from Chappell et al., 2016.

Given the initial observations that plaque VSMC-derived cells appear to be oligo-clonally derived, predictions can be made as follows: if tamoxifen dose is lowered, and therefore the proportion of labelled medial VSMCs is decreased, then plaques should still be observed containing VSMC-derived cells of one or two colours. To test this, Myh11-CreER(T2); R26R-Confetti; ApoE$^{-/-}$ mice were injected with 1 mg of tamoxifen (a 10-fold reduction in dose) which induced at a labelling frequency of ~40%. Following the HFD protocol described above (**Figure 20 A**), many unlabelled plaques and plaques where a single coloured region occupied a large part of the plaque area were observed (**Figure 25, Appendix B**). Within the section displayed in **Figure 25** a large proportion of the lumen is occupied by a plaque which is, likely the result of multiple plaques merging. The right and left portions are unlabelled, the top portion contains RFP+/red cells occupying the cap and the core while the bottom portion is split in two with RFP+/red and YFP+/yellow cells. The size of the monochromatic regions

observed in animals with reduced labelling frequency was comparable to what was found in high-density labelled animals, suggesting that large regions are not the result of multiple cells of the same colour expanding but that a single cell is capable of massive expansion through multiple rounds of proliferation.

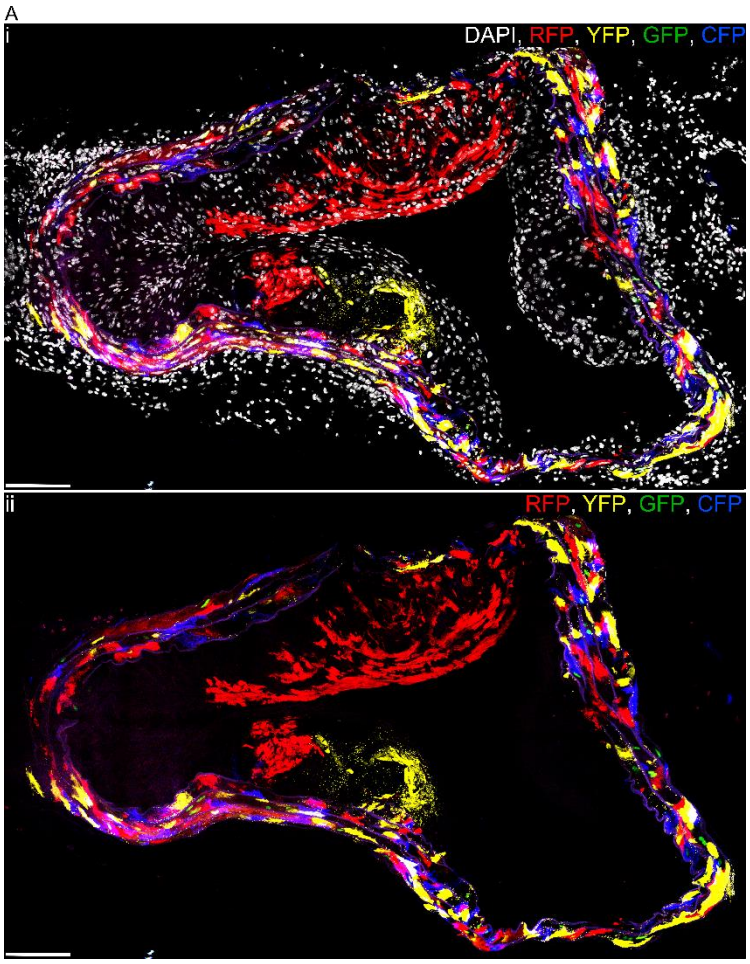

Figure 25: Animals labelled at medium density develop plaques with several large monochromatic regions, which span both the cap and core

A, An atherosclerotic plaque from a medium density-labelled (1x 1 mg tamoxifen) Confetti ApoE$^{-/-}$ animal following 16 weeks of high fat diet. Signals from fluorescent proteins are shown with (**i**) and without (**ii**) nuclear DAPI (white). Scale bars are 100 µm. From Chappell et al., 2016.

The experiments here strongly suggest that monochromatic regions within lesions are generally the progeny of a single cell, signifying that VSMC-derived cells in atherosclerotic lesions are typically formed by the oligo-clonal expansion of very few VSMCs. This observation is similar to that of Feil et al. (2014) who demonstrated using the Confetti tracing system, recombined by the Sm22a-Cre(T2) that, macroscopically, plaques appeared a single colour. Importantly, however, they used a relatively low labelling frequency (11%) and did not section or clear the plaque to image throughout so could not definitively confirm this. Furthermore, Feil et al. (2014) used a Sm22α-CreER(T2) transgene which is not specifically recombined within VSMCs (Shen et al. 2012; Espagnolle et al. 2014; Proweller et al.

2006; Zhang et al. 2006). The clonality hypothesis was first proposed by Benditt and Benditt in 1973 and the experiments here confirm their hypothesis with one adjustment, that the VSMC-derived component of a plaque is not necessarily mono-clonal but can consist of the progeny of several VSMCs (i.e. oligo-clonal). Furthermore, it does not appear that migration of VSMCs independent of proliferation contributes to late-stage plaque cellularity as singlet cells of a different colour were not observed within monochromatic regions; however, this may be a factor during earlier stages.

5.3 Progeny of single VSMCs can take on different phenotypes

Given that plaques are typically mono/oligo-clonal regarding their VSMC-derived component it seems logical to suggest that the progeny a single VSMC can trans-differentiate into the multiple VSMC-derived cells which can occupy a plaque (**section 1.5**). To test the plasticity of single VSMCs, sequential cryo-sections were stained for either the VSMC marker aSma or Mac3, a marker upregulated in VSMCs which adopt a macrophage-like state (**Figure 26 and 28**). aSma+ cells were frequently located within the cap and shoulder regions of an atherosclerotic plaque and less so within core of the plaque (**Figure 26**), similar to other studies (Shankman et al. 2015).

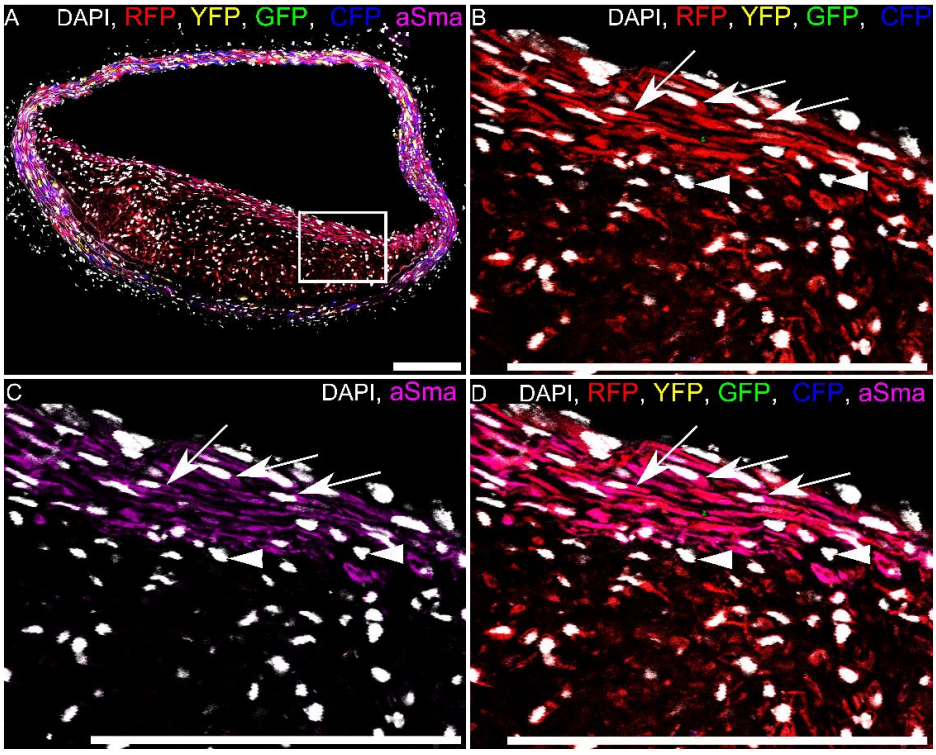

Figure 26: VSMC-derived aSma+ cells locate to the cap of an atherosclerotic plaque
Immunostaining for aSma of a plaque cryo-section from a high density-labelled animal (10x 1 mg tamoxifen), containing RFP-expressing VSMC-derived cells. Signals for fluorescent proteins, nuclear DAPI (white) and aSma (magenta) are shown as indicated on each image. The region outlined in **A** are magnified in **B, C, D**. Arrows in **B, C, D** point to RFP+ aSma+ cells, arrow heads point to RFP- aSma- cells. Scale bars are 150 µm. Adapted from Chappell et al.,2016

Quantification of all stained plaque sections (**Appendix B**) showed that 72% (±26) and 64% (±25) of Confetti+ cells within the shoulder and cap regions were aSma+. In contrast only 15% (±21) of Confetti+ cells within the core were aSma+ (**Figure 27**). Others who have lineage traced VSMCs in atherosclerosis using a single coloured reporter suggest that 18% (Shankman et al. 2015) and 30% (Albarrán-Juárez et al. 2016) of VSMC-derived cells are aSma+, these studies do not sub-categorise the plaque into multiple regions. Within this study, without plaque region sub-categorisation, on average 50% (±15) of all VSMC-derived cells were aSma+, which is 32% and 20% higher than the studies by Shankman et al. (2015) and Albarrán-Juárez et al. (2016). This varitation might be due to differences between mice in different facilities, the details with which positive cells were defined/scored and/or the fact that two regions (cap and core) which are highly aSma+ were scored here, compared to one region (core) which contains less aSma+ cells. No significant difference between vascular region and individual mice regarding the porpotion of Confetti+ cells or all cells (DAPI) which were aSma+ was observed (**Figure 27 C-F**), suggesting that variation is between individual plaques. The majority of aSma+ cells (97% ±7) were Confetti+ and therefore VSMC-derived, this result is consistent with studies which have shown that bone marrow-derived cells can, but rarely, upregulate aSma (Yu et al. 2011). Others have, however, suggested that up to 31% of aSma+ cells are not VSMC-derived and that 17% of aSma+ cells are derived from macrophage cells (Albarrán-Juárez et al. 2016). The former result is hard to reconcile, but again may be due to differences in how positive cells were scored or perhaps differences in labelling frequencies. One possible reason for the latter claim is that Albarrán-Juárez et al. (2016) use a constitutively active Cre recombinase (rather than a tamoxifen inducible Cre), driven by the myeloid marker gene LysM, which might be induced in VSMC-derived cells which have entered the plaque.

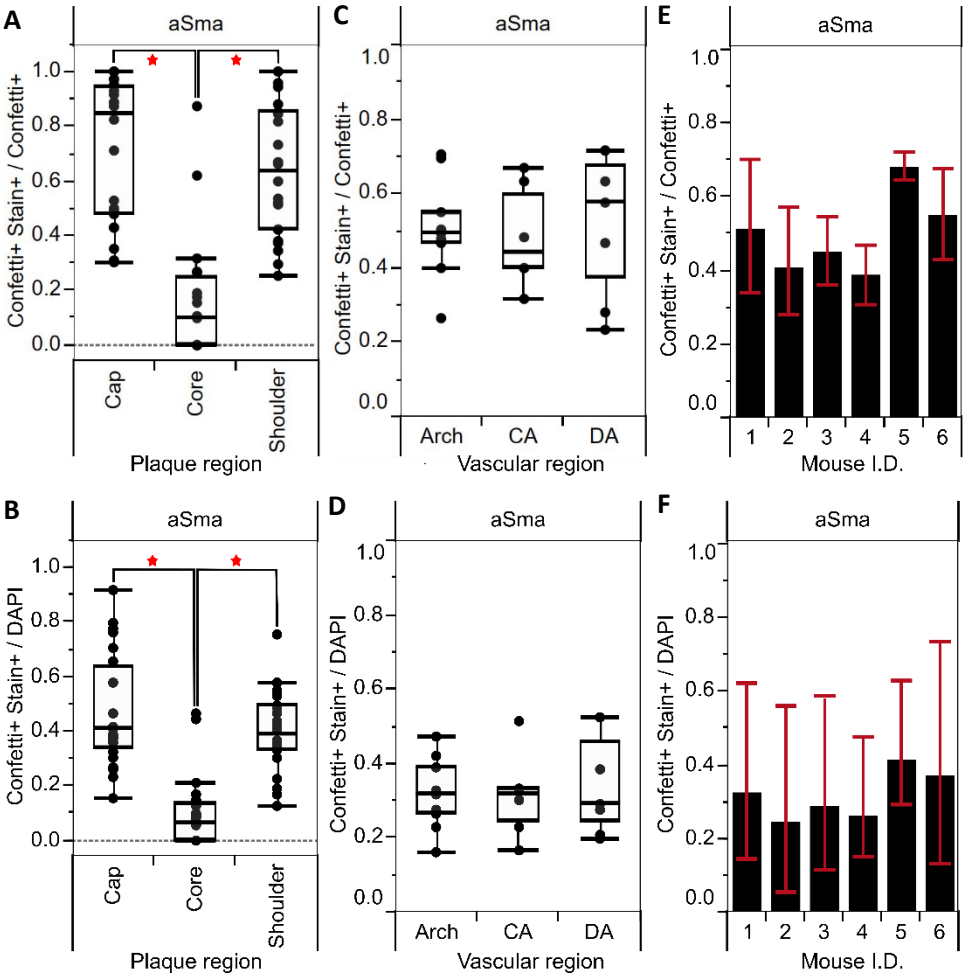

Figure 27: Quantification of Confetti+ aSma+ cells in plaques

Box plots and bar charts showing the proportion of cells that express the Confetti reporter and stain positive for aSma (Confetti+ Stain+), relative to all cells expressing the Confetti reporter (**A, C, E**) and all cells which stain positive for DAPI (**B, D, F**). **A** and **B** are stratified by plaque region. **C** and **D** are stratified by vascular region, Arch = aortic arch, CA = carotid arteries, DA = descending aorta. **E** and **F** are stratified by individual mouse. A red star indicates a significant difference ($p<0.05$) determined by a two-way ANOVA. Data are from 23 plaques from 6 animals. All data is from animals labelled at high density (10x 1 mg tamoxifen). Adapted from Chappell et al., 2016.

Mac3-staining of cryo-sections sequential to those stained for aSma identify that Mac3+ cells are predominately located within the core of the plaque (**Figure 28**), which is similar to what was shown in other studies using macrophage markers such as Lgals3 (Shankman et al. 2015).

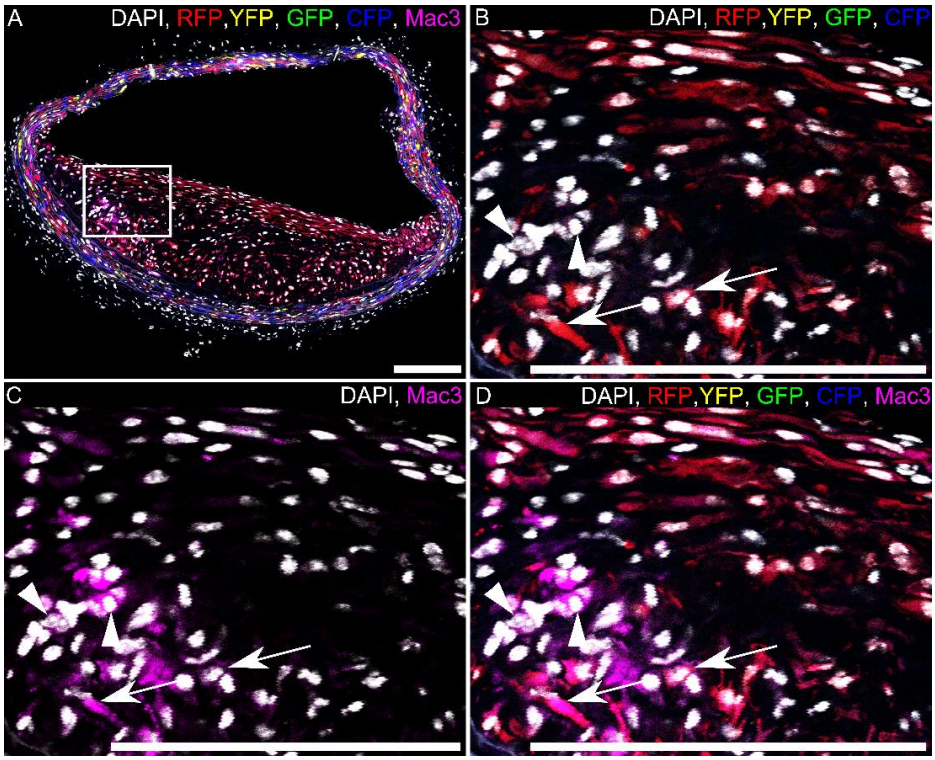

Figure 28: VSMC-derived Mac3+ cells locate to the core of an atherosclerotic plaque
Immunostaining for Mac3 of a plaque cryo-section from a high density-labelled animal (10x 1 mg tamoxifen), containing RFP-expressing VSMC-derived cells. Signals for fluorescent proteins, nuclear DAPI (white) and Mac3 (magenta) are shown as indicated on each image. The region outlined in **A** are magnified in **B, C, D**. Arrows in **B, C, D** point to RFP+ Mac3+ cells, arrow heads point to RFP- Mac3+ cells. Scale bars are 150 µm. Adapted from Chappell et al., 2016.

On average 48% (±28) of Confetti+ and 29% (±19) of all (DAPI) core cells were Mac3+, whereas only a small proportion of Confetti+ cap (15% ±19) and shoulder (26% ±20) cells were Mac3+ (**Figure 29 A, B**). These results suggest that VSMC-derived cells within the plaque core are more likely to trans-differentiate into macrophage-like cells compared to cap and shoulder cells. Similarly, Shankman et al. (2015) found that 30% of all VSMC-derived cells were positive for the macrophage marker Lgals3. Of all the Mac3+ cells counted 72% (±20) were Confetti+, and therefore VSMC derived. Previous studies have shown that only 16% of plaques cells expressing CD68 were VSMC-derived (Albarrán-Juárez et al. 2016), this difference may be due to the fact that CD68 is a stricter method of staining for macrophage-like cells. The proportion of Confetti+ Mac3+ cells relative to Confetti+ or all cells (DAPI) did not differ over vascular region or mice, except in one case between mice 1 and 3 regarding the proportion of Confetti+ cells which are also Mac3+ (**Figure 29 C-F**). Which, again, shows the trend that inter-plaque differences accounts for most of the variation observed.

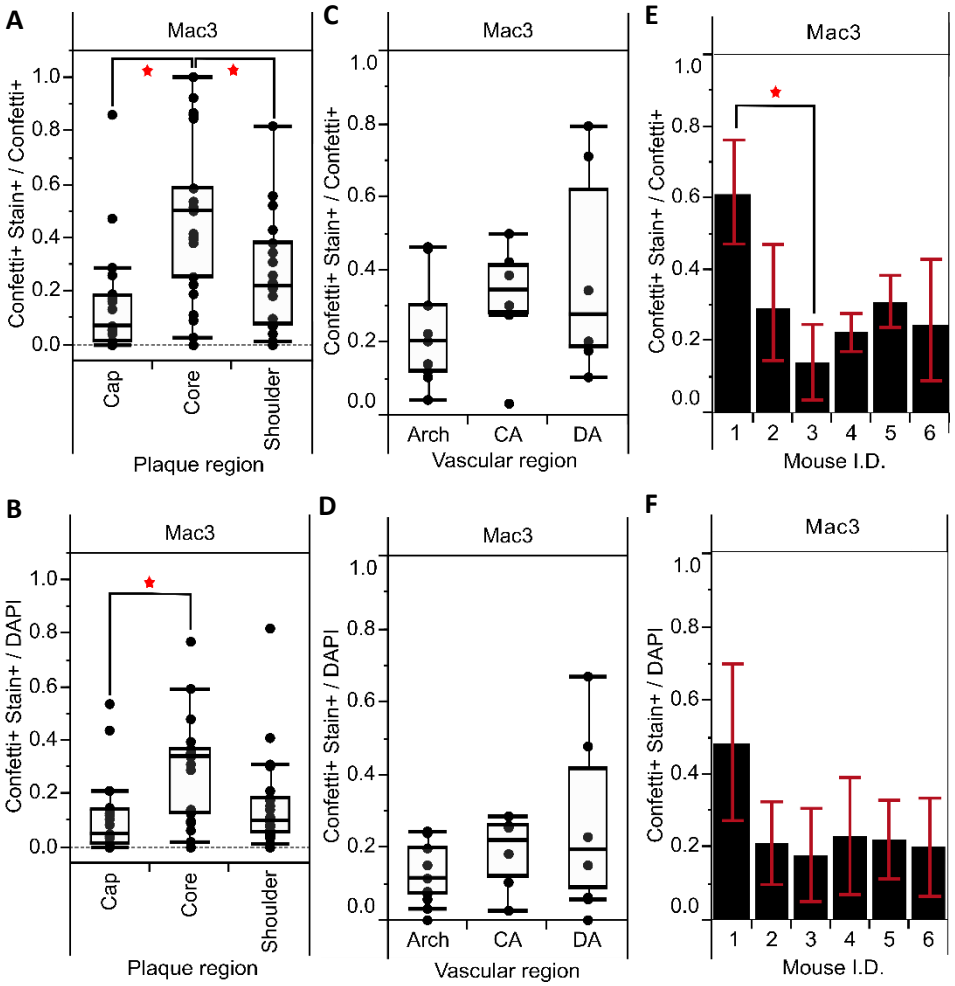

Figure 29: Quantification of Confetti+ Mac3+ cells in plaques

Box plots and bar charts showing the proportion of cells that express the Confetti reporter and stain positive for Mac3 (Confetti+ Stain+), relative to all cells expressing the Confetti reporter (**A, C, E**) and all cells which satin positive for DAPI (**B, D, F**). **A** and **B** are stratified by plaque region. **C** and **D** are stratified by vascular region, Arch = aortic arch, CA = carotid arteries, DA = descending aorta. **E** and **F** are stratified by individual mouse. A red star indicates a significant difference ($p<0.05$) determined by a two-way ANOVA. Data are from 23 plaques from 6 animals. All data is form animal labelled at high density (10x 1 mg tamoxifen). Adapted from Chappell et al., 2016.

As Confetti+, Mac3+ cells and aSma+ cells were detected in all regions of the plaque (**Figures 27 and 29**), questions regarding the plasticity of a single VSMC-derived cell were raised. For example, can one cell express both proteins at once or can, for example, Mac3 only be expressed following the downregulation of aSma. To test this, plaques were co-stained for both proteins, however, as the entirety of the useable light spectrum is already being used to image all Confetti colours, DAPI and a single immuno-stain stain, this proved problematic. To overcome this, only red or blue-monochromatic plaques were selected and the aSma stain was visualised in the channel normally reserved for GFP (488 laser). Co-staining revealed that a proportion of Confetti+ cells express both

aSma and Mac3 (26% ±20**, Figure 30**). The majority of these VSMC-derived cells located to the plaque core, however, were generally within the region bordering the core and cap (**Figure 30**). This is in agreement with recent single cell RNA data suggesting that co-expression of inflammatory and VSMC-markers is present in VSMC-derived plaque cells (Albarrán-Juárez et al. 2016). Of the 1100 Confetti-negative cells counted less than 0.03% were double positive for both Mac3 and aSma, suggesting that co-expression of VSMC and macrophage markers are typically restricted to VSMC-derived plaque cells.

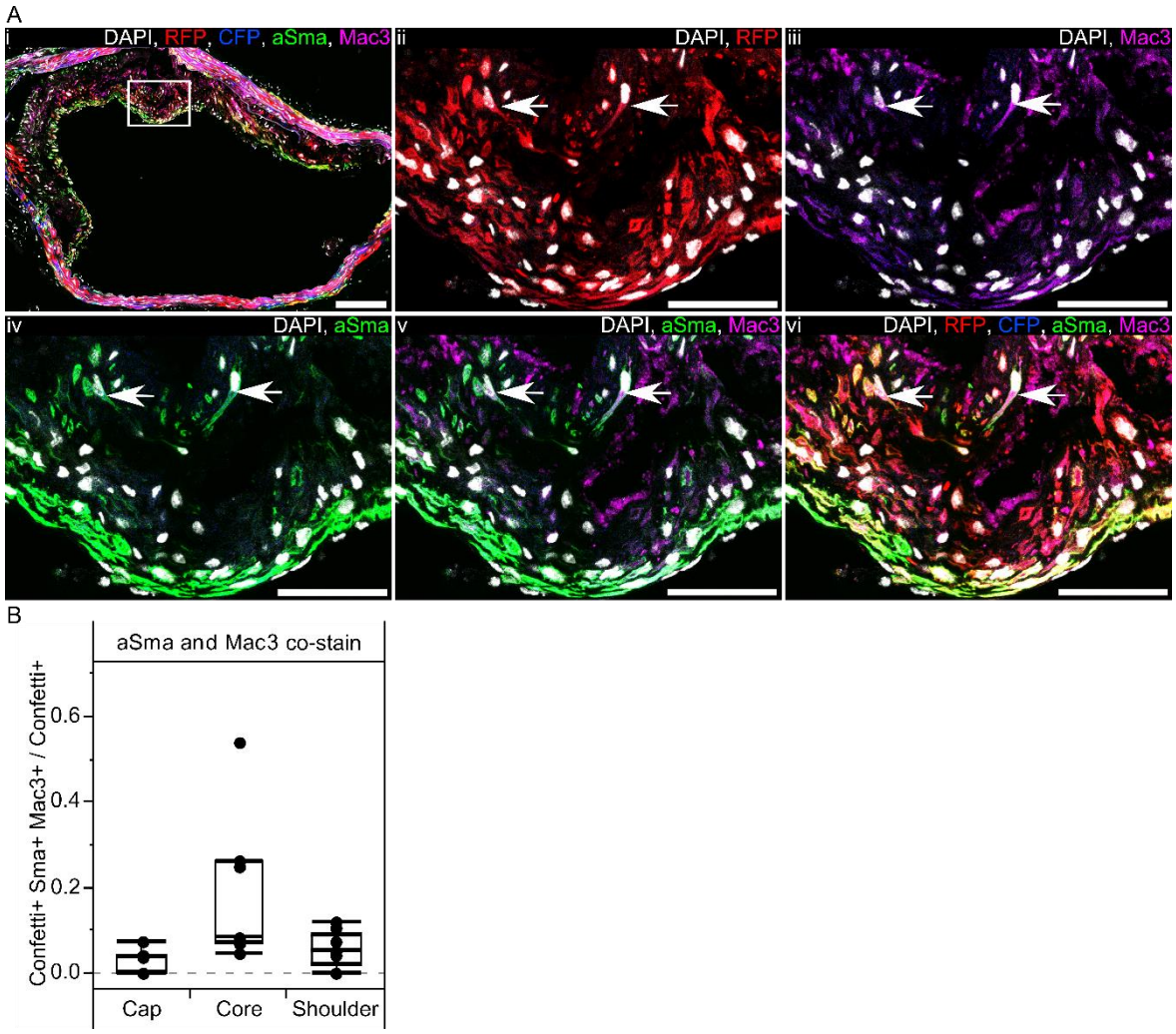

Figure 30: VSMC-derived plaque cells can express both aSma and Mac3

A, Arterial cryo-section containing RFP-expressing VSMC-derived cells, co-stained for aSma and Mac3. The region outlined in (**i**) is magnified in (**ii-iv**). Arrows point to RFP+ Mac3+ aSma+ cells. Scale bars are 150 µm (**i**) and 50 µm (**ii-vi**). Signals for fluorescent proteins, nuclear DAPI (white), aSma (green) and Mac3 (magenta) are shown as indicated on each image. **B,** Box plot showing the proportion of cells expressing the Confetti reporter (Confetti+) which co-stain for aSma and Mac3 (Confetti+Sma+Mac3+) within different plaque regions (7 plaques from 6 mice). Only red and blue plaques were used for this analysis as the 488 channel was required for aSma imaging. All data is from animals labelled at high density (10x 1 mg tamoxifen). Adapted from Chappell et al., 2016.

In total, 27/37 monochromatic regions in 23 plaques contained single cells expressing aSma or Mac3. Given that monochromatic plaque regions will generally arise from clonal proliferation of a single VSMC this suggest that, at least a proportion of, individual VSMCs have the propensity to generate plaques cells of different phenotypes. Several plaques, however, contained monochromatic regions which occupied only the core or the cap (for example **Figure 22 C, D**) raising the question whether particular VSMCs will preferentially occupy a particular plaque region and therefore either regional phenotype (aSma+ cap and Mac3+ core). To test whether VSMCs are preferentially biased towards either the aSma+ cap or Mac3+ core, the positions of 126 monochromatic regions in 82 plaques form 16 high density-labelled animals were scored with respect to the plaques cap and core (**Figure 31**).

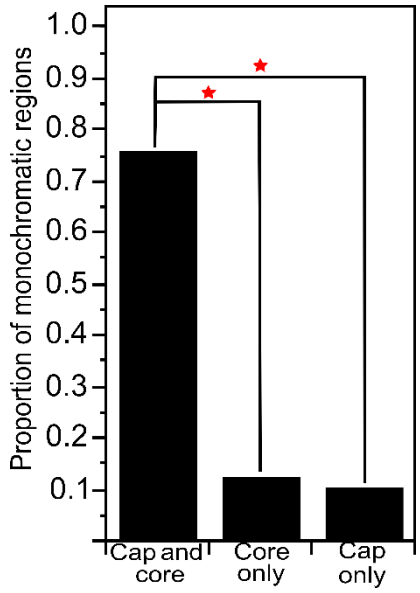

Figure 31: Monochromatic regions occupy both the cap and core regions of the plaque more frequently than just the cap or core
Bar chart showing the proportion of monochromatic regions which occupy both the cap and core or only a single region within an atherosclerotic plaque (126 regions in 82 plaques from 16 high density-labelled animals). A red star indicates a significant difference ($p<0.05$) determined by a t-test. Adapted from Chappell et al., 2016.

The majority of monochromatic regions (96/126) spanned both plaque domains with a few restricted to either the cap (11%) or core (13%) (**Figure 31**). The frequency at which single monochromatic regions occupied both plaque regions was significantly larger than expected by independent chance labelling of two proximate uni-potent clones of the same colour ($\chi^2=228$, $p<0.01$, 3 degrees of freedom, n=96; statistical analysis for each colour is detailed in the Methods Chapter, **section 3.17**). Furthermore, 14/17 plaques from the animals labelled at a ~40% labelling efficiency (example shown in **Figure 25**) contained monochromatic regions which spanned both the cap and core plaque regions. This data therefore suggests that VSMC-derived cells originating from the clonal expansion of a single VSMC do not preferentially locate to either plaque region nor associated phenotype. One hypothesis explaining the observed occurrence of monochromatic regions locating to either the cap or the core,

but not both, may be due to the way in which a plaque grows. For example, a process whereby one cell grows underneath or over the top of a pre-existing plaque, creating a layered effect.

5.4 Medial VSMCs that do not form monochromatic regions in the plaque still phenotypically switch

Given that the evidence in **sections 5.2 and 5.3** suggests that the VSMC-derived component of an atherosclerotic plaque is oligo-clonally-derived, formed through the expansion of a few VSMCs, questions are raised regarding what the response of the remaining medial-VSMCs is to atherosclerosis causing stimuli. To test the extent of phenotypic modulation in medial cells in response to disease, VSMCs adjacent to and directly underneath plaques were analysed in aSma and Mac3 stained plaque cryo-sections. To enable this analysis to be unbiased by proliferating VSMCs which are connected to the plaque, only medial-VSMCs expressing a different colour to those within the atherosclerotic plaque were analysed. Results show that the medial VSMCs directly under plaques lose their characteristic, elongated morphology, a proportion of these VSMCs downregulate aSma expression and upregulate Mac3 expression (**Figure 32**). This therefore suggests that medial VSMCs underneath an atherosclerotic plaque undergo phenotypic switching.

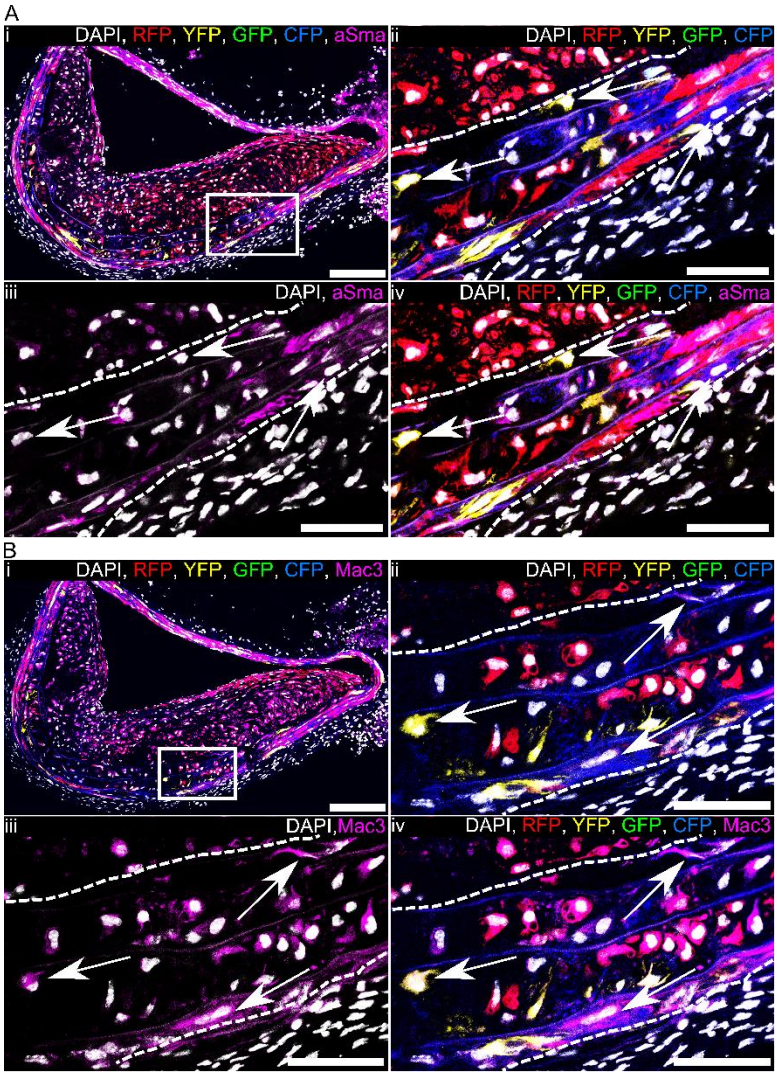

Figure 32: VSMCs within the media directly underlying atherosclerotic plaques undergo phenotypic switching without contributing to the cell mass of the lesion

A, B, Serial cryo-sections from artery of high density-labelled (10x 1 mg tamoxifen) animal containing a plaque with RFP+ VSMC-derived cells, stained for aSma (**A**) and Mac3 (**B**). The region outlined in (**i**) is magnified in (**ii-iv**), white dotted lines outline the media. Signals for fluorescent proteins, nuclear DAPI (white), aSma (magenta, **A**) and Mac3 (magenta, **B**) are shown as indicated on each image. Arrows in (**A**) point to aSma-negative cells within the media, which express the Confetti reporter (excluding RFP expressing cells). Arrows in (**B**) point to Mac3-positive cells within the media, which express the Confetti reporter (excluding RFP expressing cells). Scale bars are 150 µm in (**i**) and 50 µm in (**ii-vi**). Adapted from Chappell et al., 2016.

Quantification of plaque sections showed that there was a 30% reduction in Confetti+ aSma+ cells in the media lying directly under the plaque compared to the comparatively healthy media adjacent to the plaque (**Figure 33**). A similar reduction (54%) has previously been observed by (Shankman et al. 2015). VSMCs underlying the plaque were also frequently more often Mac3+ (33%) compared to those adjacent to the plaque (5%) (**Figure 33**). VSMCs therefore seem capable of phenotypic change independent of proliferating. If indeed these medial VSMCs had proliferated, then small coloured medial patches would be observed. Whether the phenotypic change is in response to or a cause of neointimal/plaque growth is un-resolved in this study, but is possibly more reasonable to suggest that it is in response to the plaque environment, as VSMCs underneath the plaque will be exposed to a highly pro-inflammatory environment.

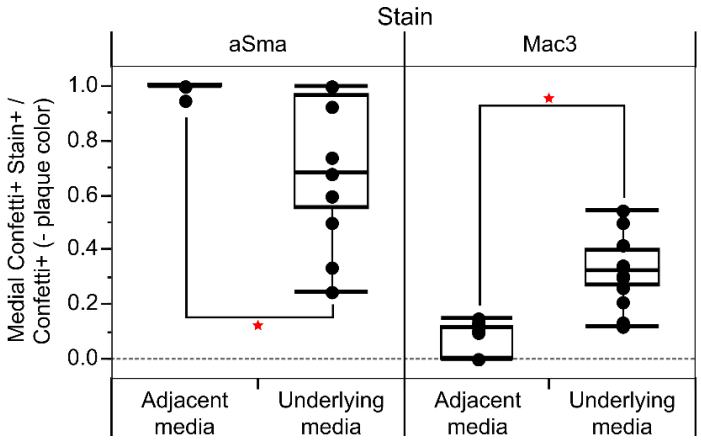

Figure 33: Quantification of aSma+ and Mac3+ medial VSMCs directly underneath and adjacent to an atherosclerotic plaque

A) Box plot quantifying the proportion of cells expressing the Confetti reporter, which stain positive for aSma or Mac3 (Confetti+ Stain+), relative to all Confetti+ cells. Only cells containing confetti fluorescent proteins not found in the plaque (-plaque colour) within the media underlying or adjacent to a plaque were counted (based on 17 plaques, selected from the 23 analysed in **Figures 26-29**, from 6 animals). Red stars indicate a significant difference based on a two-way ANOVA, $p<0.05$. All data is from animals labelled at high density (10x 1 mg tamoxifen). Adapted from Chappell et al., 2016.

5.5 Conclusions from the atherosclerosis experiments

The experiments here were performed to test the hypothesis that the VSMC-derived component of atherosclerotic plaques are clonally derived (as hypothesised by Benditt and Benditt 1973 and Feil et al. 2014) and whether the progeny of single VSMCs are capable of taking on both the aSma+ cap phenotype and the Mac3+ core phenotype. To test for clonality, the multi-colour lineage tracing Confetti system combined with the Myh11-CreER(T2) was used in combination with the $ApoE^{-/-}$ mice fed a HFD for 16-19 weeks. These mice developed large atherosclerotic plaques, imaging cross-sections of these plaques using confocal microscopy show that a large proportion of cells (65.5%) within a plaque are Confetti+ (**Figures 20, 21 and 22**), and are therefore VSMC-derived, which has been demonstrated previously (Shankman et al. 2015; Gomez et al. 2013). However, in contrast to the mosaic, stochastic labelling observed in the vascular wall, VSMC-derived cells within plaques were found in large monochromatic regions (**Figures 20 and 22**). The number of monochromatic regions per plaque was typically one or two (53% and 40%) with a few plaques containing three or four (6% and 2%, **Figure 23**), however these regions rarely intermingled, suggesting that plaques are oligo-clonal.

To test if the progeny of single VSMCs can take on the aSma+ cap and Mac3+ core cell phenotypes within a plaque, cryo-sections were stained for these markers (**Figures 26- 29**). Results showed that monochromatic VSMC-derived regions contained aSma+ cap cells and Mac3+ core cells, also observed

was a small proportion of cells which stained positive for both these markers (**Figure 30**). These results therefore confirm that VSMCs are capable of trans-differentiating into cells with different plaque phenotypes. Given that some plaques were observed to be mono-clonal it is likely that a single VSMC has the potential to trans-differentiate into all other known VSMC-derived cell types which were not tested here (e.g. MSC-like and myofibroblast-like cells, Shankman et al. 2015).

Finally, to test whether medial VSMCs, which do not contribute to cells within the plaque, phenotypically switch, VSMCs adjacent to and directly underneath plaques were analysed in aSma and Mac3 stained plaque cryo-sections. Results from this experiment demonstrated that VSMCs positioned within the media underneath the plaque phenotypically switch (down regulating aSma and upregulating Mac3) more often than medial VSMC adjacent to the plaque (**Figures 32 and 33**). Furthermore, these phenotypically switched VSMCs do not proliferate, and if they are able to enter the plaque they do not survive long enough to be detected in these experiments.

The most interesting question raised form experiments within this Chapter relates to the fact that the VSMC-derived cells within a plaque are derived from oligo-clonal expansion of a few single VSMCs and why, for example, other VSMCs in close proximity do not also respond in this proliferative way. Possible explanations for this finding are that only a few VSMCs contain the potential to proliferate and trans-differentiate, contributing to plaque development. In contrast, perhaps, all VSMCs are equi-potent and rely on some specific environmental or stochastic cues in order to react in this way. Other possible mechanisms will be discussed in detail in **sections 9.2 and 9.3**.

Chapter 6: VSMC proliferation and plasticity in an injury model of neointimal formation

The observation made in **Chapter 5** that plaques are oligo-clonally derived suggests that very few VSCMs proliferate in response to disease and that this low frequency response may be an inherent feature of VSMCs in response to atherosclerosis causing-stimuli. As discussed previously (**section 2.2**), the ApoE$^{-/-}$ HFD model induces the formation of complex atherosclerotic plaques which contain multiple inflammatory molecules, lipids and immune cells, all of which might affect the way in which VSMCs behave. To test whether the low frequency response seen in the HFD model is an inherent feature of VSMCs, it is possible to use other methods to induce VSMC proliferation.

Common methods to induce VSMC proliferation in vivo often rely on surgical techniques to injure an artery without causing its rupture. There are multiple methods which can be employed to achieve this, including wire-injury, carotid ligation and balloon injury (Xu, 2004). Injury models are typically described as modelling restenosis, a disease which occurs in humans following angioplasty to treat coronary artery disease, in which neointimal lesions containing VSMCs and ECM develop (Levine, Chodos, and Loscalzo 1995; Schwartz, deBlois, and O'Brien 1995). The two most commonly used models are wire injury, in which a thin wire is inserted into an artery and used to scrape the endothelial cells off a portion of the intima (Lindner, Fingerle, and Reidy 1993), and carotid ligation, in which the blood flow through a carotid artery is prevented by ligating the artery with a piece of suture (**section 2.3**, Kumar and Lindner 1997). Both models result in an acute proliferation of VSMCs within 2-4 weeks. Wire Injury is a technically challenging technique and the degree to which complete denudation of endothelial cells is achieved can be variable, furthermore the resulting neointima is relatively small compared to other techniques (Lindner, Fingerle, and Reidy 1993; Kumar and Lindner 1997). Carotid ligation, however, leads to the development of large neointima with intact endothelium, which by 4 weeks post-surgery can reduce lumen size by ~80% (Kumar and Lindner 1997). Carotid ligation effectively stops all forward blood flow from where the carotid artery bifurcates, this disruption in blood flow leads to a rapid proliferation of VSMCs. Indeed, Kumar and Lindner (1997) report that by day 5 post-ligation, the VMSC replication index is approximately 23.4% within the media and 27.6% within the developing intima, in the following 2 weeks medial proliferation falls sharply while intimal proliferation remained high up until the end of week 4. Herring et al. (2014), have previously shown, using the Myh11-CreER(T2) transgene, that mature VSMCs contribute to the formation of the neointima. VSMCs within the ligated artery also undergo classical features of phenotypic switching, including a downregulation of contractile markers (e.g. Myh11, Tagln, Acta2) and activation of the NF-κB pathway (Yoshida et al. 2013; B. Paul Herring et al. 2017). One major difference between the carotid ligation model and the ApoE$^{-/-}$ HFD model is the lack of immune cell involvement, as

monocytes/macrophages are not detectable within the carotid ligation-induced neointima (Kumar and Lindner, 1997). As carotid ligation is technically less challenging than wire-injury and a more effective method to induce proliferation of VSMCs/neointimal development (Lindner, Fingerle, and Reidy 1993; Kumar and Lindner 1997), this method was chosen to test whether the low frequency response is a common feature of VSMCs in response to disease/injury.

To test if a small number of VSMCs clonally proliferate to form injury-induced neointima, as seen within the ApoE$^{-/-}$ HFD model (**Chapter 5**), carotid ligation was performed on Myh11-CreER(T2); Rosa26-Confetti mice. Due to the rapid proliferation of VSMCs caused by carotid ligation, this model is used here to try to 'switch' more VSMCs to a proliferative phenotype than seen in the chronic, but less severe protocol used to induce atherosclerosis. Indeed, as previously suggested, the replicative index of VSMCs following carotid ligation is around 25% as early as 5 days post-surgery (Kumar and Lindner, 1997), which suggests that more VSMCs are capable of proliferating and remodelling arteries in response to injury.

Aims

1. Determine if a low proportion of cells proliferate following carotid ligation, as observed in the HFD atherosclerosis model
2. Test the extent of phenotypic switching of VSMCs in the carotid ligation model of neointimal growth

6.1 Carotid ligation surgery induces clonal expansion of few VSMCs to create large coherent VSMC- derived monochromatic patches

To test if, similar to the ApoE$^{-/-}$ HFD model, few cells clonally expand in a more severe, carotid ligation, model of VSMC proliferation, Myh11-CreER(T2); Rosa26-Confetti mice were labelled at high frequency (10 x 1 mg tamoxifen) prior to ligation of the left carotid artery (**Figure 34 A**). Non-ligated right carotid arteries showed stochastic labelling of VSMCs, as expected, and no neointimal growth, indicating there was no proliferation in this artery post-surgery of the left carotid artery (**Figure 34 B**). In contrast, the neointima formed in the left carotid artery 28 days after ligation surgery was composed of large contiguous monochromatic VSMC-derived patches, which occupied defined volumes (**Figure 34 C**). This result is similar to that seen in the HFD model and suggests that the neointima is formed by the clonal proliferation of a small proportion of VSMCs. Confetti+ VSMCs only intermingled where two or more coloured patches met/overlapped (**Figure 34 C iii**). The majority of high density labelled animals

analysed (11/12) displayed 2-8 coloured patches per artery, with one artery displaying 20 patches (**Appendix C**). This variation is likely explained by the fact that the carotid ligation model of neointimal growth is variable in the degree to which it affects the entire artery, with some arteries being remodelled throughout and others in just defined regions. Indeed, the number of patches correlated with the size of the remodelled area (R^2=0.7).

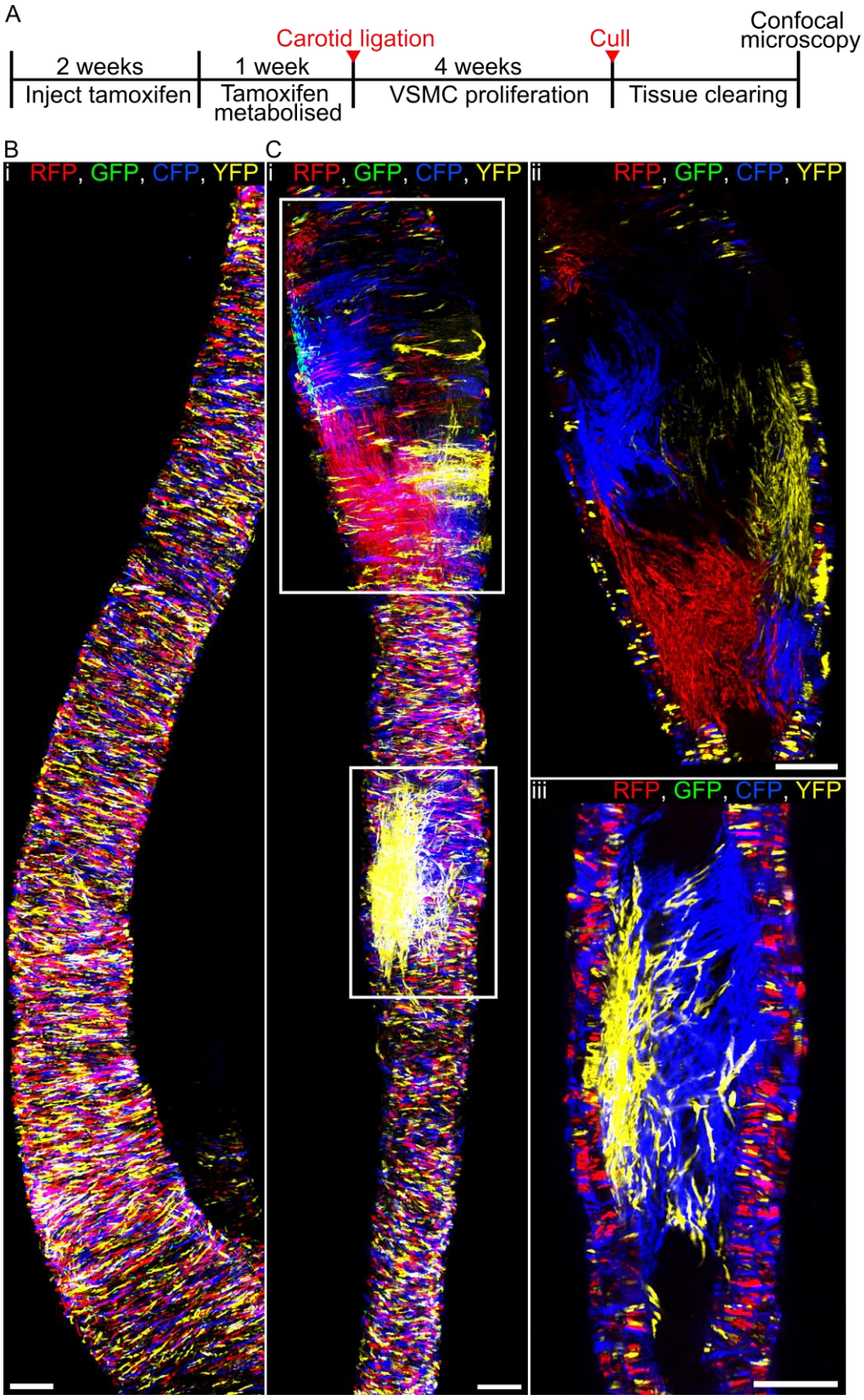

Figure 34: A subset of VSMCs proliferate to form the injury-induced neointima

A, Experimental protocol for carotid artery ligation studies. **B, C,** Whole-mount control right carotid artery (**B**) or ligated left carotid artery (**C**) from a high density-labelled animal (10x 1 mg tamoxifen), 28 days post-surgery (the point of ligation is 20-100 µm superior to the top of the ligated artery (**Ci**) as shown). Maximal projection of confocal Z-stack covering the entire artery is shown in (**B**) and (**C i**), whereas (**C ii, iii**) show magnified longitudinal cross section of the regions outlined in (**C i**). All scale bars are 150 µm. From Chappell et al., 2016.

Similar to the atherosclerosis model, patches of all colours were observed following ligation at frequencies comparable to labelling frequencies (**Figure 35**), again confirming that recombination does not confer a selective advantage to cells expressing a particular fluorescent protein.

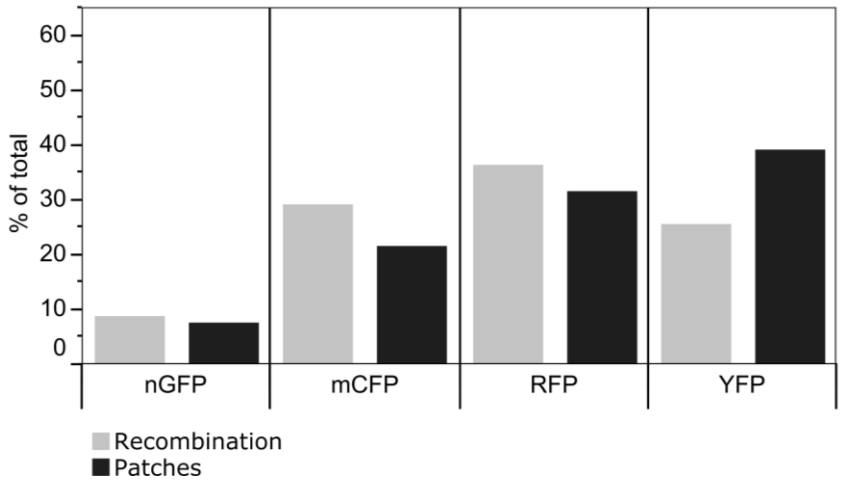

Figure 35: Colour distribution observed in carotid ligation patches
Bar chart showing the proportions of each of the Confetti colours in VSMCs directly after recombination (light grey) and in monochromatic regions within carotid ligation induced neointima (dark grey). All data is from high density-labelled animals (10x 1 mg tamoxifen). Adapted from Chappell et al., 2016.

To determine the size of patches (cells per patch), confocal images of whole-mount, ligated, carotid arteries were processed (using Imaris) to surface render individual patches or cells in 3D. The volume was then calculated for each rendered surface, using the volume function within Imaris. By dividing the patch volume with the average volume for a single cell (with the same colour as the patch) it is possible to approximate the number of cells per patch. This figure ranged from 48 to > 7000 cells/patch with a mean of 962 and median of 436 cells/patch (**Figure 36, Appendix C**). Intra-animal patch size variation was similar to inter-animal variation, suggesting that this size range is not associated with slight differences in the ligation surgery between animals. The large patch sizes observed suggest that a single cell has vast expansionary capabilities (i.e. between 6-9 rounds of uniform doubling to create patches with 128-1024 cells) in order to remodel such large sections of the artery.

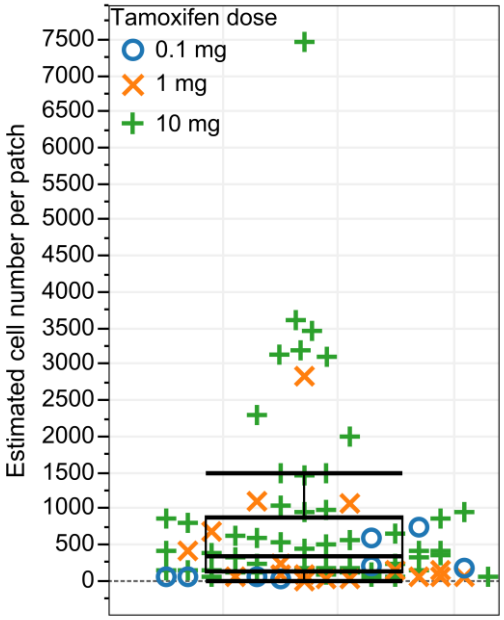

Figure 36: Patch sizes in remodelled arteries

Box plot showing the size of individual monochromatic patches. The patch sizes of low density-labelled (blue circles), medium density-labelled animals (orange crosses) and high density-labelled animals (green crosses) are displayed. Results are from 52 patches from 12 high density-labelled (10x 1 mg), 15 patches from 4 medium density-labelled (1x 1 mg) and 8 patches from 4 low density-labelled animals (1x 0.1 mg). Adapted from Chappell et al., 2017

To determine whether large monochromatic, neointimal, patches are the result of chance merging of independent clones of the same colour, carotid ligation was performed on animals injected with lower doses of tamoxifen (1x 0.1 and 1x 1 mg per animal), which induces ~40% and ~1% labelling of VSMCs, respectively. Compared to high density labelled arteries following carotid ligation, medium and low density labelled arteries contained fewer coloured patches (**Figure 37, Appendix C**), which is expected as fewer medial VSMCs are labelled. While patches in the low and medium density labelled arteries were similar in size to many of the patches in the high density labelled animals, the mean (363 cells/patch) and median (98 cells/patch) patch size was lower (**Figure 36**). This suggests that very large patches (>1500 cells) may arise from the chance merging of independent clones of the same colour, however, the fact that large isolated patches are still observed in the low density labelled artery demonstrates clonality.

The results from these carotid ligation experiments, therefore, demonstrate that a small subset of VSMCs undergo multiple rounds of division (~9 to reach the medium cells/patch) to generate the neointima following carotid ligation-induced vascular injury. This is similar to the results observed in the ApoE$^{-/-}$ HFD model (**Chapter 5**), in which few VSMCs clonally expand within atherosclerotic plaques. To quantify the proportion of cells that clonally expand in the ligation model, VSMC cellularity within the carotid medial layer of 5000 cells/mm^2 (Clarke et al. 2006), and carotid artery diameter of

0.47 mm (Lacolley et al. 2001) was used to calculate the number of VSMCs/mm of vessel: (2π(0.5*0.47)1)5000 = 7382 cells/mm of vessel. Based on the measurements collected from this study, the average number of patches/mm of remodelled artery was 2.7 ± 1.0 (**Appendix C**), therefore less than 0.1% of VSMC are actively expanding to contribute to neointimal formation 28 days post ligation.

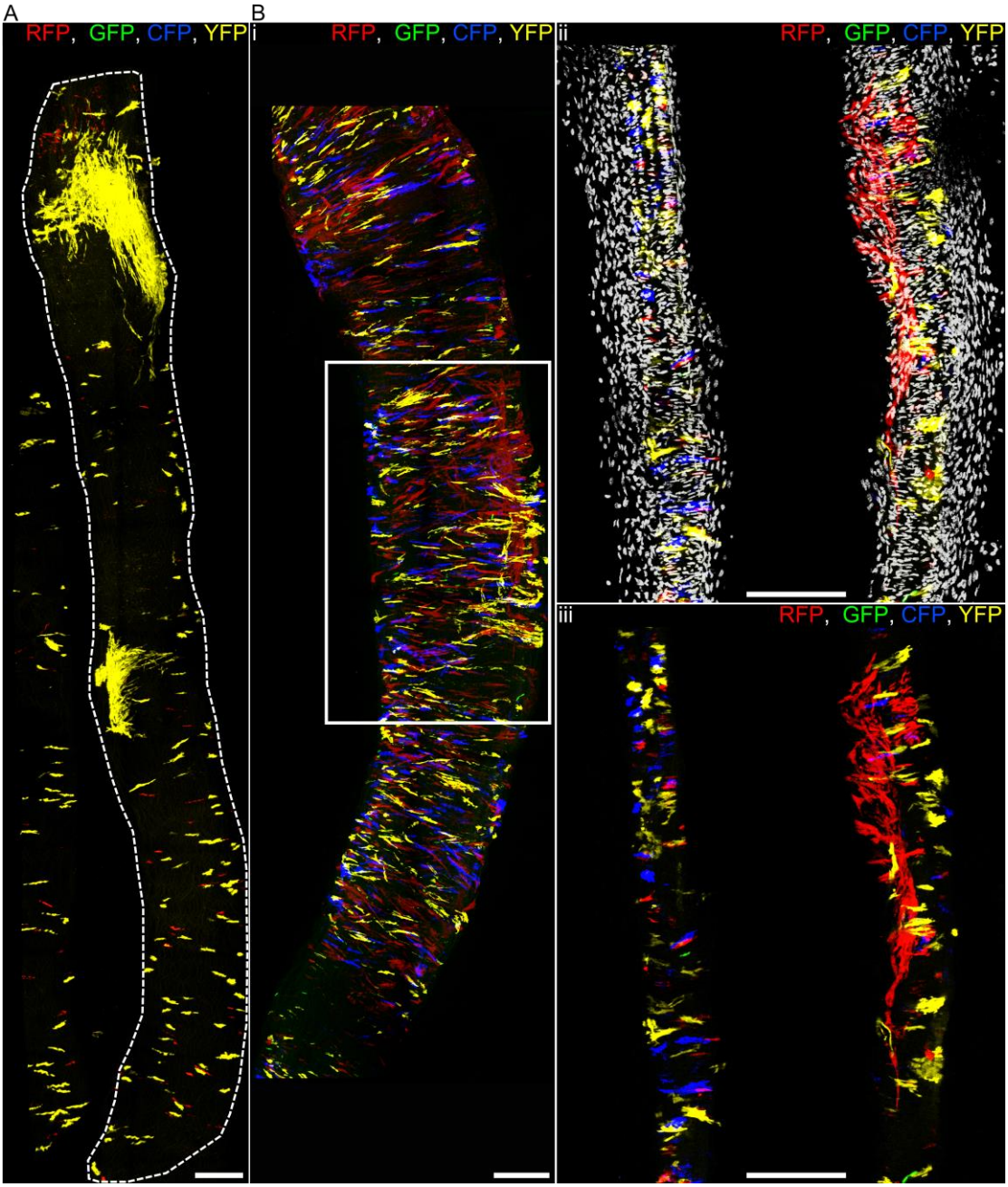

Figure 37: A subset of VSMCs proliferate to form the injury-induced neointima

A, B (**i**) Maximal confocal Z-stack projection of whole-mounted ligated left carotid artery from a low density-labelled (**A**) and mid density-labelled (**B**) animals (1x 0.1 mg and 1x 1mg tamoxifen, respectively), analysed 28 days post-ligation. Region outlined in (**B i**) is shown as a magnified longitudinal section in (**B ii**) and (**B iii**) with and without DAP (white). All scale bars are 150 µm. Adapted from Chappell et al., 2016.

The results within this section, confirm that in a second model of CVD, few VSMCs respond to an environmental stimulus known to elicit a proliferative VSMC response. Importantly, here it is demonstrated just how few VSMCs respond in such cases and raises the possibility that this low frequency response is an inherent feature of VSMCs.

6.2 Neointimal VSMCs are mostly in a contractile state 28 days post carotid ligation surgery

To investigate whether clonal proliferation following vascular injury is accompanied by similar phenotypic changes to those observed in the atherosclerosis model (i.e. decreased aSma and increased Mac3 expression), cross-sections of carotid arteries (which had previously been imaged as whole-mount) were stained for aSma and Mac3. Control staining in non-ligated right carotid arteries showed that all VSMCs stained positive for the contractile marker aSma while no Mac3 staining was detected (**Figure 38**).

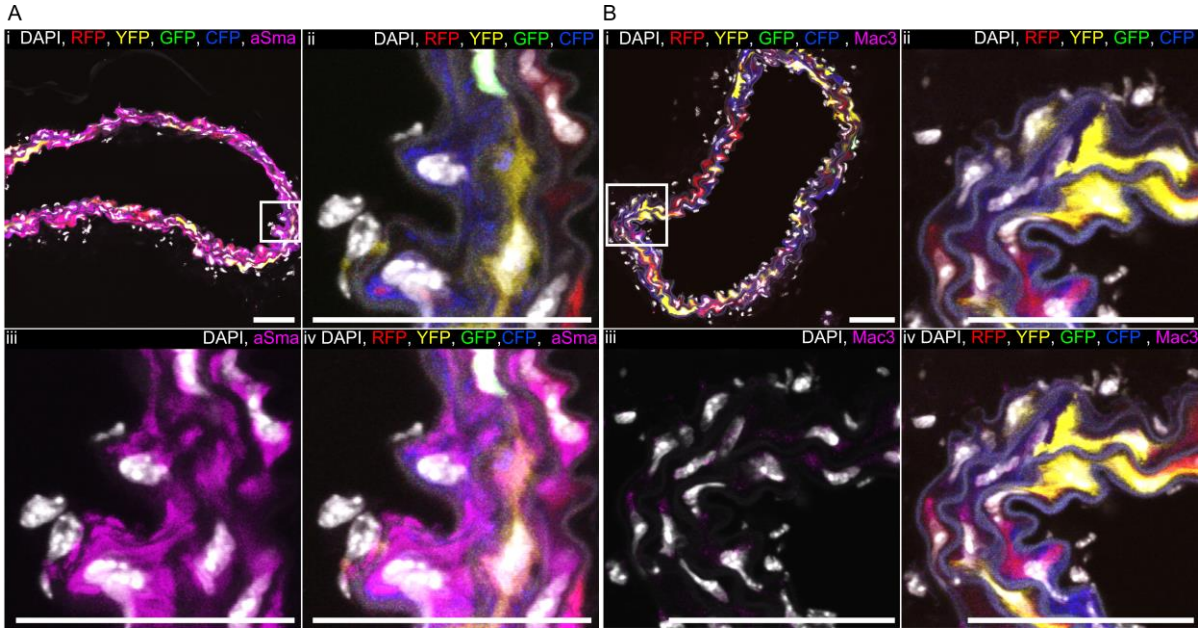

Figure 38: Right carotid artery immunostaining controls

A-D, Single confocal scans from Z-stacks of 14 µm cryo-sections from the control right carotid artery of a high density-labelled (10x 1 mg tamoxifen) animal, 28 days after ligation of the left carotid artery stained for aSma (**A**) or Mac-3 (**B**). Panels (**ii-iv**) are magnified images of the regions outlined in (**i**). Signals for fluorescent proteins, DAPI (white), aSma (magenta) and Mac3 (magenta) are shown as indicated on each image. Scale bars are 50 µm. Adapted from Chappell et al., 2016.

Serial sections from the ligated left carotid artery stained for aSma and Mac3 showed that while the majority of Confetti+ cells were aSma+ (68%) a proportion of the VSMC-derived cells had downregulated their expression of this contractile protein (**Figure 39 B, E**). Other studies examining earlier stages following carotid ligation suggest that the majority of VSMCs within the ligated artery downregulate aSma (Yoshida et al. 2013; B. Paul Herring et al. 2017). It is, therefore, possible that

aSma downregulation in VSMCs following ligation-surgery is transient, returning to near normal levels 28 days post-surgery. The proportion of Confetti+ aSma+ cells (68%) seen in carotid arteries 28 days post ligation (**Figure 39 E**) was similar to the proportion of Confetti+ cells within the cap and shoulder regions from the $ApoE^{-/-}$ HFD model which were also aSma+ (82 and 62%, respectively, **Figure 27**). There was, however, no specific localisation of Confetti+ aSma+/aSma- cells within the injury-induced neo-intima. Mac3 was upregulated in a subset (34%) of VSMC-derived cells within the neointima (**Figure 39 C, E**), however the staining was typically less intense when compared to Mac3 staining within atherosclerotic plaques (**Figure 28**). These results indicate that the injury-induced neointimal Confetti+ cells are modulating their phenotype although less severely than the Confetti+ atherosclerotic plaque cells.

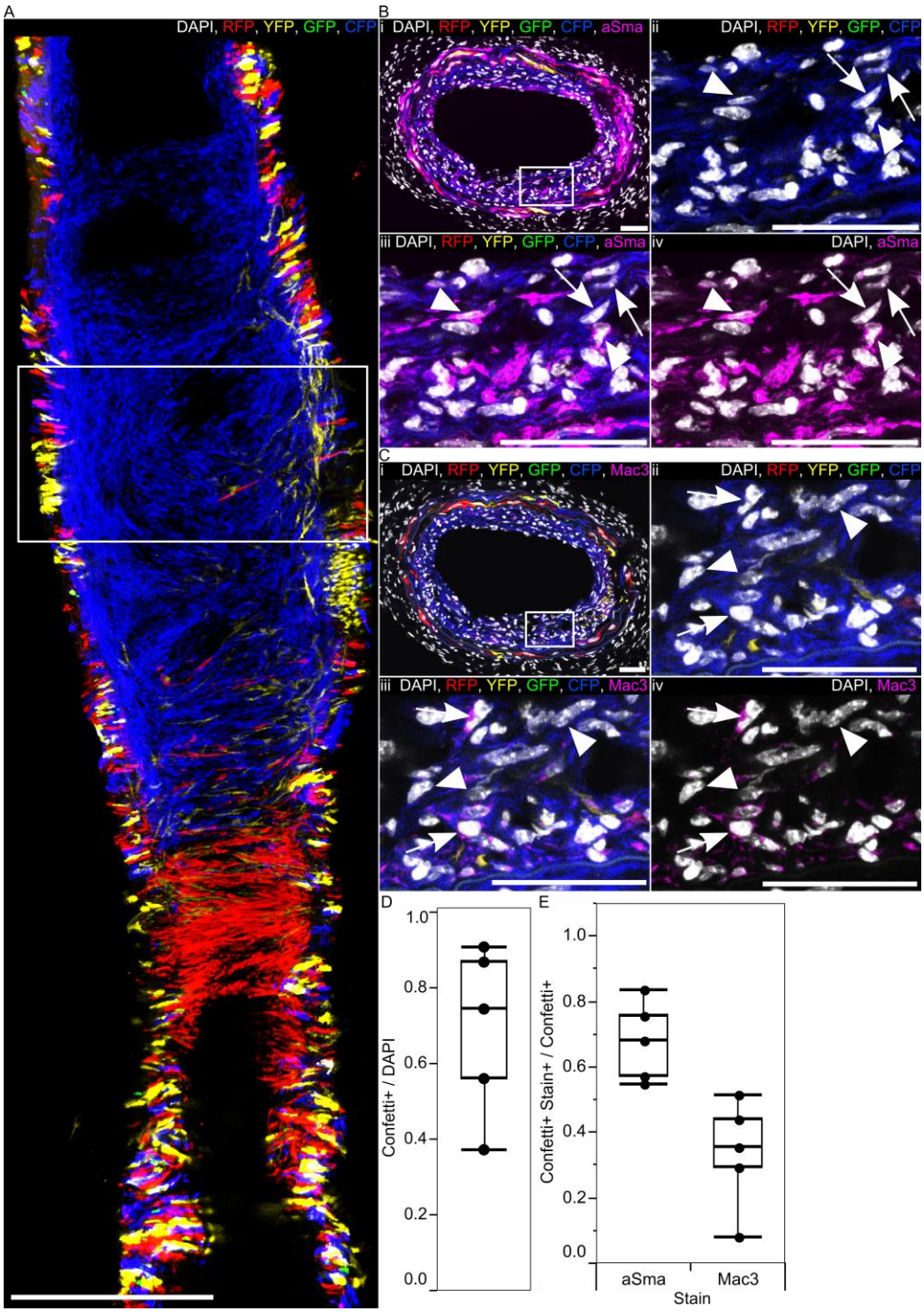

Figure 39: Injury-induced VSMC-derived neointima contains few phenotypically switched VSMCs

A, Maximal projection of three central scans (7 µm apart) of a confocal Z-stack of a whole-mount ligated left carotid artery from a high-density (10x 1 mg tamoxifen) labelled animal, 28 days post-ligation. Scale bar is 300 µm. **B, C,** Transverse cryo-sections from the region outlined in (**A**), stained for aSma (**B**) or Mac3 (**C**); the region outlined in (**i**) is magnified in (**ii-iv**). Arrows point to cells expressing the Confetti reporter (Confetti+) that do not stain for aSma (**B**) and Confetti+ Mac3+ cells (**C**) within the neointima. Arrow heads point to Confetti+ aSma+ cells (**B**) or Confetti+ Mac3- cells (**C**) within the neointima. Scale bars are 50 µm. Signals for fluorescent proteins, nuclear DAPI (white), aSma (magenta, **B**) and Mac3 (magenta, **C**) are shown as indicated on each image. **D,** Box plot showing the proportion of all cells (DAPI) within the neointima which express the Confetti reporter (Confetti+). **E,** Box plot displaying the proportion of Confetti+ neointimal cells that stain positive for aSma or Mac3 (Stain+) (based on 5 regions from 4 animals). All data is from high density-labelled (10x 1 mg tamoxifen) animals. From Chappell et al., 2016.

To further test the phenotypic modulation of VSMC-derived cells in the injury-induced neointimal model, cryo-sections were stained with Smmhc, which marks fully differentiated VSMCs and is downregulated in the earliest stages of phenotypic switching (Rensen, Doevendans, and van Eys 2007). Results showed that Smmhc staining in the neointima is similar to that in the control right carotid artery, with only few Confetti+ cells showing no staining for Smmhc (**Figure 40**), further suggesting that within the carotid ligation model, VMSCs exist primarily in a contractile state at day 28 post ligation.

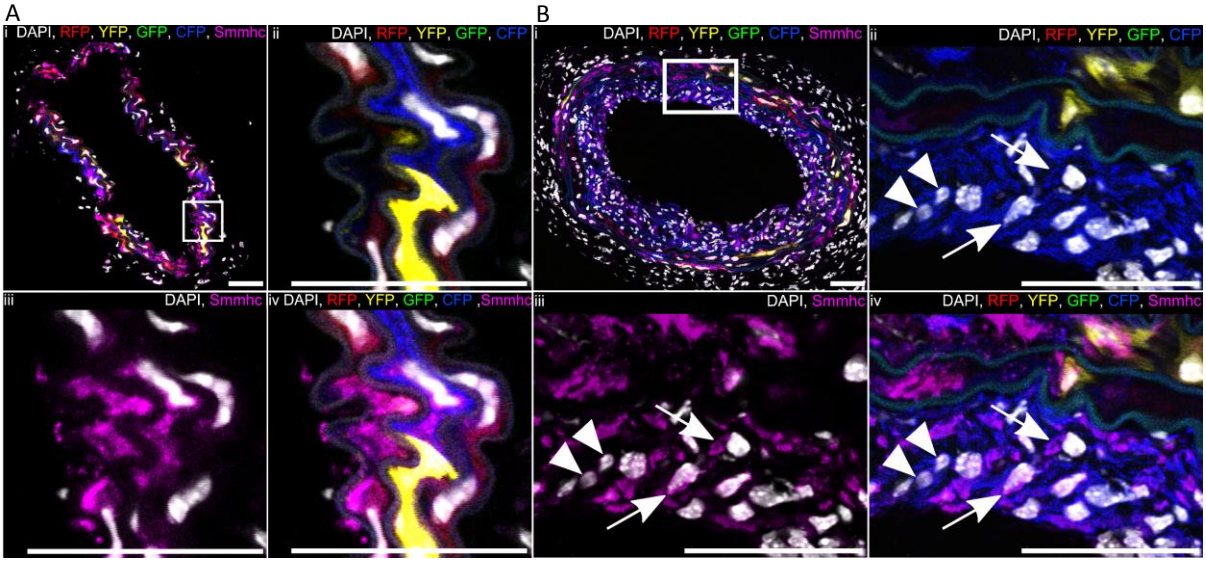

Figure 40: Smmhc immuno-staining in a control right carotid artery and ligated left carotid artery
A, B, Single confocal scans from Z-stacks of 14 µm cryo-sections from the control right carotid artery (**A**) and left carotid artery 28 days post-ligation (**B**) in high density-labelled (10x 1 mg tamoxifen) animals, stained for Smmhc. Panels (**ii-iv**) are magnified regions outlined in (**i**). Arrows point to cells co-expressing the Confetti reporter and Smmhc, whereas arrow heads point to cells that express the Confetti reporter, but do not stain for Smmhc. Signals for fluorescent proteins, DAPI (white) and Smmhc (magenta) are shown as indicated on each image. Scale bars are 50 µm. Adapted from Chappell et al., 2016.

The contractile phenotype seen here is likely only seen in the latter stage post-injury. For example, Herring et al. (2017), observed that 3 days post-ligation there was an almost complete loss of contractile markers accompanied by an increase in inflammatory markers such as Spp1, Il1β and Il6. Their study determined this using qPCR following mRNA extraction from all cells in the left carotid artery post injury, therefore indicating that the majority of VSMCs first respond by modulating their gene expression away from the contractile phenotype and towards a synthetic phenotype. Baetta et al. (2000) also observed, 6 and 12 hours post carotid artery injury (using a perivascular collar in rabbits), that the majority of VSMCs within the injured carotid artery had upregulated expression of

signal transducers and activators of transcription 6 (Stat6), further supporting the idea that the majority of VSMCs phenotypically switch following injury.

6.3 Migration of VSMCs, independent of proliferation, into injury-induced neointima is not observed

The neointimal patches formed from VSMC-derived cells in the ligation model were always connected to medial patches of the same colour (**Figure 41**) suggesting that VSMC proliferation initially occurs within the media and that progeny then migrate through the elastic laminae where they continue dividing to form the neointima. This is consistent with time course studies that have determined a high rate of medial proliferation soon after injury (Kumar and Lindner 1997). Coherent neointimal patches did not contain singlet VSMCs of a different colour (**Figures 34 and 41**), which would be observed if many randomly labelled cells migrated from the medial wall, suggesting that migration of VSMCs independent of proliferation does not significantly contribute to neointimal growth. Similarly, within the ApoE$^{-/-}$ HDF model, monochromatic patches within atherosclerotic plaques did not contain singlet cells of a different colour (**Figures 20 and 22**), suggesting that only proliferative VSMCs are able to enter and/or survive the neointima/plaque environment.

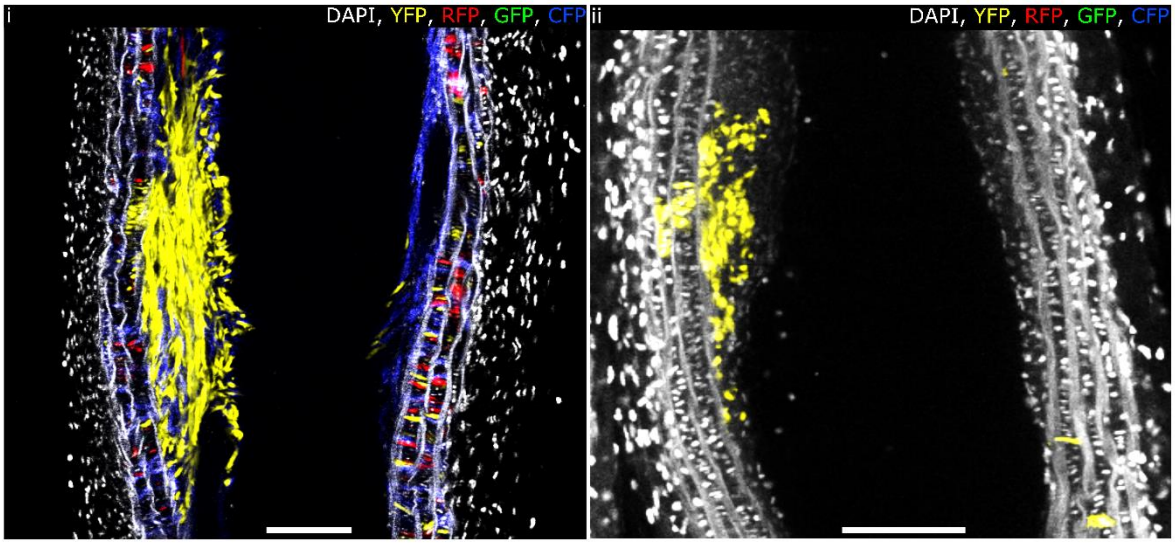

Figure 41: Clonal VSMC-derived patches span both media and neointima
Longitudinal cross section of the left carotid artery from animals labelled at high density (10x 1 mg tamoxifen, **i**) or low density (1x 0.1 mg tamoxifen, **ii**), which were analysed 28 days post-surgery, showing that individual VSMC-derived clones are "anchored" in the medial layer. A single scan of a confocal Z-stack, which intersects the middle of the vessel, is shown. Signals for fluorescent proteins and DAPI (white) are shown. Scale bars are 100 µm. From Chappell et al., 2016.

The observation made in this section that VSMCs do not migrate into the neointima independent of subsequent proliferation is in direct contradiction to several previous studies (**section 1.7**, Zahradka

et al. 2004; Yu et al. 2011; Clowes and Schwartz 1985). For example, Yu et al. (2011) suggest that approximately 40% of neointimal cells migrate independent of proliferation following carotid ligation, this observation is based on the detection of the thymidine analogue BrdU, which was diluted in the animals drinking water for the entire 28 days post-surgery. Furthermore, Clowes and Schwartz (1985), using a carotid balloon injury model in rats, also observed that 40% of neointimal cells had not proliferated, based on ^{3}H-thymidine detection, which was delivered using osmotic pumps following surgery. However, even if 1% of VSMCs migrated into the neointima and survived independent of proliferation, singlet VSMCs would be detected in neointimal, monochromatic patches of a different colour. Two possible explanation for why Clowes and Schwartz (1985) and Yu et al. (2011) detected such a high number of cells that were negative for proliferation markers within the neointima are: (1) as neither study used lineage tracing methods to accurately identify the progeny of VSMCs, they may be detecting blood- or adventitial-derived cells which invade the neointima; and (2) that methods to label proliferating VSMCs are not 100% efficient.

To test what the proliferative index is within this study, mice were injected with EdU 5 days a week following carotid ligation surgery. Results showed that a high proportion of Confetti+ VSMCs were EdU+ (47% ±2, **Figure 42**), although many cells were EdU-negative, suggesting that they did not proliferate. However, given that the neointima in monochromatic patches are derived from the clonal expansion of a single VSMC, the EdU method used here to label proliferating VSMCs cannot be 100% efficient. It is possible that this is also the case for the ^{3}H-thymidine and BrdU methods used by Clowes and Schwartz (1985) and Yu et al. (2011), respectively, explaining why they also see such a high number of non-labelled neointimal cells. There are several reasons why strategies for labelling proliferating cells may not be 100% efficient. For instance, the use of ^{3}H-thymidine suffers from poor resolution and a low signal-to-noise ratio, which makes detecting positive cells challenging (Salic and Mitchison 2008). BrdU methods may also suffer from antibody penetration issues and the harsh staining conditions necessary to denature double stranded DNA (Rakic 2002; Salic and Mitchison 2008).

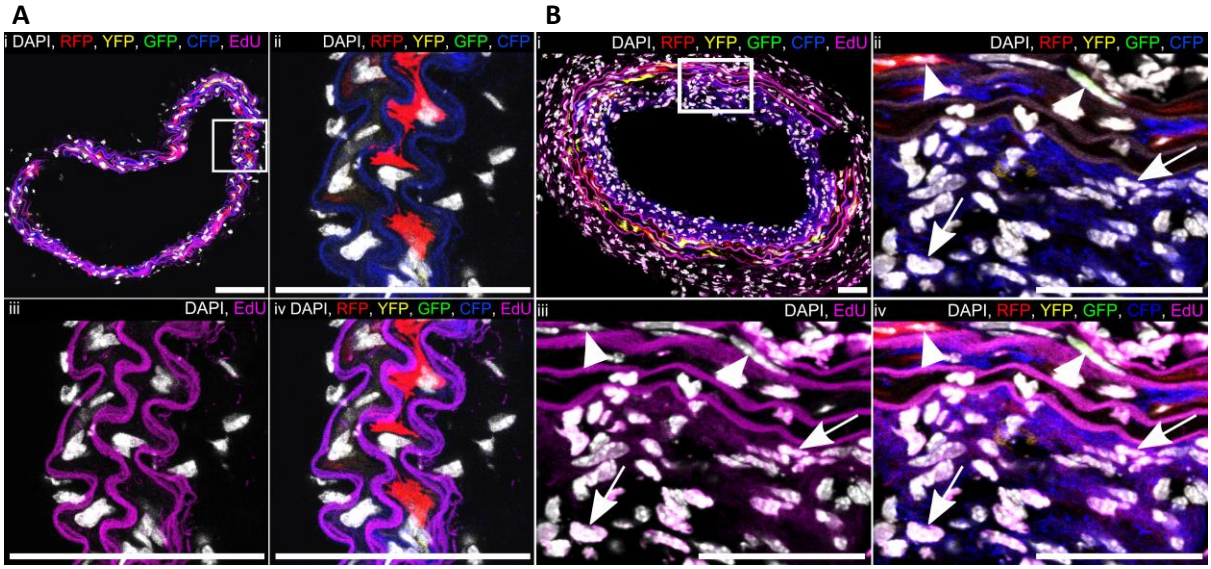

Figure 42: EdU staining in carotid ligation-induced neointima

A, B, Single confocal scans from Z-stacks of 14 µm cryo-sections from the control right carotid artery (**A**) and the left carotid artery (**B**) 28 days post-ligation in high density-labelled animals (10x 1mg tamoxifen) stained for EdU. For each cryo-section, the region outlined in (**i**) is magnified in (**ii-iv**). Arrows point to cells co-expressing the Confetti reporter and EdU, whereas arrow heads point to cells that express the Confetti reporter, but do not stain for EdU. Signals for the fluorescent proteins, DAPI (white) and EdU (magenta) are shown as indicated on each image. Scale bars are 50 µm. From Chappell et al., 2016.

6.4 Conclusions from the carotid ligation experiments

The carotid ligation model of neointimal growth was performed here to determine whether, similar to the ApoE$^{-/-}$ HFD model of atherosclerosis (**Chapter 5**), a few original VSMCs proliferate in response to arterial injury/disease. Results within this Chapter show that when carotid ligation is performed on high density labelled Myh11-CreER(T2); R26R-Confetti animals, large (mean=962 and median=436 cell) contiguous monochromatic patches of VSMC-derived cells make up the newly formed neointima (**Figures 34 and 36**). Reducing the labelling frequency of Confetti+ VSMCs resulted in fewer isolated monochromatic patches, which confirm that these regions are derived from the clonal expansion of single VSMCs (**Figures 36 and 37**). Based on the number of medial cells and neointimal patches/mm of artery, less than 0.1% of medial VSMCs clonally expand to remodel the artery and form the newly derived neointima. The low proportion of VSMCs which proliferate in response to the ligation model is, therefore, similar to what was previously seen in the ApoE$^{-/-}$ HFD model of atherosclerosis (**Chapter 5**), suggesting that the low frequency response to injury/disease could be an inherent feature of VSMCs.

In contrast to the ApoE$^{-/-}$ HFD model (**Chapter 5**), fewer VSMC-derived cells observed in injury-induced neointima, 28 days post injury, present a synthetic phenotype (i.e. irregular morphology and expression of the macrophage marker Mac3, **Figures 28, 29 and 39**), which was more typical of VSMCs located to the cap of an atherosclerotic plaque (i.e. elongated and aSma+, **Figures 26, 27 and 39**).

However, studies examining phenotypic switching of VSMCs just days after carotid ligation showed that all VSMCs within an injured artery downregulate contractile markers and upregulate markers of inflammation (Yoshida et al. 2013; Herring et al. 2017). It is therefore possible that following surgery the initial phenotypic switch of VSMCs away from the contractile phenotype is transient, with VSMC-derived cells returning to a more contractile phenotype once the neointima is fully formed.

Both, the carotid ligation experiments performed here and the atherosclerosis experiments in **Chapter 5** show that no monochromatic VSMC-derived patches within a plaque or injury-induced neointima contain singlet cells of another colour. This suggests that migration of VSMCs from the media into the neointima does not happen independently of proliferation, otherwise singlet cells would be observed. This is in direct contrast to observations made by (Yu et al. 2011; Clowes and Schwartz 1985) who suggest, based on in vivo methods to label proliferative cells, that up to 40% of non-proliferative, migratory VSMCs form the injury-induced neointima. To test the proportion of VSMCs-derived cells that were positive for proliferation within the neo-intima, EdU was injected into mice 5 days a week following carotid ligation surgery. Results demonstrated that less than 50% of VSMC-derived cells within a monochromatic patch were EdU+. However, as these patches were derived from the expansion of single VSMCs, this suggests that the EdU labelling strategy used here is not 100% efficient, which could be the case for labelling strategies used by Yu et al. (2011), and Clowes and Schwartz (1985).

Chapter 7: VSMC proliferation and plasticity in the Ang II perfusion model of AAA

Models of AAA have been intensely studied to understand the sequence of cellular events leading to aortic aneurysm and rupture (Daugherty and Casis, 2004, and discussed in **sections 1.9, 1.10 and 2.4**). Important steps in the progression of AAA are noted as: (1) the medial accumulation of macrophages and degradation of elastin; (2) Dissection of the vascular wall and appearance of vascular haematoma; and (3) A profound inflammatory response, including the infiltration of B and T lymphocytes (Saraff et al., 2003). VSMCs are typically described in regard to their apoptosis, which is increased in models of AAA, along with elastin break-down this leads to the degeneration of the vascular wall (Thompson 1996; López-Candales et al. 1997; Rowe et al. 2000). Several studies have reported that VSMCs phenotypically switch in AAA, downregulating the contractile proteins aSma and Sm22a (Ailawadi et al., 2009) and upregulating production of MMPs (Airhart et al., 2014). However, to date no studies have specifically lineage traced VSMCs within AAA. Given the known potential for VSMCs to phenotypically switch and be unidentifiable by traditional contractile markers (e.g. Myh11 and aSma, Gomez and Owens, 2012) there is a possibility that previous studies have missed an important role of VSMCs in the progression of AAA. Particularly as, in late stages of AAA there is often prominent remodelling and neovascularisation of aneurysmal tissue (Saraff et al., 2003) which, in other models of CVD, is often supported by/involves VSMCs, for example the HFD/carotid ligation models (**Chapter's 5 and 6**).

The work within this Chapter was initiated following experiments performed by Dr. Marc Clement, in which, the Ang II infusion model of AAA (**described in sections 2.4 and 3.13**) resulted in the appearance of large, coherent regions of aSma+ cells within the intraluminal thrombus of the aneurysm. To understand whether these aSma+ cells are VSMC-derived and to see if VSMCs clonally proliferate within AAA, the Myh11CreER(T2); R26R-Confetti mice were subjected to the Ang II infusion protocol for 28 days (**section 2.4**) and the tissue was analysed by confocal microscopy of cryo-sections.

This results chapter is based on a collaboration between the groups of Dr. Helle Jorgensen and Prof. Ziad Mallet. Mini-pump surgery and tissue removal was performed by Dr. Marc Clement while cryo-sectioning, immuno-staining and imaging was performed by Joel Chappell.

Aims

1. Determine if the observed aSma+ population of cells within the intraluminal thrombus, following the Ang II perfusion model of AAA, are VSMC-derived
2. Determine if VSMCs clonally proliferate in AAA
3. Examine potential molecular mechanisms leading to the proliferative response of VSMCs

7.1 The Ang II, anti-TGF-β model of AAA induces an outward clonal expansion of VSMCs at thrombotic sites and medial proliferation at sites of elastic lamina breaks

To test if VSMCs proliferate within AAA, 6-week-old Myh11CreER(T2); R26R-Confetti mice were labelled at high density (10x 1 mg tamoxifen), and subjected to mini-pump surgery in which an Ang II loaded mini-pump was inserted subcutaneously into each mouse, this was followed by 3 injections per week of anti-TGF-β for 28 days. The Ang II/anti-TGF-β protocol used here caused the development of aneurysms primarily within the abdominal region of the aorta, which macroscopically appeared as small bulges along the length of the aorta (data not shown). To investigate VSMC involvement in the development of these aneurysms the abdominal aorta was cryo-sectioned and imaged by confocal microscopy (**Figure 43 A**).

Imaged cryo-sections showed that within the developed intraluminal thrombus, Confetti+ cells were frequently (in 3/5 mice, **Appendix D**) detected in large patches (**Figure 43 B**). VSMC-derived patches within the thrombus were typically composed of several coherent patches expressing different colours, suggesting that several VSMCs clonally expand to remodel the aneurysmal tissue. Compared to the VSMC-derived patches observed in the HFD atherosclerosis/carotid ligation models of CVD they were, typically more heterogeneous, containing more colours within a given region with more intermingling of colours. For example, **Figure 43** (**B ii**) shows a large region containing VSMC-derived cells, RFP expression is predominant, with some interspersed yellow cells, suggesting that a red and yellow clone have merged. Furthermore, where VSMCs had not entered the thrombus/where no thrombus had developed, there was frequently large medial patches with multiple cells of the same colour, indicating that a single cell had expanded within a particular medial layer (**Figure 43 C**). This could suggest that, at least in some cases, VSMCs proliferate within the media prior to invading the thrombus.

The observation that large VSMC-derived, monochromatic patches within the thrombus and media exist following the Ang II/anti-TGF-β protocol clearly show that VSMCs proliferate within AAA through massive clonal expansion. This phenomenon has not yet been reported within in the literature, with

the majority of studies regarding apoptosis as the key VSMC event (Thompson 1996; López-Candales et al. 1997; Rowe et al. 2000). Some studies have however reported highly proliferative/migratory VSMCs taken from AAA tissue when analysed in culture (Patel et al. 1996). Out of the five mice analysed, three contained VSMC-derived outgrowths and all contained medial monochromatic patches and breaks within the elastic lamina (**Appendix D**). However, similar to other studies there was a large degree of heterogeneity between mice in terms of phenotype severity (Daugherty, Manning, and Cassis 2001), and is likely the result of a combination of factors, including where initial micro-tears occur within the aortic wall (Trachet et al. 2017).

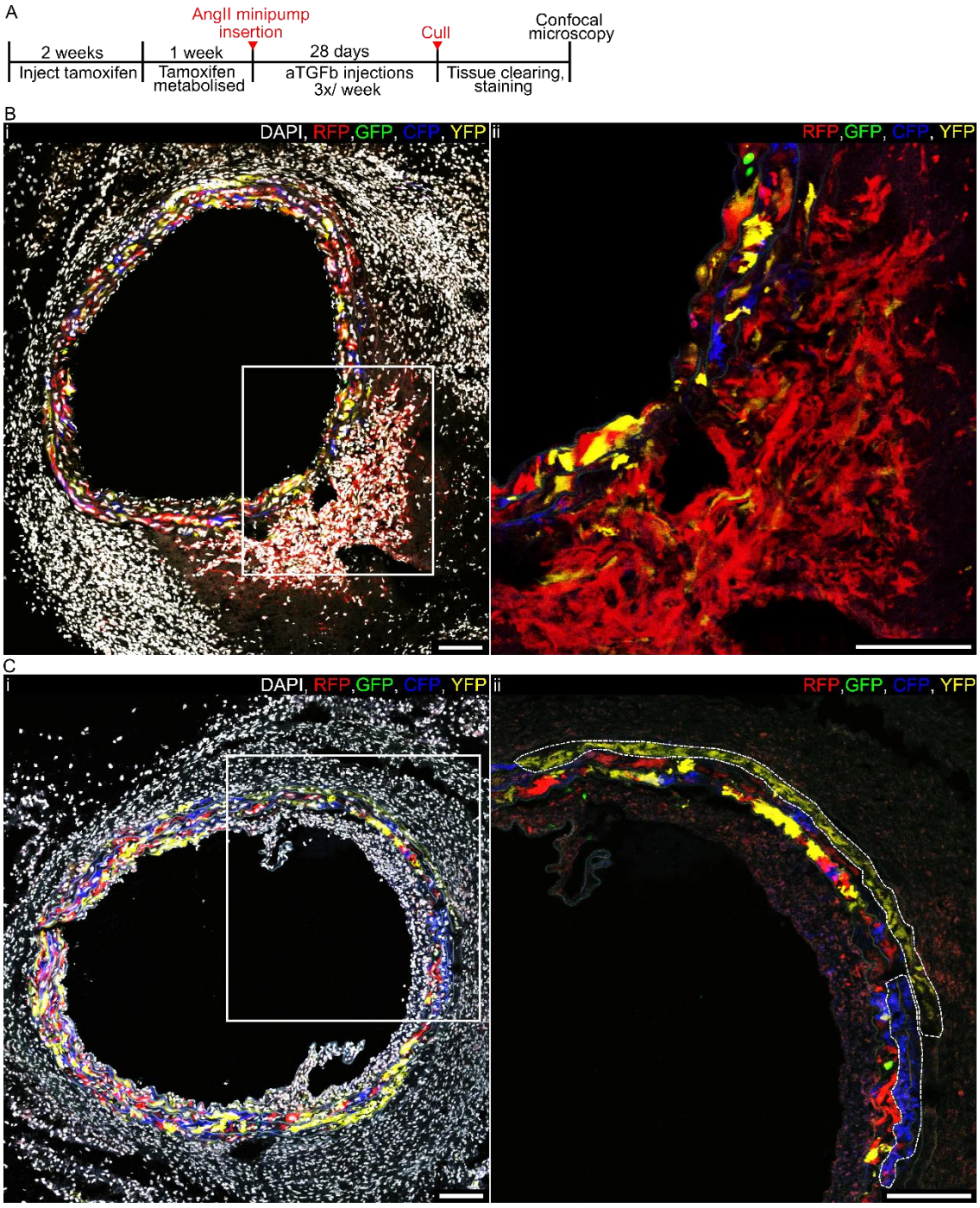

Figure 43: VSMCs clonally expand in the Ang II + anti-TGF-β model of AAA

A, Experimental protocol for the Ang II + anti-TGF-β, AAA studies. **B and C,** AAA cryo-sections from high density-labelled animals (10x 1 mg tamoxifen) presenting outward remodelling of VSMCs within the aneurysmal tissue of the abdominal aorta into the thrombus (**B**) and within the media (**C**). The regions outlined in (**i**) are magnified in (**ii**). Dashed white lines in (**C ii**) encircle VSMC-derived cells of the same colour expanded within a single medial layer. Fluorescent protein and DAPI (grey) is shown as indicated. Scale bars are 100 µm.

To determine if the VSMC-derived outgrowths were aSma+, and therefore related to the original observation by Dr. Clement (discussed above), cryo-sections were stained for aSma. Results showed that aSma staining co-localised with the Confetti+ outgrowths, although staining was typically less intense compared to the media, indicating that some downregulation of aSma had occurred within these cells (**Figure 44**). Furthermore, no aSma+ patches were detected which were not Confetti+. Confetti- aSma- cells were detected within the Confetti+ outgrowths, and are likely the results of invading macrophages and resident adventitial cells, which are similarly observed in other studies (Saraff et al. 2003; Rateri et al. 2011). These results confirm that the aSma+ patches observed by Dr. Clement are VSMC-derived.

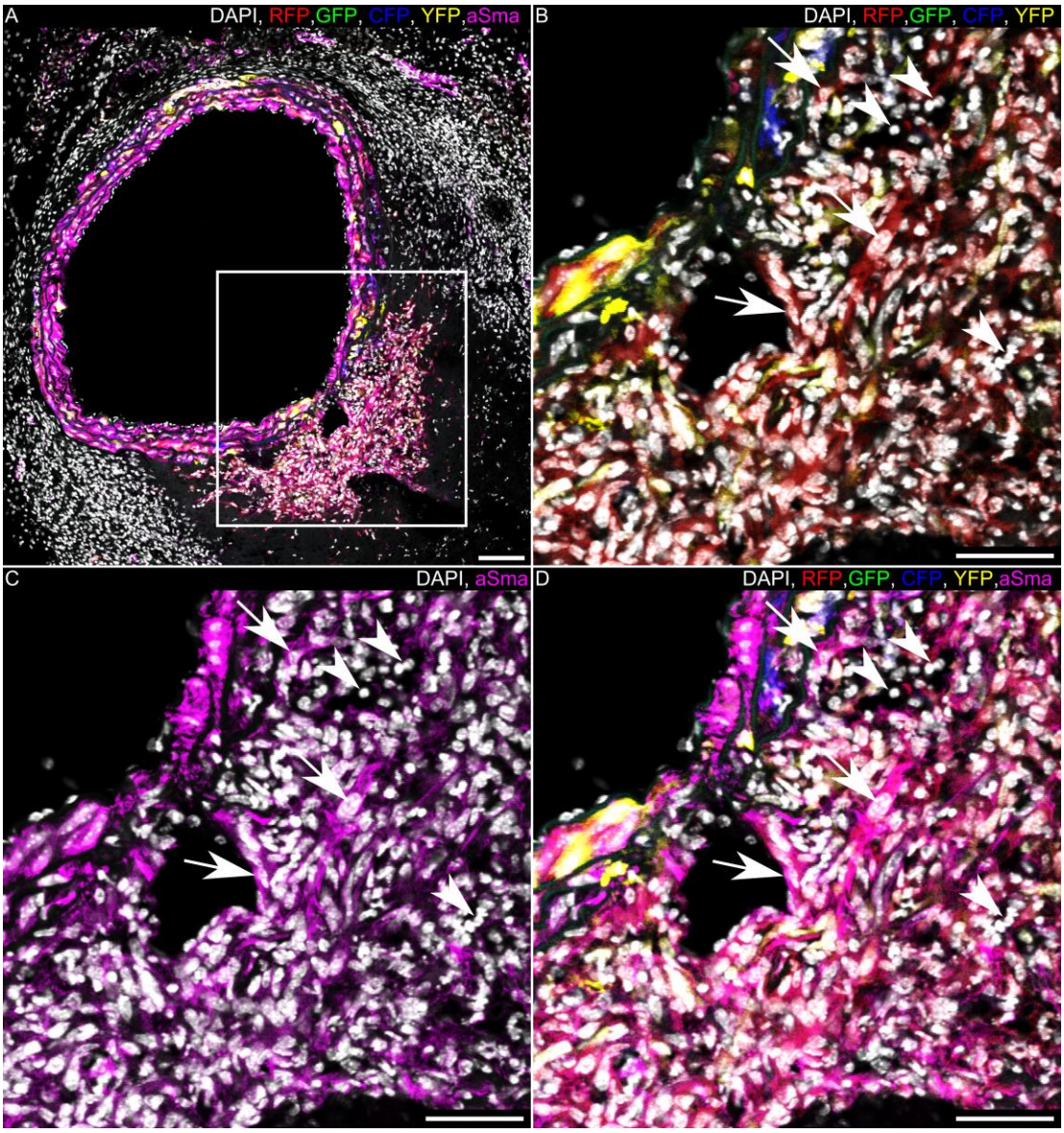

Figure 44: VSMC-derived patches within the Ang II + anti-TGF-β model of AAA co-localise with aSma
A, AAA cryo-section from high density-labelled animals (10x 1 mg tamoxifen) presenting outward remodelling of VSMCs into the thrombus with aSma staining. The region outlined in (**A**) is magnified in (**B, C and D**) fluorescent protein, DAPI (grey) and aSma (magenta) is indicated at the top of each panel. Arrows point to Confetti+ aSma+ cells, arrow heads point to Confetti- aSma- cells. Scale bars are 100 µm.

Also observed within cryo-sections from all mice with AAA were dilated areas within the media containing Confetti+ monochromatic patches, Confetti-negative cells and even regions containing no cells at all (**Figure 45**). While VSMC death, infiltration of immune cells and medial degradation is known to occur in AAA (Saraff et al. 2003; Rateri et al. 2011), proliferation of VSMCs to fill these dilated regions is not documented. Whether VSMCs which proliferate in response to their environment fill a space in which other VSMC have left empty through apoptosis, or if proliferating VSMCs invade the space around them killing less fit cells is undetermined. Experiments which lineage trace VSMCs in early stages of AAA could be used to determine the sequence of events by which monochromatic patches grow and single non-proliferative VSMCs die.

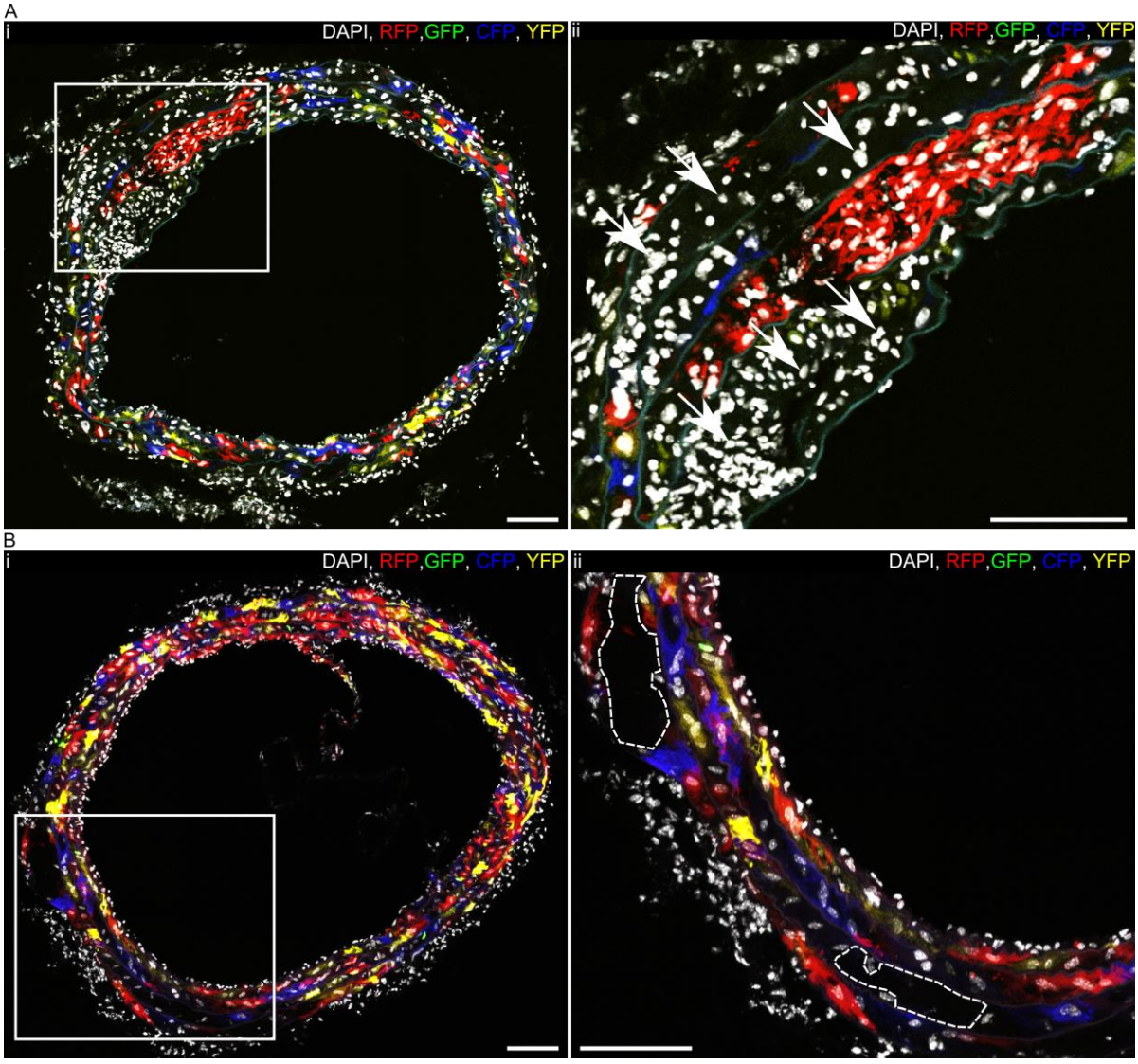

Figure 45: Medial dilation in AAA

A and B, AAA cryo-sections from high density-labelled animals (10x 1 mg tamoxifen) presenting medial dilation. Dilated areas are either filled with Confetti+ or Confetti- cells (**A**) or contain no cells (**B**). The region outlined in (**i**) is magnified in (**ii**). Arrows in (**A i**) point to Confetti-negative cells and the white dashed line in (**B ii**) encircles areas containing no cells. Fluorescent protein and DAPI (grey) is indicated at the top of each panel. Scale bars are 100 µm.

7.2 anti-TGF-β is not responsible for the VSMC response in the Ang II perfusion model on an ApoE$^{-/-}$ background

To further understand the proliferative response from VSMC-derived cells it is important to consider the factors causing this response. Both Ang II and TGF-β are known to affect VSMCs, for example Ang II has been shown to increase VSMC contractility (Dostal, Murahashi, and Peach 1990) but can also contribute to the proliferative phenotype of VSMCs (Zhang et al. 2012). In contrast, TGF-β is vital for the development and maturation of VSMCs from pre-cursor cells (Sinha et al. 2004) but can promote the proliferative and migratory phenotype of mature VSMCs (Zhu et al. 2015). To investigate whether VSMC proliferation within AAA results from the artificial blocking of TGF-β signalling, which might directly induce VSMC phenotypic switching, Ang II mini-pumps were inserted into ApoE$^{-/-}$ mice which were divided into two groups. One group received no anti-TGF-β while the other was injected with anti-TGF-β two weeks following Ang II mini-pump insertion.

Of the nine mice which did not receive anti-TGF-β only one contained a thrombotic outgrowth of VSMCs (**Appendix D**) which demonstrated large monochromatic regions, suggesting massive clonal expansion of multiple cells (**Figure 46 A**). All nine of these mice, however, contained breaks within the elastic lamina along with medial patches of VSMC-derived cells (**Appendix D, Figure 46 B**). Zero out of five animals receiving anti-TGF-β had an outgrowth of VSMCs, but similar to mice which did not receive anti-TGF-β, all contained elastic lamina breaks and medial proliferation (**Appendix D, Figure 47**). It should be noted that medial proliferation occurred in relatively healthy-looking media (**Figure 46 B**) and dilated media (**Figure 47**) in both mice which received and did not receive anti-TGF-β. The similar phenotypes observed between the two groups of animals (i.e. +/- anti-TGF-β) is expected, as previous studies have shown that while anti-TGF-β increases severity of the AAA phenotype in wildtype mice it has little effect in ApoE$^{-/-}$ mice (Wang et al. 2010). Furthermore, the observation that anti-TGF-β administration has little effect on the AAA-VSMC phenotype in Ang II infused ApoE$^{-/-}$ animals suggests that factors other than those directly related to TGF-β are causing VSMCs to proliferate.

One possible reason for the lack of VSMC outgrowths in the ApoE$^{-/-}$ mice (1/14) compared to the wild type mice (3/5) is that the ApoE$^{-/-}$ AAA phenotype was typically, in these experiments, not severe enough to develop a thrombus in which VSMCs could grow into. Given that there was still substantial medial proliferation of VSMCs within the ApoE$^{-/-}$ mice this suggests that thrombus formation is reliant on other factors than VSMC proliferation, although this is expected as thrombus formation is known to occur in response to platelet activation (Liu et al. 2012).

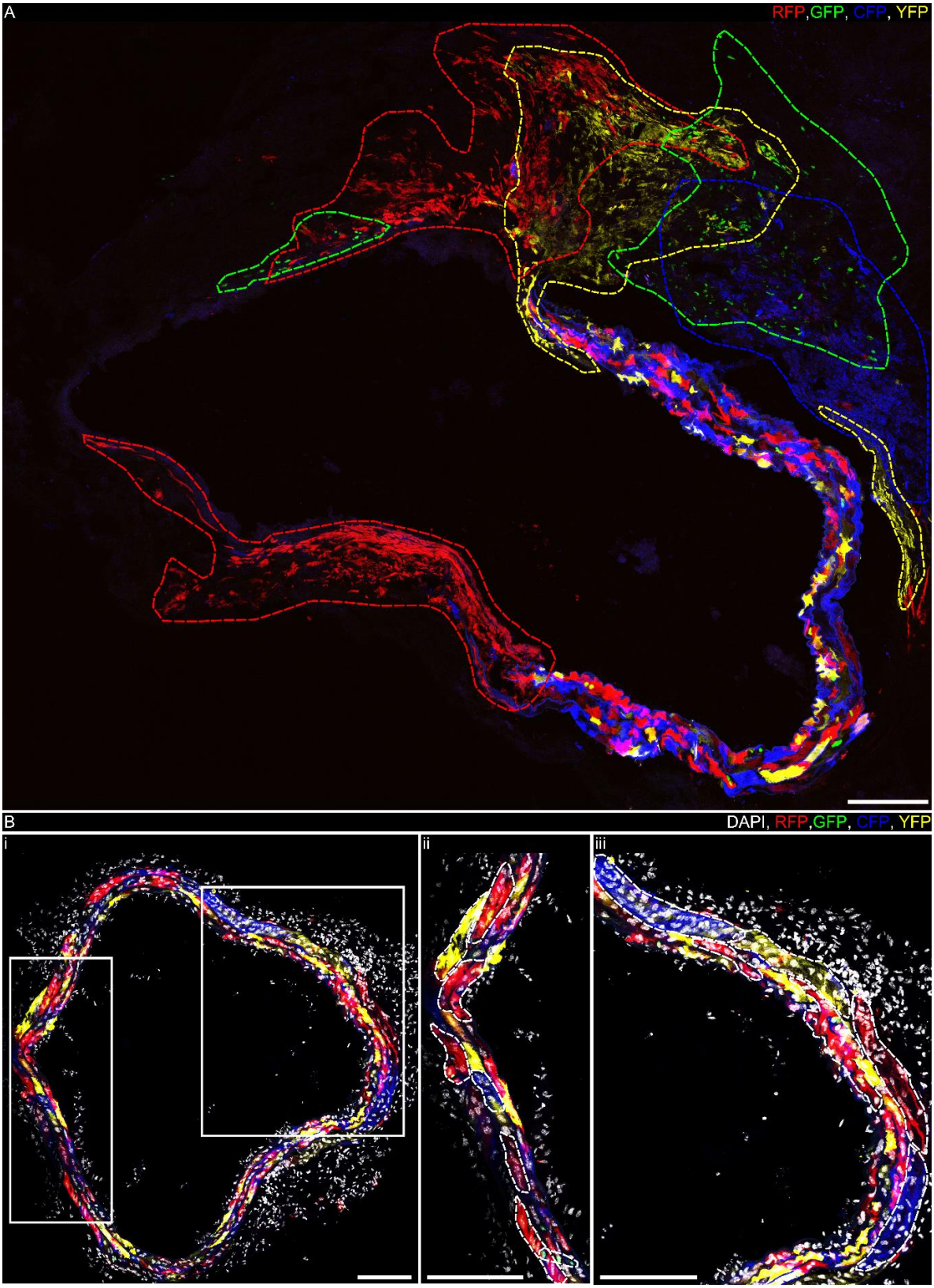

Figure 46: VSMC clonal expansion in the Ang II model of AAA on the ApoE$^{-/-}$ background
A and B, AAA cryo-sections from high density-labelled animals (10x 1 mg tamoxifen) presenting VSMC outgrowth (**A**) and medial expansion of VSMCs (**B**). The region outlined in (**B i**) is magnified in (**B ii and iii**). Coloured and white dashed lines in (**A and B ii and iii**) encircle VSMC-derived patches. Fluorescent protein and DAPI (grey) is indicated at the top of each panel. Scale bars are 150 µm.

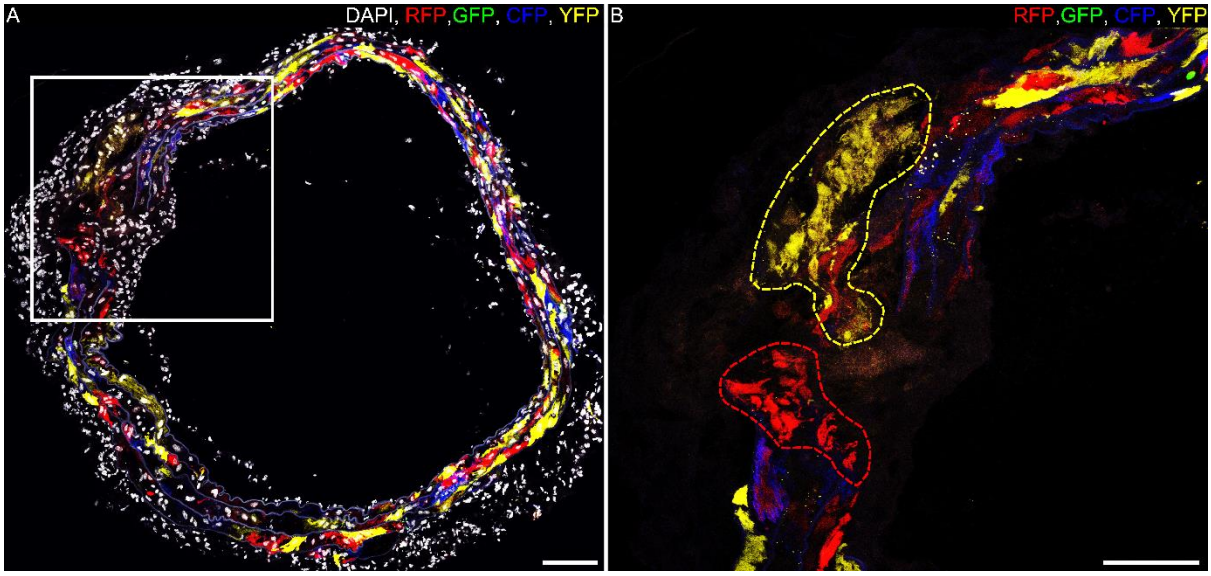

Figure 47: VSMC clonal expansion in the Ang II + anti-TGF-β model of AAA on the ApoE$^{-/-}$ background
A, AAA cryo-sections from a high density-labelled animal (10x 1 mg tamoxifen) presenting medial expansion of VSMCs. The region outlined in (**A**) is magnified in (**B**), coloured dashed lines in (**B**) encircle VSMC-derived medial patches. Fluorescent protein and DAPI (grey) is indicated at the top of each panel. Scale bars are 100 μm.

7.3 Proliferating VSMC-derived cells in AAA, frequently co-localise with the platelet marker CD41

To investigate potential mechanisms behind VSMC proliferation within the the AAA model, and whether VSMC proliferation follows or causes elastic lamina breaks, leading to subsequent infiltration by blood cells, cryo-sections were stained for the platelet marker CD41. Platelets are known to release PDGF-BB, which is a potent activator of the VSMC phenotypic switch to a synthetic state (Li et al. 1997; Hao, Gabbiani, and Bochaton-Piallat 2003), and could therefore be causing VSMCs to proliferate.

All models of AAA used in these studies showed that where breaks occurred to the elastic lamina, the media was often observed to be positive for CD41, indicating medial infiltration of platelets and likely other blood-derived cells. CD41 often co-localised with Confetti+ monochromatic patches within the media and thrombus, however, there were some Confetti+ patches which did not co-localise with CD41 but were close to an area positive for CD41 (**Figure 48**). Furthermore, CD41 frequently located to medial areas which were occupied by Confetti-negative cells (**Figure 48**), indicating that medial VSMCs may also be dying when exposed to platelets and other inflammatory cells.

Given that certain Confetti+ monochromatic patches exist which do not stain positive for CD41 (white dashed line in **Figure 48 B**) this could suggest that VSMCs are phenotypically switching/proliferating in response to other signals, for example the systemic circulation of Ang II. However, large Confetti+ patches in dilated medial layers and within thrombus were always CD41+ or surrounded by CD41+ cells, suggesting that platelets may have a role in the vast expansion of VSMC-derived clones. While there is no published data on the role of platelets within AAA specifically regarding VSMCs, one study has found that by blocking platelet activation using a P2Y(12) receptor antagonist; thrombus development, inflammatory cell infiltration and MMP-9 expression was reduced (Dai et al. 2009). Importantly VSMCs are known to upregulate MMP-9 in AAA (Airhart et al. 2014), which may indeed be induced by PDGF-BB release from platelets, as it is known to potently switch VSMCs to a synthetic phenotype (Yoshida et al. 2007).

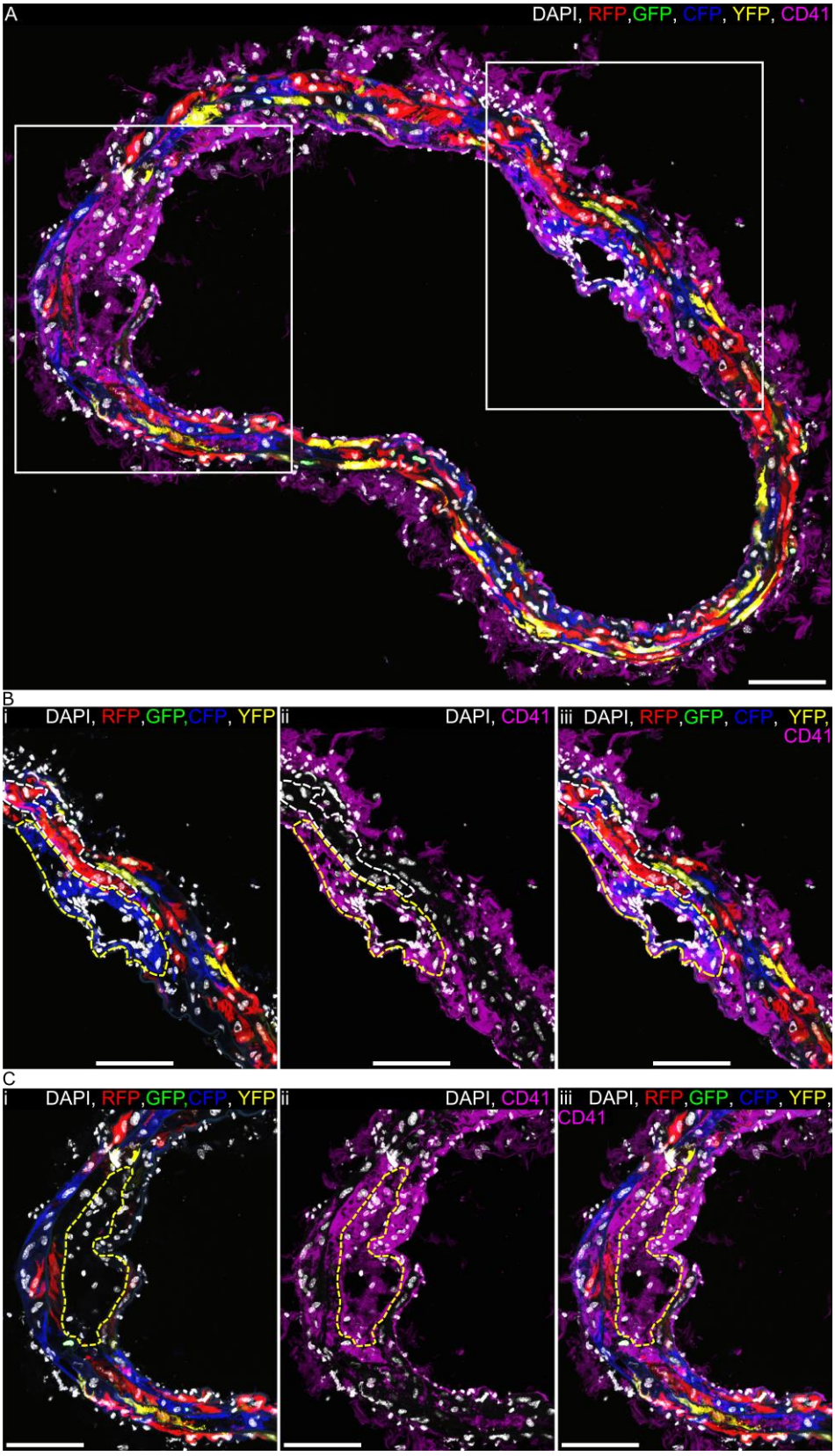

Figure 48: CD41 staining in AAA

A, AAA cryo-sections from a high density-labelled animal (10x 1 mg tamoxifen) presenting medial expansion of VSMCs. The regions outlined in (**A**) are shown in (**B and C**). Yellow dashed lines in (**B**) encircle a Confetti+ monochromatic patch which is CD41+. White dashed lines in (**B**) encircle a VSMC-derived patch which is CD41-negative. Yellow dashed lines in (**C**) encircle Confetti- CD41+ cells. Fluorescent protein and DAPI (grey) is indicated at the top of each panel. Scale bars are 100 µm.

7.4 A high proportion of VSMCs phenotypically modulate/proliferate within the AAA model

The Ang II models of AAA presented here show similar results in regard to VSMC oligo-clonality when compared to the HFD atherosclerosis (**Chapter 5**) and carotid ligation (**Chapter 6**) models (i.e. large monochromatic VSMC-derived patches are observed within the remodelling vasculature). A noticeable difference however is the proportion of VSMCs which are responding to disease in AAA. As discussed previously in the HFD atherosclerosis model, plaques were typically derived from one or two cells, and this was not accompanied by multiple small VSMC-derived patches within the media (**section 5.2**). Furthermore, within the carotid ligation model it was determined that <0.1% of cells proliferated in response to surgery to form the neo-intima (**section 6.1**). Within the Ang II models of AAA however, multiple large patches can be observed in the thrombus (**Figure 46 A**), furthermore the media typically contains many small patches of cells (**Figure 46 B**). This shows that the AAA model is able to push a higher proportion of VSMCs to proliferate and suggests that more if not all VSMCs have the potential for this response. It should, however, be noted that only the abdominal aorta was examined within the AAA studies compared to the descending thoracic aorta, aortic arch and carotid arteries in the ApoE$^{-/-}$ HFD studies (**Chapter 5**) and the left carotid artery in the carotid ligation studies (**Chapter 6**). As VSMCs within different regions are derived from different embryological pre-cursor cells (Wang et al. 2015), there may be regional differences in the proportion of VSMCs which respond/are capable of responding. Given that medial monochromatic, VSMC-derived, patches within AAA are typically space restrained this could explain the small numbers of cells in each patch, and only when full medial break down, platelet release of Pdgf-β and thrombus formation occurs, can these VSMCs truly expand to their full potential.

As discussed previously VSMCs are not usually noted for their proliferative role within AAA, and in fact most studies talk about their apoptosis and role in the degeneration of the vascular wall (Thompson 1996; López-Candales et al. 1997; Rowe et al. 2000). Whether the proliferation of VSMCs seen here is an attempt to: (1) repair the injured vasculature/replace apoptosed VSMCs; or (2) an aberrant loss of control by the proliferating VSMC-derived cells which contribute to degeneration of the vascular wall through, for example, MMP production is unknown, and will be investigated further in subsequent experiments. The former is however perhaps more likely as VSMCs would provide structural integrity to the vasculature which is undergoing extreme pressure not to break apart. Supporting this notion is work by Park et al. (2013) who implanted VSMC-like progenitor cells (muscle-derived stem cells stimulated with Pdgf-B in vitro) into elastase-induced AAA in rats, and found a decreased rate of aneurysm and MMP expression suggesting that VSMC have a role in protecting from the severe AAA disease phenotype.

7.5 Conclusions from the AAA experiments

Results from this section suggest that, within the Ang II + anti-TGF-β model of AAA, VSMCs clonally expand within the aneurysmal, intraluminal thrombus and media of tissue experiencing breaks within the elastic lamina and other characteristics of AAA such as medial dilation and infiltration of non-VSMC-derived cells (**Figures 43 and 45**). Furthermore, VSMC-derived clones within the intraluminal thrombus co-localise with aSma (**Figure 44**), confirming that the aSma+ regions observed previously (data not shown) are VSMC-derived. No literature has specifically studied VSMC proliferation in AAA and VSMCs have not been lineage traced within AAA until now.

When anti-TGF-β was removed from the Ang II/anti-TGF-β model of AAA and mice were placed on the $ApoE^{-/-}$ background there wes no observed difference in VSMC proliferative phenotype (**Figure 46**), suggesting that anti-TGF-β has no significant effect on the proliferative phenotype of VSMCs in this model. There was however a less severe phenotype in general with fewer occurrences of an intraluminal thrombus.

VSMC-derived patches typically co-localised with the platelet marker CD41 (yellow dashed lines in **Figure 48**), however there were exceptions (white dashed lines in **Figure 48**), suggesting mechanisms other than platelet-release of Pdgf-B is acting to phenotypically switch VSMCs. Furthermore, it is not clear whether VSMCs cause the breakdown of the elastic lamina and degradation of the vascular wall as some have suggested through their upregulation of MMPs (Airhart et al. 2014), or if VSMC are responding to elastic breaks to try to repair and remodel the tissue.

Lastly a higher proportion of VSMCs are observed to proliferate in AAA compared to the previously discussed HFD/carotid ligation models of CVD, resulting in the formation of many small medial patches (**Figure 46**). This suggests that given the right environment a high proportion/all VSMCs can phenotypically switch and proliferate.

Chapter 8: Optimisation of scRNA-seq techniques for VSMCs

The emergence of tools capable of profiling cells at the single cell level is revolutionising the way in which scientists can study the complexity of an organism. scRNA-seq has emerged as the most sensitive genome wide method to analyse the transcriptome of a single cell as it typically attempts to sequence every ploy(A) tailed mRNA sequence within each cell (Saliba et al., 2014). Multiple scRNA-seq platforms are currently available, including the C1, Smart-seq2, MARS-seq, Drop-seq, Chromium 10x and CEL-seq methods, within a field which is developing quickly (Haque et al. 2017). Each of these methods are different in the way they collect and process cells, be it using microfluidics, plate or droplet based systems, which can affect the throughput and quality of the generated data (Haque et al. 2017). scRNA-seq techniques are not, currently, conventionally applied to studying VSMCs, but could potentially reveal information regarding the heterogeneity of this population and provide detailed information regarding their phenotypic transition. Indeed, immunohistochemistry has already revealed that expression of contractile markers, as well as adhesion molecules and gap junctional proteins can differ between adjacent VSMCs (Christen et al. 2001; Frid, Moiseeva, and Stenmark 1994; Moiseeva 2001). A literature search reveals only one published paper using scRNA-seq to study VSMCS, and looks at cultured VSMCs from two different passages (P1 and P2) using the Fluidigm C1 method to isolate and analyse individual cells (Adhikari et al. 2015). Very little analysis of sequencing data was presented within this paper, but Adhikari et al. (2015) do suggest that there is a great deal of heterogeneity between individual cells within P1 and P2 regarding conventional contractile markers (Myh11, Tagln, Acta2, Cnn1, Smtn and Cald1).

Current single cell methods are technically sensitive and therefore require a degree of optimisation for each cell type. The objective of this Chapter is, therefore, to optimise two methods of scRNA-seq for use on VSMCs, which will be further used to answer particular questions (described below) in future experiments/analyses. Previous experiments within our group used the C1 microfluidics system to capture and sequence single VSMCs in an attempt to identify a small sub-population of VSMCs. However, this method suffered from several issues, including large batch effects and problems with capturing VSMCs of different sizes (data not show). To overcome these problems, the scRNA-seq method Smart-seq2 (**section 2.5**) was chosen for optimisation for use on individual VSMCs. This method relies on a plate based protocol in which single cells are isolated via FACS into single wells of a 96 well plate. Advantageously, isolating using FACS does not bias against VSMCs of different sizes and allows cells to be index sorted, which provides additional information on cell size and level of marker expression if cells are stained for a particular antibody of interest. Subsequent RT-PCR and cDNA amplification takes place within the 96-well plate (Picelli et al. 2013). Smart-seq2 experiments

performed here, were used to isolate and analyse a VSMC sub-population which express Sca1, as preliminary studies by our group have shown that these cells exist within the media but only very rarely (data not shown). This observation is supported by other studies which previously identified Sca1+ medial cells (Sainz et al. 2005). Sca1 is an interesting marker to study regarding VSMCs as it is typically associated with adult murine haematopoietic stem cells (Spangrude, Heimfeld, and Weissman 1988), with studies identifying Sca1+ adventitial cells, capable of differentiating into VSMCs and contributing to injury the response (Hu et al. 2004; Yu et al. 2016). Sca1 therefore represent the kind of marker which could be expressed by a population of VSMCs likely to proliferate in response to injury/disease.

In the past, studying heterogeneity within a cellular population, in a high-throughput manner, relied on methods such as multi-colour flow cytometry and multiplexed mass cytometry, which are able to profile unlimited cell numbers but are limited to the number of proteins which can be identified (Giesen et al. 2014). scRNA-seq techniques such as/similar to Smart-seq2 are unbiased, able to detect heterogeneity regarding unknown factors, and allow a higher resolution of analysis into single cells by attempting to sequence the entire transcriptome of each cell. However, they make the profiling of thousands of cells difficult/impossible due to high labour costs. To truly examine the heterogeneity of a cellular population at high resolution, a scRNA-seq method which is able to process thousands of cells at a time is required. The second method chosen to profile the transcriptome of individual VSMCs in this Chapter, is the Chromium 10x system for scRNA-seq, as it able to sequence up to 10,000 individual cells in one experiment, thus, making it a relatively high throughput method while requiring very little manual work (Zheng et al. 2017). The 10x system will be used to profile the heterogeneity of the VSMC population, this information will then be used to map cells onto the contractile-synthetic spectrum (discussed in **section 1.3, Figure 3**), search for rare sub-populations and examine heterogeneity in VSMC response following injury/disease.

The work within this Chapter is primarily performed as a proof of concept study to show that these scRNA-seq methods are able to analyse the transcriptome of individual VSMCs. The data generated in these experiments will be used in future analyses to profile VSMC heterogeneity and identify VSMC sub-populations. This results chapter is based on a collaboration between the groups of Dr. Helle Jorgensen and Dr. Mikhail Spivakov, future data analysis will be led by Lina Dobnikar.

Aims:

1. Optimise Smart-seq2 for analysis of VSMCs
2. Sequence and compare Confetti+ Sca1- and Confetti+ Sca1+ cells
3. Sequence healthy VSMCs using the 10x Chromium system

8.1 Smart-seq2 optimisation for VSMCs

Smart-seq2 is a sensitive technique for full-length transcriptome profiling in single cells, which is necessary when working with such small amounts of RNA, and requires careful optimisation for each cell type used. The main step requiring optimisation is the number of PCR cycles used to amplify the cDNA; amplification is needed to generate sufficient quantities of cDNA for subsequent reactions. Too little amplification will result in the loss of rare transcripts whilst too much will lead to amplification bias of more common transcripts. To optimise the number of PCR cycles to sufficiently amplify cDNA from a single VSMC, aortas from Myh11-CreER(T2); R26R-Confetti mice labelled at high density (10 x 1 mg tamoxifen) were enzymatically dissociated to a single cell suspension and Confetti+ cells were FACS sorted into a 96 well plate so that each well contains a single cell. The cells then underwent lysis and RT-PCR using the Smart-seq2 protocol (**sections 2.5 and 3.18**) to create cDNA. At this point different numbers of PCR cycles (22, 24 and 26) were used to amplify cDNA from individual cells. Samples were then analysed using an Agilent Bioanalyzer to test if cDNA was detectable. Bioanalyzer traces show that with 22 cycles cDNA was barely detectable and often no cDNA was detected at all, however 24 and 26 cycles showed consistently detectable quantities of cDNA (**Figure 49**).

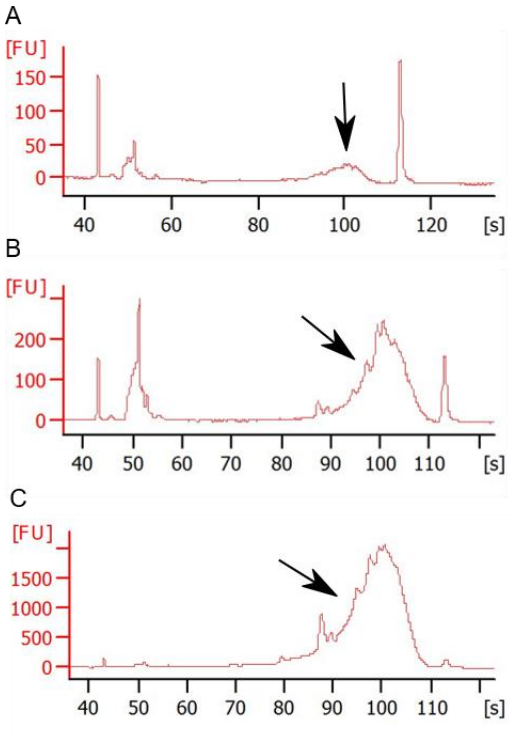

Figure 49: Bioanalyzer plots showing cDNA signal intensity from Smart-seq2 samples subjected to different PCR cycle numbers

RNA from single VSMCs went through the Smart-seq2 protocol, however, different PCR cycle numbers (22 (**A**), 24 (**B**) and 26 (**C**)) were used to amplify the cDNA. The graphs show signal intensity (fluorescence units, FU) over time in seconds (s) from the Agilent Bioanalyzer high-sensitivity DNA chips, for individual samples. Arrows point to peaks representing cDNA. Peaks at 43 and 113 (s) are internal control markers. Peaks at 50 (s) is primer dimer.

Amplified cDNA of 10 single cells from 2 separate batches (i.e. different mice, FACS sort and RT-PCR) with 24 cycles and 2 cells from a batch with 26 cycles were further processed using the Nextera XT

tagmentation kit in order to index individual transcripts so they can be matched back to their cell of origin in later analysis. Samples were then pooled together and sequenced using Illumina NextSeq 500 Mid Output 75 bp paired end sequencing. Read counts were typically between 2-6 million reads/cell for 24 cycles and 14 million for those which underwent 26 cycles of amplification (**Figure 50 A**). Gene counts, however, were similar for all cells (excluding one of low quality) with between 4000-5000 genes detected (**Figure 50 B**). Given that 26 cycles only increased the number of reads per cell and not the number of genes detected, 24 cycles were chosen for all future experiments. The number of genes detected here is comparable to the number of genes detected using Smart-seq2 in a study by Macaulay et al. (2016) which analysed hematopoietic stem cells and uses 25 PCR cycles for cDNA amplification. Other studies have detected >9000 genes/cell using Smart-seq2 when analysing embryonic stem cells (Ziegenhain et al. 2017). However, as VSMCs are typically a quiescent cell type, the number of genes detected per cell is expected to be lower compared to other cell types.

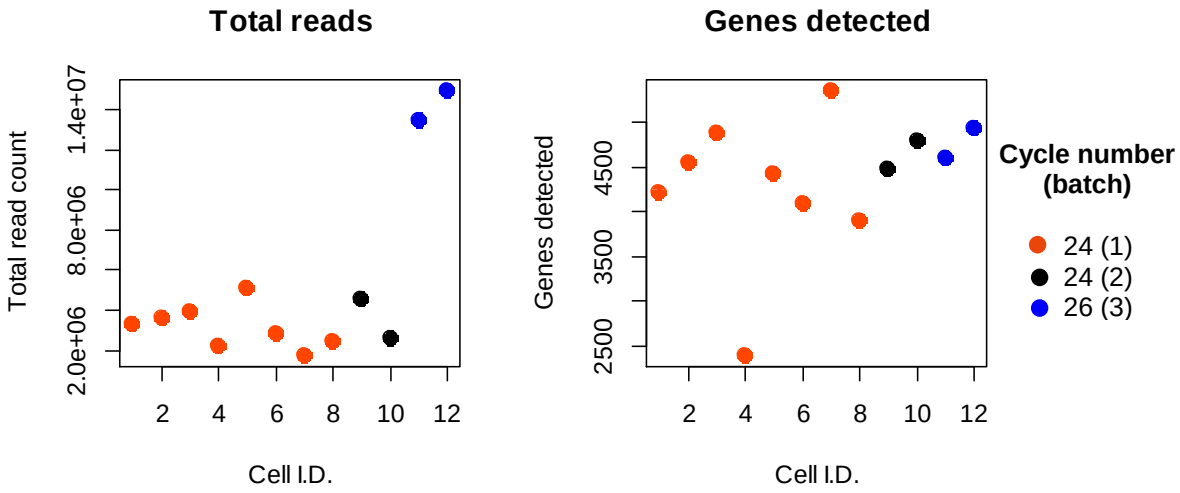

Figure 50: Total read and gene counts from single VSMCs subjected to different numbers of cDNA PCR cycles

Graphs showing the read (left panel) and gene (right panel) counts for twelve individual VSMCs which underwent the smart-seq2 protocol, each batch relates to a separate experiment. The number of cDNA amplification cycles each cell underwent is displayed in the legend.

The second factor that required optimisation concerns the concentration of ERCC spike-in controls, a common set of external RNA controls developed by the External RNA Controls Consortium. ERCC controls are a set of 92 unlabelled, poly(A) transcripts which are added to each sample after cell isolation in order to evaluate sensitivity and dynamic range of an experiment and allow differential gene expression analysis. ERCC transcripts are designed to be 250-2000 nucleotides in length and cover a concentration range of 6 logs, representing the distribution of endogenous transcript signals (Lemire et al., 2011). If, for example, too many reads from a cell map to ERCCs this suggest that the

endogenous mRNA was likely of poor quality and this cell should be excluded from further analysis. To determine the optimal amount of ERCCs to mix with each sample, different amounts of ERCC Spike-In Mix (Thermo Fischer Scientific, Cat. no. 4456740) was added to each well of a 96 well plate, already containing the RT-PCR reagents and a single VSMC. Following RT-PCR and cDNA amplification, samples were then analysed using an Agilent Bioanalyzer. As shown in **Figure 51 (B)**, addition of ERCCs at 1:10,000,000 resulted in detection of peaks corresponding to the size of prominent ERCC transcripts, whereas the broad peak resulting from cDNA generated from endogenous transcripts was barely detectable. In contrast, **Figure 51 (E)** shows that a ERCCs diluted at 1:80,000,000 are only just detectable over the endogenous RNA on the Bioanalyzer trace.

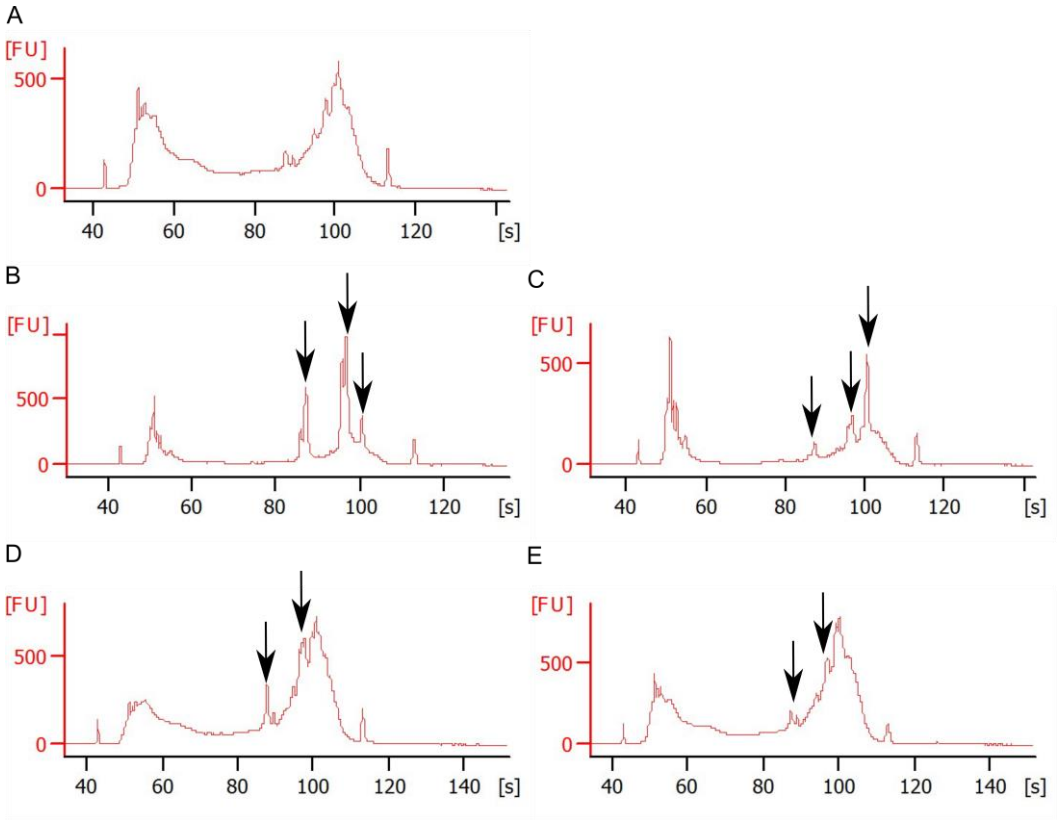

Figure 51: Bioanalyzer plots showing cDNA intensity generated from endogenous and ERCC transcripts from Smart-seq2 samples

RNA from single VSMCs went through the Smart-seq2 protocol containing different quantities of ERCC controls. **A** = 0; **B** = 1:10,000000; **C** = 1:20,000,000; **D** = 1:40,000,000; **E** = 1:80,000,000. The graphs show signal intensity (fluorescence units, FU) over time in seconds (s) observed using the Agilent Bioanalyzers high-sensitivity DNA chips, for individual VSMCs. Arrows point to peaks representing ERCC spikes, surrounded by the endogenous cDNA signal.

To further test which of the ERCC dilutions were optimal, eight single cells containing three different ERCC dilutions (1:20,000,000; 1:40,000,000; 1:80,000,000) were analysed by high-throughput

sequencing to detect the proportion of reads which mapped to ERCC transcripts compared to endogenous RNA transcripts. As shown in **Figure 52**, addition of ERCCs at 1:20,000,000 resulted in approximately 600,000 reads mapping to ERCC transcripts which equates to 20% of the total reads per cell, these values halved as the dilution halved (**Figure 52**). Other studies typically use ERCCs at a dilution which results in between 2-10% of total reads mapping to ERCC transcripts as this provides adequate coverage to detect lowly expressed ERCC transcripts without reducing the number of endogenous genes detected (Achim et al. 2015; Tung et al. 2017). Therefore, as a dilution of 1:40,000,000 gave between 7-10% of total reads mapped to ERCC transcripts, this dilution was chosen for subsequent experiments.

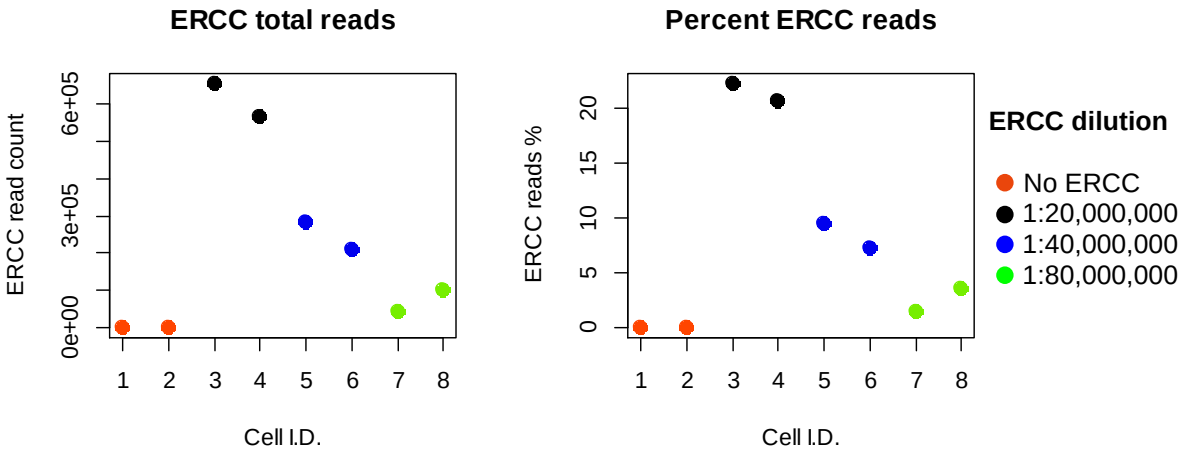

Figure 52: Total ERCC reads and the proportion of reads per cell which map to ERCC controls.
Graphs showing the number (left panel) and proportion (right panel) of reads which map to ERCCs for eight single VSMCs which underwent the Smart-seq2 protocol. The dilution of ERCC into the RT-PCR mix for each cell is displayed in the legend.

8.2 Smart-seq2 experiment: Sca1+ VSMCs

Next, the ability of the Smartseq2 protocol to identify cell-to-cell variations between VSMC populations is tested. Prior to these experiments, our group had identified a population of Sca1+ VSMCs (data not shown), this is unexpected as Sca1 is a stem cell marker typically associated with haematopoietic cells (Spangrude, Heimfeld, and Weissman 1988). Sca1+ medial cells had previously been identified by Sainz et al. (2005) but were not confirmed to be VSMCs in their study. To demonstrate the proportion of Sca1+ VSMCs, aortas from high-density labelled Myh11-CreER(T2); R26R-Confetti mice were dissociated to single cells and stained with a near infra-red viability dye and a Sca1 antibody conjugated to the APC fluorophore. These cells were then analysed by flow cytometry. Gating for singlet, live, Confetti+, Sca1+ cells revealed that approximately 0.14% of Confetti+ cells

stained positive for Sca1 (**Figure 53**). For comparison, this gating strategy with cells stained with the corresponding IgG control conjugated to APC gave a Confetti+ APC+ rate of 0.06% of cells (data not shown) suggesting that approximately 0.1% of VSMCs are Sca1+.

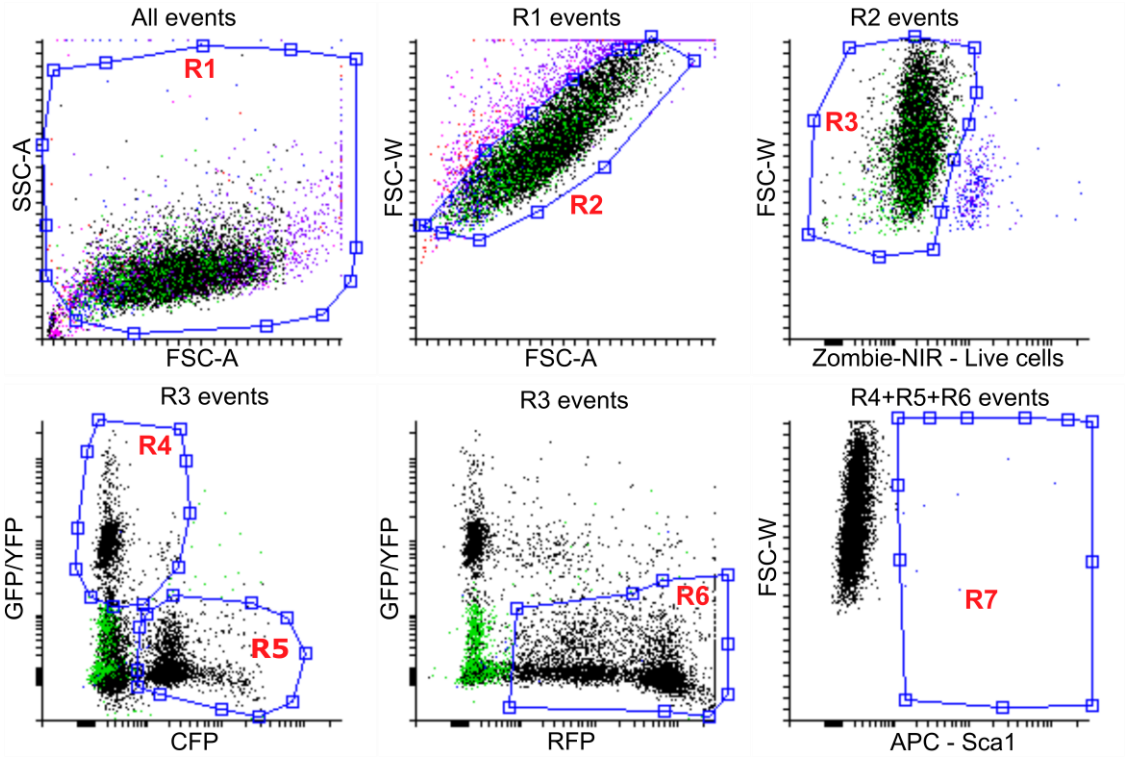

	Events	% of parent
All events	10,000	100
R1 (cells)	9,743	97.43
R2 (singlets)	8,431	86.53
R3 (live cells)	8,144	96.60
R4+R5+R6 (Confetti+ cells)	6,436	79.03
R7 (Confetti+ Sca1+)	9	0.14

Figure 53: Flow cytometry analysis of Confetti+ Sca1+ cells
VSMCs from Myh11-CreER(T2); R26R-Confetti mice were stained with a near infrared viability dye and a anit-Sca1 antibody conjugated to APC before analysis by flow cytometry. Graphs show the gates (R) used to isolate live Confetti+ Sca1+ cells. The table shows the number of events recorded in each gate (R) and the percent of cells carried on from the previous (parent) gate.

Previous results presented within the thesis, for example from the carotid ligation model (**Chapter 6**), suggest that generation of the injury-induced neointima results from the clonal expansion of very few VSMCs (<0.1%), indicating that activation of proliferation is a rare event. The observed, low proportion of cells which activate proliferation following injury raises questions regarding heterogeneity of VSMCs. For example, whether there exists a progenitor-like cell population which responds to injury or whether all cells are equi-potent, capable of responding. If the former is true, then Sca1 could

potentially be the type of gene which may mark a progenitor-like population. In order to further profile this cell type and compare them to Sca1-negative VSMCs, single cells from the aortas of nine (4 in the first batch and 5 in the second batch) Myh11-CreER(T2); R26R-Confetti mice were first dissociated to single cells. These cells were then stained with a cell viability dye and the Sca1-APC antibody and then FACS sorted into individual wells of a 96 well plate (2x plates from two different days). In total 88 Confetti+ Sca1+ (C+S+), 70 Confetti+ Sca1- (C+S-) and 26 Confetti- Sca1- (C-S-) cells were collected. All cells were subjected to the Smart-seq2 protocol (Batch 1 and 2 were processed on different days). After initial quality control, where cells were excluded if no cDNA was detected using the Quant-iT™ PicoGreen™ assay kit (**section 3.18**), 158 (84 C+S+, 48 C+S- and 26 C-S+) cells were analysed by high-throughput sequencing.

Total number of reads per cell was typically between 1-4 million (**Figure 54**) and total number of genes detected per cell was typically between 2000-8000 per cell, with a mean of 3964 (**Figure 55**). The number of ERCC reads per cell was typically between 100,000-1,000,000 with approximately 5-30% of all reads mapping to ERCCs (**Figure 56**). All cells which achieved either <100,000 reads, <1500 detected genes or where >30% of reads mapped to ERCCs were excluded from subsequent analysis, as these samples were likely of poor quality. In total, therefore, 128 cells (66 C+S+, 42 C+S- and 20 C-S+) were used for further analysis.

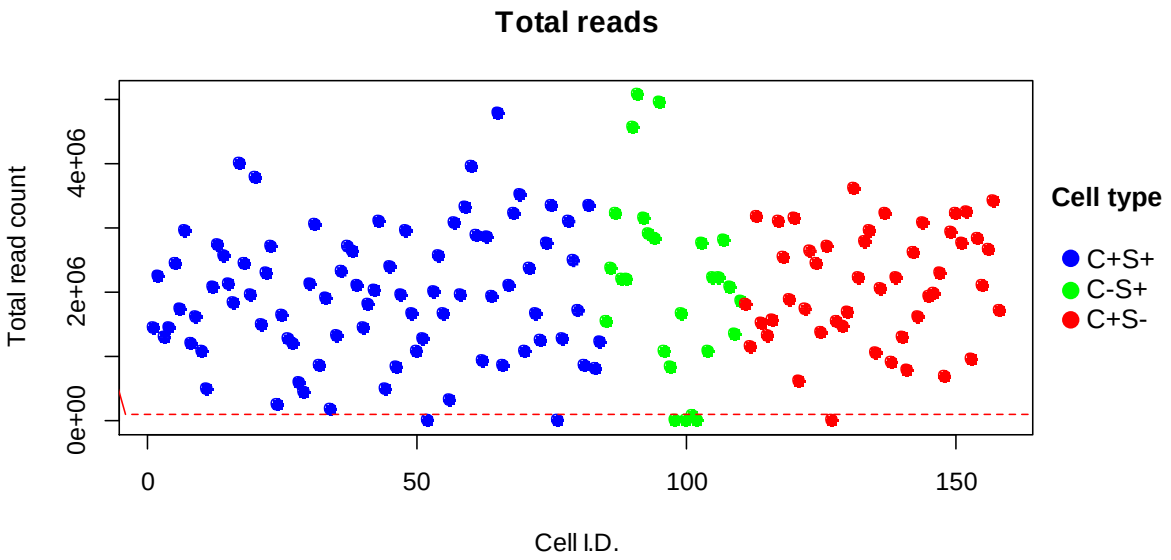

Figure 54: Total read counts from scRNA-seq analysis of sorted cell populations
Single cells from the aortas of nine Myh11-CreER(T2); R26R-Confetti mice were FACS sorted prior to scRNA-seq using the Smart-seq2 protocol. In total 154 cells were collected. Phenotype status is displayed in the legend. The red dashed line indicates a read count of 100,000, all cells below this read count were excluded from subsequent analysis. C+S+ = Confetti+ Sca1+; C-S+ = Confetti- Sca1+; C+S- = Confetti+ Sca1-.

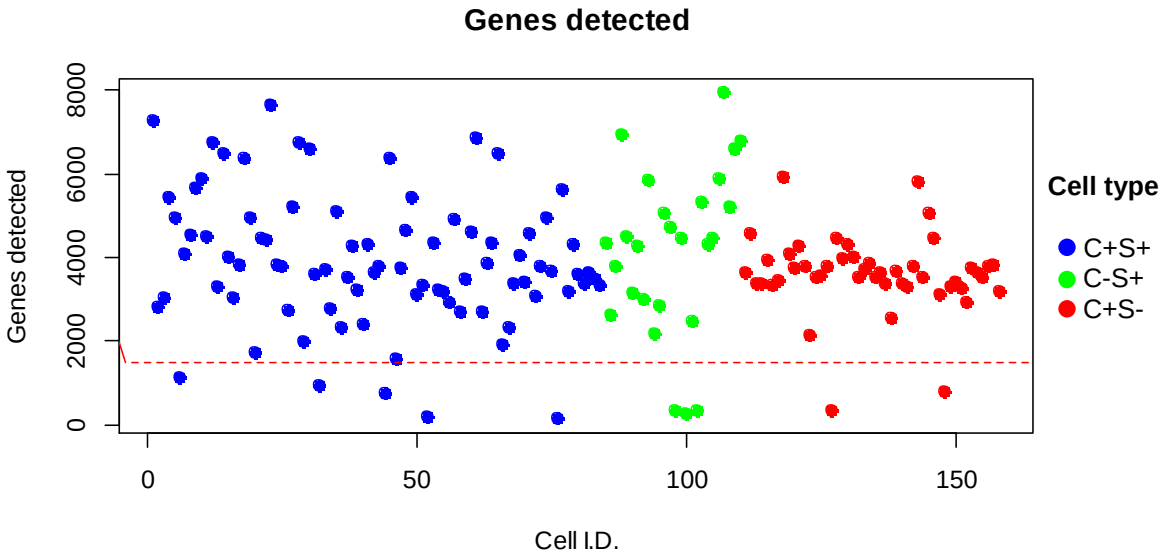

Figure 55: Total gene counts from scRNA-seq analysis of sorted cell populations
Single cells from the aortas of nine Myh11-CreER(T2); R26R-Confetti mice were FACS sorted prior to scRNA-seq using the Smart-seq2 protocol. In total 154 cells were collected. Phenotype status is displayed in the legend. The red dashed line indicates a gene count of 1500 genes, all cells below this gene count were excluded from subsequent analysis. C+S+ = Confetti+ Sca1+; C-S+ = Confetti- Sca1+; C+S- = Confetti+ Sca1-.

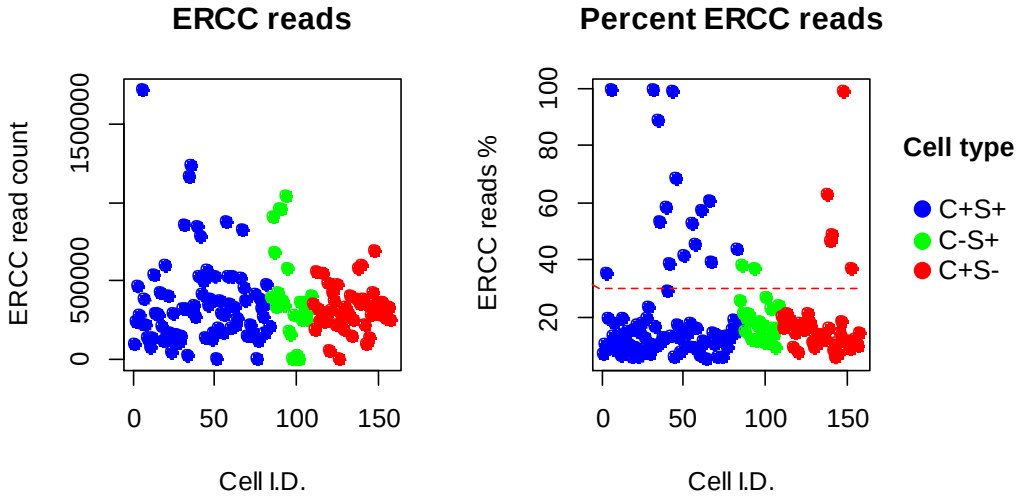

Figure 56: Total number of ERCC reads and the proportion of reads which map to ERCCs from scRNA-seq analysis of sorted cell populations

Single cells from the aortas of nine Myh11-CreER(T2); R26R-Confetti mice were FACS sorted prior to scRNA-seq using the Smart-seq2 protocol. In total 154 cells were collected. Phenotype status is displayed in the legend. The red dashed line indicates 30% of reads mapped to ERCCs, all cells above this percentage were excluded from subsequent analysis. C+S+ = Confetti+ Sca1+; C-S+ = Confetti- Sca1+; C+S- = Confetti+ Sca1-.

To investigate the sensitivity, defined here as the ability to detect ERCC control transcripts, of the Smart-seq2 method in these experiments, the number and type of ERCCs detected was analysed. Typically, between 25-45 ERCCs were detected per cell (**Figure 57**), which equates to approximately half the total number of ERCCs. This is similar to other studies using a variety of methods, including Smart-seq2, CEL-seq and Drop-seq, to sequence embryonic stem cells (Ziegenhain et al., 2017). When analysing the proportion of cells containing each individual ERCC, it was found that typically the very lowly expressed transcripts are not detected and that transcript length appears to have no difference on which transcripts are detected (**Figure 58**). While ERCC detection is a good gauge for how sensitive the experiment was it will likely differ regarding endogenous mRNA, as ERCCs are typically shorter compared to mammalian genes, have a shorter poly(A) tails and do not possess a 5' cap (Risso et al. 2014; Grun and van Oudenaarden 2015).

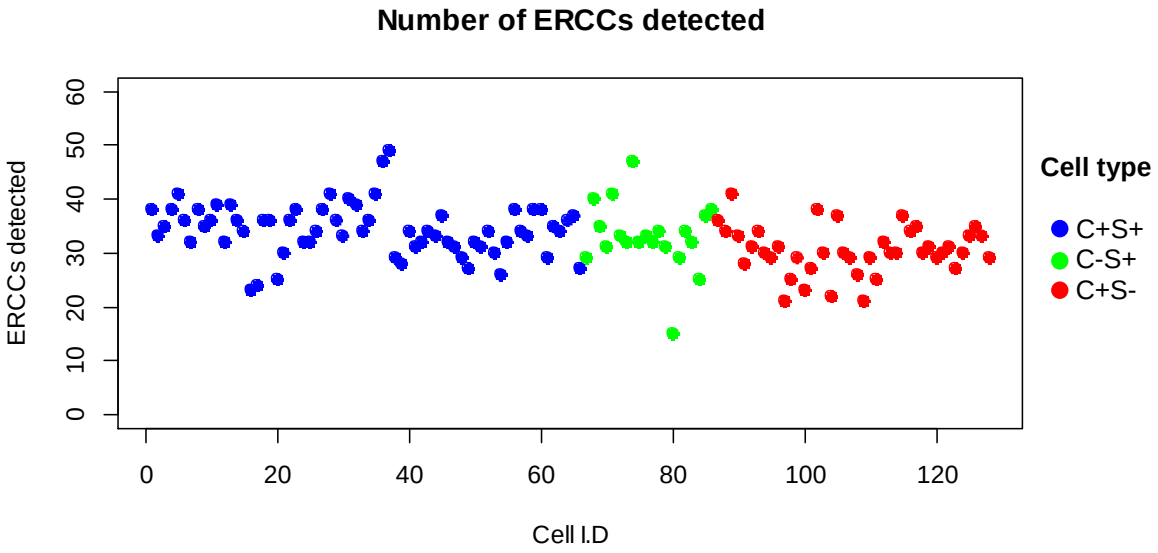

Figure 57: Number of ERCCs detected from scRNA-seq analysis of sorted cell populations

Single cells from the aortas of nine Myh11-CreER(T2); R26R-Confetti mice were FACS sorted prior to scRNA-seq using the Smart-seq2 protocol. After initial quality control 128 cells remained. In total 92 ERCCs were diluted into each cell RT-PCR mix. Phenotype status is displayed in the legend. C+S+ = Confetti+ Sca1+; C-S+ = Confetti- Sca1+; C+S- = Confetti+ Sca1-.

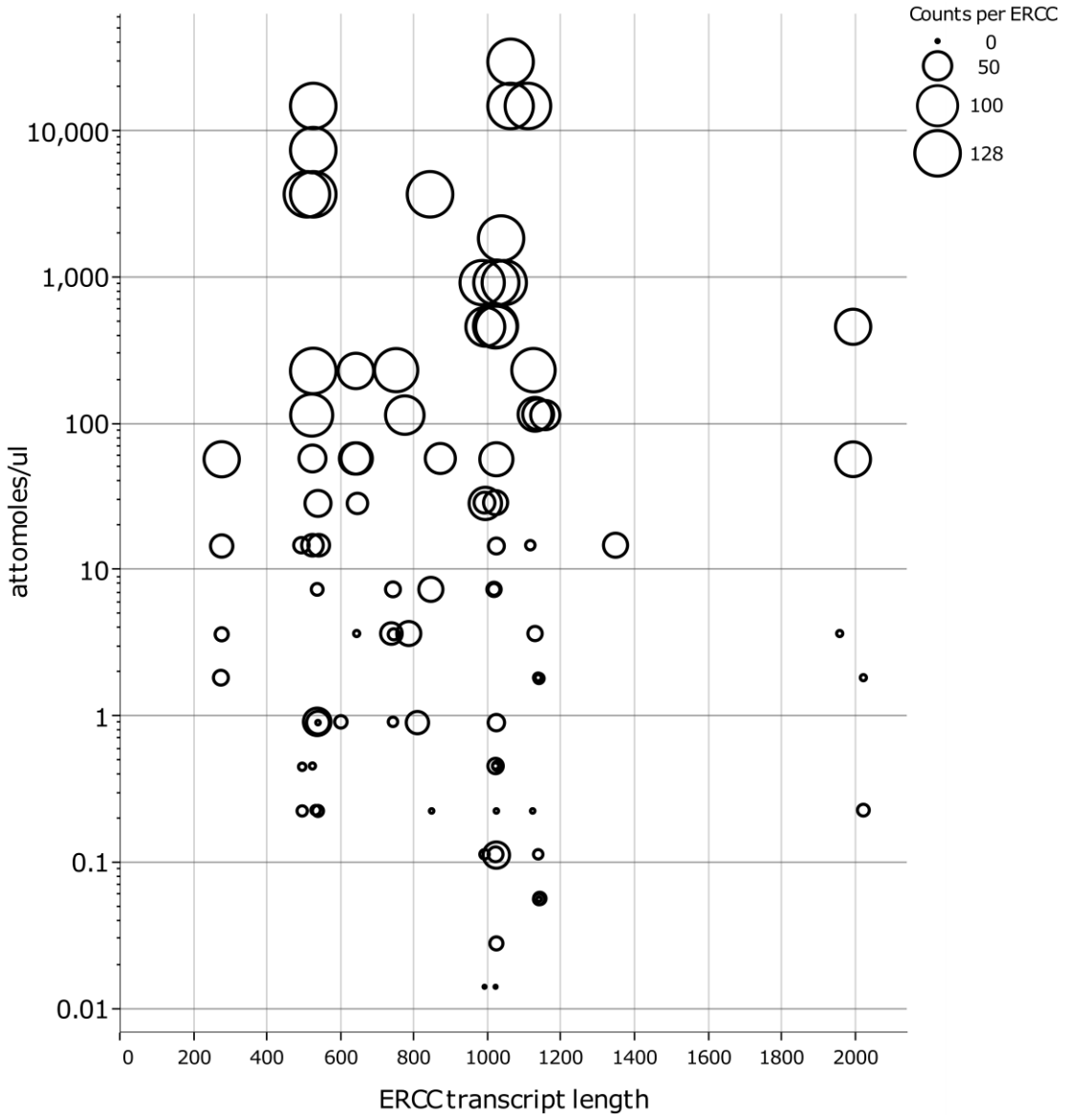

Figure 58: Number of times each ERCC is detected, their concentration and transcript length
Graph displaying the number of times each ERCC is detected at least once in all 128 cells sequenced. Each ERCC has a different transcript length and concentration, the concentration displayed here represents the concentration of each ERCC within the ERCC stock mix. Size of each point on the graph represents the number of cells each ERCC is detected in, as indicated by the legend.

Following the initial filtering of low quality cells, the sequence data was normalised using the Bioconductor scran package (Lun, Bach, and Marioni, 2016), and genes with a mean expression value below one were excluded from further analyses. Normalisation ensures that cell-to-cell differences in capture efficiency, sequencing depth and other confounding factors (for example, high dropout rates of lowly expressed genes) are accounted for, allowing for valid analysis of relative gene expression between cells (Lun, Bach, and Marioni, 2016). Myh11 and Sca1 expression was then evaluated to test if selected cell populations expressed the appropriate genes. As shown in **Figure 59,** the C+S- cells contained relatively high, normalised counts for Myh11 expression. C+S+ cells have a lower mean

expression of Myh11 compared to C+S- with a few cells expressing very low levels of Myh11. The majority of C-S+ cells express low levels of Myh11 compared to either Confetti+ group, however a few cells have high, normalised Myh11 counts. In contrast, **Figure 60** shows that Sca1 is more highly expressed in C-S+ cells which decreases in C+S+ cells and is almost completely undetectable in the majority of C+S- cells. Both these results are expected given the cell types sequenced and, importantly, these results and the quality control steps discussed above demonstrate that Smart-seq2 method is working and can be used to detect differences in gene expression between individual VSMCs. Further detailed analysis profiling each cell type is currently ongoing, and beyond the scope of this thesis.

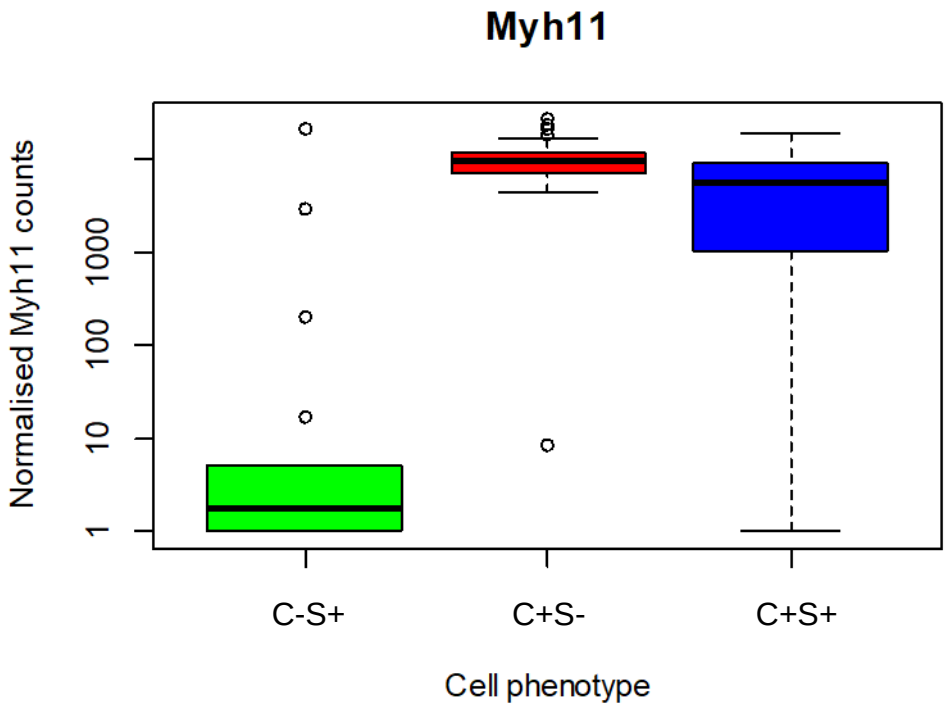

Figure 59: Normalised Myh11 counts from scRNA-seq analysis of sorted cell populations
Box plots showing the number of normalised counts for the Myh11 gene from 128 single cells using the Smart-seq2 method of scRNA-seq. C+S+ = Confetti+ Sca1+; C-S+ = Confetti- Sca1+; C+S- = Confetti+ Sca1-.

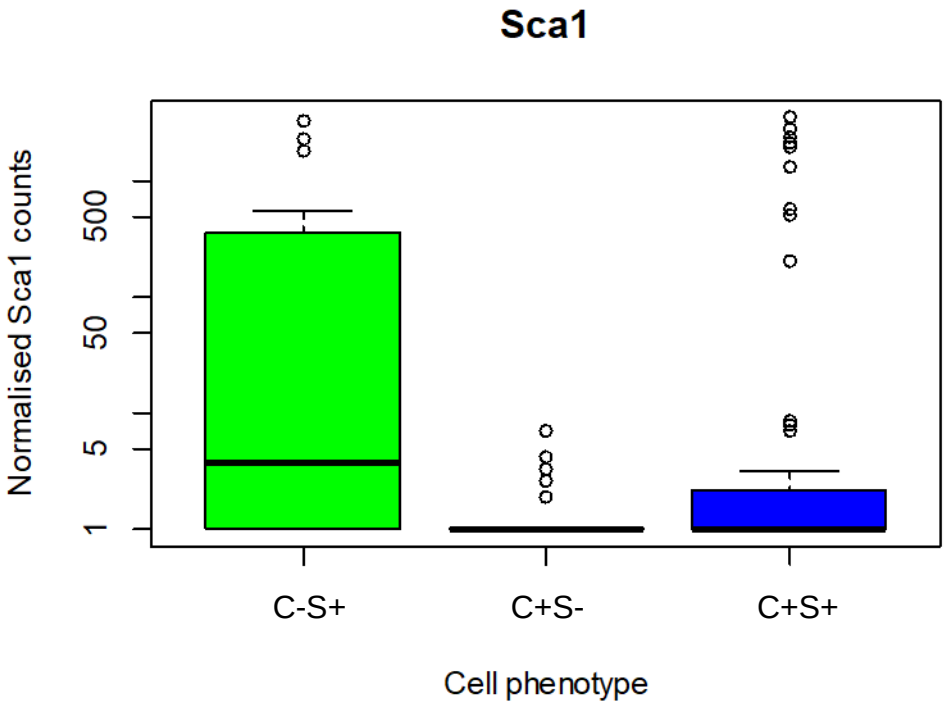

Figure 60: Normalised Sca1 counts from scRNA-seq analysis of sorted cell populations
Box plots showing the number of normalised counts for the Sca1 gene from 128 single cells using the Smart-seq2 method of scRNA-seq. C+S+ = Confetti+ Sca1+; C-S+ = Confetti- Sca1+; C+S- = Confetti+ Sca1-.

8.3 Chromium 10x experiment: VSMC heterogeneity

As discussed previously, VSMCs form a heterogeneous population (**section 1.3**), differing in regards to their expression of particular proteins, including VSMCs contractile markers (Christen et al. 2001; Frid, Moiseeva, and Stenmark 1994; Moiseeva 2001), with studies identifying different sub-populations of VSMCs (Bochaton-Piallat et al. 1996; Christen et al. 2001; Li et al. 2001). VSMCs are also hypothesised to differ in their placement on a proposed, phenotypic spectrum which ranges from contractile to synthetic (**Figure 3**, Rensen et al., 2007). Considering these ideas and given what has been shown within the HFD atherosclerosis/carotid ligation experiments (i.e. that few VSMCs respond to disease, **Chapters 5 and 6**), it is possible that heterogeneity has a functional consequence when it comes to VSMC response to disease. For example, VSMCs which proliferate to form the neo-intima/atherosclerotic plaques observed in **Chapters 5 and 6** may belong to a pre-determined response population with a distinct transcriptional profile within the healthy vascular wall. Alternatively, all cells may be capable of the proliferative response but stochastic activation of a few cells may result in the observed oligo-clonal response. To detect rare sub-populations and profile heterogeneity within the VSMC population it is necessary to capture and analyse thousands of

individual cells, which (as discussed above and in **section 2.5**) can be achieved using the Chromium 10x system, which is tested here.

To profile heterogeneity within VSMCs, the aortas of five Myh11-CreER(T2); R26R-Confetti mice labelled at high density (10 x 1 mg tamoxifen) were enzymatically dissociated to a single cell suspension and Confetti+ cells were isolated by FACS to ensure only VSMCs are analysed. The 10x system has a variable capture efficiency which will likely differ depending on the cell type used. As no information was known regarding VSMC capture efficiency in the 10x system, a predicted capture efficiency of ~50% was used based on previous experiments using other cell types (Zheng et al. 2017). Therefore, 6000 VSMC were loaded into the 10x machine with the goal of capturing 3000 cells for analysis by high-throughput sequencing. The capture efficiency was however only 12%, with only 725 cells being captured. The number of reads per cell averaged at 431,227, and typically between 1300-2500 genes were detected per cell with a mean of 2164 (**Figure 61**), however in total 14,821 different genes were detected. Compared to the Smart-seq2 method (**section 8.2**) the mean number of genes detected per cell are ~50% lower (2164/cell for 10x and 3964/cell for Smart-seq2, **Figures 55 and 61**). This was, however, not a result of the lower read counts per cell in the 10x data compared to the Smart-seq2 data, as sequencing saturation occurred at 97.4% of reads within the 10x experiments. Other studies using the 10x system to profile blood mononuclear cells and intestinal stem cells demonstrated a median of ~4500 genes per cell with a read depth of 100,000 reads per cell (Zheng et al., 2017) and ~2500 genes per cell with a read depth of 45,000-86,000 per cell (Yan et al. 2017), respectively. The lower gene counts seen when sequencing VSMCs is likely due to their quiescent phenotype.

Expression of aSma/Acta2 across the population reveals that the detected gene expression values are very variable (**Figure 62**), indicating that VSMCs are heterogeneous even in expression of one of their classical marker genes. This is similar to what was suggested by (Adhikari et al. 2015) in their experiments using the Fluidigm C1 to sequence cultured single VSMCs. However, this data requires further processing and statistical analysis to reveal a more detailed profile of heterogeneity as a degree of this variation will be technical noise. Importantly, the 10x system for scRNA-seq was successfully performed on VSMCs which will allow the detailed analysis of thousands of individual VSMCs in future experiments.

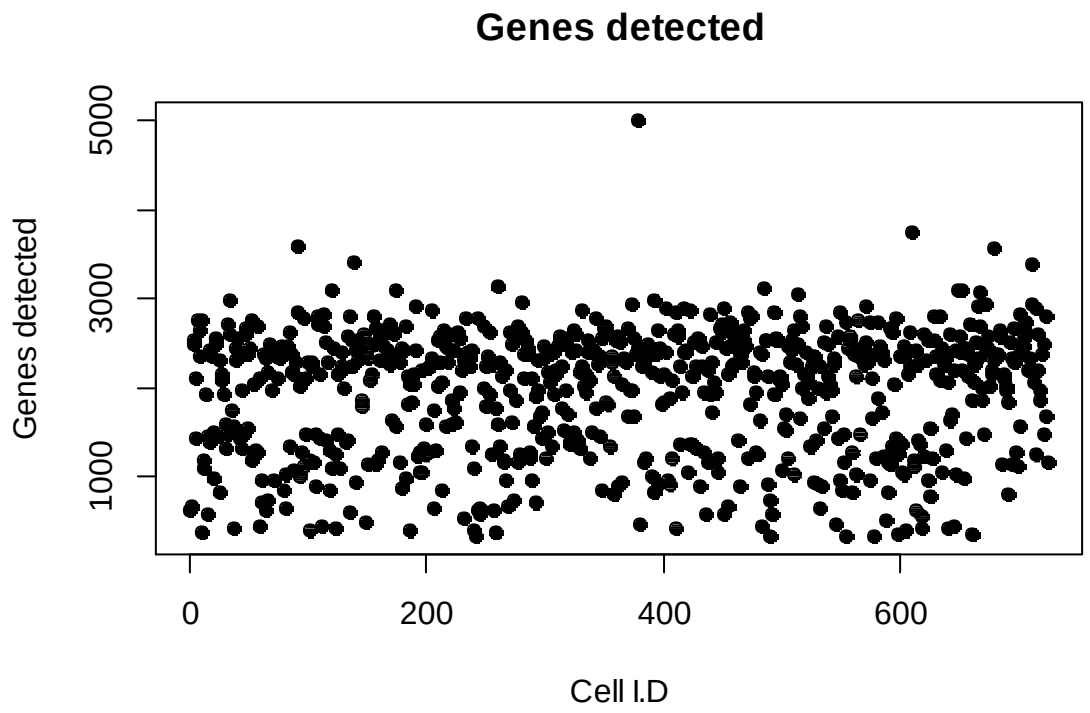

Figure 61: Number of Genes detected per cell in the 10x experiment
Graph showing the number of genes detected per cell in 725 individual VSMCs which underwent scRNA-seq using the Chromium 10x system

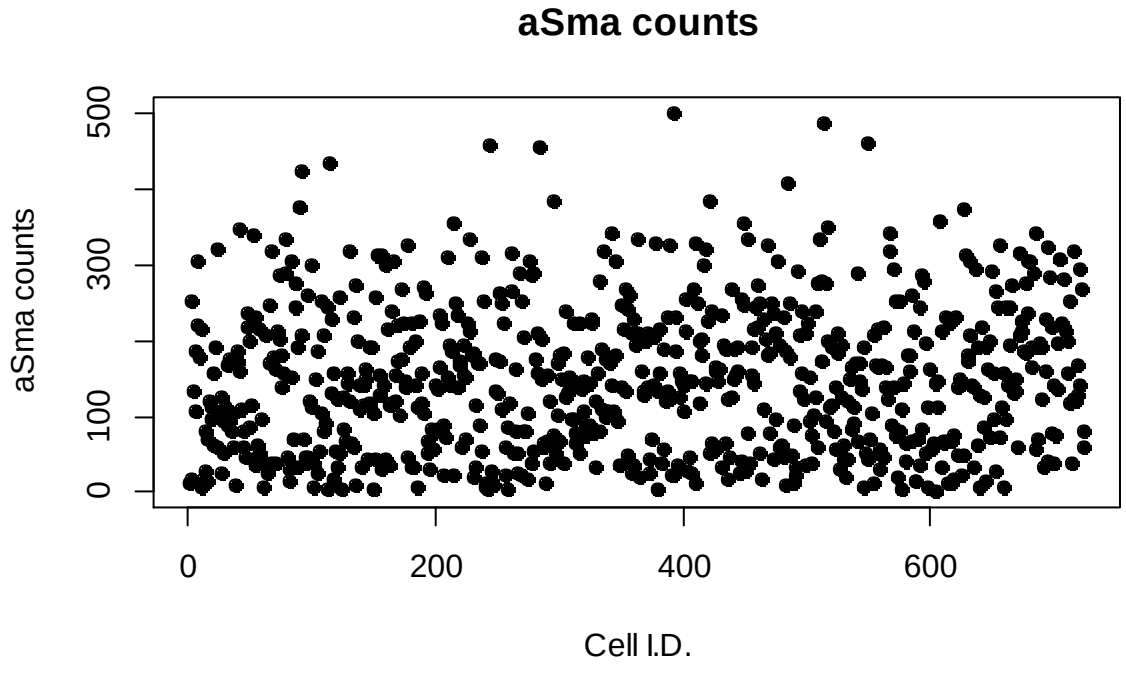

Figure 62: Number of read counts for aSma in the 10x experiment
Graph showing the number of aSma/Acta2 reads per cell in 725 individual VSMCs which underwent scRNA-seq using the Chromium 10x system

8.4 Conclusions from the scRNA-seq experiments

The observations made in **Chapter's 5, 6 and 7**, raise the question why, in a population made up of thousands of VSMCs, all of which are in close proximity to each other, did only a few cells respond proliferatively to the ApoE$^{-/-}$ HFD, carotid ligation and Ang II infusion disease models, resulting in the observed oligo-clonality. While multiple methods can be employed to answer these questions, scRNA-seq has the potential to provide detailed information regarding cell-cell heterogeneity and potentially reveal VSMC sub-populations and how they differ, which could be key in answering questions regarding oligo-clonality. As scRNA-seq methods are sensitive techniques and often require cell specific optimisations, two methods were chosen for this purpose with VSMCs.

The first method, Smart-seq2, allows specific selection of up to 96 cells per experiment using single cell FACS sorting. The work carried out within this Chapter optimised (1) the number of PCR amplification cycles (**Figures 49 and 50**), necessary to achieve sufficient amounts of cDNA for subsequent reactions; and (2) the dilution of ERCC controls (**Figures 51 and 52**), which act as an internal control within scRNA-seq experiments and can aid downstream statistical analysis. Following optimisation, the Smart-seq2 method was employed to analyse a rare population of Sca1+ VSMCs (account for ~0.1% of the entire VSMC population) and Sca1- VSMCs for comparison. In total 184 cells were collected, the dropout rate due to low quality samples was 30% meaning that 128 cells were analysed. Genes detected in each single cell typically ranged between 2000-8000 (**Figure 55**) which is comparable to other studies using scRNA-seq (Macaulay et al. 2016; Ziegenhain et al. 2017). The number of ERCCs detected was also similar to studies which have employed Smart-seq2 to sequence other cell types (Ziegenhain et al., 2017), confirming that this method is working correctly on single VSMCs.

Finally, the Chromium 10x system, which allows simultaneous processing of up to 10,000 single cells was used in order to profile VSMC heterogeneity and detect rare sub-populations. In total, 725 individual VSMCs were analysed, the number of genes detected per cell was typically between 1300-2500, which is ~50% lower than the Smart-seq2 method. The number of genes detected per cell was also lower when compared to other studies using the 10x system to analyse other cell types (Zheng et al., 2017) which may be due to VSMCs being a quiescent cell type. Further detailed analysis will hopefully allow new insights into the heterogeneity of VSMCs from healthy vasculature.

The Smart-seq2 and 10x methods detailed here to perform scRNA-seq can now be used to perform different experiments/analyses on VSMCs. The Smart-seq2 method will be used to investigate transcriptional changes in VSMCs in the early stages post carotid ligation. Specifically, carotid ligation

will be performed on Myh11-CreER(T2); Rosa26-STOP-floxedYFP mice which also contain a Ki67-RFP knock-in reporter (Basak et al. 2014). Proliferating (RFP+) VSMCs-derived (YFP+) cells will then be isolated by FACS 1-5 days post-surgery and analysed by Smart-seq2 to reveal early transcriptional changes in VSMCs which proliferate in response to injury. The 10x system will be used to analyse VSMC-derived cells from entire plaques to assess the transcriptional programmes in the phenotypically different, trans-differentiated, VSMCs-derived cells which are known to occupy atherosclerotic plaques (Shankman et al. 2015).

CHAPTER 9: Discussion

9.1 The confetti system for CVD analysis

Chapter's 4-7 within this thesis were based on analysis using multi-colour, VSMC specific, stable lineage labelling. This lineage tracing system, was successfully combined with three models of CVD, and analysed with conventional immuno-staining of cryo-sections. Additionally, a method to image whole-mount, cleared carotid arteries after carotid ligation was developed (**Chapter 6**). Which allowed detailed analysis of remodelled surfaces (i.e. neointimal patches) by rendering the imaged arteries in 3D, using the software Imaris. As expected based on previous studies using the same Cre, recombination was specific to VSMCs for all tissues analysed (Gomez et al. 2013). A potential caveat is that, as noted in **section 2.1,** the Myh11-Cre is not driven by the endogenous Myh11 Gene. While studies suggest that this Cre-transgene faithfully recapitulates endogenous gene expression (Wirth et al. 2008; Nemenoff et al. 2011), differences under certain circumstances/the extent to which it may be active in cells which express very low levels of Myh11 are difficult to determine. Importantly, however, recombination of the confetti reporter was not detected in bone marrow cells (**Table 3**), which are the only other cell type know to express Myh11, seen only in cultured cells treated with PDGF (Wu et al. 2007).

The method for analysing whole-mount carotid arteries was developed by combining multiple techniques necessary for clearing and mounting the tissue, imaging large samples with multiple fluorescent molecules and analysing data in 3D. This method proved advantageous over standard techniques which rely on sectioning tissue, primarily because it allows quantification of the number and size of neointimal patches throughout the whole artery (**Figures 34, 36, 37**), instead of a few sections which are assumed to be the average across the whole tissue. Furthermore, the number of VSMC-derived cells within a contiguous, mono-chromatic, neointimal patch could also be analysed, which would be technically challenging/impossible using sectioning alone. The method used here for whole-mount analysis would be useful in future studies, to quantify and compare phenotypic parameters (such as size and cellularity) of the neointima between mice under different physiological conditions, throughout the whole artery. For example, to test the effects of gene knockout/drug treatment in reducing the size of the neointima. While the whole-mount method was also tried for atherosclerotic plaque samples it was not possible to image through the dense, lipid-laden, core. To compensate, thick vibratome sections (**Figure 22**) allowed visualisation of how far monochromatic regions could extend throughout the artery while thin cryo-sections (**Figures 20, 26 and 28**) taken from

multiple vascular regions within each mouse allowed for immuno-staining. To avoid false positive cell scoring while analysing immuno-stained cryo-sections, all quantification was performed within Imaris in 3D, which allows section manipulation to ensure all cells were scored accurately.

9.2 VSMC oligo-clonality in models of CVD

Studies described in **Chapters 5 and 6** identified that VSMC-derived cells, which make up the majority of cells within injury-induced neointima and HFD-induced atherosclerotic plaques, are typically oligo-clonally derived. As discussed (**section 5.2**) this observation extends and supports the previous hypothesis/studies of Benditt and Benditt (1973) and Feil et al. (2014) who suggest that plaques could be mono-clonally derived. While the studies within this thesis are performed in mice, Benditt and Benditt (1973) originally tested human atherosclerotic plaques by detecting X-inactivation patterns, however, for technical reasons, this study was not able to definitively confirm that plaques were mono-clonal (**section 1.6**). It is tempting to extrapolate the oligo-clonality result from this thesis to human plaques especially given the evidence from Benditt and Benditt (1973). However, given that human plaques will likely be larger than those in mice and differences exist between mouse and human physiology, for example humans contain VSMCs within the intima at certain points in the vasculature (Doran, Meller, and McNamara 2008), this may not be the case. To definitively confirm mono/oligo-clonality within humans, this may require deep sequencing of atherosclerotic plaques combined with statistical analysis, such as that developed by Simons (2016) to detect clonal architecture of the epidermis in human.

The oligo-clonality seen in both the carotid ligation and HFD models suggest that the number of VSMCs which proliferate in response to disease is extremely low and that these cells go through multiple rounds of proliferation to form such large monochromatic regions (**Figures 20, 22, 34, 37, 39**). These observations could therefore explain findings which suggest that replicative exhaustion, telomere shortening and senescent cells are a prominent feature in human atherosclerotic plaques (Gardner et al. 2015; Matthews et al. 2006). Senescence and telomere shortening of VSMCs are highly correlated with increasing severity of atherosclerosis. Furthermore, the inability of VSMCs to proliferate and subsequent thinning of the VSMC-derived fibrous cap can result in plaque rupture (Newby, Libby, and van der Wal 1999; Matthews et al. 2006). As discussed by Braganza and Bennett (2001), prevention of deaths from atherosclerosis is shifting from controlling the absolute size of a plaque to the improving the stability of plaques by increasing the VSMC/fibrous content of a plaque. Based on the studies describe here, an increase in VSMC plaque content could be achieved in three ways: (1) preventing

the death of VSMCs (e.g. by reducing oxidative stress which is known to cause senescence/cell death, Matthews et al. 2006); (2) decreasing the proportion of non-VSMC/lipid content of the plaque; and (3) increasing the proportion of VSMCs which respond to disease. The first two suggestions have been studied, for example, statins capable of lowering cholesterol have reduced clinical events and have been shown to increase collagen, decrease lipid content and decrease VSMC death within atherosclerotic plaques (Sacks et al. 1996; Crisby et al. 2001). The third suggestion, is counter-intuitive as it may result in larger plaques, however in the long term this may be beneficial if the large monochromatic regions which contain thousands of cells are experiencing replicative exhaustion and can no longer proliferate. Reducing the size of monochromatic regions while increasing their number may therefore be beneficial, how this could be achieved though is not yet obvious.

The observation that the progeny of only a few cells exist within the diseased site in the carotid ligation and HFD atherosclerosis models suggests this 'low frequency response' could be an inherent feature of VSMCs. One possible explanation for this is the potential existence of a specialised 'response' population of medial VSMCs. This idea has previously been discussed regarding MVSMCs, in which non-Myh11 expressing medial cells are responsible for proliferating and remodelling injured arteries (Tang et al. 2012). However this view has been widely disputed as lineage tracing has definitively shown that mature Myh11-expressing cells can proliferate and trans-differentiate in response to disease (Gomez et al. 2013; Herring et al. 2014; Feil et al. 2014; Chappell et al. 2016). One study has, however, demonstrated that within the pulmonary vasculature there exists a mature Myh11-expressing VSMC progenitor population located at the pulmonary arteriole muscular-unmuscular border (Sheikh et al. 2015). Unlike other VSMCs, these cells express platelet-derived growth factor receptor-β (PDGFR-β) and are said to be 'primed' for phenotypic modulation/proliferation, as following hypoxia-induced pulmonary hypertension they express Klf4. In each arteriole a single primed cell then migrates, dedifferentiates and clonally expands to give rise to VSMCs within the distal region of the arteriole, which is normally only occupied by ECs, thus contributing to the pulmonary hypertension disease phenotype (Sheikh et al. 2015). It is tempting to expand their result to the result seen within this thesis as it would explain the observed oligo-clonal phenotype, however the necessary studies using the PDGFR-β–CreER(T2) mice have yet to be performed. Furthermore, it is worth noting that, unlike the pulmonary arterioles, within the vascular regions studied here (aortic arch, carotid arteries and descending aorta) there is no specific niche, such as the arterial muscular-unmuscular junction for these cells to exist. Preliminary studies, within our group, to test if PDGFR-β+ cells exist within the media of the aorta have identified that a low proportion of medial cells stain-positive with an anti-PDGFR-β antibody (data not shown). However, further tests are needed to show this

conclusively, and whether these PDGFR-β+ cells are primed for proliferation, as in the study by Sheikh et al. (2015).

As monochromatic regions within plaques/neointima did not contain singlet cells expressing a different confetti colour (**Figures 20, 22, 34, 37, 39**), this work strongly suggests that cell migration independent of proliferation is not frequent in either the HFD or carotid ligation models of CVD. As discussed previously (**section 6.3**), this is in contrast to studies which suggest that up to 40% of VSMC-derived cells in neointima and plaques have migrated independent of proliferation (Clowes and Schwartz 1985; Yu et al. 2011). One possible reason for these contrasting results is that methods for labelling and detecting proliferating cells is not 100% efficient. Indeed, the EdU method used in this study only labelled 47% of cells which had proliferated in the ligation model (**Figure 42, section 6.3**), which is likely due to inefficiencies in the methods used to perform EdU labelling/detection. While only the progeny of few cells form the, relatively, late stage plaques/neointima observed in **Chapters 5 and 6**, it is possible that a higher proportion of VSMCs initially proliferate in the early stages of these disease models. For example, as discussed by both Chappell et al. (2016) and Gomez and Owens (2016), more VSMCs may proliferate early on in disease development but through processes such as clonal selection or cell competition the progeny of only a few cells/clones survive. Selection of dominant clones may manifest in several different ways: (1) it may be the result of a few hyper-proliferative cells which simply outcompete other clones; (2) the expansion of particular clones may relate to not only a clone's ability to proliferate but also survive the plaque environment; and (3) a few VSMC-derived clones may inhibit the clonal expansion of surrounding VSMCs. Without further studies, these questions relating to the initial response will remain unanswered. However, addressing these questions can potentially be done using the Confetti system by analysing clones in earlier stages of disease to see if, for example, the neointima/media contains a greater number of smaller clones compared to the late stage neointima.

Another possible explanation for oligo-clonality is that all VSMCs have the same potential to phenotypically switch and contribute to disease but only those cells in the right position within this environment respond. For example, Lu et al. (2017) suggest that VSMC clonality could, in part, be explained by the difficult process which VSMCs undertake when migrating through small fenestrations within the elastic laminae, which only appear in regions where ECs have taken on an athero-prone phenotype. Therefore, it is possible that only a few VSMCs make it into the plaque in the first place, and once they begin to proliferate they might reduce the probability that other VSMCs can migrate into the plaque.

The Ang II model of AAA complicates the hypothesis that only few VSMCs proliferate in response to injury/disease. While large outgrowths of clonally derived-VSMCs are observed within the thrombus, within the media there seems to be a more general response from VSMCs, noted in their morphology (i.e. VSMCs appear larger and more irregularly shaped) and the occurrence of many small (4-5 cell) patches (**Figures 44 and 46**). The more general response within the media might be a result of the systemic administration of Ang II and anti-TGF-B, and/or the subsequent breaks within the elastic lamina which allows infiltration of blood components, including platelets. Therefore, many cells within the media may be more directly exposed to signals known to potently induce VSMC proliferation (e.g. Pdgf-BB, Blank and Owens 1990), compared to VSMCs within the media of arteries which have undergone the ligation or HFD models of CVD. It therefore appears that a larger proportion of cells are capable of phenotypic switching than eluded to in the carotid ligation and HFD models. However, the reason why only a few cells go on to massive expansion within the thrombus is still unresolved, but could partially relate to the clonal selection hypotheses discussed above. Another explanation for why so few cells expand into the thrombus of AAA animals relates back to the hypothetical spectrum of phenotypes, formulated by Rensen, Doevendans, and van Eys (2007), on which VSMCs lie. Each position on this hypothesised spectrum contains VSMCs with a different propensity and possible range of phenotypic switching (**Figure 3, section 1.3**). Therefore, it is possible that, due to the inherent heterogeneity within this population, those VSMCs which have only proliferated to a small degree are not capable of the massive proliferation seen by cells forming the large mono-chromatic patches.

9.3 Potential molecular mechanisms for the low frequency response

Regardless of the proportion of VSMCs which are capable of initial or minor responses and whether clonal competition etc. is involved in this response, only a few medial cells go through massive proliferation and survive compared to VSMCs in close proximity. All cells within diseased regions are likely exposed to a similar environment (e.g. hypercholesterolemia, oscillating blood flow or systemic Ang II exposure), this therefore raises questions regarding mechanisms which prime VSMCs to expand and become dominant (Gomez and Owens 2016).

Possible mechanism may rely on genetic and/or epigenetic priming of individual VSMCs. For example, Jaiswal et al. (2014) showed that somatic mutations in a subset of myeloid cells resulted in clonal expansion of these cells and correlated with an increased incidence of CVD. Furthermore, the genes noted to contain these mutations were typically genes responsible for epigenetic alterations (e.g. DNA (cytosine-5)-methyltransferase 3A, Tet methylcytosine dioxygenase 2 and Additional Sex Combs Like

1, Transcriptional Regulator). If similar mechanisms are present within VSMCs, somatic mutations in a very small number of VSMCs could confer proliferative/survival advantages which would result in the observed oligo-clonal phenotype (Gomez and Owens 2016). Indeed, somatic mutations, as a cause of VSMC-proliferation, have been discussed multiple times in the history of research into atherosclerosis. This is primarily due to the monoclonal hypothesis (Benditt and Benditt 1973, discussed in **section 1.6**) and other similarities atherosclerosis appears to share with cancer (Andreassi et al. 2000; Weakley et al. 2010). For example, Penn et al. (1986) showed that when DNA taken from human atherosclerotic plaques is transfected into a fibroblast cell line and injected into nude mice, these mice develop tumours which contain human DNA. Furthermore, the reason Benditt and Benditt (1973) first tested plaques for their mono-clonality was due to their similarity with uterine leiomyomas (benign smooth muscle tumours of the uterus) known to be mono-clonally derived, and like atherosclerotic plaques are present in all, female, adults (Mashal et al. 1994; Schwartz and Murry 1998). Similar to how uterine leiomyomas have been found to contain chromosomal rearrangements, unstable atherosclerotic plaques have been observed which contain chromosome 7 trisomy and tetrasomy (Schwartz and Murry 1998; Matturri et al. 2001).

Distinct epigenetic programmes within VSMCs could also be responsible for the differences in how VSMCs respond to their environment. Given the known VSMC heterogeneity (**section 1.3**) and the importance of epigenetic modulation in phenotypic switching (**section 1.11**) it is highly plausible that epigenetic programmes exist which regulate lineage memory creating a 'response like-population'. Cherepanova et al. (2016), for example, show that hydroxymethylation of the Oct4 promoter within VSMCs activates this pluripotency factor which seems to be necessary for VSMC migration/proliferation, as VSMC-specific Oct4 knockout mice contain atherosclerotic plaques with fewer VSMC-derived cells. While the frequency of DNA hydroxmethylation of the Oct4 gene within medial VSMCs is not known, such mechanisms could be responsible for the observed low frequency response (Gomez and Owens 2016).

However, differences in how cells respond to an environmental stimulus may not necessarily be the result of distinct genetic/epigenetic programmes. Within an organism there is an interplay between random biochemical interactions and precise deterministic processes such as those underlying development. To reconcile this interplay the statistical law of large numbers can be applied and in a sense, remove the significance of single particles/molecules (Raj and van Oudenaarden 2008). However, as DNA (and the genes encoded within) is present in such low numbers within a single cell and gene transcription and translation are inherently random processes, involving the movement and interaction of a host of molecules, this statistical 'averaging out' cannot take place. Random gene

fluctuations can, therefore, lead to vast cellular differences between otherwise identical populations of cells (Raj and Oudenaarden, 2008). Indeed, Sigal et al. (2006) suggest that stochastic processes can cause a large degree of human cell to cell variability regarding protein levels, which can persist as what they define as "memory noise" for several days. The transcriptional and translation variability, caused by stochastic processes within a single cell, can thus generate phenotypic variability and the potential for differences in the responses to an identical stimulus between cells of the same population (Sigal et al. 2006).

9.4 Multi-potent VSMCs

Results from **Chapter 5** demonstrate that VSMCs belonging to the same clone, and therefore derived from a single VSMC, contribute to aSma+ cap cells (**Figures 26 and 27**) and Mac3+ core cells (**Figures 28 and 29**). Given that large plaques were observed containing single coloured clones (**Figures 20, 22 and 23**) it is also likely that a single VSMC can contribute to the other cell types which VSMCs are capable of turning in to within the plaque environment, for example mesenchymal stem cell-like cells and myofibroblasts like-cells (Shankman et al. 2015). This suggests that single VSMCs, capable of responding to injury, are multi-potent and that trans-differentiation into distinct VSMC-derived cell types does not rely on specific subpopulations of VSMCs. The order in which VSMCs trans-differentiate into different cell types is not yet known, nor whether they can switch phenotype once they have acquired a specific state. As a small proportion of aSma+ Mac3+ VSMC-derived cells were observed (**Figure 30**), typically within the border region between the cap and the core, this suggests that VSMCs could inter-convert between phenotypes depending on the environment they are exposed to. Opitz et al. (2007) have similarly observed that VSMCs which have switched to a synthetic phenotype in vitro are able to return to a contractile state under physiological conditions of shear stress. These studies therefore suggest that plaque stabilisation may be achieved if therapeutics are able to bias proliferating VSMCs towards the, contractile, protective cap phenotype.

9.5 VSMCs in AAA

The Ang II model of AAA was discussed in **section 2.5**. Early studies suggested that this model has many similarities with AAA seen in humans, for example, accumulation of macrophages, medial dissection and thrombus development (Saraff et al. 2003; Barisione et al. 2006; Rateri et al. 2011). A few differences are also noted, including the location of aneurysms. Within the Ang II model they

typically locate to the suprarenal compared to infrarenal region of the aorta (Saraff et al. 2003). However, Trachet et al (2017) suggest that Ang II induced AAA is actually a model of aortic dissection rather than aneurysm, based on their observation of the sequence of events, starting with medial micro tears and finishing in the development of an intramural haematoma. Within the literature, the distinction between AAA and aortic dissection is not always clear and is confounded by the fact that dissection can occur within AAA (Saraff et al. 2003). However, these diseases can be separated in their pathophysiology. Aortic dissections occur when there is a tear in the aortic wall which results in the splitting of wall layers and haemorrhaging, whereas AAA is the result of a degenerative, proteolytic and inflammatory phenotype (Baumann et al., 2013). One major difference between these two diseases is the involvement of VSMCs. In AAA, VSMCs death contributes to the degeneration of the medial wall (Raffort et al., 2017), whereas VSMC phenotypic switching and proliferation is often noted as an integral part in the pathophysiology of aortic dissection (Feng et al., 2016; An et al., 2017).

The AAA studies presented within this thesis (**Chapter 7**) identified that a large proportion of VSMCs phenotypically switch, that many small patches within the media are generated and in some instances large medial patches or patches within the thrombus are observed. Given that many VSMCs proliferate in response to Ang II infusion, this further raises questions regarding how similar Ang II infusion reflects aneurysm, particularly as lineage tracing of VSMCs has not been performed in other models of AAA. Phenotypic switching (i.e. VSMCs with a synthetic phenotype) is often observed in aortic dissection (Feng et al. 2016; An et al. 2017) but again, there are no studies which specifically lineage trace VSMCs, detailing their proliferation. The results from **Chapter 7** are therefore difficult to put into definitive context, for example VSMC proliferation could be a common feature of both AAA and aortic dissection or only one of these diseases. Indeed, the degeneration of the vascular wall may require an initial proliferation of VSMCs, followed by the upregulation of VSMC MMP production leading to further break down of the elastin/collagen structures supporting the wall. Before VSMC proliferation can be classified as an actual stage in the cellular progression of either disease, more work needs to be performed to definitively classify what the Ang II infusion model represents and if the VSMC response can be demonstrated in other models of AAA and/or aortic dissection. Most importantly studies need to examine the role of VSMCs in human AAA and determine if VSMC proliferation occurs.

It will also be interesting to see whether the proliferating VSMCs seen in the Ang II infusion model are attempting to remodel the vascular wall (i.e. by trying to prevent the breakdown of the wall and provide structural support) or if indeed VSMC MMP production/trans-differentiation into, for example, macrophage-like cells contributes to disease development.

9.6 scRNA-seq techniques – what they will be used for now

In response to the lineage tracing which was carried out in this thesis, methods were required which allow the investigation of individual cells at high resolution. This is in order to identify possible sub-populations which might act as a 'response' population following disease and to map differential VSMC responses to injury/disease. scRNA-seq was chosen as this approach analyses the transcriptome of individuals cells, which will allow the investigation of VSMC heterogeneity.

There are an abundant number of scRNA-seq protocols, each using slightly different methods and machinery. Due to the high technical sensitivity of these methods they require careful optimisation for each cell type used. Two methods of scRNA-seq were therefore chosen to optimise for the use with VSMCs and perform preliminary experiments to check their efficiency/performance. The first, Smart-seq2, is a manual method for scRNA-seq which is relatively inexpensive, this method is usually performed for 96 cells at a time and is therefore relatively low-throughput. However, Smart-seq2 is a very sensitive method regarding the number of genes it can detect, relative to other techniques (Picelli et al. 2014; Ziegenhain et al. 2017). The second method uses the Chromium 10x protocol, an automated system than can sequence thousands of individual cells, but is relatively costly and can suffer from cell capture inefficiencies. Both methods were able to generate transcriptional data from individual VSMCs, discussed in **Chapter 8**, with information being gained regarding the optimal PCR cycle number required to amplify cDNA within the Smart-seq2 method (**Figure 50**) and the cell capture efficiency of VSMCs using the 10x system (**section 8.3**).

Importantly these methods have now generated data from a large number of healthy VSMCs and the rare population of Sca1+ VSMCs. The aim is to now use these data to answer some of the questions asked throughout this thesis. Firstly, data from healthy VSMCs will be analysed to reveal heterogeneity within this population and determine if sub-populations exist which could act as a 'response population'. Subsequent lineage tracing and gene knock out studies could then be employed to test physiological function/relevance of observed cell populations, which is important as scRNA-seq analysis can be complicated by the inherent noise within single cell techniques (Brennecke et al. 2013). It will also be interesting to see whether a picture emerges which is suggestive of the phenotypic spectrum hypothesis (**Figure 3, section 1.3**), i.e. VSMC profiles which represent different positions along the spectrum, functional studies could then be used to determine the potential for VSMCs at different starting positions to move up or down this spectrum. Importantly once VSMC population heterogeneity is understood, this will provide a baseline for comparisons to future studies which will sequence phenotypically modulated VSMCs within injury-induced neointima and atherosclerotic

plaques. Indeed, understanding the early transcriptional changes in VSMCs which are phenotypically switching could, potentially, provide valuable information regarding ways in which therapeutics could bias proliferating VSMCs towards a desired fate or stop them from proliferating in the first place.

Applying scRNA-seq analyses to study VSMCs has the potential to revolutionise our understanding of this heterogeneous cell type and reveal the molecular mechanisms responsible for their ability to trans-differentiate/phenotypically switch, which if nothing else, is an exciting prospect.

Appendices

Appendix A. Experimental animals used for atherosclerosis studies

Animal no.	Back-crosses*	Tamoxifen dose (mg)	HFD (weeks)	Plaques analysed	Analysis method
1	2	10	17	4	vibratome
2	2	10	12†	2	vibratome
3	2	10	19	10	vibratome
4	2	10	18	8	cryo
5	2	10	18	8	cryo
6	2	10	18	7	cryo
7	2	10	14†	9	cryo
8	2	10	18	8	cryo
9	2	10	17	10	cryo
10	2	10	17	1	vibratome
11	2	10	16	2	cryo
12	2	10	16	2	cryo
13	2	10	16	4	cryo
14	2	10	16	3	cryo
15	2	10	16	3	cryo
16	2	10	16	1	cryo
17	2	1	16	2	cryo
18	2	1	16	3	cryo
19	2	1	16	4	cryo
20	2	1	16	4	cryo
21	2	1	16	1	cryo
22	2	0.1	13†	0‡	vibratome
23	2	0.1	11†	0	vibratome
24	2	0.1	14	0	vibratome
25	2	0.1	14	0	vibratome

* Number of backcrosses to C57bl/6.

† Animals were analysed prematurely due to health issues unrelated to cardiovascular defects (e.g. fighting or warts).

‡ One monochromatic region was observed, but this was not included in analysis.

Adapted from Chappell et al., 2016

Appendix B. Plaque information

Animal no.	Plaque no.	Tamoxifen dose (mg)	Vascular region*	Colours per plaque	aSma	Mac3	DS†	EdU
1	1	10	CA	2 (RFP, YFP)	-	-	-	-
1	2	10	DA	2 (RFP, YFP)	-	-	-	-
1	3	10	AA	1 (RFP)	-	-	-	-
1	4	10	CA	2 (YFP, nGFP)	-	-	-	-
2	5	10	AA	2 (RFP, mCFP)	-	-	-	-
2	6	10	AA	2 (nGFP, RFP)	-	-	-	-
3	7	10	CA	2 (nGFP, RFP)	-	-	-	-
3	8	10	CA	2 (YFP, nGFP)	-	-	-	-
3	9	10	AA	2 (RFP, mCFP)	-	-	-	-
3	10	10	AA	2 (RFP, YFP)	-	-	-	-
3	11	10	AA	2 (RFP, mCFP)	-	-	-	-
3	12	10	CA	1 (RFP)	-	-	-	-
3	13	10	CA	1 (RFP)	-	-	-	-
3	14	10	CA	2 (RFP, YFP)	-	-	-	-
3	15	10	CA	1 (YFP)	-	-	-	-
3	16	10	AA	2 (RFP, nGFP)	-	-	-	-
4	17	10	CA	1 (YFP)	-	-	-	-
4	18	10	CA	2 (mCFP, nGFP)	+	+	-	-
4	19	10	AA	2 (RFP, mCFP)	-	-	-	-
4	20	10	AA	2 (RFP, YFP)	-	-	-	-
4	21	10	AA	1 (RFP)	+	+	+	-
4	22	10	AA	1 (YFP)	-	-	-	-
4	23	10	DA	1 (RFP)	+	+	+	-
4	24	10	?	1 (RFP)	-	-	-	-
5	25	10	DA	3 (RFP, YFP, mCFP)	+	+	-	-
5	26	10	CA	1 (RFP)	+	+	-	-
5	27	10	AA	2 (RFP, mCFP)	-	-	-	-
5	28	10	CA	1 (RFP)	+	+	-	-
5	29	10	AA	1 (mCFP)	+	+	-	-
5	30	10	AA	1 (RFP)	+	+	-	-
5	31	10	?	1 (RFP)	-	-	-	-
5	32	10	?	1 (RFP)	-	-	+	-
6	33	10	CA	1 (RFP)	-	-	-	-
6	34	10	CA	1 (mCFP)	-	-	-	-
6	35	10	CA	1 (mCFP)	+	+	-	-
6	36	10	AA	1 (RFP)	-	-	+	-
6	37	10	DA	1 (RFP)§	+	+	-	-
6	38	10	AA	1 (mCFP)	+	+	-	-
6	39	10	DA	1 (RFP)	+	+	-	-
7	40	10	DA	1 (mCFP)	-	-	-	-
7	41	10	DA	1 (mCFP)	-	-	-	-
7	42	10	DA	1 (RFP)	-	-	+	-
7	43	10	CA	2 (RFP, YFP)	+	+	-	-
7	44	10	AA	2 (RFP, YFP)	+	+	-	-
7	45	10	?	4 (RFP, YFP, mCFP, nGFP)	+	+	-	-
7	46	10	CA	1 (YFP)	-	-	-	-
7	47	10	AA	2 (RFP, mCFP)	+	+	+	-
7	48	10	?	2 (RFP, nGFP)	-	-	-	-
8	49	10	DA	1 (RFP)	-	-	-	-
8	50	10	DA	1 (mCFP)	+	+	-	-
8	51	10	??	1 (RFP)	-	-	-	-
8	52	10	AA	2 (RFP, mCFP)	-	-	-	-

8	53	10	AA	1 (RFP)	+	+	+	-
8	54	10	DA	2 (RFP, mCFP)	+	+	-	-
8	55	10	CA	2 (RFP, YFP)	+	+	-	-
8	56	10	AA	2 (mCFP, RFP)	-	-	-	-
9	57	10	AA	3 (RFP, YFP, mCFP)	-	-	-	-
9	58	10	AA	1 (RFP)	-	-	-	-
9	59	10	DA	1 (RFP)	-	-	-	-
9	60	10	AA	2 (mCFP, RFP)	+	+	+	-
9	61	10	AA	1 (YFP)	-	-	-	-
9	62	10	AA	1 (RFP)	-	-	-	-
9	63	10	AA	2 (RFP, YFP)	+	+	-	-
9	64	10	DA	1 (RFP)	-	-	-	-
9	65	10	?	3 (mCFP, RFP, YFP)	-	-	-	-
9	66	10	DA	1 (mCFP)	-	-	-	-
10	67	10	DA	1 (YFP)	-	-	-	-
11	68	10	CA	3 (RFP, YFP, mCFP)	-	-	-	-
11	69	10	CA	1 (RFP)	-	-	-	+
12	70	10	AA	2 (RFP, YFP)	-	-	-	+
12	71	10	DA	1 (YFP)	-	-	-	-
13	72	10	AA	2 (RFP, nGFP)	-	-	-	+
13	73	10	DA	2 (RFP, mCFP)	-	-	-	+
13	74	10	AA	1 (RFP)	-	-	-	+
13	75	10	DA	2 (YFP, nGFP)	-	-	-	+
14	76	10	AA	1 (RFP)	-	-	-	+
14	77	10	CA	2 (RFP, YFP)	-	-	-	-
14	78	10	CA	3 (mCFP, RFP, YFP)	-	-	-	+
15	79	10	AA	1 (RFP)	-	-	-	-
15	80	10	CA	2 (RFP, mCFP)	-	-	-	+
15	81	10	CA	1 (RFP)	-	-	-	-
16	82	10	CA	1 (YFP)	-	-	-	-
17	83	1	AA	1 (RFP)	-	-	-	-
17	84	1	AA	2 (RFP, YFP)	-	-	-	-
18	85	1	AA	1 (RFP)	-	-	-	-
18	86	1	CA	1 (RFP)	-	-	-	-
18	87	1	DA	1 (YFP)	-	-	-	-
19	88	1	AA	1 (RFP)	-	-	-	-
19	89	1	AA	2 (RFP, YFP)	-	-	-	-
19	90	1	XA	1 (RFP)	-	-	-	-
19	91	1	CA	1 (RFP)	-	-	-	-
20	92	1	CA	1 (RFP)	-	-	-	-
20	93	1	DA	2 (RFP, YFP)	-	-	-	-
20	94	1	CA	1 (RFP)	-	-	-	-
20	95	1	AA	1 (RFP)	-	-	-	-
21	96	1	AA	1 (RFP)	-	-	-	-

* AA: ascending aorta or aortic arch. DA: descending aorta. CA: carotid artery or brachiocephalic artery. Plaques at borders between vascular regions are indicated with a question mark.
† DS: double staining for aSma and Mac3. Only done in plaques that did not contain nGFP or YFP positive cells.
§ One YFP-expressing cell was observed in this plaque.

Adapted from Chappell et al., 2016

Appendix C. Experimental animals used for carotid ligation surgery

Animal no.	Tamoxifen dose (mg)	Back-crosses*	nGFP	YFP	RFP	mCFP	Confetti patches	Measured patches†	Patch size (cell number)	Remodelled area (µm)
1	10	1	3	6	7	4	20	17	48, 52, 149, 156, 227, 375, 425, 522, 585, 872, 950, 981, 1040, 1990, 2290, 3140, 3450	4517
2	10	1	1	2	1	3	7	7	171, 409, 666, 849, 940, 1470, 3610	2391
3	10	1	1	1	0	1	3	1	178	1301
4	10	1	0	2	2	0	4	4	174, 332, 415, 508	1878
5	10	1	0	1	1	1	3	3	66, 360, 3090	1276
6	10	1	0	1	2	0	3	3	125, 151, 329	1130
7	10	1	0	2	1	1	4	3	128, 234, 7480	1609
8	10	1	0	3	3	1	7	3	52, 149, 446	2128
9	10	1	0	2	2	2	6	3	125, 805, 1495	1345
10	10	1	0	2	1	1	4	3	96, 115, 1490	1503
11	10	6	0	1	1	1	3	3	565, 612, 3200	1994
12	10	6	0	1	1	1	3	2	1097, 2827	2816
13	1	6	0	3	1	2	6	4	35, 63, 689, 1073	NA
14	1	5	2	2	2	0	6	6	50, 55, 81, 98, 148, 225	NA
15	1	6	0	1	1	0	2	2	9, 64	NA
16	1	6	0	1	1	1	3	3	24, 153, 410	NA
17	0.1	1	0	0	0	0	0	0	NA	NA
18	0.1	1	0	1	0	1	2	2	45, 170	NA
19	0.1	1	0	0	0	0	0	0	NA	NA
20	0.1	1	0	2	1	0	3	3	65, 192, 749	NA
21	0.1	1	0	0	0	0	0	0	NA	NA
22	0.1	5	0	1	0	0	1	1	32	NA
23	0.1	6	0	1	1	0	2	2	59, 592	NA

* Number of backcrosses to C57Bl/6. † A small subset of patches was not quantified due to technical issues, such as high auto-fluorescence, which impeded surface modelling in Imaris.
NA, not applicable.

Adapted from Chappell et al., 2016

Appendix D. Experimental animals used for AAA studies

Animal no.	Genotype background	Tamoxifen dose (mg)	Anti-TGF-β	Thrombus VSMC outgrowth	Medial VSMC-derived patches	Breaks in elastic lamina
1	Wild type	10	Yes	Yes	Yes	Yes
2	Wild type	10	Yes	No	Yes	Yes
3	Wild type	10	Yes	No	Yes	Yes
4	Wild type	10	Yes	Yes	Yes	Yes
5	Wild type	10	Yes	Yes	Yes	Yes
6	ApoE$^{-/-}$	10	No	No	Yes	Yes
7	ApoE$^{-/-}$	10	No	No	Yes	Yes
8	ApoE$^{-/-}$	10	No	No	Yes	Yes
9	ApoE$^{-/-}$	10	No	No	Yes	Yes
10	ApoE$^{-/-}$	10	No	No	Yes	Yes
11	ApoE$^{-/-}$	10	No	Yes	Yes	Yes
12	ApoE$^{-/-}$	10	No	No	Yes	Yes
13	ApoE$^{-/-}$	10	No	No	Yes	Yes
14	ApoE$^{-/-}$	10	No	No	Yes	Yes
15	ApoE$^{-/-}$	10	Yes	No	Yes	Yes
16	ApoE$^{-/-}$	10	Yes	No	Yes	Yes
17	ApoE$^{-/-}$	10	Yes	No	Yes	Yes
18	ApoE$^{-/-}$	10	Yes	No	Yes	Yes
19	ApoE$^{-/-}$	10	Yes	No	Yes	Yes

References

Achim, Kaia, Jean-Baptiste Pettit, Luis R Saraiva, Daria Gavriouchkina, Tomas Larsson, Detlev Arendt, and John C Marioni. “High-Throughput Spatial Mapping of Single-Cell RNA-Seq Data to Tissue of Origin.” *Nature Biotechnology* 33, no. 5 (April 2015): 503–509. https://doi.org/10.1038/nbt.3209.

Adhikari, Neeta, Kadambari Chandra Shekar, Rodney Staggs, Zaw Win, Kerianne Steucke, Yi-Wei Lin, Li-Na Wei, Patrick Alford, Jennifer L. Hall, and International Society of Cardiovascular Translational Research. “Guidelines for the Isolation and Characterization of Murine Vascular Smooth Muscle Cells. A Report from the International Society of Cardiovascular Translational Research.” *Journal of Cardiovascular Translational Research* 8, no. 3 (April 2015): 158–163. https://doi.org/10.1007/s12265-015-9616-6.

Ailawadi, Gorav, Jonathan L Eliason, and Gilbert R Upchurch. “Current Concepts in the Pathogenesis of Abdominal Aortic Aneurysm.” *Journal of Vascular Surgery* 38, no. 3 (September 2003): 584–588. https://doi.org/10.1016/S0741-5214(03)00324-0.

Ailawadi, Gorav, Christopher W Moehle, Hong Pei, Sandra P Walton, Zequan Yang, Irving L Kron, Christine L Lau, and Gary K Owens. “Smooth Muscle Phenotypic Modulation Is an Early Event in Aortic Aneurysms.” *The Journal of Thoracic and Cardiovascular Surgery* 138, no. 6 (December 2009): 1392–9. https://doi.org/10.1016/j.jtcvs.2009.07.075.

Airhart, Nathan, Bernard H Brownstein, J Perren Cobb, William Schierding, Batool Arif, Terri L Ennis, Robert W Thompson, and John A Curci. “Smooth Muscle Cells from Abdominal Aortic Aneurysms Are Unique and Can Independently and Synergistically Degrade Insoluble Elastin.” *Journal of Vascular Surgery* 60, no. 4 (October 2014): 1033–41; discussion 1041–2. https://doi.org/10.1016/j.jvs.2013.07.097.

Albarrán-Juárez, Julián, Harmandeep Kaur, Myriam Grimm, Stefan Offermanns, and Nina Wettschureck. “Lineage Tracing of Cells Involved in Atherosclerosis.” *Atherosclerosis* 251 (August 2016): 445–453. https://doi.org/10.1016/j.atherosclerosis.2016.06.012.

Alexander, Matthew R., and Gary K. Owens. “Epigenetic Control of Smooth Muscle Cell Differentiation and Phenotypic Switching in Vascular Development and Disease.” *Annual Review of Physiology* 74, no. 1 (2012): 13–40. https://doi.org/10.1146/annurev-physiol-012110-142315.

Alexander, Matthew R, and Gary K Owens. “Epigenetic Control of Smooth Muscle Cell Differentiation and Phenotypic Switchingin Vascular Development and Disease.” *Annual Review of Physiology*, 2011. https://doi.org/10.1146/annurev-physiol-012110-142315.

An, Zhao, Yang Liu, Zhi-Gang Song, Hao Tang, Yang Yuan, and Zhi-Yun Xu. “Mechanisms of Aortic Dissection Smooth Muscle Cell Phenotype Switch.” *The Journal of Thoracic and Cardiovascular Surgery*, May 2017. https://doi.org/10.1016/j.jtcvs.2017.05.066.

Andreassi, M G, N Botto, M G Colombo, A Biagini, and A Clerico. “Genetic Instability and Atherosclerosis: Can Somatic Mutations Account for the Development of Cardiovascular Diseases?” *Environmental and Molecular Mutagenesis* 35, no. 4 (2000): 265–9.

Annabi, Borhane, Daniel Shédid, Pierre Ghosn, Rhoda L. Kenigsberg, Richard R. Desrosiers, Michel W. Bojanowski, Édith Beaulieu, Edgar Nassif, Robert Moumdjian, and Richard Béliveau. “Differential Regulation of Matrix Metalloproteinase Activities in Abdominal Aortic Aneurysms.” *Journal of Vascular Surgery* 35, no. 3 (March 2002): 539–546. https://doi.org/10.1067/mva.2002.121124.

Baetta, R, M Soma, C De Fraja, C Comparato, C Teruzzi, L Magrassi, and E Cattaneo. “Upregulation and Activation of Stat6 Precede Vascular Smooth Muscle Cell Proliferation in Carotid Artery Injury Model.” *Arteriosclerosis, Thrombosis and Vascular Biology* 20, no. 4 (2000): 931–939.

Barisione, Chiara, Richard Charnigo, Deborah A. Howatt, Jessica J. Moorleghen, Debra L. Rateri, and Alan Daugherty. “Rapid Dilation of the Abdominal Aorta during Infusion of Angiotensin II

Detected by Noninvasive High-Frequency Ultrasonography." *Journal of Vascular Surgery* 44, no. 2 (August 2006): 372–376. https://doi.org/10.1016/j.jvs.2006.04.047.

Basak, O., M. van de Born, J. Korving, J. Beumer, S. van der Elst, J. H. van Es, and H. Clevers. "Mapping Early Fate Determination in Lgr5+ Crypt Stem Cells Using a Novel Ki67-RFP Allele." *The EMBO Journal* 33, no. 18 (September 2014): 2057–2068. https://doi.org/10.15252/embj.201488017.

Basnyat, P. S., A. H. B. Biffin, L. G. Moseley, A. R. Hedges, and M. H. Lewis. "Mortality from Ruptured Abdominal Aortic Aneurysm in Wales." *British Journal of Surgery* 86, no. 6 (June 1999): 765–770. https://doi.org/10.1046/j.1365-2168.1999.01170.x.

Baumann, F., V. Makaloski, and N. Diehm. "Aortenaneurysma Und -Dissektion." *Der Internist* 54, no. 5 (May 2013): 535–542. https://doi.org/10.1007/s00108-012-3217-0.

Beery, Annaliese K, and Irving Zucker. "Sex Bias in Neuroscience and Biomedical Research." *Neuroscience and Biobehavioral Reviews* 35, no. 3 (January 2011): 565–72. https://doi.org/10.1016/j.neubiorev.2010.07.002.

Bellairs, Ruth, and Mark Osmond. *The Atlas of Chick Development*, 2009.

Benditt, E P, and J M Benditt. "Evidence for a Monoclonal Origin of Human Atherosclerotic Plaques." *Proceedings of the National Academy of Sciences of the United States of America* 70, no. 6 (1973): 1753–6.

Bennett, M R. "Apoptosis of Vascular Smooth Muscle Cells in Vascular Remodelling and Atherosclerotic Plaque Rupture." *Cardiovascular Research* 41, no. 2 (February 1999): 361–8.

Bennett, M R, G I Evan, and S M Schwartz. "Apoptosis of Human Vascular Smooth Muscle Cells Derived from Normal Vessels and Coronary Atherosclerotic Plaques." *The Journal of Clinical Investigation* 95, no. 5 (May 1995): 2266–74. https://doi.org/10.1172/JCI117917.

Bennett, Martin R. "Apoptosis in the Cardiovascular System." *Heart (British Cardiac Society)* 87, no. 5 (May 2002): 480–7.

Bennett, Martin R., Sanjay Sinha, and Gary K. Owens. "Vascular Smooth Muscle Cells in Atherosclerosis." *Circulation Research* 118, no. 4 (February 2016): 692–702. https://doi.org/10.1161/CIRCRESAHA.115.306361.

Bheda, Poonam, and Robert Schneider. "Epigenetics Reloaded: The Single-Cell Revolution." *Trends in Cell Biology* 24, no. 11 (November 2014): 712–723. https://doi.org/10.1016/j.tcb.2014.08.010.

Blank, Randal S., and Gary K. Owens. "Platelet-Derived Growth Factor Regulates Actin Isoform Expression and Growth Factor Regulates Actin Isoform Expression and Growth State in Cultured Rat Aortic Smooth Muscle Cells." *Journal of Cellular Physiology* 142, no. 3 (March 1990): 635–642. https://doi.org/10.1002/jcp.1041420325.

Blatnik, Jeffrey S., Geert W. Schmid-Schönbein, and Lanping Amy Sung. "The Influence of Fluid Shear Stress on the Remodeling of the Embryonic Primary Capillary Plexus." *Biomechanics and Modeling in Mechanobiology* 4, no. 4 (December 2005): 211–220. https://doi.org/10.1007/s10237-005-0001-2.

Bochaton-Piallat, M L, P Ropraz, F Gabbiani, and G Gabbiani. "Phenotypic Heterogeneity of Rat Arterial Smooth Muscle Cell Clones - Implications for the Development of Experimental Intimal Thickening." *Arteriosclerosis Thrombosis and Vascular Biology* 16, no. 6 (1996): 815–820.

Braganza, D M, and M R Bennett. "New Insights into Atherosclerotic Plaque Rupture." *Postgraduate Medical Journal* 77, no. 904 (February 2001): 94–8. https://doi.org/10.1136/PMJ.77.904.94.

Brennecke, Philip, Simon Anders, Jong Kyoung Kim, Aleksandra A Ko\lodziejczyk, Xiuwei Zhang, Valentina Proserpio, Bianka Baying, et al. "Accounting for Technical Noise in Single-Cell RNA-Seq Experiments." *Nature Methods* 10, no. 11 (September 2013): 1093–1095. https://doi.org/10.1038/nmeth.2645.

Cai, H, and D G Harrison. "Endothelial Dysfunction in Cardiovascular Diseases: The Role of Oxidant Stress." *Circulation Research* 87, no. 10 (November 2000): 840–4.

Cambridge Clinical School. Clinical and Biomedical Computing Unit. *Expert Reviews in Molecular Medicine.* Published by Cambridge University Press in association with the Clinical and

Biomedical Computing Unit of the University of Cambridge School of Clinical Medicine, 1997. http://journals.cambridge.org/fulltext_content/ERM/ERM4_01/S1462399402004039sup006.htm.

Campbell, Gordon R., Yasuo Uehara, Torbjorn Malmfors, and Geoffrey Burnstock. "Degeneration and Regeneration of Smooth Muscle Transplants in the Anterior Eye Chamber." *Cell & Tissue Research* 117, no. 2 (1971): 155–175.

Cao, D., Z. Wang, C.-L. Zhang, J. Oh, W. Xing, S. Li, J. A. Richardson, D.-Z. Wang, and E. N. Olson. "Modulation of Smooth Muscle Gene Expression by Association of Histone Acetyltransferases and Deacetylases with Myocardin." *Molecular and Cellular Biology* 25, no. 1 (January 2005): 364–376. https://doi.org/10.1128/MCB.25.1.364-376.2005.

Cao, Richard Y, Tim Amand, Matthew D Ford, Ugo Piomelli, and Colin D Funk. "The Murine Angiotensin II-Induced Abdominal Aortic Aneurysm Model: Rupture Risk and Inflammatory Progression Patterns." *Frontiers in Pharmacology* 1 (2010): 9. https://doi.org/10.3389/fphar.2010.00009.

Chamley-Campbell, J H, and G R Campbell. "What Controls Smooth Muscle Phenotype?" *Atherosclerosis* 40, no. 3–4 (1981): 347–57. https://doi.org/0021-9150(81)90145-3 [pii].

Chappell, Joel, Jennifer L. Harman, Vagheesh M. Narasimhan, Haixiang Yu, Kirsty Foote, Benjamin D. Simons, Martin R. Bennett, and Helle F. Jørgensen. "Extensive Proliferation of a Subset of Differentiated, yet Plastic, Medial Vascular Smooth Muscle Cells Contributes to Neointimal Formation in Mouse Injury and Atherosclerosis ModelsNovelty and Significance." *Circulation Research* 119, no. 12 (December 2016): 1313–1323. https://doi.org/10.1161/CIRCRESAHA.116.309799.

Chen, Z., and E. Tzima. "PECAM-1 Is Necessary for Flow-Induced Vascular Remodeling." *Arteriosclerosis, Thrombosis, and Vascular Biology* 29, no. 7 (July 2009): 1067–1073. https://doi.org/10.1161/ATVBAHA.109.186692.

Cheng, Y., X. Liu, J. Yang, Y. Lin, D.-Z. Xu, Q. Lu, E. A. Deitch, Y. Huo, E. S. Delphin, and C. Zhang. "MicroRNA-145, a Novel Smooth Muscle Cell Phenotypic Marker and Modulator, Controls Vascular Neointimal Lesion Formation." *Circulation Research* 105, no. 2 (July 2009): 158–166. https://doi.org/10.1161/CIRCRESAHA.109.197517.

Cherepanova, Olga A, Delphine Gomez, Laura S Shankman, Pamela Swiatlowska, Jason Williams, Olga F Sarmento, Gabriel F Alencar, et al. "Activation of the Pluripotency Factor OCT4 in Smooth Muscle Cells Is Atheroprotective." *Nature Medicine* 22, no. 6 (May 2016): 657–665. https://doi.org/10.1038/nm.4109.

Chiu, Jeng-Jiann, and Shu Chien. "Effects of Disturbed Flow on Vascular Endothelium: Pathophysiological Basis and Clinical Perspectives." *Physiological Reviews* 91, no. 1 (2011): 327–387. https://doi.org/10.1152/physrev.00047.2009.

Choke, E., G. Cockerill, W.R.W. Wilson, S. Sayed, J. Dawson, I. Loftus, and M.M. Thompson. "A Review of Biological Factors Implicated in Abdominal Aortic Aneurysm Rupture." *European Journal of Vascular and Endovascular Surgery* 30, no. 3 (September 2005): 227–244. https://doi.org/10.1016/j.ejvs.2005.03.009.

Christen, T, V Verin, M Bochaton-Piallat, Y Popowski, F Ramaekers, P Debruyne, E Camenzind, G van Eys, and G Gabbiani. "Mechanisms of Neointima Formation and Remodeling in the Porcine Coronary Artery." *Circulation* 103, no. 6 (2001): 882–888. https://doi.org/10.1161/01.CIR.103.6.882.

Cines, D B, E S Pollak, C a Buck, J Loscalzo, G a Zimmerman, R P McEver, J S Pober, et al. "Endothelial Cells in Physiology and in the Pathophysiology of Vascular Disorders." *Blood* 91, no. 10 (1998): 3527–3561.

Clarke, Murray C H, Nichola Figg, Janet J Maguire, Anthony P Davenport, Martin Goddard, Trevor D Littlewood, and Martin R Bennett. "Apoptosis of Vascular Smooth Muscle Cells Induces Features of Plaque Vulnerability in Atherosclerosis." *Nature Medicine* 12, no. 9 (September 2006): 1075–1080. https://doi.org/10.1038/nm1459.

Clowes, A W, and S M Schwartz. “Significance of Quiescent Smooth Muscle Migration in the Injured Rat Carotid Artery.” *Circulation Research* 56, no. 1 (1985). http://circres.ahajournals.org/content/56/1/139.

Collin, J, L Araujo, J Walton, and D Lindsell. “Oxford Screening Programme for Abdominal Aortic Aneurysm in Men Aged 65 to 74 Years.” *Lancet (London, England)* 2, no. 8611 (September 1988): 613–5.

Cordes, Kimberly R., Neil T. Sheehy, Mark P. White, Emily C. Berry, Sarah U. Morton, Alecia N. Muth, Ting-Hein Lee, Joseph M. Miano, Kathryn N. Ivey, and Deepak Srivastava. “MiR-145 and MiR-143 Regulate Smooth Muscle Cell Fate and Plasticity.” *Nature* 460, no. 7256 (July 2009): 705. https://doi.org/10.1038/nature08195.

Crisby, M, G Nordin-Fredriksson, P K Shah, J Yano, J Zhu, and J Nilsson. “Pravastatin Treatment Increases Collagen Content and Decreases Lipid Content, Inflammation, Metalloproteinases, and Cell Death in Human Carotid Plaques: Implications for Plaque Stabilization.” *Circulation* 103, no. 7 (February 2001): 926–33.

Dai, Jianping, Liliane Louedec, Monique Philippe, Jean-Baptiste Michel, and Xavier Houard. “Effect of Blocking Platelet Activation with AZD6140 on Development of Abdominal Aortic Aneurysm in a Rat Aneurysmal Model.” *Journal of Vascular Surgery* 49, no. 3 (March 2009): 719–727. https://doi.org/10.1016/j.jvs.2008.09.057.

Daugherty, A, M W Manning, and L A Cassis. “Antagonism of AT2 Receptors Augments Angiotensin II-Induced Abdominal Aortic Aneurysms and Atherosclerosis.” *British Journal of Pharmacology* 134, no. 4 (October 2001): 865–70. https://doi.org/10.1038/sj.bjp.0704331.

Daugherty, Alan, and Lisa Cassis. “Angiotensin II and Abdominal Aortic Aneurysms.” *Current Hypertension Reports* 6, no. 6 (November 2004): 442–446. https://doi.org/10.1007/s11906-004-0038-0.

Daugherty, Alan, and Lisa Cassis. “Chronic Angiotensin II Infusion Promotes Atherogenesis in Low Density Lipoprotein Receptor -/- Mice.” *Annals of the New York Academy of Sciences* 892, no. 1 THE METABOLIC (November 1999): 108–118. https://doi.org/10.1111/j.1749-6632.1999.tb07789.x.

Daugherty, Alan, Lisa A. Cassis, and Hong Lu. “Complex Pathologies of Angiotensin II-Induced Abdominal Aortic Aneurysms.” *Journal of Zhejiang University SCIENCE B* 12, no. 8 (August 2011): 624–628. https://doi.org/10.1631/jzus.B1101002.

Daugherty, Alan, Michael W. Manning, and Lisa A. Cassis. “Angiotensin II Promotes Atherosclerotic Lesions and Aneurysms in Apolipoprotein E–deficient Mice.” *Journal of Clinical Investigation* 105, no. 11 (June 2000): 1605–1612. https://doi.org/10.1172/JCI7818.

Davis, P H, J D Dawson, W a Riley, and R M Lauer. “Carotid Intimal-Medial Thickness Is Related to Cardiovascular Risk Factors Measured from Childhood through Middle Age: The Muscatine Study.” Circulation 104, no. 23 (2001): 2815–2819. https://doi.org/10.1161/hc4601.099486.

Davies, M J, P D Richardson, N Woolf, D R Katz, and J Mann. “Risk of Thrombosis in Human Atherosclerotic Plaques: Role of Extracellular Lipid, Macrophage, and Smooth Muscle Cell Content.” *British Heart Journal* 69, no. 5 (1993): 377–381. https://doi.org/10.1136/hrt.69.5.377.

De Caterina, R, P Libby, H B Peng, V J Thannickal, T B Rajavashisth, M A Gimbrone, W S Shin, J K Liao, and J K Liao. “Nitric Oxide Decreases Cytokine-Induced Endothelial Activation. Nitric Oxide Selectively Reduces Endothelial Expression of Adhesion Molecules and Proinflammatory Cytokines.” *The Journal of Clinical Investigation* 96, no. 1 (July 1995): 60–8. https://doi.org/10.1172/JCI118074.

De Donatis, Alina, Giusy Comito, Francesca Buricchi, Maria C. Vinci, Astrid Parenti, Anna Caselli, Guido Camici, Giampaolo Manao, Giampietro Ramponi, and Paolo Cirri. “Proliferation versus Migration in Platelet-Derived Growth Factor Signaling: The Key Role of Endocytosis.” *Journal of Biological Chemistry* 283, no. 29 (2008): 19948–19956. https://doi.org/10.1074/jbc.M709428200.

DeBakey, M E, G M Lawrie, and D H Glaeser. “Patterns of Atherosclerosis and Their Surgical Significance.” *Annals of Surgery* 201, no. 2 (February 1985): 115–31.

Dekker, Rob J., Johannes V. van Thienen, Jakub Rohlena, Saskia C. de Jager, Yvonne W. Elderkamp, Jurgen Seppen, Carlie J.M. de Vries, et al. “Endothelial KLF2 Links Local Arterial Shear Stress Levels to the Expression of Vascular Tone-Regulating Genes.” *The American Journal of Pathology* 167, no. 2 (August 2005): 609–618. https://doi.org/10.1016/S0002-9440(10)63002-7.

Dilley, R J, and S M Schwartz. “Vascular Remodeling in the Growth Hormone Transgenic Mouse.” *Circulation Research* 65, no. 5 (1989): 1233–40.

Dimmeler, S, C Hermann, J Galle, and A M Zeiher. “Upregulation of Superoxide Dismutase and Nitric Oxide Synthase Mediates the Apoptosis-Suppressive Effects of Shear Stress on Endothelial Cells.” *Arteriosclerosis, Thrombosis, and Vascular Biology* 19, no. 3 (March 1999): 656–64.

Doran, Amanda C, Nahum Meller, and Coleen a McNamara. “Role of Smooth Muscle Cells in the Initiation and Early Progression of Atherosclerosis.” *Arteriosclerosis, Thrombosis, and Vascular Biology* 28, no. 5 (2008): 812–9. https://doi.org/10.1161/ATVBAHA.107.159327.

Dostal, D E, T Murahashi, and M J Peach. “Regulation of Cytosolic Calcium by Angiotensins in Vascular Smooth Muscle.” *Hypertension (Dallas, Tex. : 1979)* 15, no. 6 Pt 2 (June 1990): 815–22. https://doi.org/10.1161/01.hyp.30.2.222.

Dourron, H. M., Gary M Jacobson, James L Park, Jianhua Liu, Daniel J Reddy, Maria L Scheel, and Patrick J Pagano. “Perivascular Gene Transfer of NADPH Oxidase Inhibitor Suppresses Angioplasty-Induced Neointimal Proliferation of Rat Carotid Artery.” *AJP: Heart and Circulatory Physiology* 288, no. 2 (October 2004): H946–H953. https://doi.org/10.1152/ajpheart.00413.2004.

Du, Kevin L, Hon S Ip, Jian Li, Mary Chen, Frederic Dandre, William Yu, Min Min Lu, Gary K Owens, and Michael S Parmacek. “Myocardin Is a Critical Serum Response Factor Cofactor in the Transcriptional Program Regulating Smooth Muscle Cell Differentiation.” *Molecular and Cellular Biology* 23, no. 7 (April 2003): 2425–37.

Elmore, James R., Bonnie F. Keister, David P. Franklin, Jerry R. Youkey, and David J. Carey. “Expression of Matrix Metalloproteinases and TIMPs in Human Abdominal Aortic Aneurysms.” *Annals of Vascular Surgery* 12, no. 3 (May 1998): 221–228. https://doi.org/10.1007/s100169900144.

Espagnolle, Nicolas, Fabien Guilloton, Frédéric Deschaseaux, Mélanie Gadelorge, Luc Sensébé, and Philippe Bourin. “CD146 Expression on Mesenchymal Stem Cells Is Associated with Their Vascular Smooth Muscle Commitment.” *Journal of Cellular and Molecular Medicine* 18, no. 1 (January 2014): 104–114. https://doi.org/10.1111/jcmm.12168.

Faury, Gilles, Mylène Pezet, Russell H. Knutsen, Walter A. Boyle, Scott P. Heximer, Sean E. McLean, Robert K. Minkes, et al. “Developmental Adaptation of the Mouse Cardiovascular System to Elastin Haploinsufficiency.” *Journal of Clinical Investigation* 112, no. 9 (November 2003): 1419–1428. https://doi.org/10.1172/JCI19028.

Feil, Susanne, Birgit Fehrenbacher, Robert Lukowski, Frank Essmann, Klaus Schulze-Osthoff, Martin Schaller, and Robert Feil. “Transdifferentiation of Vascular Smooth Muscle Cells to Macrophage-like Cells during Atherogenesis.” *Circulation Research*, 2014, 662–667. https://doi.org/10.1161/CIRCRESAHA.115.304634.

Feng, J, S Ge, L Zhang, H Che, and C Liang. “Aortic Dissection Is Associated with Reduced Polycystin-1 Expression, an Abnormality That Leads to Increased ERK Phosphorylation in Vascular Smooth Muscle Cells.” *European Journal of Histochemistry : EJH* 60, no. 4 (December 2016): 2711. https://doi.org/10.4081/ejh.2016.2711.

Filardo, Giovanni, Janet T Powell, Melissa Ashley-Marie Martinez, and David J Ballard. “Surgery for Small Asymptomatic Abdominal Aortic Aneurysms.” In *Cochrane Database of Systematic Reviews*, edited by Giovanni Filardo, CD001835. 3. Chichester, UK: John Wiley & Sons, Ltd, 2012. https://doi.org/10.1002/14651858.CD001835.pub3.

Frid, M G, E P Moiseeva, and K R Stenmark. “Multiple Phenotypically Distinct Smooth Muscle Cell Populations Exist in the Adult and Developing Bovine Pulmonary Arterial Media in Vivo.” *Circulation Research* 75, no. 4 (1994): 669–81. https://doi.org/10.1161/01.RES.75.4.669.

Fuster, V. “Lewis A. Conner Memorial Lecture. Mechanisms Leading to Myocardial Infarction: Insights from Studies of Vascular Biology.” *Circulation* 90 (1994): 2126–2146. https://doi.org/10.1161/01.CIR.90.4.2126.

Galkina, Elena, Alexandra Kadl, John Sanders, Danielle Varughese, Ian J. Sarembock, and Klaus Ley. “Lymphocyte Recruitment into the Aortic Wall before and during Development of Atherosclerosis Is Partially L-Selectin Dependent.” *The Journal of Experimental Medicine* 203, no. 5 (May 2006): 1273–1282. https://doi.org/10.1084/jem.20052205.

Galley, H. F., and N R Webster. “Physiology of the Endothelium.” *British Journal of Anaesthesia* 93, no. 1 (July 2004): 105–113. https://doi.org/10.1093/bja/aeh163.

Gardner, Sarah E., Melanie Humphry, Martin R. Bennett, and Murray C.H. Clarke. “Senescent Vascular Smooth Muscle Cells Drive Inflammation Through an Interleukin-1α–Dependent Senescence-Associated Secretory PhenotypeSignificance.” *Arteriosclerosis, Thrombosis, and Vascular Biology* 35, no. 9 (September 2015): 1963–1974. https://doi.org/10.1161/ATVBAHA.115.305896.

Geng, Y J, and P Libby. “Evidence for Apoptosis in Advanced Human Atheroma. Colocalization with Interleukin-1 Beta-Converting Enzyme.” *The American Journal of Pathology* 147, no. 2 (August 1995): 251–66.

Giesen, Charlotte, Hao A O Wang, Denis Schapiro, Nevena Zivanovic, Andrea Jacobs, Bodo Hattendorf, Peter J Schüffler, et al. “Highly Multiplexed Imaging of Tumor Tissues with Subcellular Resolution by Mass Cytometry.” *Nature Methods* 11, no. 4 (March 2014): 417–422. https://doi.org/10.1038/nmeth.2869.

Gomez, D., and G. K. Owens. “Smooth Muscle Cell Phenotypic Switching in Atherosclerosis.” *Cardiovascular Research* 95, no. 2 (July 2012): 156–164. https://doi.org/10.1093/cvr/cvs115.

Gomez, Delphine, and Gary K Owens. “Reconciling Smooth Muscle Cell Oligoclonality and Proliferative Capacity in Experimental Atherosclerosis.” *Circulation Research* 119, no. 12 (December 2016): 1262–1264. https://doi.org/10.1161/CIRCRESAHA.116.310104.

Gomez, Delphine, Laura S Shankman, Anh T Nguyen, and Gary K Owens. “Detection of Histone Modifications at Specific Gene Loci in Single Cells in Histological Sections.” *Nature Methods* 10, no. 2 (2013): 171–7. https://doi.org/10.1038/nmeth.2332.

Gomez, Delphine, Pamela Swiatlowska, and Gary K. Owens. “Epigenetic Control of Smooth Muscle Cell Identity and Lineage Memory.” *Arteriosclerosis, Thrombosis, and Vascular Biology* 35, no. 12 (December 2015): 2508–2516. https://doi.org/10.1161/ATVBAHA.115.305044.

Grobbee, D.E., and M.L. Bots. “Carotid Artery Intima-Media Thickness as an Indicator of Generalized Atherosclerosis.” *Journal of Internal Medicine* 236 (1994): 567–573.

Grun, D, and A van Oudenaarden. “Design and Analysis of Single-Cell Sequencing Experiments.” *Cell* 163, no. 4 (2015).

Guo, Dong-Chuan, Hariyadarshi Pannu, Van Tran-Fadulu, Christina L Papke, Robert K Yu, Nili Avidan, Scott Bourgeois, et al. “Mutations in Smooth Muscle α-Actin (ACTA2) Lead to Thoracic Aortic Aneurysms and Dissections.” *Nature Genetics* 39, no. 12 (December 2007): 1488–1493. https://doi.org/10.1038/ng.2007.6.

Gutterman, D D. “Adventitia-Dependent Influences on Vascular Function.” *The American Journal of Physiology* 277, no. 4 Pt 2 (October 1999): H1265–72.

Haimovici, H, and N Maier. “Experimental Canine Atherosclerosis in Autogenous Abdominal Aortic Grafts Implanted into the Jugular Vein.” *Atherosclerosis* 13, no. 3 (May 1971): 375–84. https://doi.org/10.1016/0021-9150(71)90080-3.

Hao, H., Giulio Gabbiani, and Marie-Luce Bochaton-Piallat. “Arterial Smooth Muscle Cell Heterogeneity: Implications for Atherosclerosis and Restenosis Development.” *Arteriosclerosis,*

Thrombosis, and Vascular Biology 23, no. 9 (September 2003): 1510–1520. https://doi.org/10.1161/01.ATV.0000090130.85752.ED.

Hao, Hiroyuki, Patricia Ropraz, Vitali Verin, Edoardo Camenzind, Antoine Geinoz, Michael S. Pepper, Giulio Gabbiani, and Marie Luce Bochaton-Piallat. "Heterogeneity of Smooth Muscle Cell Populations Cultured from Pig Coronary Artery." *Arteriosclerosis, Thrombosis, and Vascular Biology* 22, no. 7 (2002): 1093–1099. https://doi.org/10.1161/01.ATV.0000022407.91111.E4.

Haque, Ashraful, Jessica Engel, Sarah A. Teichmann, and Tapio Lönnberg. "A Practical Guide to Single-Cell RNA-Sequencing for Biomedical Research and Clinical Applications." *Genome Medicine* 9, no. 1 (December 2017): 75. https://doi.org/10.1186/s13073-017-0467-4.

Hashimshony, Tamar, Florian Wagner, Noa Sher, and Itai Yanai. "CEL-Seq: Single-Cell RNA-Seq by Multiplexed Linear Amplification." *Cell Reports* 2, no. 3 (September 2012): 666–673. https://doi.org/10.1016/j.celrep.2012.08.003.

Haurani, M, P PAGANO, Ruperez M., Suzuki Y., Egido J., Kübler W., Kita T., and Yokode M. "Adventitial Fibroblast Reactive Oxygen Species as Autacrine and Paracrine Mediators of Remodeling: Bellwether for Vascular Disease?" *Cardiovascular Research* 75, no. 4 (September 2007): 679–689. https://doi.org/10.1016/j.cardiores.2007.06.016.

Herring, B. Paul, April M. Hoggatt, Sarah L. Griffith, Jeanette N. McClintick, and Patricia J. Gallagher. "Inflammation and Vascular Smooth Muscle Cell Dedifferentiation Following Carotid Artery Ligation." *Physiological Genomics* 49, no. 3 (2017). http://physiolgenomics.physiology.org/content/49/3/115?hwshib2=authn%3A1505408047%3A20170913%253A9f5d9f7c-6515-4636-8895-7c6af22ba2bc%3A0%3A0%3A0%3AG1XGk%2B9pHF8OYAEYkj3gOw%3D%3D.

Herring, Brian Paul, April M Hoggatt, Christopher Burlak, and Stefan Offermanns. "Previously Differentiated Medial Vascular Smooth Muscle Cells Contribute to Neointima Formation Following Vascular Injury." *Vascular Cell* 6 (2014): 21. https://doi.org/10.1186/2045-824X-6-21.

Hiltunen, Mikko O, Mikko P Turunen, Tomi P Häkkinen, Juha Rutanen, Maria Hedman, Kimmo Mäkinen, Anna-Mari Turunen, Katriina Aalto-Setälä, and Seppo Ylä-Herttuala. "DNA Hypomethylation and Methyltransferase Expression in Atherosclerotic Lesions." *Vascular Medicine (London, England)* 7 (2002): 5–11. https://doi.org/10.1191/1358863x02vm418oa.

Hofnagel, O., Birgit Luechtenborg, Katrin Stolle, Stefan Lorkowski, Heike Eschert, Gabriele Plenz, and Horst Robenek. "Proinflammatory Cytokines Regulate LOX-1 Expression in Vascular Smooth Muscle Cells." *Arteriosclerosis, Thrombosis, and Vascular Biology* 24, no. 10 (August 2004): 1789–1795. https://doi.org/10.1161/01.ATV.0000140061.89096.2b.

Howard, E W, E C Bullen, and M J Banda. "Preferential Inhibition of 72- and 92-KDa Gelatinases by Tissue Inhibitor of Metalloproteinases-2." *The Journal of Biological Chemistry* 266, no. 20 (July 1991): 13070–5.

Hu, Yanhua, Zhongyi Zhang, Evelyn Torsney, Ali R Afzal, Fergus Davison, Bernhard Metzler, and Qingbo Xu. "Abundant Progenitor Cells in the Adventitia Contribute to Atherosclerosis of Vein Grafts in ApoE-Deficient Mice." *The Journal of Clinical Investigation* 113, no. 9 (2004): 1258–1265. https://doi.org/10.1172/JCI200419628.

Ishibashi, S, M S Brown, J L Goldstein, R D Gerard, R E Hammer, and J Herz. "Hypercholesterolemia in Low Density Lipoprotein Receptor Knockout Mice and Its Reversal by Adenovirus-Mediated Gene Delivery." *The Journal of Clinical Investigation* 92, no. 2 (August 1993): 883–93. https://doi.org/10.1172/JCI116663.

Iwata, Hiroshi, Ichiro Manabe, Katsuhito Fujiu, Tetsufumi Yamamoto, Norifumi Takeda, Kosei Eguchi, Akiko Furuya, Makoto Kuro-o, Masataka Sata, and Ryozo Nagai. "Bone Marrow-Derived Cells Contribute to Vascular Inflammation but Do Not Differentiate into Smooth Muscle Cell Lineages." *Circulation* 122, no. 20 (2010): 2048–2057. https://doi.org/10.1161/CIRCULATIONAHA.110.965202.

Jacobs, M L, A J Chin, J Rychik, J M Steven, S C Nicolson, and W I Norwood. “Interrupted Aortic Arch. Impact of Subaortic Stenosis on Management and Outcome.” *Circulation* 92, no. 9 Suppl (November 1995): II128–31.

Jaitin, Diego Adhemar, Ephraim Kenigsberg, Hadas Keren-Shaul, Naama Elefant, Franziska Paul, Irina Zaretsky, Alexander Mildner, et al. “Massively Parallel Single-Cell RNA-Seq for Marker-Free Decomposition of Tissues into Cell Types.” *Science (New York, N.Y.)* 343, no. 6172 (February 2014): 776–9. https://doi.org/10.1126/science.1247651.

Jaulmes, A., Sylvain Thierry, Brigitte Janvier, Michel Raymondjean, and Vincent Maréchal. “Activation of SPLA2-IIA and PGE2 Production by High Mobility Group Protein B1 in Vascular Smooth Muscle Cells Sensitized by IL-1.” *The FASEB Journal* 20, no. 10 (August 2006): 1727–1729. https://doi.org/10.1096/fj.05-5514fje.

Jiang, X, D H Rowitch, P Soriano, a P McMahon, and H M Sucov. “Fate of the Mammalian Cardiac Neural Crest.” *Development (Cambridge, England)* 127, no. 8 (2000): 1607–1616.

Johnsen, S. H., S. H. Forsdahl, K. Singh, and B. K. Jacobsen. “Atherosclerosis in Abdominal Aortic Aneurysms: A Causal Event or a Process Running in Parallel? The Tromso Study.” *Arteriosclerosis, Thrombosis, and Vascular Biology* 30, no. 6 (June 2010): 1263–1268. https://doi.org/10.1161/ATVBAHA.110.203588.

Johnston, K W, R B Rutherford, M D Tilson, D M Shah, L Hollier, and J C Stanley. “Suggested Standards for Reporting on Arterial Aneurysms. Subcommittee on Reporting Standards for Arterial Aneurysms, Ad Hoc Committee on Reporting Standards, Society for Vascular Surgery and North American Chapter, International Society for Cardiovascular Surgery.” *Journal of Vascular Surgery* 13, no. 3 (March 1991): 452–8.

Kim, S, H S Ip, M M Lu, C Clendenin, and M S Parmacek. “A Serum Response Factor-Dependent Transcriptional Regulatory Program Identifies Distinct Smooth Muscle Cell Sublineages.” *Molecular and Cellular Biology* 17, no. 4 (April 1997): 2266–78.

King, V. L., A. Y. Lin, F. Kristo, T. J. T. Anderson, N. Ahluwalia, G. J. Hardy, A. P. Owens, et al. “Interferon- and the Interferon-Inducible Chemokine CXCL10 Protect Against Aneurysm Formation and Rupture.” *Circulation* 119, no. 3 (January 2009): 426–435. https://doi.org/10.1161/CIRCULATIONAHA.108.785949.

Kinlay, S, and P Ganz. “Role of Endothelial Dysfunction in Coronary Artery Disease and Implications for Therapy.” *The American Journal of Cardiology* 80, no. 9A (1997): 11I–16I.

Kivioja, Teemu, Anna Vähärautio, Kasper Karlsson, Martin Bonke, Martin Enge, Sten Linnarsson, and Jussi Taipale. “Counting Absolute Numbers of Molecules Using Unique Molecular Identifiers.” *Nature Methods* 9, no. 1 (November 2011): 72–74. https://doi.org/10.1038/nmeth.1778.

Koch, A E, G K Haines, R J Rizzo, J A Radosevich, R M Pope, P G Robinson, and W H Pearce. “Human Abdominal Aortic Aneurysms. Immunophenotypic Analysis Suggesting an Immune-Mediated Response.” *The American Journal of Pathology* 137, no. 5 (November 1990): 1199–213.

Kolodgie, Frank D, Allen P Burke, Gaku Nakazawa, and R Virmani. “Is Pathologic Intimal Thickening the Key to Understanding Early Plaque Progression in Human Atherosclerotic Disease?” *ATVB* 27 (2007): 986–989.

Koltsova, Ekaterina K, Catherine C Hedrick, and Klaus Ley. “Myeloid Cells in Atherosclerosis: A Delicate Balance of Anti-Inflammatory and Proinflammatory Mechanisms.” *Current Opinion in Lipidology* 24, no. 5 (October 2013): 371–80. https://doi.org/10.1097/MOL.0b013e328363d298.

Korshunov, Vyacheslav a., and Bradford C. Berk. “Flow-Induced Vascular Remodeling in the Mouse: A Model for Carotid Intima-Media Thickening.” *Arteriosclerosis, Thrombosis, and Vascular Biology* 23 (2003): 2185–2191. https://doi.org/10.1161/01.ATV.0000103120.06092.14.

Koyama, H, E W Raines, K E Bornfeldt, J M Roberts, and R Ross. “Fibrillar Collagen Inhibits Arterial Smooth Muscle Proliferation through Regulation of Cdk2 Inhibitors.” *Cell* 87, no. 6 (December 1996): 1069–78.

Kramann, Rafael, Rebekka K Schneider, Derek P DiRocco, Flavia Machado, Susanne Fleig, Philip A Bondzie, Joel M Henderson, et al. “Perivascular Gli1+ Progenitors Are Key Contributors to Injury-Induced Organ Fibrosis.” *Cell Stem Cell* 16, no. 1 (January 2015): 51–66. https://doi.org/10.1016/j.stem.2014.11.004.

Kumar, A, and V Lindner. “Remodeling with Neointima Formation in the Mouse Carotid Artery after Cessation of Blood Flow.” *Arteriosclerosis, Thrombosis, and Vascular Biology* 17, no. 10 (October 1997): 2238–44.

Lacolley, P, P Challande, S Boumaza, G Cohuet, S Laurent, P Boutouyrie, J A Grimaud, D Paulin, J M Lamazière, and Z Li. “Mechanical Properties and Structure of Carotid Arteries in Mice Lacking Desmin.” *Cardiovascular Research* 51, no. 1 (July 2001): 178–87.

Lemire, A. Lea, K. Batten, D. Jian Gu, S. Whitley, P. and Bramlett. K. “Development of ERCC RNA Spike-In Control Mixes.” *J Biomol Tech* 22 (2011).

Levine, G N, A P Chodos, and J Loscalzo. “Restenosis Following Coronary Angioplasty: Clinical Presentations and Therapeutic Options.” *Clinical Cardiology* 18, no. 12 (December 1995): 693–703.

Li, L, J M Miano, B Mercer, and E N Olson. “Expression of the SM22alpha Promoter in Transgenic Mice Provides Evidence for Distinct Transcriptional Regulatory Programs in Vascular and Visceral Smooth Muscle Cells.” *The Journal of Cell Biology* 132, no. 5 (March 1996): 849–59.

Li, S, Y S Fan, L H Chow, C Van Den Diepstraten, E van Der Veer, S M Sims, and J G Pickering. “Innate Diversity of Adult Human Arterial Smooth Muscle Cells: Cloning of Distinct Subtypes from the Internal Thoracic Artery.” *Circulation Research* 89, no. 6 (2001): 517–525. https://doi.org/10.1161/hh1801.097165.

Li, Shaohua, Stephen Sims, Yang Jiao, Lawrence H Chow, and J Geoffrey Pickering. “Evidence From a Novel Human Cell Clone That Adult Between Noncontractile and Contractile Phenotypes.” *Circulation Research* 85 (1999): 338–348. https://doi.org/10.1161/01.RES.85.4.338.

Li, X, V Van Putten, F Zarinetchi, M E Nicks, S Thaler, L E Heasley, and R A Nemenoff. “Suppression of Smooth-Muscle Alpha-Actin Expression by Platelet-Derived Growth Factor in Vascular Smooth-Muscle Cells Involves Ras and Cytosolic Phospholipase A2.” *The Biochemical Journal* 327 (Pt 3), no. Pt 3 (November 1997): 709–16.

Libby, P. *Chapter 241. The Pathogenesis, Prevention, and Treatment of Atherosclerosis | Harrison’s Principles of Internal Medicine, 18e | AccessMedicine | McGraw-Hill Medical*. (2005).

Libby, Peter, Paul M Ridker, and Göran K Hansson. “Progress and Challenges in Translating the Biology of Atherosclerosis.” *Nature* 473, no. 7347 (2011): 317–25. https://doi.org/10.1038/nature10146.

Lindner, V, J Fingerle, and M A Reidy. “Mouse Model of Arterial Injury.” *Circulation Research* 73, no. 5 (November 1993): 792–6.

Liu, Chengyu. “Strategies for Designing Transgenic DNA Constructs.” *Methods in Molecular Biology (Clifton, N.J.)* 1027 (2013): 183–201. https://doi.org/10.1007/978-1-60327-369-5_8.

Liu, Ou, Lixin Jia, Xiaoxi Liu, Yueli Wang, Xiaolong Wang, Yanwen Qin, Jie Du, and Hongjia Zhang. “Clopidogrel, a Platelet P2Y12 Receptor Inhibitor, Reduces Vascular Inflammation and Angiotensin II Induced-Abdominal Aortic Aneurysm Progression.” *PloS One* 7, no. 12 (2012): e51707. https://doi.org/10.1371/journal.pone.0051707.

Liu, Serena, and Cole Trapnell. “Single-Cell Transcriptome Sequencing: Recent Advances and Remaining Challenges.” *F1000Research* 5 (February 2016). https://doi.org/10.12688/f1000research.7223.1.

Livet, Jean, Tamily A. Weissman, Hyuno Kang, Ryan W. Draft, Ju Lu, Robyn A. Bennis, Joshua R. Sanes, and Jeff W. Lichtman. “Transgenic Strategies for Combinatorial Expression of Fluorescent Proteins in the Nervous System.” *Nature* 450, no. 7166 (November 2007): 56–62. https://doi.org/10.1038/nature06293.

López-Candales, A, D R Holmes, S Liao, M J Scott, S A Wickline, and R W Thompson. “Decreased Vascular Smooth Muscle Cell Density in Medial Degeneration of Human Abdominal Aortic Aneurysms.” *The American Journal of Pathology* 150, no. 3 (March 1997): 993–1007.

Lu, Yao Wei, Anthony M. Lowery, Li-Yan Sun, Harold A. Singer, Guohao Dai, Alejandro P. Adam, Peter A. Vincent, and John J. Schwarz. “Endothelial Myocyte Enhancer Factor 2c Inhibits Migration of Smooth Muscle Cells Through Fenestrations in the Internal Elastic LaminaHighlights.” *Arteriosclerosis, Thrombosis, and Vascular Biology* 37, no. 7 (2017). http://atvb.ahajournals.org/content/37/7/1380.

Lun, L. Aaron T., Karsten Bach, and John C. Marioni. “Pooling across Cells to Normalize Single-Cell RNA Sequencing Data with Many Zero Counts.” *Genome Biology* 17, no. 1 (December 2016): 75. https://doi.org/10.1186/s13059-016-0947-7.

Maaten, Laurens van der. “Barnes-Hut-SNE,” January 2013. http://arxiv.org/abs/1301.3342.

Macaulay, Iain C., Valentine Svensson, Charlotte Labalette, Lauren Ferreira, Fiona Hamey, Thierry Voet, Sarah A. Teichmann, and Ana Cvejic. “Single-Cell RNA-Sequencing Reveals a Continuous Spectrum of Differentiation in Hematopoietic Cells.” *Cell Reports* 14, no. 4 (February 2016): 966–977. https://doi.org/10.1016/j.celrep.2015.12.082.

Macaulay, IC, V Svensson, C Labalette, L Ferreira, F Hamey, T Voet, SA Teichmann, and A Cvejic. “No Title.” *Cell Reports* 14, no. 4 (2016).

Mack, C P, and G K Owens. “Regulation of Smooth Muscle Alpha-Actin Expression in Vivo Is Dependent on CArG Elements within the 5’ and First Intron Promoter Regions.” *Circulation Research* 84, no. 7 (April 1999): 852–61.

Madsen, C S, C P Regan, J E Hungerford, S L White, I Manabe, and G K Owens. “Smooth Muscle-Specific Expression of the Smooth Muscle Myosin Heavy Chain Gene in Transgenic Mice Requires 5’-Flanking and First Intronic DNA Sequence.” *Circulation Research* 82, no. 8 (May 1998): 908–17.

Majesky, M. W., X. R. Dong, J. N. Regan, and V. J. Hoglund. “Vascular Smooth Muscle Progenitor Cells: Building and Repairing Blood Vessels.” *Circulation Research* 108, no. 3 (February 2011): 365–377. https://doi.org/10.1161/CIRCRESAHA.110.223800.

Majesky, Mark W. “Developmental Basis of Vascular Smooth Muscle Diversity.” *Arteriosclerosis, Thrombosis, and Vascular Biology* 27, no. 6 (2007): 1248–1258. https://doi.org/10.1161/ATVBAHA.107.141069.

Manabe, I, and G K Owens. “Recruitment of Serum Response Factor and Hyperacetylation of Histones at Smooth Muscle-Specific Regulatory Regions during Differentiation of a Novel P19-Derived in Vitro Smooth Muscle Differentiation System.” *Circulation Research* 88, no. 11 (June 2001): 1127–34.

Manning, Michael W, Lisa A Cassis, Jing Huang, Stephen J Szilvassy, and Alan Daugherty. “Abdominal Aortic Aneurysms: Fresh Insights from a Novel Animal Model of the Disease.” *Vascular Medicine* 7, no. 1 (February 2002): 45–54. https://doi.org/10.1191/1358863x02vm413ra.

Marx, Steven O, Hana Totary-Jain, and Andrew R Marks. “Vascular Smooth Muscle Cell Proliferation in Restenosis.” *Circulation. Cardiovascular Interventions* 4, no. 1 (February 2011): 104–11. https://doi.org/10.1161/CIRCINTERVENTIONS.110.957332.

Mashal, R D, M L Fejzo, A J Friedman, N Mitchner, R A Nowak, M S Rein, C C Morton, and J Sklar. “Analysis of Androgen Receptor DNA Reveals the Independent Clonal Origins of Uterine Leiomyomata and the Secondary Nature of Cytogenetic Aberrations in the Development of Leiomyomata.” *Genes, Chromosomes & Cancer* 11, no. 1 (September 1994): 1–6.

Mathers, Colin D, and Dejan Loncar. “Updated Projections of Global Mortality and Burden of Disease, 2002-2030: Data Sources, Methods and Results.” *World Health*, no. October (2005): 2002–2030. https://doi.org/10.1371/journal.pmed.0030442.

Mathers, Colin D, Dejan Loncar, J Boreham, M Thun, JC Heath, and R Doll. “Projections of Global Mortality and Burden of Disease from 2002 to 2030.” Edited by Jon Samet. *PLoS Medicine* 3, no. 11 (November 2006): e442. https://doi.org/10.1371/journal.pmed.0030442.

Matthews, Charles, Isabelle Gorenne, Stephen Scott, Nicola Figg, Peter Kirkpatrick, Andrew Ritchie, Martin Goddard, and Martin Bennett. “Vascular Smooth Muscle Cells Undergo Telomere-Based Senescence in Human Atherosclerosis: Effects of Telomerase and Oxidative Stress.” *Circulation Research* 99, no. 2 (2006): 156–164. https://doi.org/10.1161/01.RES.0000233315.38086.bc.

Matturri, L, A Cazzullo, P Turconi, A M Lavezzi, P L Vandone, L Gabrielli, G Fernández Alonso, D Grana, and J Milei. “Chromosomal Alterations in Atherosclerotic Plaques.” *Atherosclerosis* 154, no. 3 (February 2001): 755–61. https://doi.org/10.1016/S0021-9150(00)00488-3.

Mayor, R., and E. Theveneau. “The Neural Crest.” *Development* 140, no. 11 (June 2013): 2247–2251. https://doi.org/10.1242/dev.091751.

McDonald, O. G., Brian R Wamhoff, Mark H Hoofnagle, and Gary K Owens. “Control of SRF Binding to CArG Box Chromatin Regulates Smooth Muscle Gene Expression in Vivo.” *Journal of Clinical Investigation* 116, no. 1 (December 2005): 36–48. https://doi.org/10.1172/JCI26505.

McDonald, Oliver G, Brian R Wamhoff, Mark H Hoofnagle, and Gary K Owens. “Control of SRF Binding to CArG Box Chromatin Regulates Smooth Muscle Gene Expression in Vivo.” *The Journal of Clinical Investigation* 116, no. 1 (2006): 36–48. https://doi.org/10.1172/JCI26505.

McEniery, Carmel M, Ian B Wilkinson, and Albert P Avolio. “AGE, HYPERTENSION AND ARTERIAL FUNCTION.” *Clinical and Experimental Pharmacology and Physiology* 34, no. 7 (July 2007): 665–671. https://doi.org/10.1111/j.1440-1681.2007.04657.x.

Meir, Karen S, and Eran Leitersdorf. “Atherosclerosis in the Apolipoprotein-E-Deficient Mouse: A Decade of Progress.” *Arteriosclerosis, Thrombosis, and Vascular Biology* 24, no. 6 (2004): 1006–14. https://doi.org/10.1161/01.ATV.0000128849.12617.f4.

Mericskay, Mathias, Ara Parlakian, Arlette Porteu, Frédéric Dandré, Jacques Bonnet, Denise Paulin, and Zhenlin Li. “An Overlapping CArG/Octamer Element Is Required for Regulation of Desmin Gene Transcription in Arterial Smooth Muscle Cells.” *Developmental Biology* 226, no. 2 (2000): 192–208. https://doi.org/10.1006/dbio.2000.9865.

Moiseeva, E P. “Adhesion Receptors of Vascular Smooth Muscle Cells and Their Functions.” *Cardiovascular Research* 52, no. 3 (2001): 372–386.

Mozaffarian, Dariush, Emelia J. Benjamin, Alan S. Go, Donna K. Arnett, Michael J. Blaha, Mary Cushman, Sandeep R. Das, et al. “Heart Disease and Stroke Statistics—2016 Update.” *Circulation*, 2015. http://circ.ahajournals.org/content/early/2015/12/16/CIR.0000000000000350.

Nakahashi, Takeshi K, Katsuyuki Hoshina, Philip S Tsao, Eiketsu Sho, Mien Sho, John K Karwowski, Cory Yeh, Ruey-Bing Yang, James N Topper, and Ronald L Dalman. “Flow Loading Induces Macrophage Antioxidative Gene Expression in Experimental Aneurysms.” *Arteriosclerosis, Thrombosis, and Vascular Biology* 22, no. 12 (December 2002): 2017–22.

Nakashima, Yutaka, Andrew S Plump, Elaine W Raines, Jan L Breslow, and Russell Ross. “ApoE-Deficient Mice Develop Lesions of All Phases of Atherosclerosis throughout the Arterial Tree.” *Arteriosclerosis and Thrombosis : A Journal of Vascular Biology / American Heart Association* 14, no. 1 (1994): 133–40. https://doi.org/10.1161/01.ATV.14.1.133.

Nam, Douglas, Chih-Wen Ni, Amir Rezvan, Jin Suo, Klaudia Budzyn, Alexander Llanos, David Harrison, Don Giddens, and Hanjoong Jo. “Partial Carotid Ligation Is a Model of Acutely Induced Disturbed Flow, Leading to Rapid Endothelial Dysfunction and Atherosclerosis.” *American Journal of Physiology. Heart and Circulatory Physiology* 297, no. 4 (2009): H1535–43. https://doi.org/10.1152/ajpheart.00510.2009.

Neese, R. A., L. M. Misell, S. Turner, A. Chu, J. Kim, D. Cesar, R. Hoh, et al. “Nonlinear Partial Differential Equations and Applications: Measurement in Vivo of Proliferation Rates of Slow Turnover Cells by 2H2O Labeling of the Deoxyribose Moiety of DNA.” *Proceedings of the National Academy of Sciences* 99, no. 24 (November 2002): 15345–15350. https://doi.org/10.1073/pnas.232551499.

Nemenoff, R. A., H. Horita, A. C. Ostriker, S. B. Furgeson, P. A. Simpson, V. VanPutten, J. Crossno, S. Offermanns, and M. C. M. Weiser-Evans. “SDF-1 Induction in Mature Smooth Muscle Cells by

Inactivation of PTEN Is a Critical Mediator of Exacerbated Injury-Induced Neointima Formation." *Arteriosclerosis, Thrombosis, and Vascular Biology* 31, no. 6 (June 2011): 1300–1308. https://doi.org/10.1161/ATVBAHA.111.223701.

Newby, A C, P Libby, and A C van der Wal. "Plaque Instability–the Real Challenge for Atherosclerosis Research in the next Decade?" *Cardiovascular Research* 41, no. 2 (February 1999): 321–2.

Newman, W P, D S Freedman, a W Voors, P D Gard, S R Srinivasan, J L Cresanta, G D Williamson, L S Webber, and G S Berenson. *Relation of Serum Lipoprotein Levels and Systolic Blood Pressure to Early Atherosclerosis. The Bogalusa Heart Study.* Vol. 314. 3, 1986. https://doi.org/10.1056/NEJM198601163140302.

Nguyen, AT, D Gomez, RD Bell, JH Campbell, AW Clowes, G Gabbiani, CM Giachelli, et al. "Smooth Muscle Cell Plasticity: Fact or Fiction?" *Circ Res.* 112, no. 1 (2013): 17–22.

Nichterwitz, Susanne, Geng Chen, Julio Aguila Benitez, Marlene Yilmaz, Helena Storvall, Ming Cao, Rickard Sandberg, Qiaolin Deng, and Eva Hedlund. "Laser Capture Microscopy Coupled with Smart-Seq2 for Precise Spatial Transcriptomic Profiling." *Nature Communications* 7 (July 2016): 12139. https://doi.org/10.1038/ncomms12139.

Nurnberg, ST, K Cheng, A Raiesdana, R Kundu, CL Miller, JB Kim, K Arora, et al. "Coronary Artery Disease Associated Transcription Factor TCF21 Regulates Smooth Muscle Precursor Cells That Contribute to the Fibrous Cap." *PLoS Genet.* 11, no. 5 (2015).

Ogeng'o, Julius, Kevin Ongeti, Moses Obimbo, Bedu Olabu, and Phillip Mwachaka. "Features of Atherosclerosis in the Tunica Adventitia of Coronary and Carotid Arteries in a Black Kenyan Population." *Anatomy Research International* Article ID (2014): 5 pages.

Okura, Yoshifumi, Marijke Brink, Hiroyuki Itabe, Kathrin J. Scheidegger, Afksendiyos Kalangos, and Patrice Delafontaine. "Oxidized Low-Density Lipoprotein Is Associated With Apoptosis of Vascular Smooth Muscle Cells in Human Atherosclerotic Plaques." *Circulation* 102, no. 22 (2000). http://circ.ahajournals.org/content/102/22/2680.short.

Opitz, Florian, Katja Schenke-Layland, Tina U. Cohnert, and Ulrich A. Stock. "Phenotypical Plasticity of Vascular Smooth Muscle Cells—Effect of \textlessi\textgreaterIn Vitro\textless/I\textgreater and \textlessi\textgreaterIn Vivo\textless/I\textgreater Shear Stress for Tissue Engineering of Blood Vessels." *Tissue Engineering* 13, no. 10 (October 2007): 2505–2514. https://doi.org/10.1089/ten.2006.0424.

Organization, World Health. *Global Health Estimates : Death by Cause, Age, Sex and Country, 2000 - 2012. WHO*, 2014.

Owens, G K. "Regulation of Differentiation of Vascular Smooth Muscle Cells." *Physiological Reviews* 75, no. 3 (July 1995): 487–517.

Owens, G. K., Meena S Kumar, and Brian R Wamhoff. "Molecular Regulation of Vascular Smooth Muscle Cell Differentiation in Development and Disease." *Physiological Reviews* 84, no. 3 (July 2004): 767–801. https://doi.org/10.1152/physrev.00041.2003.

Paigen, B, A Morrow, P A Holmes, D Mitchell, and R A Williams. "Quantitative Assessment of Atherosclerotic Lesions in Mice." *Atherosclerosis* 68, no. 3 (1987): 231–240. https://doi.org/10.1016/0021-9150(87)90202-4.

Pannu, H., V. Tran-Fadulu, C. L. Papke, S. Scherer, Y. Liu, C. Presley, D. Guo, et al. "MYH11 Mutations Result in a Distinct Vascular Pathology Driven by Insulin-like Growth Factor 1 and Angiotensin II." *Human Molecular Genetics* 16, no. 20 (April 2007): 2453–2462. https://doi.org/10.1093/hmg/ddm201.

Parastatidis, Ioannis, Daiana Weiss, Giji Joseph, and W Robert Taylor. "Overexpression of Catalase in Vascular Smooth Muscle Cells Prevents the Formation of Abdominal Aortic Aneurysms." *Arteriosclerosis, Thrombosis, and Vascular Biology* 33, no. 10 (October 2013): 2389–96. https://doi.org/10.1161/ATVBAHA.113.302175.

Park, Hyung Sub, Geum Hee Choi, Soli Hahn, Young Sun Yoo, Ji Youl Lee, and Taeseung Lee. "Potential Role of Vascular Smooth Muscle Cell-like Progenitor Cell Therapy in the Suppression of Experimental Abdominal Aortic Aneurysms." *Biochemical and Biophysical Research*

Communications 431, no. 2 (February 2013): 326–331. https://doi.org/10.1016/j.bbrc.2012.12.099.

Patel, M. I., P. Ghosh, J. Melrose, and M. Appleberg. “SMOOTH MUSCLE CELL MIGRATION AND PROLIFERATION IS ENHANCED IN ABDOMINAL AORTIC ANEURYSMS.” *ANZ Journal of Surgery* 66, no. 5 (May 1996): 305–308. https://doi.org/10.1111/j.1445-2197.1996.tb01192.x.

PDAY research group. “Relationship of Atherosclerosis in Young Men to Serum Lipoprotein Cholesterol Concentrations and Smoking. A Preliminary Report from the Pathobiological Determinants of Atherosclerosis in Youth (PDAY) Research Group.” *JAMA : The Journal of the American Medical Association* 264, no. 23 (1990): 3018–24. https://doi.org/10.1097/00043764-199108000-00002.

Penn, A, S J Garte, L Warren, D Nesta, and B Mindich. “Transforming Gene in Human Atherosclerotic Plaque DNA.” *Proceedings of the National Academy of Sciences of the United States of America* 83, no. 20 (October 1986): 7951–5.

Pfaltzgraff, Elise R, and David M Bader. “Heterogeneity in Vascular Smooth Muscle Cell Embryonic Origin in Relation to Adult Structure, Physiology, and Disease.” *Developmental Dynamics : An Official Publication of the American Association of Anatomists* 244, no. 3 (2015): 410–6. https://doi.org/10.1002/dvdy.24247.

Picelli, Simone, \AAsa K Björklund, Omid R Faridani, Sven Sagasser, Gösta Winberg, and Rickard Sandberg. “Smart-Seq2 for Sensitive Full-Length Transcriptome Profiling in Single Cells.” *Nature Methods* 10, no. 11 (September 2013): 1096–1098. https://doi.org/10.1038/nmeth.2639.

Picelli, Simone, Omid R Faridani, \AAsa K Björklund, Gösta Winberg, Sven Sagasser, and Rickard Sandberg. “Full-Length RNA-Seq from Single Cells Using Smart-Seq2.” *Nature Protocols* 9, no. 1 (January 2014): 171–181. https://doi.org/10.1038/nprot.2014.006.

Piedrahita, Jorge A, Sunny H Zhang, John R Hagaman, Paula M Oliver, and Nobuyo Maeda. “Generation of Mice Carrying a Mutant Apolipoprotein E Gene Inactivated by Gene Targeting in Embryonic Stem Cells.” *Proceedings of the National Academy of Sciences of the United States of America* 89, no. May (1992): 4471–4475. https://doi.org/10.1073/pnas.89.10.4471.

Pleumeekers, H.J.C.M., A.W. Hoes, E. van der Does, H. Van Urk, and D.E. Grobbee. “Epidemiology of Abdominal Aortic Aneurysms.” *European Journal of Vascular Surgery* 8, no. 2 (March 1994): 119–128. https://doi.org/10.1016/S0950-821X(05)80446-3.

Pouget, C., K. Pottin, and T. Jaffredo. “Sclerotomal Origin of Vascular Smooth Muscle Cells and Pericytes in the Embryo.” *Developmental Biology* 315, no. 2 (March 2008): 437–447. https://doi.org/10.1016/j.ydbio.2007.12.045.

Proweller, Aaron, Lili Tu, John J. Lepore, Lan Cheng, Min Min Lu, John Seykora, Sarah E. Millar, Warren S. Pear, and Michael S. Parmacek. “Impaired Notch Signaling Promotes \textlessi\textgreaterDe Novo\textless/I\textgreater Squamous Cell Carcinoma Formation.” *Cancer Research* 66, no. 15 (August 2006): 7438–7444. https://doi.org/10.1158/0008-5472.CAN-06-0793.

Pugsley, M K, and R Tabrizchi. “The Vascular System. An Overview of Structure and Function.” *Journal of Pharmacological and Toxicological Methods* 44, no. 2 (2000): 333–40.

Qiu, Ping, and Li Li. “Histone Acetylation and Recruitment of Serum Responsive Factor and CREB-Binding Protein Onto SM22 Promoter During SM22 Gene Expression.” *Circulation Research* 90, no. 8 (2002). http://circres.ahajournals.org/content/90/8/858.

R Core Team. *R: A Language and Environment for Statistical Computing.*, 2016.

Raffort, Juliette, Fabien Lareyre, Marc Clément, Réda Hassen-Khodja, Giulia Chinetti, and Ziad Mallat. “Monocytes and Macrophages in Abdominal Aortic Aneurysm.” *Nature Reviews Cardiology* 14, no. 8 (April 2017): 457–471. https://doi.org/10.1038/nrcardio.2017.52.

Raj, Arjun, and Alexander van Oudenaarden. “Nature, Nurture, or Chance: Stochastic Gene Expression and Its Consequences.” *Cell* 135, no. 2 (2008): 216–26. https://doi.org/10.1016/j.cell.2008.09.050.

Rakic, Pasko. “PROGRESSNeurogenesis in Adult Primate Neocortex: An Evaluation of the Evidence.” *Nature Reviews Neuroscience* 3, no. 1 (January 2002): 65–71. https://doi.org/10.1038/nrn700.

Rastan, S. “Timing of X-Chromosome Inactivation in Postimplantation Mouse Embryos.” *Journal of Embryology and Experimental Morphology* 71 (1982): 11–24.

Rateri, Debra L., Deborah A. Howatt, Jessica J. Moorleghen, Richard Charnigo, Lisa A. Cassis, and Alan Daugherty. “Prolonged Infusion of Angiotensin II in ApoE−/− Mice Promotes Macrophage Recruitment with Continued Expansion of Abdominal Aortic Aneurysm.” *The American Journal of Pathology* 179, no. 3 (September 2011): 1542–1548. https://doi.org/10.1016/j.ajpath.2011.05.049.

Rensen, S S M, P a F M Doevendans, and G J J M van Eys. “Regulation and Characteristics of Vascular Smooth Muscle Cell Phenotypic Diversity.” *Netherlands Heart Journal : Monthly Journal of the Netherlands Society of Cardiology and the Netherlands Heart Foundation* 15, no. 3 (2007): 100–108. https://doi.org/10.1007/BF03085963.

Rhodin, Johannes A. G. “Architecture of the Vessel Wall.” In *Comprehensive Physiology*, 1–31. Hoboken, NJ, USA: John Wiley & Sons, Inc., 1980. https://doi.org/10.1002/cphy.cp020201.

Risso, Davide, John Ngai, Terence P Speed, and Sandrine Dudoit. “Normalization of RNA-Seq Data Using Factor Analysis of Control Genes or Samples.” *Nature Biotechnology* 32, no. 9 (August 2014): 896–902. https://doi.org/10.1038/nbt.2931.

Ross, Russell. “Atherosclerosis — An Inflammatory Disease.” *New England Journal of Medicine* 340, no. 2 (1999): 115–126. https://doi.org/10.1056/NEJM199901143400207.

Rowe, V L, S L Stevens, T T Reddick, M B Freeman, R Donnell, R C Carroll, and M H Goldman. “Vascular Smooth Muscle Cell Apoptosis in Aneurysmal, Occlusive, and Normal Human Aortas.” *Journal of Vascular Surgery* 31, no. 3 (March 2000): 567–76.

Ruddy, Jean Marie, Jeffrey A. Jones, Francis G. Spinale, and John S. Ikonomidis. “Regional Heterogeneity within the Aorta: Relevance to Aneurysm Disease.” *The Journal of Thoracic and Cardiovascular Surgery* 136, no. 5 (November 2008): 1123–1130. https://doi.org/10.1016/j.jtcvs.2008.06.027.

Sacks, Frank M., Marc A. Pfeffer, Lemuel A. Moye, Jean L. Rouleau, John D. Rutherford, Thomas G. Cole, Lisa Brown, et al. “The Effect of Pravastatin on Coronary Events after Myocardial Infarction in Patients with Average Cholesterol Levels.” *New England Journal of Medicine* 335, no. 14 (October 1996): 1001–1009. https://doi.org/10.1056/NEJM199610033351401.

Sainz, J., Ayman Al Haj Zen, Giuseppina Caligiuri, Corinne Demerens, Dominique Urbain, Mathilde Lemitre, and Antoine Lafont. “Isolation of ‘Side Population’ Progenitor Cells From Healthy Arteries of Adult Mice.” *Arteriosclerosis, Thrombosis, and Vascular Biology* 26, no. 2 (December 2005): 281–286. https://doi.org/10.1161/01.ATV.0000197793.83391.91.

Saliba, AE, AJ Westermann, SA Gorski, and J Vogel. “Single-Cell RNA-Seq: Advances and Future Challenges.” *Nucleic Acids Res.* 42, no. 14 (2014).

Salic, A., and T. J. Mitchison. “A Chemical Method for Fast and Sensitive Detection of DNA Synthesis in Vivo.” *Proceedings of the National Academy of Sciences* 105, no. 7 (February 2008): 2415–2420. https://doi.org/10.1073/pnas.0712168105.

Samy, A. K., B. Whyte, and G. Macbain. “Abdominal Aortic Aneurysm in Scotland.” *British Journal of Surgery* 81, no. 8 (August 1994): 1104–1106. https://doi.org/10.1002/bjs.1800810807.

Sandoo, Aamer, Jet J C S Veldhuijzen van Zanten, George S Metsios, Douglas Carroll, and George D Kitas. “The Endothelium and Its Role in Regulating Vascular Tone.” *The Open Cardiovascular Medicine Journal* 4 (December 2010): 302–12. https://doi.org/10.2174/1874192401004010302.

Saraff, K., Fjoralba Babamusta, Lisa A Cassis, and Alan Daugherty. “Aortic Dissection Precedes Formation of Aneurysms and Atherosclerosis in Angiotensin II-Infused, Apolipoprotein E-Deficient Mice.” *Arteriosclerosis, Thrombosis, and Vascular Biology* 23, no. 9 (September 2003): 1621–1626. https://doi.org/10.1161/01.ATV.0000085631.76095.64.

Sata, Masataka, Akio Saiura, Atsushi Kunisato, Akihiro Tojo, Seiji Okada, Takeshi Tokuhisa, Hisamaru Hirai, Masatoshi Makuuchi, Yasunobu Hirata, and Ryozo Nagai. “Hematopoietic Stem Cells Differentiate into Vascular Cells That Participate in the Pathogenesis of Atherosclerosis.” *Nat Med* 8, no. 4 (2002): 403–409. https://doi.org/10.1038/nm0402-403.

Sato, Yuki. “Dorsal Aorta Formation: Separate Origins, Lateral-to-Medial Migration, and Remodeling.” *Development, Growth & Differentiation* 55, no. 1 (January 2013): 113–129. https://doi.org/10.1111/dgd.12010.

Schindelin, Johannes, Ignacio Arganda-Carreras, Erwin Frise, Verena Kaynig, Mark Longair, Tobias Pietzsch, Stephan Preibisch, et al. “Fiji: An Open-Source Platform for Biological-Image Analysis.” *Nature Methods* 9, no. 7 (June 2012): 676–682. https://doi.org/10.1038/nmeth.2019.

Schwartz, S M, D DeBlois, and E R O’Brien. “The Intima. Soil for Atherosclerosis and Restenosis.” *Circulation Research* 77, no. 3 (September 1995): 445–65.

Schwartz, S M, and C E Murry. “Proliferation and the Monoclonal Origins of Atherosclerotic Lesions.” *Annual Review of Medicine* 49 (1998): 437–60. https://doi.org/10.1146/annurev.med.49.1.437.

Schwartz, Stephen M., Renu Virmani, and Michael E. Rosenfeld. “The Good Smooth Muscle Cells in Atherosclerosis.” *Curr Atheroscler Rep* 2, no. 5 (2000): 422–429. https://doi.org/10.1007/s11883-000-0081-5.

Scott, R A, N M Wilson, H A Ashton, and D N Kay. “Influence of Screening on the Incidence of Ruptured Abdominal Aortic Aneurysm: 5-Year Results of a Randomized Controlled Study.” *The British Journal of Surgery* 82, no. 8 (August 1995): 1066–70.

Shang, Yueting, Tadashi Yoshida, Brad A. Amendt, James F. Martin, and Gary K. Owens. “Pitx2 Is Functionally Important in the Early Stages of Vascular Smooth Muscle Cell Differentiation.” *The Journal of Cell Biology* 181, no. 3 (May 2008): 461–473. https://doi.org/10.1083/jcb.200711145.

Shankman, Laura S, Delphine Gomez, Olga a Cherepanova, Morgan Salmon, Gabriel F Alencar, Ryan M Haskins, Pamela Swiatlowska, et al. “KLF4-Dependent Phenotypic Modulation of Smooth Muscle Cells Has a Key Role in Atherosclerotic Plaque Pathogenesis.” *Nature Medicine* 21, no. 6 (2015): 628–37. https://doi.org/10.1038/nm.3866.

Sheikh, Abdul Q, Ashish Misra, Ivan O Rosas, Ralf H Adams, and Daniel M Greif. “Smooth Muscle Cell Progenitors Are Primed to Muscularize in Pulmonary Hypertension.” *Science Translational Medicine* 7, no. 308 (October 2015): 308ra159. https://doi.org/10.1126/scitranslmed.aaa9712.

Shen, Zhuxia, Chao Li, Ryan A Frieler, Alena S Gerasimova, Soo Jung Lee, Jing Wu, Michael M Wang, et al. “Smooth Muscle Protein 22 Alpha-Cre Is Expressed in Myeloid Cells in Mice.” *Biochemical and Biophysical Research Communications* 422, no. 4 (June 2012): 639–42. https://doi.org/10.1016/j.bbrc.2012.05.041.

Sheng, Kuanwei, Wenjian Cao, Yichi Niu, Qing Deng, and Chenghang Zong. “Effective Detection of Variation in Single-Cell Transcriptomes Using MATQ-Seq.” *Nature Methods* 14, no. 3 (January 2017): 267–270. https://doi.org/10.1038/nmeth.4145.

Sherif L, and Zahradka P. “Vascular Smooth Muscle Cell Motility: From Migration to Invasion.” *Experimental and Clinical Cardiology* 15, no. 4 (2010): 75–85.

Shikatani, Eric A., Mark Chandy, Rickvinder Besla, Cedric C. Li, Abdul Momen, Omar El-Mounayri, Clinton S. Robbins, and Mansoor Husain. “C-Myb Regulates Proliferation and Differentiation of Adventitial Sca1 \textlesssup\textgreater+\textless/Sup\textgreater Vascular Smooth Muscle Cell Progenitors by Transactivation of MyocardinHighlights.” *Arteriosclerosis, Thrombosis, and Vascular Biology* 36, no. 7 (July 2016): 1367–1376. https://doi.org/10.1161/ATVBAHA.115.307116.

Sigal, Alex, Ron Milo, Ariel Cohen, Naama Geva-Zatorsky, Yael Klein, Yuvalal Liron, Nitzan Rosenfeld, Tamar Danon, Natalie Perzov, and Uri Alon. “Variability and Memory of Protein Levels in Human Cells.” *Nature* 444, no. 7119 (2006): 643–646. https://doi.org/10.1038/nature05316.

Simons, Benjamin D. “Deep Sequencing as a Probe of Normal Stem Cell Fate and Preneoplasia in Human Epidermis.” *Proceedings of the National Academy of Sciences of the United States of America* 113, no. 1 (January 2016): 128–33. https://doi.org/10.1073/pnas.1516123113.

Singh, K, K H Bønaa, B K Jacobsen, L Bjørk, and S Solberg. “Prevalence of and Risk Factors for Abdominal Aortic Aneurysms in a Population-Based Study : The Tromsø Study.” *American Journal of Epidemiology* 154, no. 3 (August 2001): 236–44.

Sinha, S., Mark H Hoofnagle, Paul A Kingston, Mary E McCanna, and Gary K Owens. “Transforming Growth Factor- 1 Signaling Contributes to Development of Smooth Muscle Cells from Embryonic Stem Cells.” *AJP: Cell Physiology* 287, no. 6 (August 2004): C1560–C1568. https://doi.org/10.1152/ajpcell.00221.2004.

Sinha, Sanjay, Dharini Iyer, and Alessandra Granata. “Embryonic Origins of Human Vascular Smooth Muscle Cells: Implications for in Vitro Modeling and Clinical Application.” *Cellular and Molecular Life Sciences* 71, no. 12 (June 2014): 2271–2288. https://doi.org/10.1007/s00018-013-1554-3.

Smallwood, Sébastien A, Heather J Lee, Christof Angermueller, Felix Krueger, Heba Saadeh, Julian Peat, Simon R Andrews, Oliver Stegle, Wolf Reik, and Gavin Kelsey. “Single-Cell Genome-Wide Bisulfite Sequencing for Assessing Epigenetic Heterogeneity.” *Nature Methods* 11, no. 8 (August 2014): 817–820. https://doi.org/10.1038/nmeth.3035.

Snippert, Hugo J, Laurens G van der Flier, Toshiro Sato, Johan H van Es, Maaike van den Born, Carla Kroon-Veenboer, Nick Barker, et al. “Intestinal Crypt Homeostasis Results from Neutral Competition between Symmetrically Dividing Lgr5 Stem Cells.” *Cell* 143, no. 1 (2010): 134–44. https://doi.org/10.1016/j.cell.2010.09.016.

Spangrude, G J, S Heimfeld, and I L Weissman. “Purification and Characterization of Mouse Hematopoietic Stem Cells.” *Science (New York, N.Y.)* 241, no. 4861 (July 1988): 58–62.

Stegemann, Jan P, Helen Hong, and Robert M Nerem. “Mechanical, Biochemical, and Extracellular Matrix Effects on Vascular Smooth Muscle Cell Phenotype.” *Journal of Applied Physiology (Bethesda, Md. : 1985)* 98, no. 6 (2005): 2321–2327. https://doi.org/10.1152/japplphysiol.01114.2004.

Stenmark, Kurt R, Michael E Yeager, Karim C El Kasmi, Eva Nozik-Grayck, Evgenia V Gerasimovskaya, Min Li, Suzette R Riddle, and Maria G Frid. “The Adventitia: Essential Regulator of Vascular Wall Structure and Function.” *Annual Review of Physiology* 75, no. November 2012 (2013): 23–47. https://doi.org/10.1146/annurev-physiol-030212-183802.

Stringfellow, M M, P F Lawrence, and R G Stringfellow. “The Influence of Aorta-Aneurysm Geometry upon Stress in the Aneurysm Wall.” *The Journal of Surgical Research* 42, no. 4 (April 1987): 425–33.

Swedenborg, J., M. I. Mayranpaa, and P. T. Kovanen. “Mast Cells: Important Players in the Orchestrated Pathogenesis of Abdominal Aortic Aneurysms.” *Arteriosclerosis, Thrombosis, and Vascular Biology* 31, no. 4 (April 2011): 734–740. https://doi.org/10.1161/ATVBAHA.110.213157.

Tabas, I., G. Garcia-Cardena, and G. K. Owens. “The Cell Biology of Disease: Recent Insights into the Cellular Biology of Atherosclerosis.” *The Journal of Cell Biology* 209, no. 1 (2015): 13–22. https://doi.org/10.1083/jcb.201412052.

Tacke, Frank, David Alvarez, Theodore J Kaplan, Claudia Jakubzick, Rainer Spanbroek, Jaime Llodra, Alexandre Garin, et al. “Monocyte Subsets Differentially Employ CCR2, CCR5, and CX3CR1 to Accumulate within Atherosclerotic Plaques.” *The Journal of Clinical Investigation* 117, no. 1 (January 2007): 185–94. https://doi.org/10.1172/JCI28549.

Takagi, N, O Sugawara, and M Sasaki. “Regional and Temporal Changes in the Pattern of X-Chromosome Replication during the Early Post-Implantation Development of the Female Mouse.” *Chromosoma* 85, no. 2 (1982): 275–86. https://doi.org/10.1007/BF00294971.

Tam, Patrick P.L, and Richard R Behringer. “Mouse Gastrulation: The Formation of a Mammalian Body Plan.” *Mechanisms of Development* 68, no. 1–2 (November 1997): 3–25. https://doi.org/10.1016/S0925-4773(97)00123-8.

Tamarina, N A, W D McMillan, V P Shively, and W H Pearce. “Expression of Matrix Metalloproteinases and Their Inhibitors in Aneurysms and Normal Aorta.” *Surgery* 122, no. 2 (August 1997): 264–71; discussion 271–2.

Tambyraja, Andrew L., Raymond Dawson, Domenico Valenti, John A. Murie, and Roderick T. Chalmers. “Systemic Inflammation and Repair of Abdominal Aortic Aneurysm.” *World Journal of Surgery* 31, no. 6 (May 2007): 1212–1216. https://doi.org/10.1007/s00268-007-9014-6.

Tang, Fuchou, Catalin Barbacioru, Yangzhou Wang, Ellen Nordman, Clarence Lee, Nanlan Xu, Xiaohui Wang, et al. “MRNA-Seq Whole-Transcriptome Analysis of a Single Cell.” *Nature Methods* 6, no. 5 (May 2009): 377–382. https://doi.org/10.1038/nmeth.1315.

Tang, R.-h., X.-L. Zheng, T. E. Callis, W. E. Stansfield, J. He, A. S. Baldwin, D.-Z. Wang, and C. H. Selzman. “Myocardin Inhibits Cellular Proliferation by Inhibiting NF- B(P65)-Dependent Cell Cycle Progression.” *Proceedings of the National Academy of Sciences* 105, no. 9 (March 2008): 3362–3367. https://doi.org/10.1073/pnas.0705842105.

Tang, Zhenyu, Aijun Wang, Falei Yuan, Zhiqiang Yan, Bo Liu, Julia S. Chu, Jill a. Helms, and Song Li. “Differentiation of Multipotent Vascular Stem Cells Contributes to Vascular Diseases.” *Nature Communications* 3 (2012): 875. https://doi.org/10.1038/ncomms1867.

Tanous, David, Lee N Benson, and Eric M Horlick. “Coarctation of the Aorta: Evaluation and Management.” *Current Opinion in Cardiology* 24, no. 6 (November 2009): 509–515. https://doi.org/10.1097/HCO.0b013e328330cc22.

Tedgui, A, and Z Mallat. “Cytokines in Atherosclerosis: Pathogenic and Regulatory Pathways.” *Physiol Rev* 86, no. 2 (2006): 515–581. https://doi.org/86/2/515 [pii]\r10.1152/physrev.00024.2005.

Thompson, R W. “Basic Science of Abdominal Aortic Aneurysms: Emerging Therapeutic Strategies for an Unresolved Clinical Problem.” *Current Opinion in Cardiology* 11, no. 5 (September 1996): 504–18.

Thompson, Robert W. “Reflections on the Pathogenesis of Abdominal Aortic Aneurysms.” *Cardiovascular Surgery (London, England)* 10, no. 4 (August 2002): 389–94.

Tieu, Brian C., Chang Lee, Hong Sun, Wanda LeJeune, Adrian Recinos, Xiaoxi Ju, Heidi Spratt, et al. “An Adventitial IL-6/MCP1 Amplification Loop Accelerates Macrophage-Mediated Vascular Inflammation Leading to Aortic Dissection in Mice.” *Journal of Clinical Investigation* 119, no. 12 (December 2009): 3637–3651. https://doi.org/10.1172/JCI38308.

Trachet, Bram, Lydia Aslanidou, Alessandra Piersigilli, Rodrigo A. Fraga-Silva, Jessica Sordet-Dessimoz, Pablo Villanueva-Perez, Marco F.M. Stampanoni, Nikolaos Stergiopulos, and Patrick Segers. “Angiotensin II Infusion into ApoE-/- Mice: A Model for Aortic Dissection Rather than Abdominal Aortic Aneurysm?” *Cardiovascular Research* 31, no. 10 (June 2017): 270–U102. https://doi.org/10.1093/cvr/cvx128.

Trapnell, Cole, Davide Cacchiarelli, Jonna Grimsby, Prapti Pokharel, Shuqiang Li, Michael Morse, Niall J Lennon, Kenneth J Livak, Tarjei S Mikkelsen, and John L Rinn. “The Dynamics and Regulators of Cell Fate Decisions Are Revealed by Pseudotemporal Ordering of Single Cells.” *Nature Biotechnology* 32, no. 4 (March 2014): 381–386. https://doi.org/10.1038/nbt.2859.

Trigueros-Motos, L., J. M. Gonzalez-Granado, C. Cheung, P. Fernandez, F. Sanchez-Cabo, A. Dopazo, S. Sinha, and V. Andres. “Embryological-Origin-Dependent Differences in Homeobox Expression in Adult Aorta: Role in Regional Phenotypic Variability and Regulation of NF- B Activity.” *Arteriosclerosis, Thrombosis, and Vascular Biology* 33, no. 6 (June 2013): 1248–1256. https://doi.org/10.1161/ATVBAHA.112.300539.

Tromp, Gerard, Helena Kuivaniemi, Irene Hinterseher, and David J. Carey. “Novel Genetic Mechanisms for Aortic Aneurysms.” *Current Atherosclerosis Reports* 12, no. 4 (July 2010): 259–266. https://doi.org/10.1007/s11883-010-0111-x.

Tung, Po-Yuan, John D Blischak, Chiaowen Joyce Hsiao, David A Knowles, Jonathan E Burnett, Jonathan K Pritchard, and Yoav Gilad. “Batch Effects and the Effective Design of Single-Cell Gene Expression Studies.” *Scientific Reports* 7 (January 2017): 39921. https://doi.org/10.1038/srep39921.

Vallabhaneni, Srinivasa R., Geoffrey L. Gilling-Smith, Thien V. How, Stuart D. Carter, John A. Brennan, and Peter L. Harris. “\textlessb\textgreaterHeterogeneity of Tensile Strength and Matrix Metalloproteinase Activity in the Wall of Abdominal Aortic Aneurysms\textless/B\textgreater.” *Journal of Endovascular Therapy* 11, no. 4 (August 2004): 494–502. https://doi.org/10.1583/04-1239.1.

VanderLaan, Paul a., Catherine a. Reardon, and Godfrey S. Getz. “Site Specificity of Atherosclerosis: Site-Selective Responses to Atherosclerotic Modulators.” *Arteriosclerosis, Thrombosis, and Vascular Biology* 24, no. 1 (2004): 12–22. https://doi.org/10.1161/01.ATV.0000105054.43931.f0.

Virmani, R, M Robinowitz, J C Geer, P P Breslin, J C Beyer, and H a McAllister. “Coronary Artery Atherosclerosis Revisited in Korean War Combat Casualties.” *Archives of Pathology & Laboratory Medicine* 111, no. 10 (1987): 972–6.

Wang, Gang, Laureen Jacquet, Eirini Karamariti, and Qingbo Xu. “Origin and Differentiation of Vascular Smooth Muscle Cells.” *The Journal of Physiology* 593, no. 14 (July 2015): 3013–30. https://doi.org/10.1113/JP270033.

Wang, Haidong, Mohsen Naghavi, Christine Allen, Ryan M Barber, Zulfiqar A Bhutta, Austin Carter, Daniel C Casey, et al. “Global, Regional, and National Life Expectancy, All-Cause Mortality, and Cause-Specific Mortality for 249 Causes of Death, 1980–2015: A Systematic Analysis for the Global Burden of Disease Study 2015.” *The Lancet* 388, no. 10053 (October 2016): 1459–1544. https://doi.org/10.1016/S0140-6736(16)31012-1.

Wang, Yu, Hafid Ait-Oufella, Olivier Herbin, Philippe Bonnin, Bhama Ramkhelawon, Soraya Taleb, Jin Huang, et al. “TGF-β Activity Protects against Inflammatory Aortic Aneurysm Progression and Complications in Angiotensin II–infused Mice.” *Journal of Clinical Investigation* 120, no. 2 (February 2010): 422–432. https://doi.org/10.1172/JCI38136.

Wang, Zhigao, Da-Zhi Wang, Dirk Hockemeyer, John McAnally, Alfred Nordheim, and Eric N. Olson. “Myocardin and Ternary Complex Factors Compete for SRF to Control Smooth Muscle Gene Expression.” *Nature* 428, no. 6979 (March 2004): 185–189. https://doi.org/10.1038/nature02382.

Wasteson, Per, Bengt R Johansson, Tomi Jukkola, Silke Breuer, Levent M Akyürek, Juha Partanen, and Per Lindahl. “Developmental Origin of Smooth Muscle Cells in the Descending Aorta in Mice.” *Development (Cambridge, England)* 135, no. 10 (2008): 1823–1832. https://doi.org/10.1242/dev.020958.

Weakley, Sarah M, Jun Jiang, Panagiotis Kougias, Peter H Lin, Qizhi Yao, F Charles Brunicardi, Richard A Gibbs, and Changyi Chen. “Role of Somatic Mutations in Vascular Disease Formation.” *Expert Review of Molecular Diagnostics* 10, no. 2 (March 2010): 173–85. https://doi.org/10.1586/erm.10.1.

Wills, Quin F, Kenneth J Livak, Alex J Tipping, Tariq Enver, Andrew J Goldson, Darren W Sexton, and Chris Holmes. “Single-Cell Gene Expression Analysis Reveals Genetic Associations Masked in Whole-Tissue Experiments.” *Nature Biotechnology* 31, no. 8 (July 2013): 748–752. https://doi.org/10.1038/nbt.2642.

Wirth, Angela, Zoltán Benyó, Martina Lukasova, Barbara Leutgeb, Nina Wettschureck, Stefan Gorbey, Petra Orsy, et al. “G12-G13-LARG-Mediated Signaling in Vascular Smooth Muscle Is Required for Salt-Induced Hypertension.” *Nature Medicine* 14, no. 1 (2008): 64–68. https://doi.org/10.1038/nm1666.

Wolinsky, H., and S. Glagov. “A Lamellar Unit of Aortic Medial Structure and Function in Mammals.” *Circulation Research* 20, no. 1 (1967): 99–111. https://doi.org/10.1161/01.RES.20.1.99.

Wu, Ying-chen, Lei Cui, Gang Li, Shuo Yin, Yong-juan Gao, and Yi-lin Cao. "[PDGF-BB Initiates Vascular Smooth Muscle-like Phenotype Differentiation of Human Bone Marrow Mesenchymal Stem Cells in Vitro]." *Zhonghua Zheng Xing Wai Ke Za Zhi = Zhonghua Zhengxing Waike Zazhi = Chinese Journal of Plastic Surgery* 23, no. 4 (July 2007): 335–9.

Xin, M., E. M. Small, L. B. Sutherland, X. Qi, J. McAnally, C. F. Plato, J. A. Richardson, R. Bassel-Duby, and E. N. Olson. "MicroRNAs MiR-143 and MiR-145 Modulate Cytoskeletal Dynamics and Responsiveness of Smooth Muscle Cells to Injury." *Genes & Development* 23, no. 18 (September 2009): 2166–2178. https://doi.org/10.1101/gad.1842409.

Xu, Qingbo. "Mouse Models of Arteriosclerosis: From Arterial Injuries to Vascular Grafts." *The American Journal of Pathology* 165, no. 1 (July 2004): 1–10. https://doi.org/10.1016/S0002-9440(10)63270-1.

Yan, Kelley S., Claudia Y. Janda, Junlei Chang, Grace X. Y. Zheng, Kathryn A. Larkin, Vincent C. Luca, Luis A. Chia, et al. "Non-Equivalence of Wnt and R-Spondin Ligands during Lgr5+ Intestinal Stem-Cell Self-Renewal." *Nature* 545, no. 7653 (May 2017): 238–242. https://doi.org/10.1038/nature22313.

Yang, P, MS Hong, C Fu, BM Schmit, Y Su, SA Berceli, and Z Jiang. "Preexisting Smooth Muscle Cells Contribute to Neointimal Cell Repopulation at an Incidence Varying Widely among Individual Lesions." *Surgery*, 2015.

Yao, Q., M.-A. Renault, C. Chapouly, S. Vandierdonck, I. Belloc, B. Jaspard-Vinassa, J.-M. Daniel-Lamaziere, et al. "Sonic Hedgehog Mediates a Novel Pathway of PDGF-BB-Dependent Vessel Maturation." *Blood* 123, no. 15 (April 2014): 2429–2437. https://doi.org/10.1182/blood-2013-06-508689.

Yoshida, T., Q. Gan, Y. Shang, and G. K. Owens. "Platelet-Derived Growth Factor-BB Represses Smooth Muscle Cell Marker Genes via Changes in Binding of MKL Factors and Histone Deacetylases to Their Promoters." *AJP: Cell Physiology* 292, no. 2 (August 2006): C886–C895. https://doi.org/10.1152/ajpcell.00449.2006.

Yoshida, T., Mark H Hoofnagle, and Gary K Owens. "Myocardin and Prx1 Contribute to Angiotensin II-Induced Expression of Smooth Muscle -Actin." *Circulation Research* 94, no. 8 (April 2004): 1075–1082. https://doi.org/10.1161/01.RES.0000125622.46280.95.

Yoshida, T., Sanjay Sinha, Frédéric Dandré, Brian R Wamhoff, Mark H Hoofnagle, Brandon E Kremer, Da-Zhi Wang, Eric N Olson, and Gary K Owens. "Myocardin Is a Key Regulator of CArG-Dependent Transcription of Multiple Smooth Muscle Marker Genes." *Circulation Research* 92, no. 8 (May 2003): 856–864. https://doi.org/10.1161/01.RES.0000068405.49081.09.

Yoshida, Tadashi, Maho Yamashita, Chihiro Horimai, and Matsuhiko Hayashi. "Smooth Muscle-Selective Inhibition of Nuclear Factor-KB Attenuates Smooth Muscle Phenotypic Switching and Neointima Formation Following Vascular Injury." *Journal of the American Heart Association* 2, no. 3 (May 2013): e000230. https://doi.org/10.1161/JAHA.113.000230.

Yu, Baoqi, Mei Mei Wong, Claire M. F. Potter, Russell M. L. Simpson, Eirini Karamariti, Zhongyi Zhang, Lingfang Zeng, et al. "Vascular Stem/Progenitor Cell Migration Induced by Smooth Muscle Cell-Derived Chemokine (C-C Motif) Ligand 2 and Chemokine (C-X-C Motif) Ligand 1 Contributes to Neointima Formation." *STEM CELLS* 34, no. 9 (September 2016): 2368–2380. https://doi.org/10.1002/stem.2410.

Yu, Haixiang, Murray C.H. Clarke, Nichola Figg, Trevor D. Littlewood, and Martin R. Bennett. "Smooth Muscle Cell Apoptosis Promotes Vessel Remodeling and Repair via Activation of Cell Migration, Proliferation, and Collagen Synthesis." *Arteriosclerosis, Thrombosis, and Vascular Biology* 31, no. 11 (2011). http://atvb.ahajournals.org/content/31/11/2402.long.

Yuan, Falei, Dong Wang, Kang Xu, Jixian Wang, Zhijun Zhang, Li Yang, Guo-Yuan Yang, and Song Li. "Contribution of Vascular Cells to Neointimal Formation." *PloS One* 12, no. 1 (2017): e0168914. https://doi.org/10.1371/journal.pone.0168914.

Zahradka, Peter, Greg Harding, Brenda Litchie, Shawn Thomas, Jeffrey P Werner, David P Wilson, and Natalia Yurkova. "Activation of MMP-2 in Response to Vascular Injury Is Mediated by

Phosphatidylinositol 3-Kinase-Dependent Expression of MT1-MMP." *American Journal of Physiology. Heart and Circulatory Physiology* 287, no. 6 (2004): H2861–70. https://doi.org/10.1152/ajpheart.00230.2004.

Zaman, A.G, G Helft, S.G Worthley, and J.J Badimon. "The Role of Plaque Rupture and Thrombosis in Coronary Artery Disease." *Atherosclerosis* 149, no. 2 (2000): 251–266. https://doi.org/10.1016/S0021-9150(99)00479-7.

Zengin, E., Fariba Chalajour, Ursula M Gehling, Wulf D Ito, Hendrik Treede, Heidrun Lauke, Joachim Weil, Hermann Reichenspurner, Nerbil Kilic, and Süleyman Ergün. "Vascular Wall Resident Progenitor Cells: A Source for Postnatal Vasculogenesis." *Development* 133, no. 8 (April 2006): 1543–1551. https://doi.org/10.1242/dev.02315.

Zhang, H., S. Gu, B. Al-Sabeq, S. Wang, J. He, A. Tam, C. Cifelli, et al. "Origin-Specific Epigenetic Program Correlates with Vascular Bed-Specific Differences in Rgs5 Expression." *The FASEB Journal* 26, no. 1 (January 2012): 181–191. https://doi.org/10.1096/fj.11-185454.

Zhang, Jifeng, Wei Zhong, Taixing Cui, Maozhou Yang, Xing Hu, Kefeng Xu, Changqing Xie, et al. "Generation of an Adult Smooth Muscle Cell-Targeted Cre Recombinase Mouse Model." *Arteriosclerosis, Thrombosis, and Vascular Biology* 26, no. 3 (March 2006): e23–4. https://doi.org/10.1161/01.ATV.0000202661.61837.93.

Zhang, Ming-Jie, Yi Zhou, Lei Chen, Yan-Qin Wang, Xu Wang, Yan Pi, Chang-Yue Gao, Jing-Cheng Li, and Li-Li Zhang. "An Overview of Potential Molecular Mechanisms Involved in VSMC Phenotypic Modulation." *Histochemistry and Cell Biology* 145, no. 2 (February 2016): 119–130. https://doi.org/10.1007/s00418-015-1386-3.

Zhang, Z., M. Wang, X.-H. Fan, J.-H. Chen, Y.-Y. Guan, and Y.-B. Tang. "Upregulation of TRPM7 Channels by Angiotensin II Triggers Phenotypic Switching of Vascular Smooth Muscle Cells of Ascending Aorta." *Circulation Research* 111, no. 9 (October 2012): 1137–1146. https://doi.org/10.1161/CIRCRESAHA.112.273755.

Zheng, Grace X. Y., Jessica M. Terry, Phillip Belgrader, Paul Ryvkin, Zachary W. Bent, Ryan Wilson, Solongo B. Ziraldo, et al. "Massively Parallel Digital Transcriptional Profiling of Single Cells." *Nature Communications* 8 (January 2017): 14049. https://doi.org/10.1038/ncomms14049.

Zheng, Jian-Pu, Donghong Ju, Jianbin Shen, Maozhou Yang, and Li Li. "Disruption of Actin Cytoskeleton Mediates Loss of Tensile Stress Induced Early Phenotypic Modulation of Vascular Smooth Muscle Cells in Organ Culture." *Experimental and Molecular Pathology* 88, no. 1 (February 2010): 52–57. https://doi.org/10.1016/j.yexmp.2009.10.006.

Zhu, Shui-Bo, Jian Zhu, Zi-Zi Zhou, Er-Ping Xi, Rong-Ping Wang, and Yu Zhang. "TGF-B1 Induces Human Aortic Vascular Smooth Muscle Cell Phenotype Switch through PI3K/AKT/ID2 Signaling." *American Journal of Translational Research* 7, no. 12 (2015): 2764–74.

Ziegenhain, Christoph, Beate Vieth, Swati Parekh, Björn Reinius, Amy Guillaumet-Adkins, Martha Smets, Heinrich Leonhardt, Holger Heyn, Ines Hellmann, and Wolfgang Enard. "Comparative Analysis of Single-Cell RNA Sequencing Methods." *Molecular Cell* 65, no. 4 (February 2017): 631–643.e4. https://doi.org/10.1016/j.molcel.2017.01.023.

Zong, Chenghang, Sijia Lu, Alec R Chapman, and X Sunney Xie. "Genome-Wide Detection of Single-Nucleotide and Copy-Number Variations of a Single Human Cell." *Science (New York, N.Y.)* 338, no. 6114 (December 2012): 1622–6. https://doi.org/10.1126/science.1229164.